# Angiogenesis
# the genetic regulation of vascular development

Angiogenesis - the genetic regulation of vascular development

# Angiogenesis
# the genetic regulation of vascular development

Angiogenese
de genetische regulatie van vaatontwikkeling

**Proefschrift**

ter verkrijging van de graad van doctor aan de
Erasmus Universiteit Rotterdam
op gezag van de
rector magnificus

Prof.dr. H.A.P. Pols

en volgens besluit van het College voor Promoties.
De openbare verdediging zal plaatsvinden op

**dinsdag 8 april 2014 om 13.30 uur**
door

**Remco Anton Haasdijk**

geboren te Doetinchem

ERASMUS UNIVERSITEIT ROTTERDAM

## *Promotiecommissie*

**Promotor**
> Prof.dr. D.J.G.M. Duncker

**Overige leden**
> Prof.dr. S. Schulte-Merker
> Prof.dr. E.J.G. Sijbrands
> Dr. J. Essers

**Copromotoren**
> Dr. H.J. Duckers
> Dr. C. Cheng

**Paranimfen**
> Susan Geurts-Groen
> Carien Kloek

이것은 너를 위한 것이다

# *Contents*

# Proposition

## Stellingen

## *Stellingen*

1.  Leden van de Rho-GTPase familie vormen een sleutelrol in de regulatie van vaatontwikkeling - *dit proefschrift*.

2.  Intra-oculaire injectie van siRNA gericht tegen een specifiek gen geeft een betrouwbaar beeld van het *in vivo* effect van dit gen op de retinale vaatontwikkeling - *dit proefschrift*.

3.  De stimulerende werking van 9430020K01Rik (KIAA1462) op endotheelcel proliferatie tijdens angiogenese, verloopt via modulatie van de RhoA activiteit - *dit proefschrift*.

4.  Tagln2 onderdrukt vaatuitgroei door actine depolymerisatie en vermindering van de VEGFR-2 turnover - *dit proefschrift*.

5.  Tijdens angiogenese is Thsd1 essentieel voor vaatstabilisatie - *dit proefschrift*.

6.  Remming van angiogenese ter bestrijding van tumorgroei heeft mogelijk een averechts effect - *Physiol Rev. 2011;91(3):1071-1121*.

7.  Dagelijkse consumptie van pure chocolade verlaagd het risico op coronair vaatlijden - *Curr Atheroscler Rep. 2011;13(6):447-452*.

8.  In families met een erfelijke afwijking in het mitochondriaal DNA hebben kinderen met drie biologische ouders de toekomst - *Hum Mol Genet. 2011;20(R2):R168-R174*.

9.  Ook laboratoriummuizen zitten er graag warmpjes bij - *PLoS One. 2012;7(3):e32799*.

10. Binnen de plantenbiologie heeft 'auxine' dezelfde uitwerking op wetenschappers, als 'VEGF' binnen de vasculaire ontwikkelingsbiologie: ze hebben beide een stimulerend effect - *Nat Rev Genet. 2009;10(5):305-317*.

11. Mensen die zich helemaal niet inlaten met de wetenschappen en zich alleen door de natuur laten leiden, zijn verreweg het gelukkigst - *Desiderius Erasmus*.

# Chapter 1


## Introduction

For centuries, many scientists are fascinated by the organisation of the vascular network. The Greek philosopher and polymath *Aristotle* (384 BC) was one of the first man who described the vasculature. He wrote: "the system of blood vessels in the body may be compared to those of water-courses which are constructed in gardens: they start from one source, or spring, and branch off into numerous channels, and then into still more, and so on progressively, so as to carry a supply to every part of the garden".[1] Over time, many models of the vascular system have been developed. In 1628, it was the English biologist and physician *William Harvey* (1578 AD) who published in his book *Exercitatio Anatomica de Motu Cordis et Sanguinis in Animalibus* (Anatomical Exercises on the Motion of the Heart and Blood in Animals) our current model of the vascular system that blood circulates in a closed circuit.[2] Until then, less was known about blood vessel development. With the discovery of the microscope in the 17th century by *Antonie van Leeuwenhoek* (1632 AD), scientists observed for the first time vessel sprouting in thin transparent tissues. It was *John Hunter* - a Scottish surgeon (1728 AD) - who identified growing vessels in healing wounds and embryos.[3,4] The first observation of angiogenesis was made in 1853 by *Meyer* who described spindle-shaped structures arising from capillaries in tadpole tails, which later became tubular.[5,6] Over the last decades, knowledge about blood vessel development has increased by the advances of molecular biology. Today, scientists unravel the factors that stimulate angiogenesis in ischemic tissues and wound healing, and those that inhibit tumour growth and metastasis to develop better medical treatments for cancer and cardiovascular diseases.

## *Vessel formation*

During embryonic development, the vascular network is formed by both vasculogenesis and angiogenesis to provide oxygen to the developing organism. Hypoxic conditions initiate vessel formation by upregulating angiogenic factors like vascular endothelial growth factor (VEGF).[7,8]

**Vasculogenesis**
Vasculogenesis refers to the initial events of blood vessel formation in which angioblasts - endothelial precursor cell - differentiate into endothelial cells (EC), which assemble into a primitive vascular plexus.[1]

In the mouse at embryonic day (E)7.5 vascular development starts with the differentiation of mesodermal cells into haemangioblasts, leading to the formation of primitive blood islands. Then, haemangioblasts at the centre forms haematopoietic stem

cells, while those on the edge give rise to angioblasts. They further differentiate into ECs and assemble into tubular structures, forming the primitive vascular plexus (Figure 1A).[9]
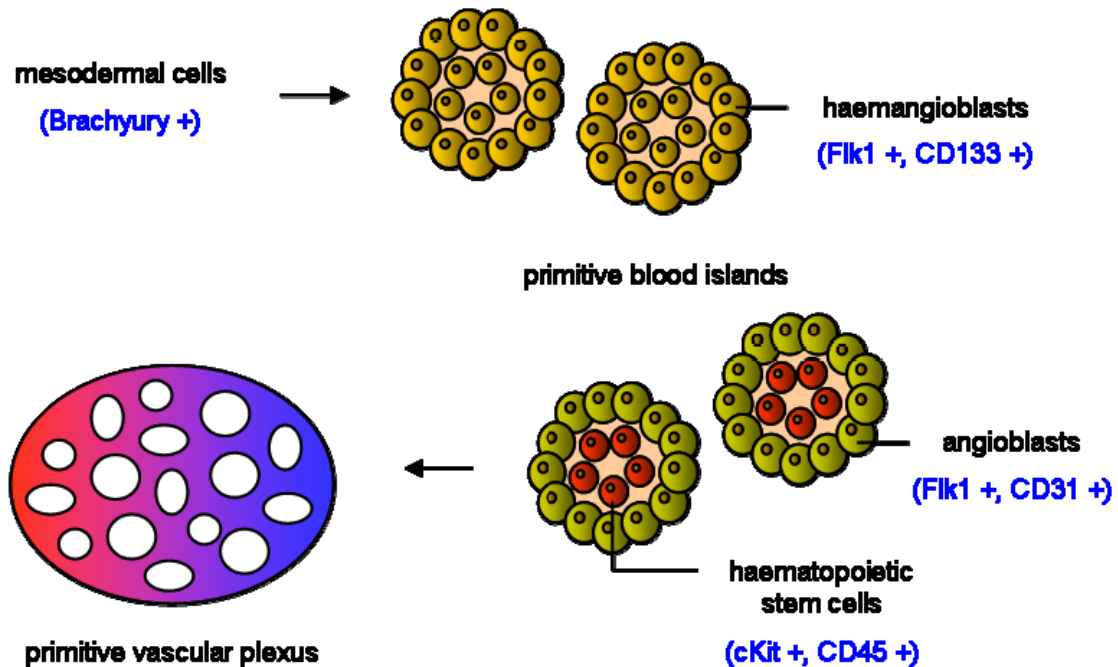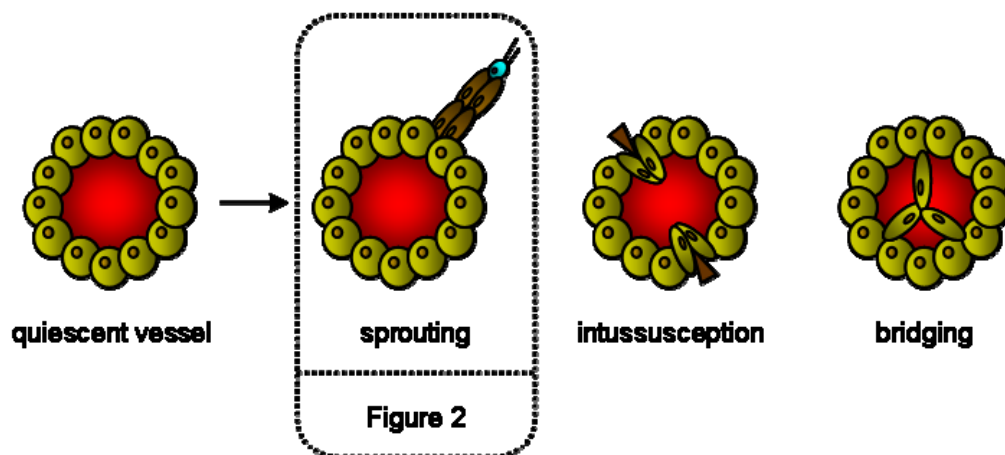


**Figure 1. Vessel formation.** (**A**) Vasculogenesis: the formation of blood vessels. Transcription factor *Brachyury* is needed for mesodermal cell differentiation into haemangioblasts, followed by the formation of primitive blood islands. Haemangioblasts give rise to angioblasts and haematopoietic stem cells. The angioblasts assemble into a primitive vascular plexus. Cell markers (blue). (**B**) Angiogenesis: the formation of new capillaries by sprouting from pre-existing small blood vessels. Quiescent vessels expand by sprouting: growth of a newly formed vessel branch or stalk toward an angiogenic stimulus (for a more detailed description see Figure 2), intussusception: splitting of an existing blood vessel in two, and bridging: splitting of an existing vessel by the formation of transendothelial bridges.

**Angiogenesis**

The formation of new capillaries by sprouting from pre-existing small blood vessels is known as angiogenesis.[1]

In the mouse at E8.5 the primitive vascular plexus expand by subsequent sprouting. Thereafter, angiogenesis can also take place by intussusception - the internal division of pre-existing vessels without sprouting - and vessels can also divide longitudinal into daughter vessels by the formation of transendothelial bridges (Figure 1B).[10]

**VEGF**

Vessel formation is regulated by many different angiogenic factors. One of the best known is VEGF, also known as VEGF-A. There are four different isoforms: $VEGF_{121}$, $VEGF_{165}$, $VEGF_{189}$ and $VEGF_{206}$, of which $VEGF_{165}$ is the most active one. $VEGF_{165}$ is a freely diffusible protein, but can also be sequestered in the extracellular matrix (ECM).[11-13] Mouse embryos lacking one VEGF allele dies between E11 and 12. They display defective vascularisation in several organs.[14]

VEGF stimulates angiogenesis by signalling through VEGF receptor 2 (VEGFR-2), also known as fetal liver kinase (Flk1) or kinase domain receptor (Kdr), and its neuropilin (NRP) co-receptor 1 and 2. Binding of VEGF to VEGFR-2 results in dimerisation and ligand-dependent tyrosine phosphorylation, activating downstream signalling cascades.[11,12] Kdr-knockout mice die *in utero* between E8.5 and 9.5 as a consequence of disturbed blood island formation and organised blood vessel development.[15] Thus, VEGF and VEGFR-2 are important factors in vascular development.

## *Molecular basis of vessel branching*

The various processes involved in blood vessel formation will be explained in more detail based on sprouting angiogenesis, starting with a quiescent vessel (Figure 2A).[7] Sprouting begins in the presence of pro-angiogenic factors and will continue until quiescence is re-established.[16]

**Hypoxia-inducible factor**

In response to hypoxic conditions, pro-angiogenic factors will be upregulated. Vessel perfusion or the amount of oxygen is measured by oxygen sensing enzymes - prolyl hydroxylase domain proteins (PHD) - expressed at the surface of ECs. When sufficient oxygen is available, PHDs hydroxylate the hypoxia-inducible transcription factor (HIF), after which it is targeted for proteasomal degradation by the Von Hippel-Lindau tumour-suppressor protein.[12,16-19]

**A**       quiescent vessel

- lumen
- basement membrane
- pericytes
- endothelial cells

blood flow

**B**       tip cell selection

- pericyte detachment (Ang2)
- basement membrane degradation (MMPs)
- tip cell selection (VEGFR-2, Dll4 - Notch)
- angiogenic factors (VEGF, FGF)
- filopodia formation (Cdc42)
- loosening junctions
- vasodilatation (eNOS, NO)
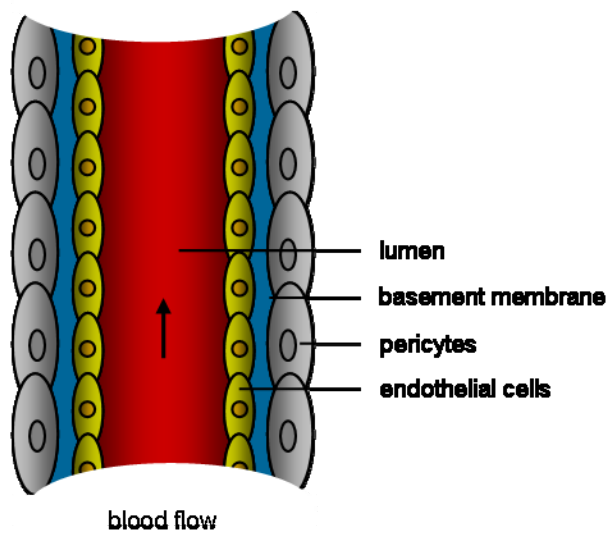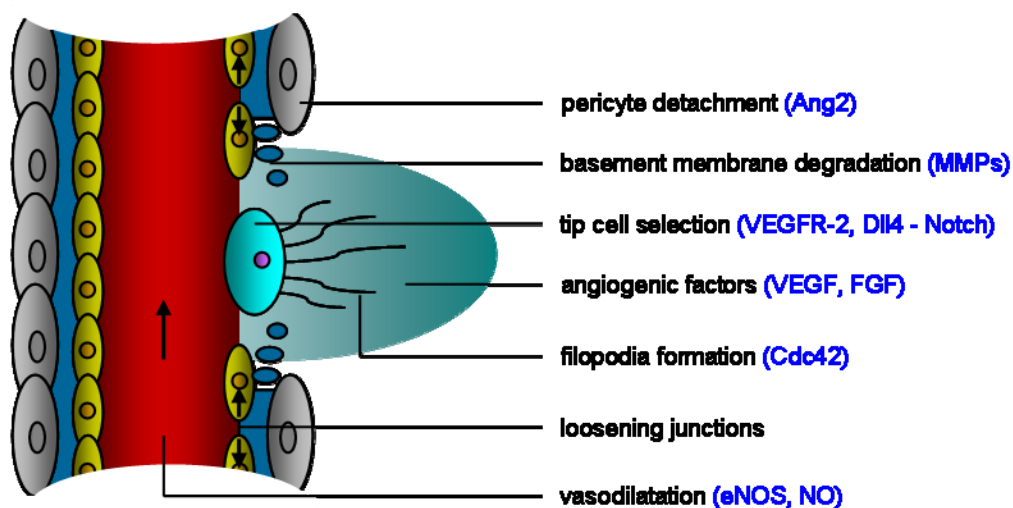
**Figure 2. Vessel branching.** The various processes involved in sprouting angiogenesis: (**A**) Quiescent vessels consist of a monolayer of endothelial cells (EC), interconnected by adherens and tight junctions. These ECs are enfolded by pericytes which suppress EC proliferation. Both cell types are anchored via integrins to a common basement membrane composed of extracellular matrix proteins to prevent resident ECs leaving their position. (**B**) Tip cell formation requires pericyte detachment, basement membrane degradation and disruption of EC junctions.

**C**      tip cell guidance



phalanx cell    *survival*

stalk cell    *proliferation*

attraction    (VEGF - VEGFR-2)

tip cell    *migration*

repulsion    (slit - Robo4

netrin 1 - UNC5B

semaphorins - NRP1

ephrin - EPH)

Figure 3

**D**      **vessel stabilisation**                    **vessel regression**



barrier function

(VE-cadherin)

Figure 4

apoptosis

(hypoperfusion,

Klf2 ↓)

survival

(VEGF, FGF

Klf2 ↑)

mural cell recruitment

(PDGF - PDGFR-β

Ang1 - Tie2

EDG1 and TGF-β)
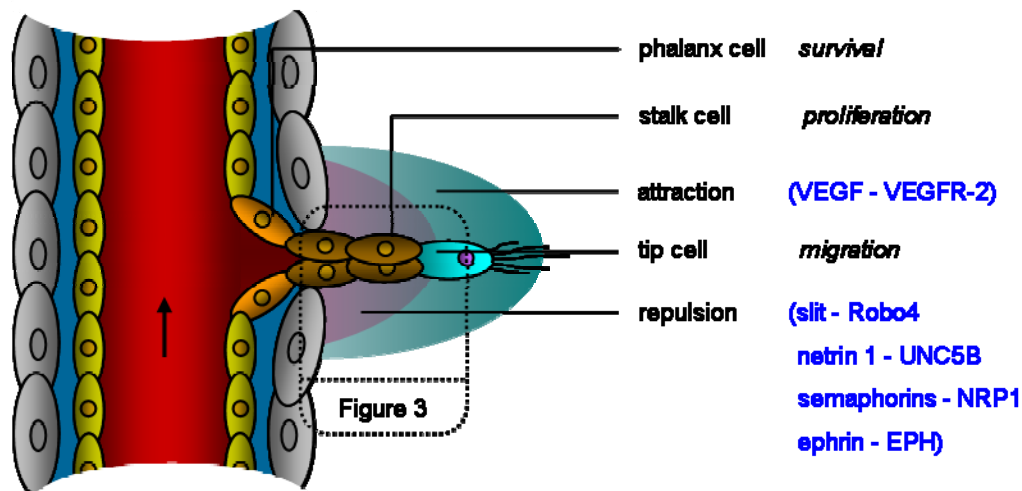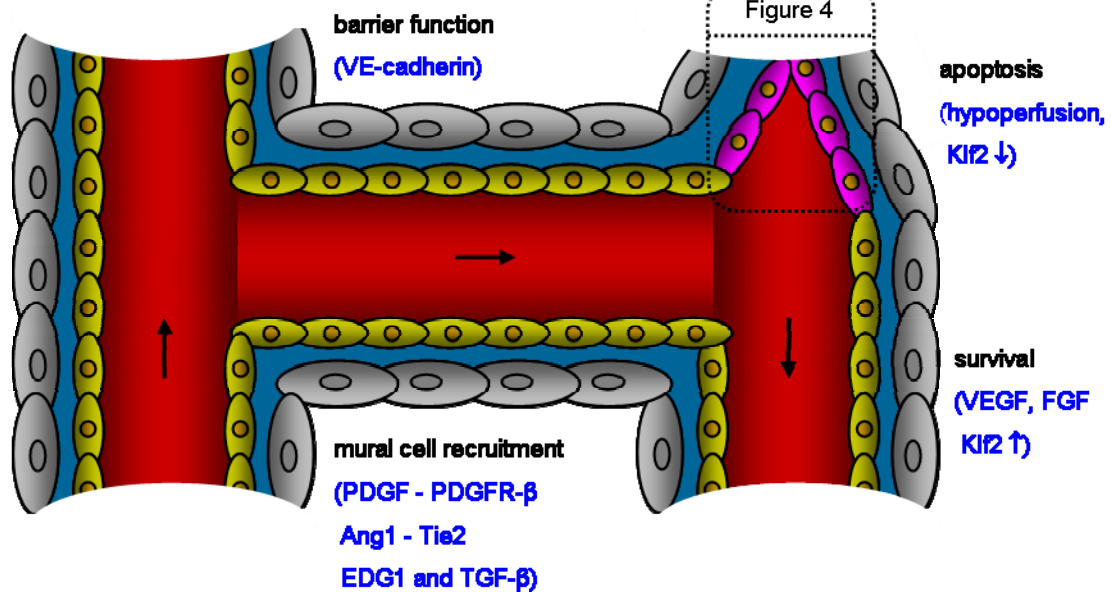
(**C**) Tip cells navigate in response to attractant and repulsive signals, and adhere to the extracellular matrix to migrate. Stalk cells behind the tip cell proliferate (for a more detailed description see Figure 3) and form a lumen. VE-cadherin is upregulated by phalanx cells for vessel stabilisation. (**D**) After tip cell fusion the initial endothelial barrier function is restored by VE-cadherin. Lumen formation allows perfusion which promote basement membrane deposition, mural cell recruitment and production of survival signals. Vessel regression appear when perfusion remains (for a more detailed description see Figure 4). Factors involved in the molecular basis of vessel branching (blue).

In hypoxic conditions, PHDs become inactive which results in diminished HIF degradation. So HIF can interact with hypoxia responsive elements to induce transcriptional activity of pro-angiogenic factors, initiating vessel sprouting.[12,16-18] Absence of HIF in mice results in abnormal vascular development and embryonic lethality.[20] Thus, HIF functions as a switch of vessel branching.

**Tip cell selection**

When a quiescent vessel sense a pro-angiogenic factor, pericytes will detach from the vessel wall by proteolytic degradation of the basement membrane, mediated by matrix metalloproteinases (MMP). Thereafter, break down of the basement membrane results in the liberation of several pro-angiogenic factors sequestered in the ECM like VEGF and fibroblast growth factor (FGF), and generate also anti-angiogenic factors by cleaving plasma proteins, matrix molecules or the proteases themselves to prevent excessive sprouting.[21-23] VEGF stimulates vasodilatation via endothelial nitric oxide synthase (eNOS) activation and release of NO, and induce the disruption of intercellular connections between ECs leading to an increased permeability of the vessel wall. Plasma proteins will extravasate and lay down a temporal ECM to which the ECs migrate.[7,12] FGF works pro-angiogenic by inducing the release of pro-angiogenic factors in a positive feedback loop.[24] Further pericyte detachment is stimulated by the release of angiopoietin 2 (Ang2) by ECs (Figure 2B).[25]

Once the pericytes have detached from the basement membrane and degradation of the ECM has taken place, one EC - known as the tip cell - become selected to lead the newly formed vessel branch or stalk. The neighbours of the tip cell become stalk cells. This selection process is controlled by the Notch pathway. In response to a VEGF gradient, all ECs upregulate the expression of the Notch ligand Dll4 by activation of VEGFR-2. The EC expressing Dll4 more quickly or at higher levels become a tip cell. Dll4 then activates Notch in the neighbouring ECs or stalk cells, downregulating VEGFR-2 while upregulating VEGF receptor 1 (VEGFR-1) which is involved in limiting tip cell formation. In this way, stalk cells become less responsive to the sprouting activity of VEGF.[7,16,26,27] Overall, tip cells express higher levels of Dll4, while stalk cells reveal high Notch activity which promotes EC proliferation.[28]

**Proliferation**

The link between proliferative signals from cell surface receptors, such as VEGFR-2 or integrin, to transcription factors which finally modulate cell cycle progression is formed by the Ras-Raf-MEK-ERK pathway. Ligand binding to its surface receptor leads to activation of focal adhesion kinase (FAK) via its N-terminal FERM domain. Structurally, FAK also contains a central tyrosine kinase domain, proline-rich regions and a focal adhesion-targeting (FAT) domain at the C-terminus. Receptor ligation to the FERM domain leads to

autophosphorylation of Y397 in the central tyrosine kinase domain. *c*-Src is recruited, unfolding to transphosphorylate Y925 in the FAT domain. Via the Grb-2/mSOS complex the Ras-Raf-MEK-ERK pathway is activated (Figure 3A).[9]
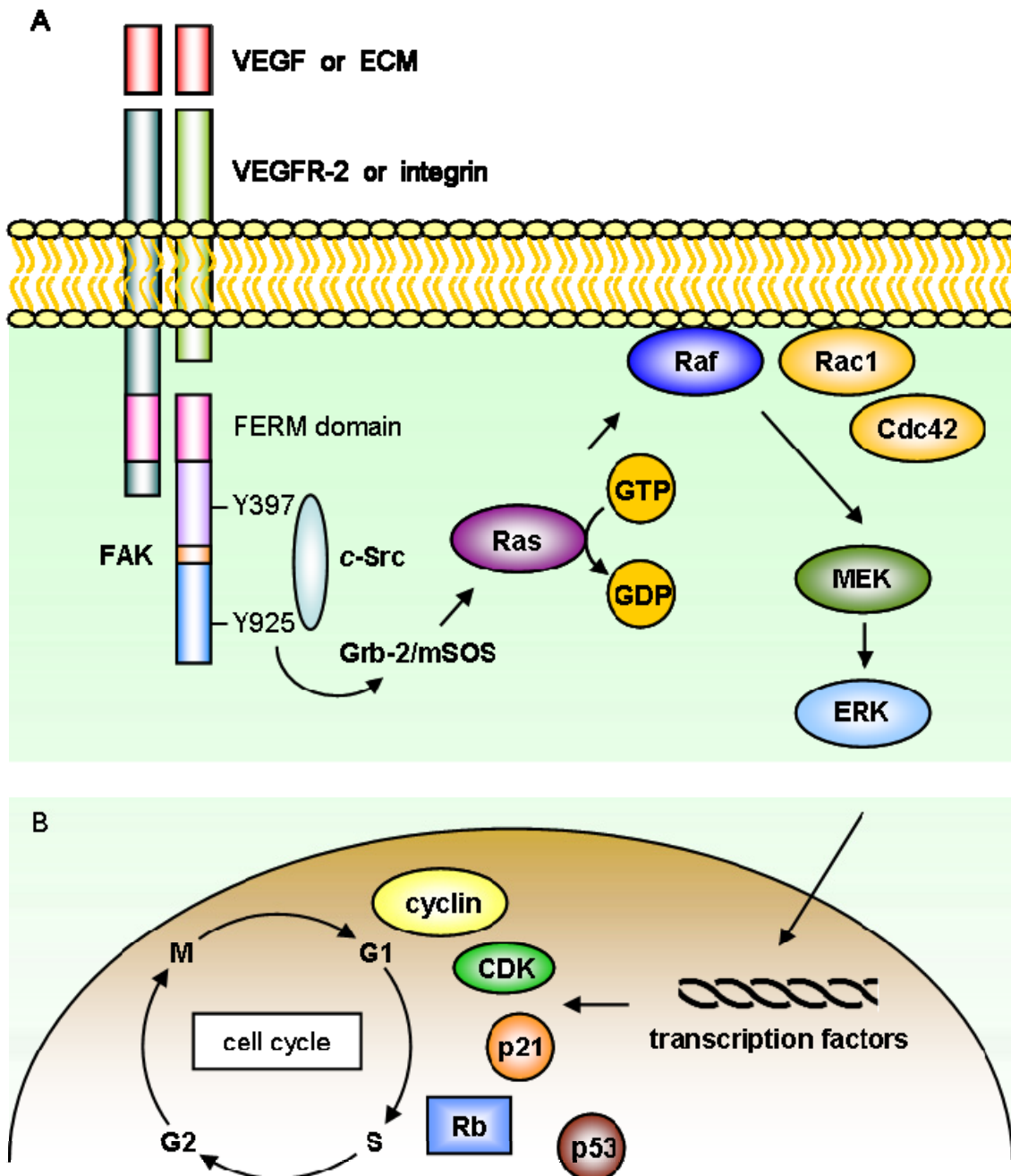


**Figure 3. Proliferation.** (**A**) Overview of the Ras-Raf-MEK-ERK pathway. FAK transduce signals from the membrane receptor to the Grb-2/mSOS complex which induce Ras activity by the exchange of GDP with GTP. Then, Raf is translocated to the cell membrane where it is activated by Rac1 or Cdc42, after which it activates its downstream effectors MEK and ERK. (**B**) ERK modulate transcription factors which are involved in the expression of cell cycle regulators such as cyclins, CDKs, CDK inhibitors and other regulatory proteins.

Ras is activated due to the exchange of GDP with GTP. Then, Raf is translocated to the cell membrane where it can be activated by Rac1 or Cdc42 of the Rho-GTPase family. The effect of Raf activation on cell cycle progression depends on the level and duration of Raf activation. In the short term, Raf stimulates cyclin-induced cell cycle progression, while prolonged Raf signalling leads to cell cycle arrest induced by the cyclin-dependent kinase (CDK) inhibitor p21.[29] Raf phosphorylates its substrate MAPK/ERK kinase (MEK) which activates extracellular signal-regulated kinase (ERK). Next, ERK modulate numerous transcription factors which are involved in cell cycle regulation.[30]

These transcription factors regulate the expression of cyclins (cyclin D1, D2 and E), CDKs (CDK2, 4 and 6), CDK inhibitors (p16, p21 and p27), and regulatory proteins like retinoblastoma (Rb) and p53. All these proteins activate or inactivate 'check points' which determine the progression of the cell cycle from one phase to the next. During these 'check points' the cell status is monitored to ensure that an earlier process is complete. In response to DNA damage, repair genes can be activated or the cell undergo programmed cell death or apoptosis. In some cases, proliferative ECs receive cell cycle arrest signals which induce lumen formation or morphogenic differentiation (Figure 3B).[9,30,31]

**Tip cell guidance**

The tip cell has to sense the environment for guidance cues. For this reason, filopodia are formed at the tip cell which is regulated by Cdc42. One of the attractive cues is VEGF, while slit proteins, netrin 1, semaphorins and ephrin works repulsive (Figure 2C).[16,27]

The response to VEGF differ from tip cells, stalk cells and phalanx cells because of their unique molecular characteristics. Tip cells exhibit a migratory response to VEGF and show an upregulation of Dll4. Stalk cells undergo proliferation and show upregulation of Notch, while VEGF signalling in phalanx cells leads to a survival response mediated by increased levels of VE-cadherin.[32]

Slit proteins bind to its Roundabout 4 (Robo4) receptor and is involved in vessel stabilisation.[16] Netrin 1 binds the UNC5B receptor and suppress vessel growth by stimulating filopodia retraction of ECs.[33] Most semaphorins suppress angiogenesis by binding NRP1 - co-receptor of VEGFR-2 - in a competitive way with VEGF.[34,35] Ephrin binds to the ephrin (EPH) receptor and regulates vessel morphogenesis, especially arterial and venous specification. Ephrin-B2 is mainly expressed in arterial ECs, whereas ephrin-B4 marks venous ECs.[16,36] Finally, all these guidance cues determine the direction of tip cell migration.

**Migration**

Migration to a gradient of soluble guidance cues is known as chemotaxis. Two other mechanisms also determine EC migration: haptotaxis, migration toward a gradient of immobilised ligands such as integrins or components of the ECM, and mechanotaxis,

migration generated by mechanical forces like shear stress. The process of migration can be divided into six following steps: sensing of guidance cues by filopodia, cellular extension by the formation of lamellipodia, attachment of the protrusions to the ECM via focal adhesion (FA) sites, contraction of stress fibres, rear release by FA disassembly and finally recycling of the adhesive and signalling components.[11,37]

When filopodia at the tip cell has determined the direction of migration, lamellipodia are formed for protrusion at the leading edge. Formation of lamellipodia is associated with microtubule elongation by actin polymerisation, promoted by Rac activity. Activation of Rac is induced by VEGFR-2 or integrins.[38] The next step in migration is FA assembly. FAs are sites where ECs are anchored to the ECM of the basement membrane via integrins. Intracellular, integrins are linked to the actin cytoskeleton by proteins such as FAK, vinculin, paxillin and talin. As mentioned before, FAK has an important role in signal transduction to induce EC proliferation. After that, FAK also regulates FA assembly and disassembly which allows adhesion and release of the EC important for migration.[39] FAK-knockout mice die *in utero* between E8.5 and 9.0 as a result of defective migration and abnormal angiogenesis.[9] Integrin signalling at FA sites can be activated by changes in the density of the ECM or by shear stress. Pressure forces generated by shear stress at the apical surface of the EC are transmitted to the integrins at the basal side of the endothelium via the actin cytoskeleton. Beside Rac activation for lamellipodia formation, integrins can also activate RhoA which is an important mediator in stress fibre formation and contraction, pulling the trailing edge to the direction of migration.[40] After that, adhesive and signalling components were recycled.[11] In general, integrins, FAK, and the Rho-GTPases Cdc42, Rac and RhoA have an important role in cell migration.

**Lumen formation**

When the newly formed vessel branch increases in length by EC proliferation and migration, a vascular lumen has to be formed. Lumen formation takes place by two different mechanisms: cell hollowing, in which a lumen is created by fusion of intracellular vacuoles and interconnections with vacuoles from neighbouring cells, or cord hollowing, in which a luminal cavity is created by changes in cell shape via contraction of the actin cytoskeleton and rearrangement of cellular junctions, followed by exposure to negatively charged glycoproteins at the luminal side of the ECs.[16,41]

**Vessel stabilisation**

When two newly formed vessel branches or sprouts come close together, filopodia of both tip cells interact and start to form a branch anastomosis by tip cell fusion.[7] This process is facilitated by macrophages.[42] Once the contact between tip cells is established, VE-cadherin primarily strengthened the connection by the formation of adherens junctions.[43]

VE-cadherin is a transmembrane protein of which the extracellular domain shows homotypic interactions forming zipper-like adhesions, while the cytoplasmic domain is linked by β-catenin and p120 - also known as CTNND1 - to the actin cytoskeleton for junction stabilisation. Loss of β-catenin results in defective cell adhesion and failure of cadherin-catenin complexes to associate with the actin cytoskeleton. Complex formation of CTNND1 with VE-cadherin maintains VE-cadherin at the plasma membrane, whereas VE-cadherin alone cycles on and off the plasma membrane by exocytosis and endocytosis.[44-46] Soluble CTNND1 regulates the activity of the Rho-GTPases, especially RhoA. As mentioned before, RhoA plays an important role in stress fibre formation during migration, but also in EC proliferation by Rb-induced G1–S-phase transition.[47] VE-cadherin mediates contact inhibition of cell growth by diminishing VEGFR-2-stimulated EC proliferation. Mice deficient for VE-cadherin show a normal differentiation of ECs, but vascular remodelling and integrity are defected, resulting in vascular malformations and death at midgestation.[48] It seems that VE-cadherin is more required during angiogenesis instead of vasculogenesis.

Further stabilisation of the newly formed vessel branch takes place by deposition of ECM proteins into the basement membrane and recruitment of mural cells (Figure 2D).[7,8] Four molecular pathways are involved in mural cell recruitment: platelet-derived growth factor (PDGF) - PDGF receptor (PDGFR)-β, sphingosine-1-phosphate receptor (S1PR) or endothelial differentiation sphingolipid G-protein-coupled receptor 1 (EDG1), angiopoietin 1 (Ang1) - Tie2 receptor, and the transforming growth factor (TGF)-β signalling pathway.

Tip cells release PDGF to attract mural cells expressing PDGFR-β. In response, these mural cells anchor to the newly formed basement membrane, which encloses the layer of stalk cells.[49,50] Lack of PDGFR-β in mice results in insufficient recruitment of mural cells, leading to an increase in EC growth, loss of vessel integrity and haemorrhage.[51] To consolidate the EC-pericyte contacts, stalk cells upregulate EDG1 expression at the apical surface of the EC, which induces N-cadherin trafficking to the basal side of the endothelium where they form connections between ECs and pericytes.[8,52] EDG1-knockout mice exhibit an alteration in ECM production and EC-pericyte interaction which results in diminished vessel maturation.[53] Also EC-EC contacts have to tighten up to make the newly formed vessel branch leak-resistant. This process is regulated by Ang1 - produced by mural cells - which upregulate the endothelial Tie2 receptor, leading to Tie2 clustering *in trans* at cell-cell junctions. After that, Ang1 also stimulates ECM protein deposition in the basement membrane, mural coverage, and release of PDGF and TGF-β by ECs.[7,8,25] Next, mural cells differentiate into vascular smooth muscle cells (vSMC) induced by TGF-β signalling. Downstream of TGF-β, the balance between Alk1 and Alk5, which is regulated by endoglin (Eng), determines the pro-angiogenic or anti-angiogenic effect of TGF-β. The Alk1 pathway induces break down of the basement membrane by upregulating MMP expression, while Alk5 prevents ECM degradation via plasminogen activator inhibitor (PAI)-1

expression in ECs which indirectly inhibits MMP activation.[8,54] Deficiency of Eng impairs mural cell development and results in arteriovenous malformations.[55]

## Vessel quiescence

Finally, the expression of pro-angiogenic factors is reduced as a consequence of oxygen delivery by blood vessel perfusion, inducing a quiescent phenotype of ECs. To maintain vessel quiescence, ECs have to produce survival factors in low levels such as VEGF or FGF.[12,56] Other survival factors are cerebral cavernous malformation (CCM) proteins 1-3. Loss of these proteins results in the development of abnormal vascular structures, characterised by thin-walled, dilated blood vessels with gaps between the ECs.[57] Blood vessel perfusion or shear stress also activates Krüppel-like factor 2 (Klf2) which upregulate eNOS expression and the anticoagulant factor Thrombomodulin, keeping blood vessels dilated, perfused and free of clots. Thereafter, Klf2 downregulates VEGFR-2 preventing tip cell formation. All these survival factors extend the endothelial half-life time to several years.[7,16]

## Vessel regression

Hypoperfused vessel branches show less Klf2 expression which results in vessel regression by programmed cell death or apoptosis, characterised by cell shrinkage, chromatin condensation and fragmentation of the cell into apoptotic bodies that are absorbed by macrophages.[16,31,58]

Beside hypoxia and loss of survival factors, apoptosis can also be initiated by detachment of ECs from their surrounding tissue, DNA damage or disruption of the cell cycle. Based on the way of initiation, two main pathways of apoptosis can be distinguished: the extrinsic or death-receptor pathway, and the intrinsic or mitochondrial pathway.[31,59]

The extrinsic pathway is activated by binding of tumour necrosis factor (TNF) at the death-receptor. The intracellular death domain of the death-receptor attracts the Fas-associated death domain (FADD) protein, forming a death-inducing signalling complex (DISC) which activates the 'initiator' cysteine aspartyl-specific protease (caspase) 8 and 10 by proteolytic cleavage (Figure 4A).[59,60] The intrinsic pathway can be activated via upregulation of p53 expression as a consequence of DNA damage, or loss of survival factors, resulting in less FAK-PI3K-Akt signalling.[9,30] Also crosstalk between the two pathways is possible via activated caspase 8. All of these signals are mediated by the pro-apoptotic Bcl2 family proteins - BAX, BAD and BID - leading to cytochrome *c* release from the intermembraneous space of mitochondria into the cytosol where an apoptosome is formed, composed of cytochrome *c*, apoptotic protease activating factor 1 (APAF1), ATP and the inactive 'initiator' caspase 9. At the apoptosome caspase 9 is activated by proteolytic cleavage (Figure 4B).[59,61] The 'initiator' caspases activate the 'executioner' caspases 3, 6 and 7 which will cleave each other to amplify the proteolytic cascade.
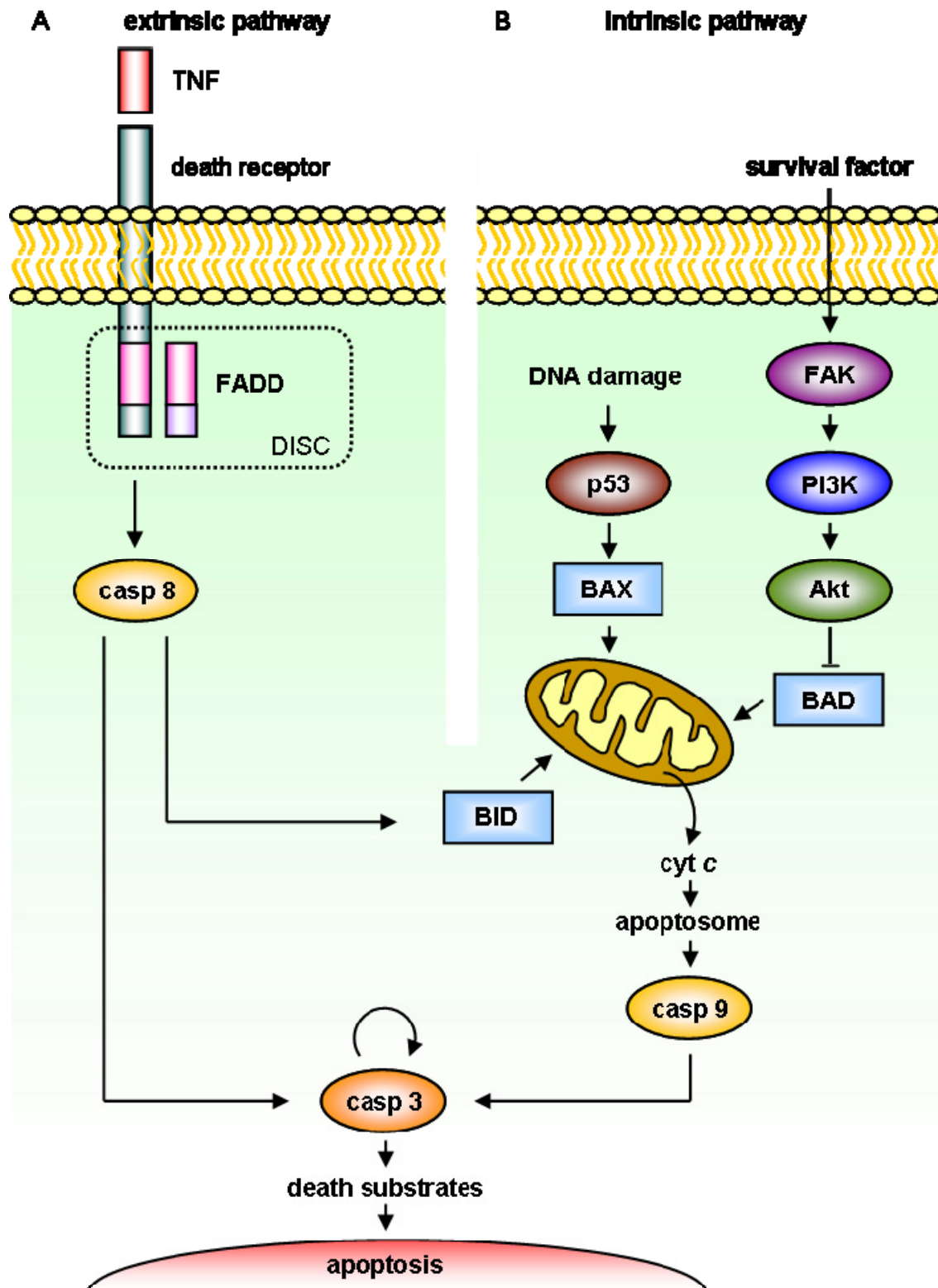
**Figure 4. Vessel regression.** Apoptosis can be induced through (**A**) death receptors at the cell surface (extrinsic pathway) or through (**B**) mitochondria (intrinsic pathway). Induction of apoptosis leads to activation of the 'initiator' caspases 8 and 9, followed by activation of the 'executioner' caspase 3, cleaving the death substrates which finally results in apoptosis.

Finally, cellular death substrates are cleaved, resulting in cellular self destruction. For example, cleavage of nuclear lamins results in chromatin condensation, whereas cleavage of cytoskeleton proteins - like actin - leads to cell fragmentation and the formation of apoptotic bodies.[59,62,63]


## *Vascular development and pathology*


Vessel formation leads to a vascular network that reaches nearly every part of the body. For this reason, deviations of normal vascular development or disruptions in the maintenance of the inner vascular lining contribute to the aetiology or worsening of many diseases. One of these is atherosclerosis.

**Atherosclerosis**

Atherosclerosis develops mainly at places with disturbed shear stress, like branch points. In combination with elevated levels of serum cholesterol and subsequent accumulation of oxidised low-density lipoprotein (LDL) in the intimal layer, endothelial dysfunction will develop, which is characterised by an imbalance of endothelium-derived vessel relaxing factors and contracting factors.[64,65] Endothelial dysfunction leads to plaque formation, characterised by chronic vascular inflammation and the accumulation of lipids, cholesterol, calcium, fibrous elements and cellular debris within the intimal layer of arteries. During plaque formation microvessels sprouted from the vasa vasorum - a network of small blood vessels in the adventitial layer that supply large blood vessels - into the medial layer of the vessel wall, making the plaque highly vulnerable for rupture and thrombus formation which can finally result in myocardial infarction or stroke.[66-69]

Inward vessel growth sprouted from the vasa vasorum is initiated by a highly hypoxic microenvironment in the core area of the plaque and pro-angiogenic factors such as PDGF.[70] This process of vessel branching is associated with increased MMP activity in the surrounding tissue like in normal angiogenesis. Also the intercellular connections between ECs become disrupted, diminishing endothelial barrier function. Normally, plasma proteins will extravasate and lay down a temporal ECM to which the ECs migrate, but in case of atherosclerotic plaque formation, next to this, inflammatory cells will enter the medial layer which promote further inflammation.[7,12,71] The highly inflammatory environment leads to failure of vessel stabilisation as seen by a lack of EC-pericyte contacts. Loss of these pericytes makes it possible for ECs to hyperproliferate resulting in tortuous vessel branches that are highly susceptible to intraplaque haemorrhage. Repeated intraplaque haemorrhages leads to atherosclerotic plaque instability, fissuring and rupture, followed by thrombus formation which can finally result in blood vessel occlusion and clinical manifestations.[71-73]

**ApoE-knockout mice**

To study atherosclerosis, transgenic mice were generated. Mice are normally very resistant to develop atherosclerosis, but genetic manipulations - apolipoprotein E (ApoE)-knockout - in combination with a high cholesterol diet results in massive hypercholesterolemia, leading to extensive atherosclerotic plaque formation that has many features in common with human lesions. This process is accelerated by placing a cylindrical device with a tapered lumen around the carotid artery, which leads to a high shear stress field. Deviations in shear stress upstream and downstream from the device deregulates EC function and maintenance of the inner vascular lining, which results in atherosclerotic plaque formation. In ApoE-knockout mice subendothelial microvessel formation has been observed in advanced atherosclerotic lesions.[74,75]

## *Indentifying new genes involved in angiogenesis*

In the previous sections a general overview has been given about vessel formation in normal and pathological conditions, in particularly atherosclerosis. Insight into the molecular players during the various stages of vascular development can provide clues to improve medical treatment of many diseases. For example, understanding the role of different (new) factors in the process of vessel stabilisation may possibly help to diminish intraplaque haemorrhage in atherosclerotic plaque formation. In order to identify new molecular players involved in angiogenesis, we carried out a genome-wide microarray screen for candidate regulatory genes.

**Study design**

The gene expression profiles of Flk1-positive angioblasts at various stages of vascular development during mouse embryogenesis were compared with the profiles of Flk1-negative cells. This resulted in a list of genes that were upregulated during vascular development. Next, for all one-to-one orthologues to zebrafish of the upregulated genes, RNA expression in the vascular network of zebrafish was determined by whole-mount *in situ* hybridisation. If gene expression was seen in the vasculature, the gene was silenced by morpholino (MO)-knockdown technology to assess gene function *in vivo*. Then, the mammalian relevance of the gene was studied in a mouse model of retinal vascularisation. To further validate the molecular influence on vessel formation, *in vitro* models such as a 2D matrigel network-formation assay were used. In these models, gene expression was influenced by targeted siRNA knockdown or adenovirus-induced overexpression. When the signalling pathway of the gene becomes clear, rescue experiments at different levels of the

signalling cascade were carried out. Finally, the functional implications of the gene were elucidated in knockout mice.

## Outline of this thesis

The first part of this thesis focuses on the process of EC proliferation and migration, which is important in the outgrowth of a newly formed vessel branch or stalk. In chapter 2, the role of 9430020K01Rik in EC proliferation is studied. Loss of 9430020K01Rik resulted in impaired vessel outgrowth as a consequence of less Rb phosphorylation, leading to an arrest in G1–S-phase transition. Cell cycle progression could also be influenced by the activity of cyclins and CDK inhibitors, which is regulated by Klf7, as shown in chapter 3. The role of Tagln2 in migration is described in chapter 4. Unravelling the function of Tagln2 by targeted siRNA knockdown showed an effect on tip cell formation and migration. The second part of this thesis describes the process of vessel stabilisation and quiescence. In chapter 5 we describe the role of Thsd1 in normal vessel formation, but also in the vulnerable plaque. Thsd1 is crucial for establishing endothelial barrier function by Rac1-dependent regulation of the actin cytoskeleton. Vessel quiescence, which is maintained by the CCM1-3 proteins, is reviewed in chapter 6. The third part of this thesis describes processes in vessel regression. Stimulation of apoptosis by Fgd5 is described in chapter 7, while the inhibiting role of Tnfaip8l1 is unfolded in chapter 8. Finally, the results obtained in these studies are discussed in chapter 9 of this thesis.

## References

1. Conway EM, Collen D, Carmeliet P. Molecular mechanisms of blood vessel growth. *Cardiovasc Res.* 2001;49(3):507-521.
2. Aird WC. Discovery of the cardiovascular system: from Galen to William Harvey. *J Thromb Haemost.* 2011;9(Suppl 1):118-129.
3. Skalak TC. Angiogenesis and microvascular remodelling: a brief history and future roadmap. *Microcirculation.* 2005;12(1):47-58.
4. Hunter J. In: Treatise on the Blood, Inflammation, and Gunshot Wounds. London; 1794.
5. Tomanek RJ, Schatteman GC. Angiogenesis: new insights and therapeutic potential. *Anat Rec.* 2000;261(3):126-135.
6. Meyer J. Ueber die Neubildung von Blutgefässen. In Plastischen Exudaten seröser Membranen und in Hautwunden. *Ann Charité (Berlin).* 1853;4:41-140.

7. Carmeliet P, Jain RK. Molecular mechanisms and clinical applications of angiogenesis. *Nature.* 2011;473(7347):298-307.

8. Jain RK. Molecular regulation of vessel maturation. *Nat Med.* 2003;9(6):685-693.

9. Wary KK, Kohler EE, Chatterjee I. Focal adhesion kinase regulation of neovascularisation. *Microvasc Res.* 2012;83(1):64-70.

10. Djonov V, Schmid M, Tschanz SA, Burri PH. Intussusceptive angiogenesis: its role in embryonic vascular network formation. *Circ Res.* 2000;86(3):286-292.

11. Lamalice L, Le Boeuf F, Huot J. Endothelial cell migration during angiogenesis. *Circ Res.* 2007;100(6):782-794.

12. Ferrara N, Gerber HP, LeCouter J. The biology of VEGF and its receptors. *Nat Med.* 2003;9(6):669-676.

13. Tischer E, Mitchell R, Hartman T, Silva M, Gospodarowicz D, Fiddes JC, Abraham JA. The human gene for vascular endothelial growth factor. Multiple protein forms are encoded through alternative exon splicing. *J Biol Chem.* 1991;266(18):11947-11954.

14. Carmeliet P, Ferreira V, Breier G, Pollefeyt S, Kieckens L, Gertsenstein M, Fahrig M, Vandenhoeck A, Harpal K, Eberhardt C, Declercq C, Pawling J, Moons L, Collen D, Risau W, Nagy A. Abnormal blood vessel development and lethality in embryos lacking a single VEGF allele. *Nature.* 1996;380(6573):435-439.

15. Shalaby F, Rossant J, Yamaguchi TP, Gertsenstein M, Wu XF, Breitman ML, Schuh AC. Failure of blood-island formation and vasculogenesis in Flk1-deficient mice. *Nature.* 1995;376(6535):62-66.

16. Potente M, Gerhardt H, Carmeliet P. Basic and therapeutic aspects of angiogenesis. *Cell.* 2011;146(6):873-887.

17. Majmundar AJ, Wong WJ, Simon MC. Hypoxia-inducible factors and the response to hypoxic stress. *Mol Cell.* 2010;40(2):294-309.

18. Pugh CW, Ratcliffe PJ. Regulation of angiogenesis by hypoxia: role of the HIF system. *Nat Med.* 2003;9(6):677-684.

19. Maxwell PH, Wiesener MS, Chang GW, Clifford SC, Vaux EC, Cockman ME, Wykoff CC, Pugh CW, Maher ER, Ratcliffe PJ. The tumour suppressor protein VHL targets hypoxia-inducible factors for oxygen-dependent proteolysis. *Nature.* 1999;399(6733):271-275.

20. Kotch LE, Iyer NV, Laughner E, Semenza GL. Defective vascularisation of HIF-1alpha-null embryos is not associated with VEGF deficiency but with mesenchymal cell death. *Dev Biol.* 1999;209(2):254-267.

21. Arroyo AG, Iruela-Arispe ML. Extracellular matrix, inflammation and the angiogenic response. *Cardiovasc Res.* 2010;86(2):226-235.

22. Nyberg P, Xie L, Kalluri R. Endogenous inhibitors of angiogenesis. *Cancer Res.* 2005;65(10):3967-3979.

23. Carmeliet P. Angiogenesis in health and disease. *Nat Med.* 2003;9(6):653-660.

24. Beenken A, Mohammadi M. The FGF family: biology, pathophysiology and therapy. *Nat Rev Drug Discov.* 2009;8(3):235-253.

25. Augustin HG, Koh GY, Thurston G, Alitalo K. Control of vascular morphogenesis and homeostasis through the angiopoietin-Tie system. *Nat Rev Mol Cell Biol.* 2009;10(3):165-177.

26. Jakobsson L, Franco CA, Bentley K, Collins RT, Ponsioen B, Aspalter IM, Rosewell I, Busse M, Thurston G, Medvinsky A, Schulte-Merker S, Gerhardt H. Endothelial cells dynamically compete for the tip cell position during angiogenic sprouting. *Nat Cell Biol.* 2010;12(10):943-953.

27. Phng LK, Gerhardt H. Angiogenesis: a team effort coordinated by Notch. *Dev Cell.* 2009;16(2):196-208.

28. Phng LK, Potente M, Leslie JD, Babbage J, Nygvist D, Lobov I, Ondr JK, Rao S, Lang RA, Thurston G, Gerhardt H. Nrarp coordinates endothelial Notch and Wnt signalling to control vessel density in angiogenesis. *Dev Cell.* 2009;16(1):70-82.

29. Woods D, Parry D, Cherwinski H, Bosch E, Lees E, McMahon M. Raf-induced proliferation or cell cycle arrest is determined by the level of Raf activity with arrest mediated by p21Cip1. *Mol Cell Biol.* 1997;17(9):5598-5611.

30. Chang F, Steelman LS, Shelton JG, Lee JT, Navolanic PM, Blalock WL, Franklin R, McCubrey JA. Regulation of cell cycle progression and apoptosis by the Ras/Raf/MEK/ERK pathway (Review). *Int J Oncol.* 2003;22(3):469-480.

31. Davis CD, Emenaker NJ, Milner JA. Cellular proliferation, apoptosis and angiogenesis: molecular targets for nutritional preemption of cancer. *Semin Oncol.* 2010;37(3):243-257.

32. Warren CM, Iruela-Arispe ML. Signalling circuitry in vascular morphogenesis. *Curr Opin Hematol.* 2010;17(3):213-218.

33. Adams RH, Eichmann A. Axon guidance molecules in vascular patterning. *Cold Spring Harb Perspect Biol.* 2010;2(5):a001875.

34. Serini G, Maione F, Giraudo E, Bussolino F. Semaphorins and tumour angiogenesis. *Angiogenesis.* 2009;12(2):187-193.

35. Neufeld G, Cohen T, Shraga N, Lange T, Kessler O, Herzog Y. The neuropilins: multifunctional semaphorin and VEGF receptors that modulate axon guidance and angiogenesis. *Trends Cardiovasc Med.* 2002;12(1):13-19.

36. Pitulescu ME, Adams RH. Eph/ephrin molecules - a hub for signalling and endocytosis. *Genes Dev.* 2010;24(22):2480-2492.

37. Li S, Huang NF, Hsu S. Mechanotransduction in endothelial cell migration. *J Cell Biochem.* 2005;96(6):1110-1126.

38. Small JV, Stradal T, Vignal E, Rottner K. The lamellipodium: where motility begins. *Trends Cell Biol.* 2002;12(3):112-120.

39. Romer LH, Birukov KG, Garcia JG. Focal adhesions: paradigm for a signalling nexus. *Circ Res.* 2006;98(5):606-616.

40. Katsumi A, Orr AW, Tzima E, Schwartz MA. Integrins in mechanotransduction. *J Biol Chem.* 2004;279(13):12001-12004.

41. Iruela-Arispe ML, Davis GE. Cellular and molecular mechanisms of vascular lumen formation. *Dev Cell.* 2009;16(2):222-231.

42. Fantin A, Vieira JM, Gestri G, Denti L, Schwarz Q, Prykhozhij S, Peri F, Wilson SW, Ruhrberg C. Tissue macrophages act as cellular chaperones for vascular anastomosis downstream of VEGF-mediated endothelial tip cell induction. *Blood.* 2010;116(5):829-840.

43. Dejana E, Tournier-Lasserve E, Weinstein BM. The control of vascular integrity by endothelial cell junctions: molecular basis and pathological implications. *Dev Cell.* 2009;16(2):209-221.

44. Quadri SK. Cross talk between focal adhesion kinase and cadherins: role in regulating endothelial barrier function. *Microvasc Res.* 2012;83(1):3-11.

45. Vestweber D. VE-cadherin: the major endothelial adhesion molecule controlling cellular junctions and blood vessel formation. *Arterioscler Thromb Vasc Biol.* 2008;28(2):223-232.

46. Xiao K, Garner J, Buckley KM, Vincent PA, Chiasson CM, Dejana E, Faundez V, Kowalczyk AP. p120-Catenin regulates clathrin-dependent endocytosis of VE-cadherin. *Mol Biol Cell.* 2005;16(11):5141-5151.

47. Noren NK, Niessen CM, Gumbiner BM, Burridge K. Cadherin engagement regulates Rho family GTPases. *J Biol Chem.* 2001;276(36):33305-33308.

48. Gory-Fauré S, Prandini MH, Pointu H, Roullot V, Pignot-Paintrand I, Vernet M, Huber P. Role of vascular endothelial-cadherin in vascular morphogenesis. *Development.* 1999;126(10):2093-2102.

49. Gaengel K, Genové G, Armulik A, Betsholtz C. Endothelial-mural cell signalling in vascular development and angiogenesis. *Arterioscler Thromb Vasc Biol.* 2009;29(5):630-638.

50. Cleaver O, Melton DA. Endothelial signalling during development. *Nat Med.* 2003;9(6):661-668.

51. Hellström M, Gerhardt H, Kalén M, Li X, Eriksson U, Wolburg H, Betsholtz C. Lack of pericytes leads to endothelial hyperplasia and abnormal vascular morphogenesis. *J Cell Biol.* 2001;153(3):543-553.

52. Lucke S, Levkau B. Endothelial functions of sphingosine-1-phosphate. *Cell Physiol Biochem.* 2010;26(1):87-96.

53. Kluk MJ, Hla T. Signalling of sphingosine-1-phosphate via the S1P/EDG-family of G-protein-coupled receptors. *Biochim Biophys Acta.* 2002;1582(1-3):72-80.

54. Goumans MJ, Valdimarsdottir G, Itoh S, Rosendahl A, Sideras P, ten Dijke P. Balancing the activation state of the endothelium via two distinct TGF-beta type I receptors. *EMBO J.* 2002;21(7):1743-1753.

55. Pardali E, Goumans MJ, ten Dijke P. Signalling by members of the TGF-beta family in vascular morphogenesis and disease. *Trends Cell Biol.* 2010;20(9):556-567.

56. Murakami M, Nguyen LT, Zhuang ZW, Moodie KL, Carmeliet P, Stan RV, Simons M. The FGF system has a key role in regulating vascular integrity. *J Clin Invest.* 2008;118(10):3355-3366.

57. Gore AV, Lampugnani MG, Dye L, Dejana E, Weinstein BM. Combinatorial interaction between CCM pathway genes precipitates haemorrhagic stroke. *Dis Model Mech.* 2008;1(4-5):275-281.

58. Rodriguez M, Schaper J. Apoptosis: measurement and technical issues. *J Mol Cell Cardiol.* 2005;38(1):15-20.

59. Igney FH, Krammer PH. Death and anti-death: tumour resistance to apoptosis. *Nat Rev Cancer.* 2002;2(4):277-288.

60. Schmitz I, Kirchhoff S, Krammer PH. Regulation of death receptor-mediated apoptosis pathways. *Int J Biochem Cell Biol.* 2000;32(11-12):1123-1136.

61. Zamzami N, Kroemer G. The mitochondrion in apoptosis: how Pandora's box opens. *Nat Rev Mol Cell Biol.* 2001;2(1):67-71.

62. Savill J, Fadok V. Corpse clearance defines the meaning of cell death. *Nature.* 2000;407(6805):784-788.

63. Rathmell JC, Thompson CB. The central effectors of cell death in the immune system. *Annu Rev Immunol.* 1999;17:781-828.

64. Stroka DM, Burkhardt T, Desbaillets I, Wenger RH, Neil DA, Bauer C, Gassmann M, Candinas D. HIF-1 is expressed in normoxic tissue and displays an organ-specific regulation under systemic hypoxia. *FASEB J.* 2001;15(13):2445-2453.

65. Wiesener MS, Turley H, Allen WE, Willam C, Eckardt KU, Talks KL, Wood SM, Gatter KC, Harris AL, Pugh CW, Ratcliffe PJ, Maxwell PH. Induction of endothelial PAS domain protein-1 by hypoxia: characterisation and comparison with hypoxia-inducible factor-1alpha. *Blood.* 1998;92(7):2260-2268.

66. Libby P, Ridker PM, Hansson GK. Progress and challenges in translating the biology of atherosclerosis. *Nature.* 2011;473(7347):317-325.

67. Weber C. Noels H. Atherosclerosis: current pathogenesis and therapeutic options. *Nat Med.* 2011;17(11):1410-1422.

68. Jackson SP. Arterial thrombosis - insidious, unpredictable and deadly. *Nat Med.* 2011;17(11):1423-1436.

69. Michel JB, Delbosc S, Ho-Tin-Noé B, Leseche G, Nicoletti A, Meilhac O, Martin-Ventura JL. From intraplaque haemorrhages to plaque vulnerability: biological consequences of intraplaque haemorrhages. *J Cardiovasc Med (Hagerstown).* 2012;13(10):628-634.

70. Boucher P, Gotthardt M. LRP and PDGF signalling: a pathway to atherosclerosis. *Trends Cardiovasc Med.* 2004;14(2):55-60.

71. Cheng C, Chrifi I, Pasterkamp G, Duckers HJ. Biological mechanisms of microvessel formation in advanced atherosclerosis: the big five. *Trends Cardiovasc Med.* 2013;23(5):153-164.

72. Le Dall J, Ho-Tin-Noé B, Louedec L, Meilhac O, Roncal C, Carmeliet P, Germain S, Michel JB, Houard X. Immaturity of microvessels in haemorrhagic plaques is associated with proteolytic degradation of angiogenic factors. *Cardiovasc Res.* 2010;85(1):184-193.

73. Lusis AJ. Atherosclerosis. *Nature.* 2000;407(6801):233-241.

74. Cheng C, van Haperen R, de Waard M, van Damme LC, Tempel D, Hanemaaijer L, van Cappellen GW, Bos J, Slager CJ, Duncker DJ, van der Steen AF, de Crom R, Krams R. Shear stress affects the intracellular distribution of eNOS: direct demonstration by a novel *in vivo* technique. *Blood.* 2005;106(12):3691-3698.

75. Glass CK, Witztum JL. Atherosclerosis: the road ahead. *Cell.* 2001;104(4):503-516.

# Chapter 2

## 9430020K01Rik (KIAA1462): a new regulator of endothelial cell proliferation in angiogenesis

R.A. Haasdijk, D.M.A. Hermkens, D. Tempel
J.A.A. Demmers, E.H.M. van de Kamp, L.A.J. Blonden
S. Schulte-Merker, C. Cheng, H.J. Duckers

## *Abstract*

**Objective** - Aberrant proliferation of endothelial cells and vascular smooth muscle cells is involved in the progression of cardiovascular diseases such as coronary artery disease (CAD). Previously, it has been shown that a missense variant in the KIAA1462 gene increases the risk of CAD. Using a genome-wide microarray screen for new angiogenic factors during embryogenesis, we identified 9430020K01Rik (KIAA1462) as a potential regulator of vascular growth. However, the biological function of KIAA1462 remains unknown. Here, we sought to characterise the role of KIAA1462 during blood vessel formation.

**Methods and Results** - Functional knockdown of KIAA1462 in zebrafish embryos resulted in epiboly, whereas 9430020K01Rik-knockout mice exhibited suppressed blood vessel formation in the retina and heart tissue. Flow cytometric analysis of cultured endothelial cells suggested that blockage of G1–S-phase transition in KIAA1462-depleted cells might be the cause of impaired vessel development. To clarify the molecular mechanism by which KIAA1462 regulates cell proliferation, liquid chromatography-mass spectrometry was carried out and reveals CTNND1 as an active binding partner of KIAA1462. Knockdown of KIAA1462 impaired downstream signalling of CTNND1 via RhoA, leading to inhibition of ROCK2 and Rb and reduced G1–S-phase transition.

**Conclusion** - KIAA1462 is essential in endothelial cell proliferation during vascular development by direct CTNND1 complex interaction and RhoA-dependent regulation of the G1–S-phase transition.

## *Introduction*

Cardiovascular diseases - including coronary artery disease (CAD) - is a major and highly frequent complication in the aging Western population and has a large impact on morbidity and mortality. CAD is the primary cause of myocardial infarction and is mostly the result from complications of atherosclerotic plaque formation.[1] Atherosclerosis is a disease of the vascular wall in which a slow progression of lipid deposition and inflammation lead to narrowing of the vessel lumen and finally obstruction of coronary flow.[2-5] Leukocyte extravasation - characteristic for inflammation - and vascular homeostasis are regulated by the endothelium, a monolayer of endothelial cells (EC) lining the vessel wall. These ECs are connected by adherens, tight and gap junctions. Previous studies have shown that endothelial junctional proteins - like VE-cadherin - play an essential role in the regulation of vascular permeability, cell proliferation and angiogenesis.[6,7] Pathological misbalance causes endothelial dysfunction which is a prominent feature in the development, progression and clinical manifestation of atherosclerosis and CAD.[8] Considering the clear association between endothelial function and cardiovascular disease, the molecular mechanisms that are involved in maintaining vascular homeostasis and prevention of CAD are crucial for the development of new diagnostics and therapeutics. However, the genetic regulation underlying endothelial dysfunction and subsequent CAD remains unknown.

Recently, genome-wide association studies have detected a missense variant (p.S1002T) in the KIAA1462 gene - on chromosome 10p11.23 - which increases the risk of CAD by 15%.[9,10] Although this finding marks KIAA1462 as a genetic risk factor for CAD, the exact role in the pathophysiology remains to be elucidated.

In search of new angiogenic factors - using a genome-wide microarray screen -, we identified KIAA1462 as a candidate gene which is possibly involved in angiogenesis and endothelial regulation. The KIAA1462 gene encodes a 148 kDa protein without any known domains, but contains a proline-rich region. Thereafter, KIAA1462 shows some structural similarity with Rho-associated coiled-coil containing protein kinase (ROCK), suggesting a potential role in Rho signalling.[11-13] Immunolocalisation studies revealed that KIAA1462 is a component of VE-cadherin-based cell-cell junctions in ECs.[14] However, the protein function of KIAA1462 in angiogenesis and the pathophysiology of CAD remains to be clarified.

In this study, we sought to characterise the role of KIAA1462 during blood vessel formation and pathogenesis of CAD *in vitro* using primary cell cultures and *in vivo* using a zebrafish and a murine retinal vascular development model. Functional knockdown of KIAA1462 in zebrafish resulted in epiboly, whereas 9430020K01Rik-knockout mice - the mouse orthologue of KIAA1462 - exhibited suppressed blood vessel formation in the retina and heart tissue. KIAA1462 depletion in cultured ECs showed blockage of G1–S-phase

transition, regulated by RhoA activity via catenin (cadherin-associated protein), delta 1 (CTNND1). Our results reveal the importance of KIAA1462-mediated modulation of RhoA and EC proliferation in angiogenesis.

## *Methods*

This study was carried out in accordance with the Council of Europe Convention (ETS123)/Directive (86/609/EEC) for the protection of vertebrate animals used for experimental and other scientific purposes and with the approval of the National and Local Animal Care Committee.

**Zebrafish**
Zebrafish (*Danio rerio*) were maintained under standard laboratory conditions.

**Morpholino injection**
Morpholinos (MO) against Loc100001168 (KIAA1462) were obtained from Gene Tools (Philomath, USA) and resuspended in Milli-Q water containing 0.2% phenol red. Different doses of the MO were injected into single-cell stage zebrafish embryos as previously described.[15] The following zebrafish MO was used: 5'-ATT GGT TCT GCG CTC TGA GAA AAG C-3' (MO Loc100001168-ATG).

**Mice**
Plugged FVB/N mice (*Mus musculus*) were ordered at Harlan (Indianapolis, USA). C57BL/6J mice were obtained from laboratory stock. They were maintained under standard husbandry conditions.

**Isolation of Flk1-positive and Flk1-negative cells from mouse embryos**
From eight to sixteen days post-fertilisation (dpf), embryos were collected from plugged FVB/N mice and homogenised. Cells were stained with PE-conjugated anti-mouse Flk1 antibody 1:50 (555308; BD, Breda, The Netherlands). Hoechst (Sigma-Aldrich, Zwijndrecht, The Netherlands) was used to select dead cells. Flk1-positive/Hoechst-negative cells and Flk1-negative/Hoechst-negative cells were sorted on a BD FACSCanto™ (Breda, The Netherlands). Isolation of mRNA was carried out using the RNeasy Mini Kit from Qiagen (Venlo, The Netherlands).

## Microarray analysis

Double stranded cDNA was generated from 5 μg mRNA. Biotin-labelled RNA was synthesised using the BioArray™ HighYield™ RNA Transcript Labeling Kit from ENZO Life Sciences (Raamsdonksveer, The Netherlands). After clean-up and fragmentation, approximately 20 μg of labelled cRNA was hybridised to the GeneChip® Mouse Genome 430 2.0 Array (Affymetrix, Santa Clara, USA). Rosetta Resolver® (Rosetta Biosoftware, Cambridge, USA) was used to get quantile normalised raw data from the arrays. These data were merged into OmniViz® (BioWisdom, Cambridge, UK) and a threshold minimum for intensities was set at 30. Fold differences were calculated from log averages determined by the different experimental conditions.

## Mouse model of retinal vascularisation

Two-day old C57BL/6J mice pups were anesthetised by placement on ice. One microlitre of 9430020K01Rik targeting siRNA (si-9430020K01Rik) (1.33 μg/μl) was injected into the left eye using a 33-Gauge needle (World Precision Instruments, Berlin, Germany). As a control, one microlitre of scrambled non-targeting siRNA (si-sham) (1.33 μg/μl) was injected into the right eye. siRNA was obtained from Thermo Fisher Scientific (Breda, The Netherlands). The following mix of mouse si-9430020K01Rik was used: 5'-AGG AAA GGG CAG AGA GGA UUU-3' – 5'-GGA AAA GGC CCC AGG AAA AUU-3' – 5'-AGA GCC AGC CAU UGG GAA AUU-3'. Mice pups were killed five days after intra-ocular injection. The retinas were stained with Alexa Fluor® 488-conjugated isolectin GS-IB$_4$ 1:200 (I21411; Invitrogen, Bleiswijk, The Netherlands) before assessment under a fluorescence microscope (Axiovert S100; Carl Zeiss, Sliedrecht, The Netherlands). Image analysis of the number of junctions, tubules and total tubule length was carried out using Angiosys Image Analysis Software 1.0 (TCS CellWorks, Buckingham, UK). Validation of adequate 9430020K01Rik knockdown in the retina (two days after intra-ocular injection) was achieved by quantitative real time PCR using the following mouse primers: 5'-CAG CAC CAT GTG AGG ACA AA-3' (forward) and 5'-ATG CGG TTT TCA GAG TTG CT-3' (reverse) (Biolegio, Nijmegen, The Netherlands).

## Generation of 9430020K01Rik-knockout mice

9430020K01Rik-knockout mice were generated starting with JM8A3 mouse embryonic stem cells (ES cell) from Knockout Mouse Project (KOMP, *www.komp.org*) Repository, project ID: CDS46781 in which out-of-frame exon 3 is replaced with a LacZ reporter gene and Neomycin selection marker by homologous recombination. After that, the Neomycin selection marker was removed by treatment of ES cells with cre recombinase. Neo-negative cells were used to generate a C57BL/6.9430020K01Rik*tm1(KOMP)Mbp/MCL*-knockout mouse line. Founder mice and offspring were genotyped on DNA-isolated toe biopsies by PCR using the following mouse primers: 5'-CCA CCA TAG GGA CCA ATG TTT CAA AGG

TGG-3' (forward wt and KO), and 5'-GTT CTT TCC AGT CCC TGG GAC ACA GGG AGC-3' (reverse wt) and 5'-CCT TGG GCA AGA ACA TAA AGT GAC CCT CCC-3' (reverse KO) (Biolegio, Nijmegen, The Netherlands). Transgenic mice used in the present study were homozygous.

**Isolectin staining**

Formalin-fixed, paraffin-embedded sections of heart tissue of 9430020K01Rik-knockout mice were mounted on super-frost glass slides. Deparaffinised slides were treated with 3% hydrogen peroxide in methanol (20 min) to block the endogenous peroxidase activity, followed by rinsing with phosphate-buffered saline (PBS). After that, slides were pre-incubated for 15 minutes with 5% bovine serum albumin (BSA)/PBS to block non-specific binding and then incubated overnight at 4°C with peroxidase-conjugated isolectin GS-IB$_4$ 1:20 (L5391; Sigma-Aldrich, Zwijndrecht, The Netherlands). After rinsing PBS, slides were visualised with 3,3'-diaminobenzidine (Dako DAB solution K3468; Dako, Heverlee, Belgium) (30 sec) as the chromogen. Slides were counter-stained with haematoxylin for 10 seconds. Negative controls were prepared using omission of peroxidase-conjugated isolectin GS-IB$_4$.

**Cell cultures**

Primary cultures of human umbilical vein endothelial cells (HUVEC) were cultured in EBM®-2 medium supplemented with a commercial BulletKit, 10% foetal calf serum (FCS) and 1% penicillin/streptomycin (Lonza, Breda, The Netherlands). Primary aorta-derived human vascular smooth muscle cells (vSMC) were cultured in SmGM®-2 medium supplemented with a commercial BulletKit, 10% FCS and 1% penicillin/streptomycin (Lonza, Breda, The Netherlands). HeLa and sarcoma cells were cultured in Dulbecco's modified Eagle's medium (DMEM) supplemented with 10% FCS (Cambrex, Wiesbaden, Germany). Cells were cultured at 37°C in 5% $CO_2$. Passages three to six were used throughout the study.

**Immunofluorescence**

HUVECs - transfected with si-sham or KIAA1462 targeting siRNA (si-KIAA1462) - were grown in gelatin-coated 48-wells. After 24 hours, the cells were fixed in 4% formaldehyde and permeabilised with 0.2% Triton® X-100. Cells were incubated overnight at 4°C with antibodies against KIAA1462 1:50 (custom made; Eurogentec, Maastricht, The Netherlands), CTNND1 1:10 (HPA015955; Sigma-Aldrich, Zwijndrecht, The Netherlands) or VE-cadherin 1:50 (sc-6458; Santa Cruz Biotechnology, Heidelberg, Germany). For the detection of the primary antibodies Alexa Fluor® 488 or 546 1:100 (Invitrogen, Bleiswijk, The Netherlands) was used. The nucleus was stained with 4,6-diamidino-2-phenylindole (DAPI) in Vectashield® mounting medium (H-1200; Vector Laboratories, Burlingame,

USA). Cells were visualised with a fluorescence microscope (Axiovert S100; Carl Zeiss, Sliedrecht, The Netherlands).

**Targeted siRNA knockdown**

HUVEC were grown to 60-70% confluence and DharmaFECT1 Transfection Reagent was used to transfect 5 ng siRNA (Thermo Fisher Scientific, Breda, The Netherlands). The following mix of human si-KIAA1462 was used: 5'-CGG GAA GAG GUG AGA GUA AUU-3' – 5'-CAG CAU CAC GCG AGG AUA AUU-3' – 5'-GGA UGA GAG UCC UGA GCU UUU-3'. Si-sham was used as a control. Knockdown of KIAA1462 was validated by quantitative real time PCR analysis and Western blot two days post-transfection using the following human primers: 5'-AGA GCT GGA GTG AGG AGC TG-3' (forward) and 5'-TCC ATT CCG TTG CTA ACC TC-3' (reverse) (Biolegio, Nijmegen, The Netherlands), and anti-human KIAA1462 antibody 1:100 (custom made; Eurogentec, Maastricht, The Netherlands). Beta-actin primers 5'-TCC CTG GAG AAG AGC TAC GA-3' (forward) and 5'-AGC ACT GTG TTG GCG TAC AG-3' (reverse) (Biolegio, Nijmegen, The Netherlands) were used as housekeeping gene, while beta-actin antibody 1:500 (ab8229; Abcam, Cambridge, UK) was used as a loading control.

**2D matrigel network-formation assay**

To induce network-formation, HUVECs - transfected with si-sham or si-KIAA1462 - were cultured on a 2D Matrigel$^{TM}$ matrix (BD, Breda, The Netherlands). The tubules were stained by Calcein-AM (BD, Breda, The Netherlands) after 24 hours of network-formation. Each condition was assessed by fluorescence microscopy (Axiovert S100; Carl Zeiss, Sliedrecht, The Netherlands). Image analysis of the number of junctions, tubules and total tubule length was carried out using Angiosys Image Analysis Software 1.0 (TCS CellWorks, Buckingham, UK).

**Cell proliferation assay**

EC proliferation *in vitro* was evaluated by culturing HUVECs - transfected with si-sham or si-KIAA1462 - in gelatin-coated 6-wells and counting them at different time points.

In brief, 50,000 cells were seeded and incubated in EBM$^{®}$-2 medium supplemented with 0.2% FCS for 4 hours to synchronise the cell cycle. Thereafter, HUVECs were trypsinised after 0, 8, 24 and 48 hours, and counted with a Bürker-Türk. At all time points the amount of cells was expressed as percentage, whereas time point zero the amount of cells was expressed as 100%.

**Cell cycle assay**

For cell cycle experiments, HUVECs - transfected with si-sham or si-KIAA1462 - were trypsinised and fixed in 70% ice-cold ethanol overnight at 4°C. After being washed in PBS,

the cells were resuspended in 300 μl PBS containing 69 μM propidium iodide (PI), 37 mM sodium citrate and 200 μg RNase. Cell cycle profile was measured on a BD FACSCanto[TM] (Breda, The Netherlands).

To analyse bromodeoxyuridine (BrdU) incorporation during replication, cells were incubated for 24 hours with 1 μM BrdU at 37°C in 5% $CO_2$. After fixation in 70% ice-cold ethanol overnight at 4°C, cells were washed in PBS and resuspended in pepsin solution for 20 minutes. Thereafter, the cells were washed in PBS with 0.1% BSA and 0.5% Tween 20, resuspended in 2 M HCl for 12 minutes at 37°C, and then neutralised in 0.1 M $Na_2B_4O_7$ (pH 8.5). After being washed in PBS with 0.1% BSA and 0.5% Tween 20, cells were incubated with FITC-conjugated anti-human BrdU antibody 1:50 (ab74545; Abcam, Cambridge, UK) for 1 hour on ice. Next, the cells were washed in PBS with 0.1% BSA and 0.5% Tween 20, and resuspended in PBS with 0.1% BSA containing PI and RNase. BrdU incorporation was measured on a BD FACSCanto[TM] (Breda, The Netherlands).

**LC-MS**

Binding partners of KIAA1462 were identified by liquid chromatography-mass spectrometry (LC-MS) as previously described.[16]

**Co-immunoprecipitation**

To immunoprecipitate protein complexes, magnetic beads (Dynabeads®; Invitrogen, Bleiswijk, The Netherlands) were conjugated with 10 μg anti-human KIAA1462 antibody (custom made; Eurogentec, Maastricht, The Netherlands). The coated magnetic beads were then added to protein cell lysates of HUVECs (20 μg total protein in 100 μl incubation buffer supplied by the Dynabeads® system) and incubated overnight at 4°C. The beads were washed three times in washing buffer (Invitrogen, Bleiswijk, The Netherlands) before the immunoprecipitated protein complexes were eluted from the magnetic beads with elution buffer (Invitrogen, Bleiswijk, The Netherlands). Protein complexes were analysed using a 12.5% SDS-PAGE gel, followed by immunoblotting using anti-human antibodies against KIAA1462 1:100 (custom made; Eurogentec, Maastricht, The Netherlands) and CTNND1 1:500 (HPA015955; Sigma-Aldrich, Zwijndrecht, The Netherlands).

**qPCR**

To determine whether knockdown of KIAA1462 interfered with cellular processes, qPCR analysis was carried out using HUVEC cDNA in combination with the following human primers: 5'-AGA GCT GGA GTG AGG AGC TG-3' (forward) and 5'-TCC ATT CCG TTG CTA ACC TC-3' (reverse) for KIAA1462, and 5'-TGG GAA TCT TTT CCT GTC TG-3' (forward) and 5'-GAA CAC TGA GAC AGT ATG CC-3' (reverse) for SKP2 (Biolegio, Nijmegen, The Netherlands). Beta-actin primers 5'-TCC CTG GAG AAG AGC

TAC GA-3' (forward) and 5'-AGC ACT GTG TTG GCG TAC AG-3' (reverse) (Biolegio, Nijmegen, The Netherlands) were used as housekeeping gene.

**Western blot**

To determine whether knockdown of KIAA1462 interfered with cellular processes, Western blot analysis was carried out using HUVEC protein lysates. At 72 hours post-transfection, HUVECs were serum starved for 4 hours and replenished with EBM®-2 medium supplemented with a commercial BulletKit for 40 minutes. Cells were lysed in NP40 Cell Lysis Buffer (Invitrogen, Bleiswijk, The Netherlands) and analysed on a 12.5% SDS-PAGE gel, followed by immunoblotting using anti-human antibodies against KIAA1462 1:100 (custom made; Eurogentec, Maastricht, The Netherlands), RhoA 1:100 (ab54835; Abcam, Cambridge, UK), ROCK2 1:100 and phosphorylated-ROCK2 (T249) 1:500 (ab56661 and ab83514; Abcam, Cambridge, UK), and retinoblastoma (Rb) 1:500 and phosphorylated-Rb (T821) 1:500 (ab39690 and ab122893; Abcam, Cambridge, UK). Beta-actin antibody 1:500 (ab8229; Abcam, Cambridge, UK) was used as a loading control. Protein bands were visualised by the Odyssey® Infrared Imaging System and analysed by Odyssey 3.0 software (LI-COR Biotechnology, Cambridge, UK).

**RhoA activation assay**

RhoA activity was measured using the G-LISA® RhoA Activation Assay Biochem Kit™ from Cytoskeleton (Denver, USA) according to the instruction manual.

**Statistical analysis**

Data were reported as mean ± standard error of the mean (SEM). Statistical significance was evaluated using a Student's $t$-test and was accepted at $P < 0.05$ (* $P < 0.05$, ** $P < 0.01$ in the figures).

## *Results*

**Expression of 9430020K01Rik is upregulated during mouse embryogenesis**

To identify new genes involved in angiogenesis, a genome-wide microarray analysis was carried out followed by validation of the results by qPCR. Gene expression profiles of Flk1-positive angioblasts at various stages of murine embryonic development were compared with the profiles of Flk1-negative cells. 9430020K01Rik was upregulated in Flk1-positive angioblasts from 8 to 16 dpf. Expression levels were highest upregulated around 8 to 10 dpf, which coincides with the period of early angiogenesis in murine development and suggests a potential role of 9430020K01Rik in blood vessel formation (Figure 1).
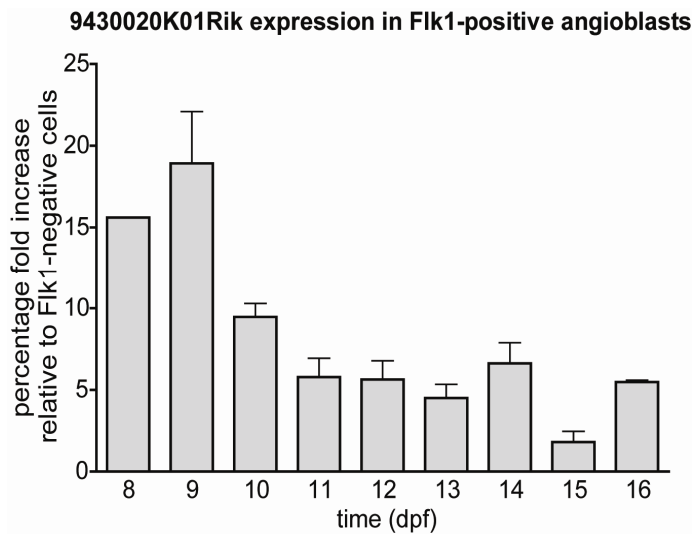
**9430020K01Rik expression in Flk1-positive angioblasts**



**Figure 1. 9430020K01Rik is upregulated in Flk1-positive angioblasts during mouse development.** Endogenous expression level of 9430020K01Rik in Flk1-positive angioblasts during murine embryonic development from 8 to 16 days post-fertilisation (dpf) compared with Flk1-negative cells as analysed by qPCR. The expression level of 9430020K01Rik in Flk1-negative cells was arbitrarily set to one (n = 4; mean ± SEM). The highest upregulation was detected around day 8 to 10, which coincides with the period of angiogenesis in murine development.

## 9430020K01Rik knockdown in the developing retinal vasculature of neonatal mice suppresses blood vessel formation

To assess the function of 9430020K01Rik *in vivo*, the gene was silenced during the development of the retinal vasculature of neonatal mice. To determine the optimal moment of 9430020K01Rik knockdown, 9430020K01Rik mRNA expression in the murine retina was evaluated during postnatal development by qPCR analysis. 9430020K01Rik mRNA levels were adjusted to CD31 mRNA levels to compensate for changes in percentage of ECs. High expression levels of 9430020K01Rik were mainly observed around 3 days post-partum, which corresponds with the period of plexus formation (Figure 2A). Based on these findings, 9430020K01Rik knockdown was induced in the first week of retinal vascular development by intra-ocular injection of a siRNA pool composed of three different 9430020K01Rik targeting siRNA sequences in two-day old wild-type C57BL/6J mouse pups and compared with controls injected with a scrambled non-targeting siRNA pool. Efficient knockdown of 9430020K01Rik was observed two days after intra-ocular injection (Figure 3). Loss of 9430020K01Rik expression affected the outgrowth of the vasculature toward the retinal borders (Figure 2B).
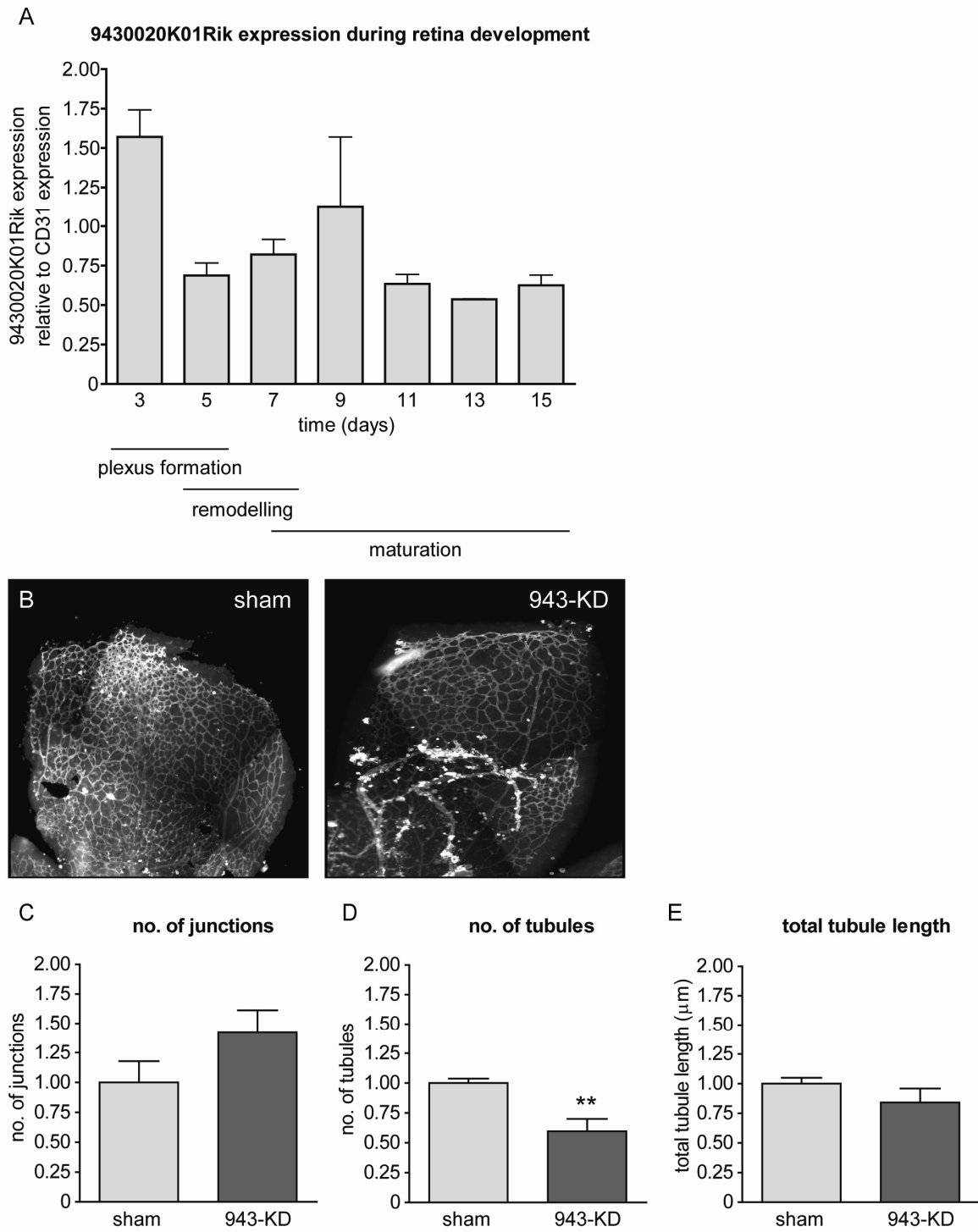
**Figure 2. 9430020K01Rik depletion during murine retinal vascular development results in diminished vascular growth.** (**A**) Endogenous expression level of 9430020K01Rik in the developing retinal vasculature of neonatal mice from 3 to 15 days after birth compared with CD31 expression in the retina (n = 3; mean ± SEM). 9430020K01Rik is highly expressed around day 3, which coincides with the period of plexus formation. (**B**) Retinas stained with isolectin GS-IB$_4$. (**C-E**) Quantification by means of the dimensions of the vascular network showed a reduction in the total number of vessels after 9430020K01Rik knockdown (943-KD): (**C**) number of junctions, (**D**) number of tubules and (**E**) total tubule length (n = 10; mean ± SEM).

Assessment and quantification of the number of vascular branches, the total number of vessels and the total tubule length after visualisation of the vasculature by isolectin GS-IB$_4$ staining, showed a reduction in the total number of vessels between si-9430020K01Rik and si-sham injected eyes five days after intra-ocular injection, while there was no difference observed in the number of vascular branches and the total tubule length (Figure 2C-E). These data indicate that 9430020K01Rik has an essential role in vessel outgrowth during vascular development.
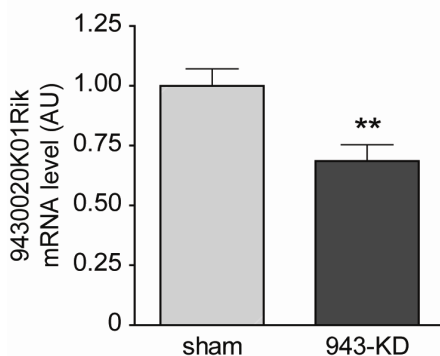


**Figure 3. 9430020K01Rik depletion in the developing retinal vasculature of neonatal mice after siRNA targeting.** Endogenous expression level of 9430020K01Rik in the retina after intra-ocular injection of 9430020K01Rik targeting siRNA (943-KD) showed a reduction in expression levels of 9430020K01Rik as analysed by qPCR (n = 10; mean ± SEM).

## KIAA1462 is highly expressed in cultured endothelial cells and vascular smooth muscle cells

To clarify the molecular mechanism underlying the impaired vessel outgrowth, we first validated the endothelial expression of 9430020K01Rik in cultured cells. The expression level of the 9430020K01Rik human orthologue - also known as KIAA1462 - was determined in a number of different cell types. In a comparison between HUVECs, vSMCs, HeLa and sarcoma cells, the highest mRNA expression level of KIAA1462 was observed in HUVECs and vSMCs (Figure 4). Intracellular immunofluorescent detection of KIAA1462 in HUVECs demonstrated that the protein was mainly located at the plasma membrane (Figure 5A).
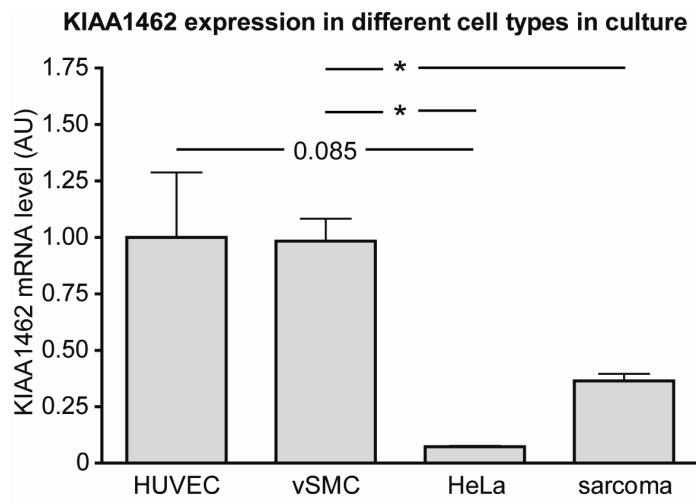
**Figure 4. KIAA1462 expression in different cell types in culture.** KIAA1462 was highly expressed in HUVEC and vSMC compared with HeLa and sarcoma cells, as demonstrated by qPCR analysis (n = 3; mean ± SEM).
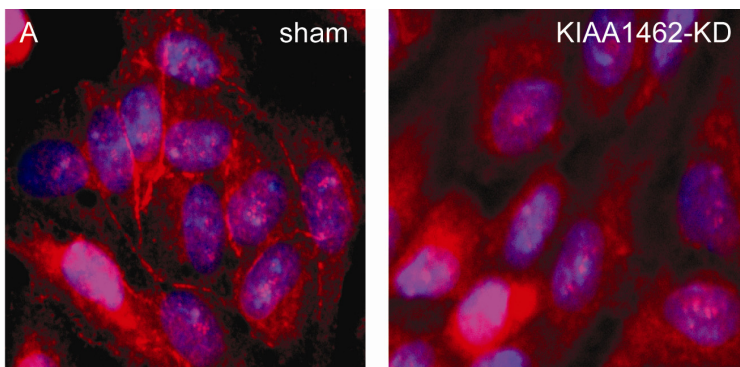


**Figure 5. KIAA1462 knockdown in cultured endothelial cells inhibits vascular network-formation.** (A) KIAA1462 was mainly located at cell-cell contacts, as demonstrated by immunofluorescent staining. KIAA1462 (red) and nuclei (blue) (n = 3).

**Knockdown of KIAA1462 inhibits vascular network-formation *in vitro***

To further assess the function of KIAA1462 in cultured ECs, knockdown of KIAA1462 in HUVECs was induced by transfection of si-KIAA1462 and compared with si-sham transfected and untransfected controls. In si-KIAA1462 transfected cells, endogenous KIAA1462 expression was significantly lower than in the control cultures on both mRNA (Figure 6A) and protein level (Figure 6B).

To investigate the effect of KIAA1462 knockdown on vascular network-formation, *in vitro* network-formation experiments with HUVECs were carried out. Knockdown of KIAA1462 had an inhibitory effect on the number of junctions, capillary tubules and the total tubule length when compared with cultures transfected with equimolar of si-sham or untransfected controls (Figure 5B-E). These data corresponds with the *in vivo* findings in which vessel outgrowth was also impaired. The process of vessel growth is determined by many different factors. One of these is cell proliferation.
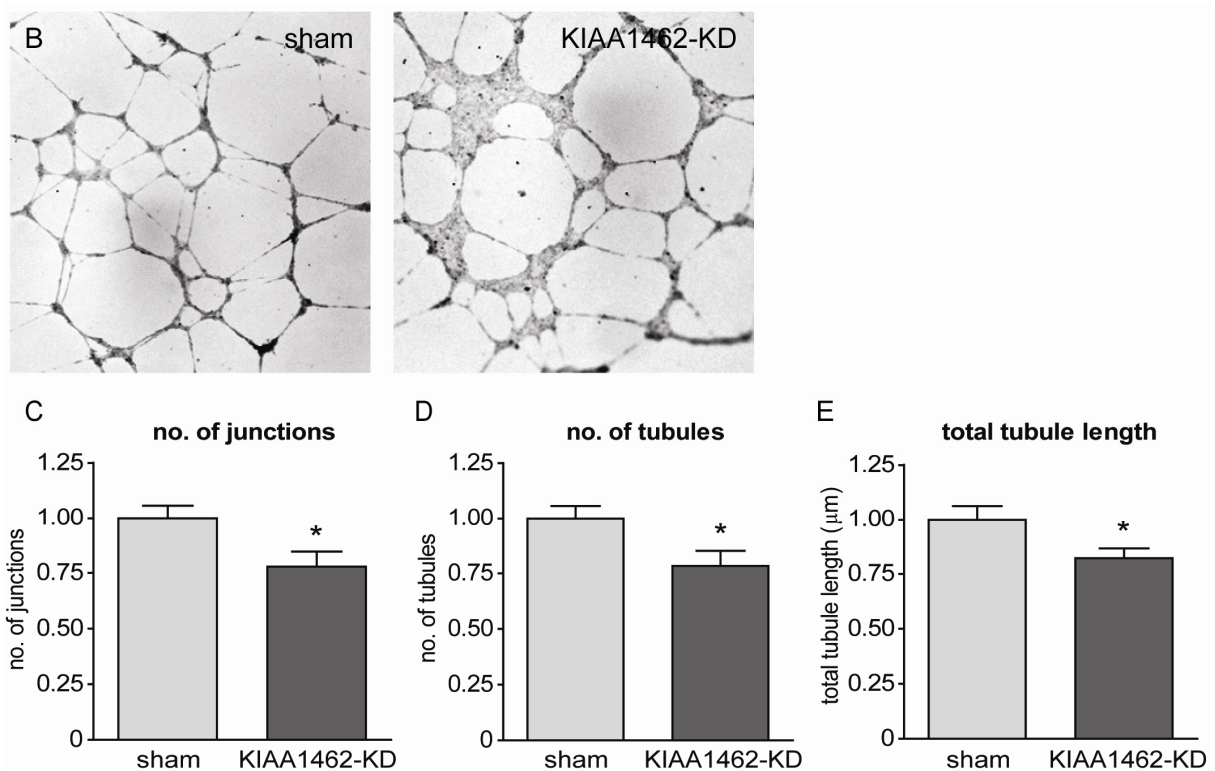


(**B**) Assessment of network-formation capacity for KIAA1462-silenced ECs (KIAA1462-KD) in a 2D matrigel experiment. Tubules were stained by Calcein-AM uptake. (**C-E**) Quantification of the vascular network showed a delay in network-formation in KIAA1462-KD HUVECs: (**C**) number of junctions, (**D**) number of tubules and (**E**) total tubule length (n = 5; mean ± SEM).
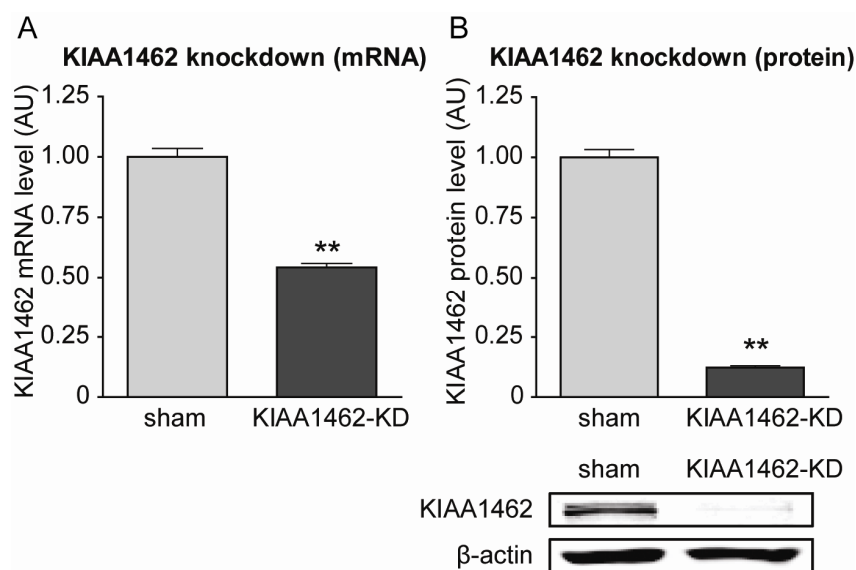
**Figure 6. siRNA-mediated knockdown of KIAA1462 in cultured endothelial cells.** (**A**) qPCR analysis of HUVECs transfected with KIAA1462 targeting siRNA (KIAA1462-KD) showed a reduction in mRNA expression levels of KIAA1462. (**B**) Western blot analysis of KIAA1462-KD in HUVECs showed a reduction in protein expression levels of KIAA1462 (n = 3; mean ± SEM).

## KIAA1462 knockdown in HUVECs reduces cell proliferation through a blockade of G1–S-phase transition

To determine the effect of KIAA1462 on cell proliferation *in vitro*, a proliferation assay was carried out. Cell proliferation was reduced after knockdown of KIAA1462 in HUVECs (Figure 7A). Sufficient cell cycle progression is necessary for proliferation. We therefore assessed the effect of KIAA1462 silencing on the cell cycle. Flow cytometric analysis of PI demonstrated that knockdown of KIAA1462 in HUVECs blocks the G1–S-phase transition (Figure 7B-D). To further validate these findings, BrdU incorporation during cell cycle was measured. BrdU incorporation was decreased after knockdown of KIAA1462 in HUVECs (Figure 7E, F). Together, these data suggest that KIAA1462 regulates cell proliferation by G1–S-phase transition.
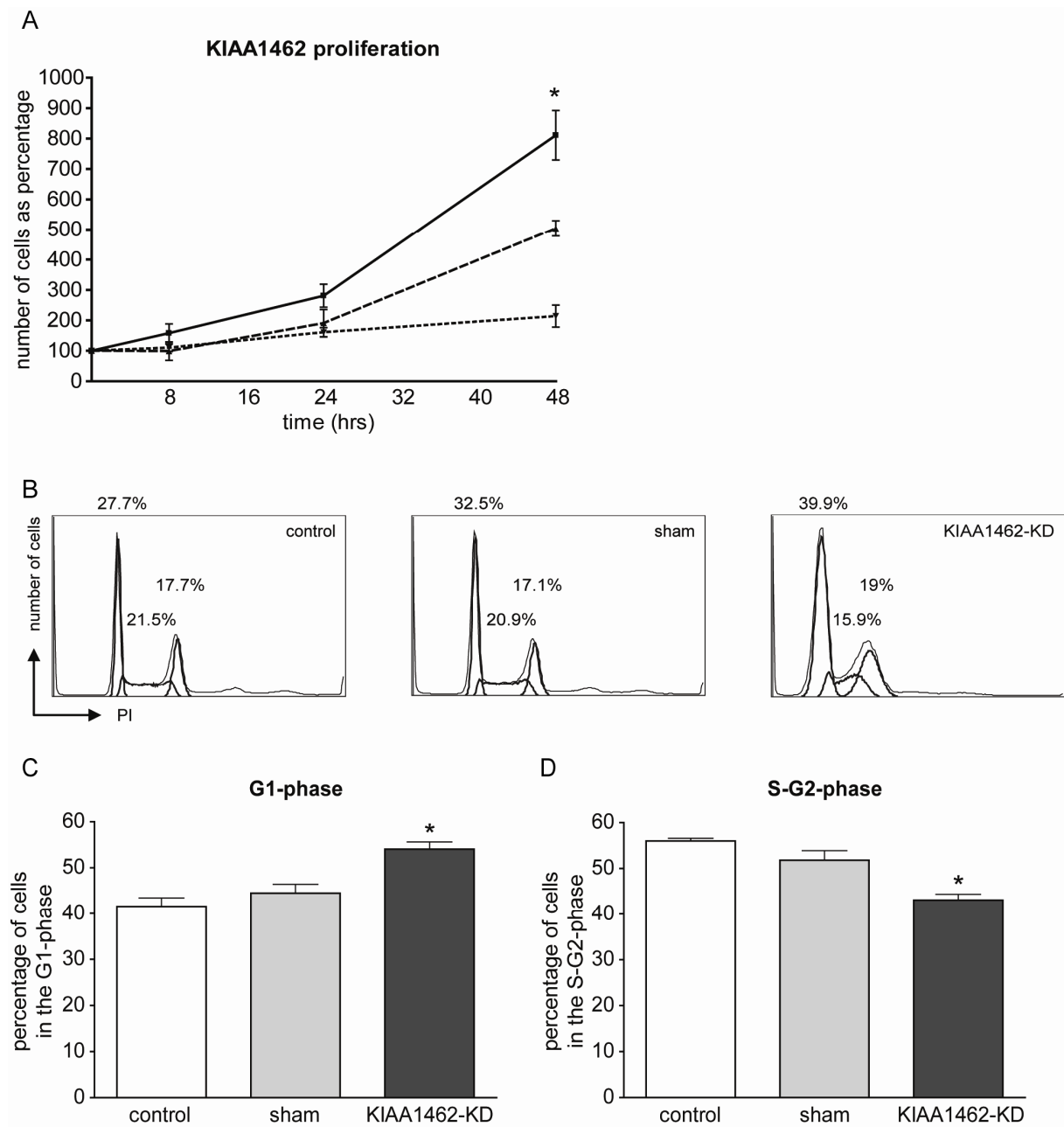
**Figure 7. KIAA1462 regulates cell proliferation through G1–S-phase transition.** (**A**) Averaged curves of cell proliferation of HUVECs. ⸻: control, – – –: sham adenovirus, ⋯⋯: KIAA1462 knockdown (KIAA1462-KD). (**B**) Representative flow cytometric analysis of HUVECs. (**C-D**) Quantification of the G1 and S–G2-phase of the cell cycle in HUVECs showed a blockade in G1–S-phase transition after KIAA1462-KD, as analysed by flow cytometry: (**C**) G1-phase and (**D**) S–G2-phase (n = 3; mean ± SEM).
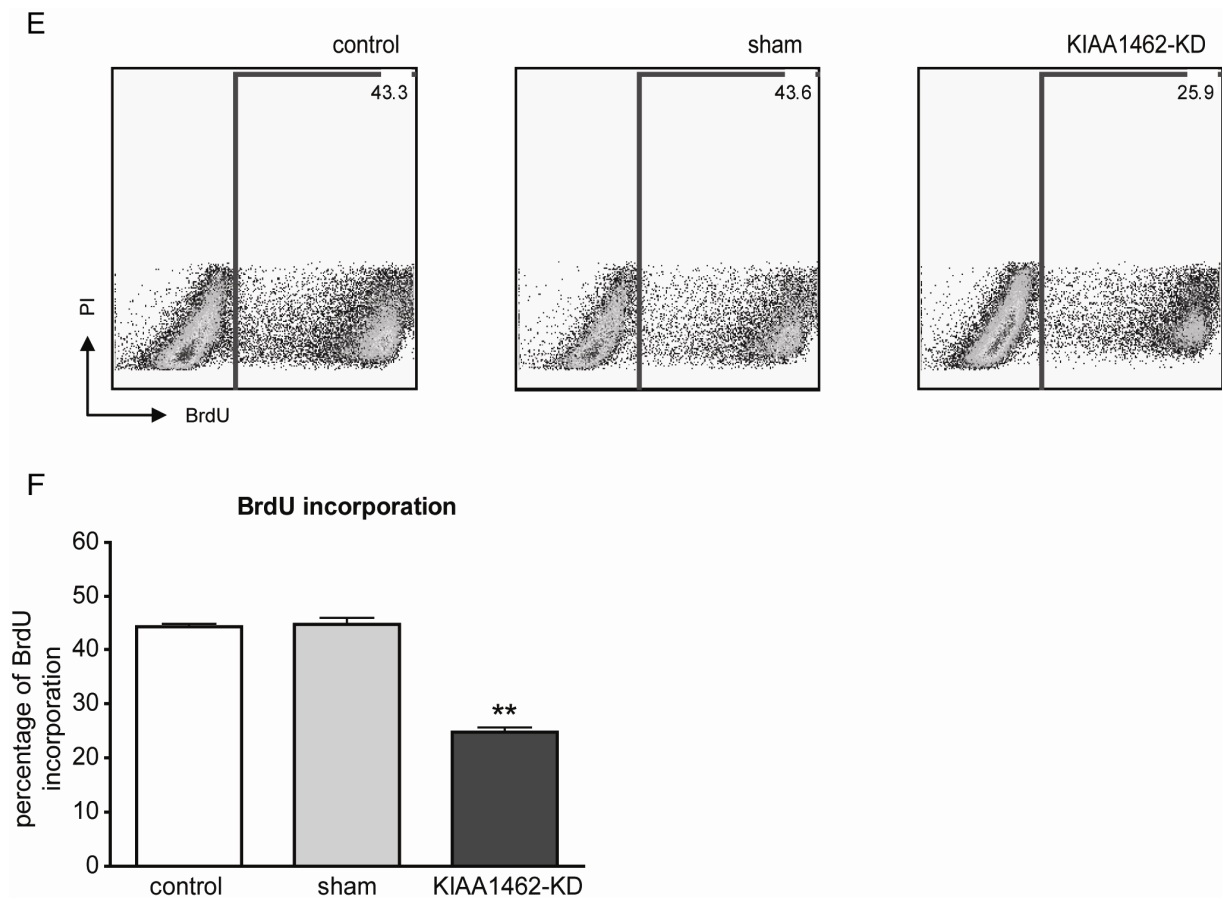
(**E**) Representative flow cytometric analysis of HUVECs. (**F**) Quantification of BrdU incorporation during cell cycle in HUVECs showed a decrease in BrdU incorporation after KIAA1462-KD, as analysed by flow cytometry (n = 4; mean ± SEM).

## Interaction of KIAA1462 with CTNND1 modulates RhoA activity

To clarify the influence of KIAA1462 on cell cycle control, we identified the binding partners of KIAA1462 by LC-MS. As shown in Table 1 and Figure 8, CTNND1 is one of the candidates to form a protein complex with KIAA1462, since CTNND1 as well as KIAA1462 are both situated at the plasma membrane. This was verified by co-localisation studies of KIAA1462 and CTNND1 in cultured ECs, which demonstrated a co-localisation of both proteins at the cell membrane (Figure 9A). To validate the binding of CTNND1 to KIAA1462, co-immunoprecipitation was carried out. It was showed that KIAA1462 and CTNND1 could indeed form a protein complex (Figure 9B).

**Table 1. Candidate binding partners of KIAA1462 identified by LC-MS.**

| Binding partners of KIAA1462 by LC-MS | | The Human Protein Atlas (Version 10.0) subcellular location |
|---|---|---|
| gene | description | |
| ACTR2 | ARP2 actin-related protein 2 homolog (yeast) | cytoplasm |
| AFAP1L1 | actin filament-associated protein 1-like 1 | nucleus, mitochondria |
| ARHGAP11A | Rho-GTPase activating protein 11A | nucleus, nucleoli, cytoplasm |
| ATAD3B | ATPase family, AAA domain containing 3B | - |
| ATP1A1 | ATPase, Na+/K+ transporting, alpha 1 polypeptide | - |
| CALD1 | caldesmon 1 | plasma membrane, cytoskeleton (actin filaments) |
| CDK1 | cyclin-dependent kinase 1 | cytoplasm, nucleus |
| CSRP1 | cysteine and glycine-rich protein 1 | cytoplasm, cytoskeleton (actin filaments) |
| CTNNB1 | catenin (cadherin-associated protein), beta 1 | plasma membrane |
| *CTNND1* | *catenin (cadherin-associated protein), delta 1* | *plasma membrane* |
| DDX17 | DEAD (Asp-Glu-Ala-Asp) box helicase 17 | - |
| DDX3X | DEAD (Asp-Glu-Ala-Asp) box polypeptide 3, X-linked | cytoplasm |
| DST | dystonin | nucleus, cytoplasm, cytoskeleton (microtubules) |
| EEF1G | eukaryotic translation elongation factor 1 gamma | - |
| EEF2 | eukaryotic translation elongation factor 2 | cytoplasm, Golgi apparatus |
| FBLIM1 | filamin binding LIM protein 1 | vesicles, cell junctions |
| FLOT1 | flotillin 1 | Golgi apparatus, plasma membrane, vesicles |
| FLOT2 | flotillin 2 | nucleus, cytoplasm, mitochondria |
| FXR1 | fragile X mental retardation, autosomal homolog 1 | cytoplasm |
| GNB1 | guanine nucleotide binding protein (G protein), beta polypeptide 1 | plasma membrane, Golgi apparatus |
| GNB2 | guanine nucleotide binding protein (G protein), beta polypeptide 2 | plasma membrane, Golgi apparatus |

| Binding partners of KIAA1462 by LC-MS | | The Human Protein Atlas (Version 10.) subcellular location |
|---|---|---|
| gene | description | |
| GSN | gelsolin | cytoskeleton (actin filaments) |
| H2AFV | H2A histone family, member V | - |
| *KIAA1462* | *KIAA1462* | *plasma membrane, vesicles* |
| LMNA | lamin A/C | nucleus |
| LRRFIP1 | leucine-rich repeat (in FLII) interacting protein 1 | cytoplasm |
| MCM7 | minichromosome maintenance complex component 7 | nucleus |
| PABPC1 | poly(A) binding protein, cytoplasmic 1 | cytoplasm |
| PCMT1 | protein-L-isoaspartate (D-aspartate) O-methyltransferase | cytoplasm |
| PDLIM5 | PDZ and LIM domain 5 | Golgi apparatus, cytoskeleton (actin filaments), nucleoli, cytoplasm |
| PKM2 | pyruvate kinase, muscle | cytoplasm, plasma membrane |
| PLS3 | plastin 3 | - |
| PPIA | peptidylprolyl isomerase A (cyclophilin A) | - |
| PRKDC | protein kinase, DNA-activated, catalytic polypeptide | - |
| PRPF3 | PRP3 pre-mRNA processing factor 3 homolog (*S. cerevisiae*) | nucleus, cytoplasm |
| PTRF | polymerase I and transcript release factor | - |
| RAN | RAN, member RAS oncogene family | - |
| RAP1B | RAP1B, member RAS oncogene family | - |
| RPL27A | ribosomal protein L27a | - |
| RPL9 | ribosomal protein L9 | cytoplasm, nucleoli |
| RPS3A | ribosomal protein S3A | - |
| RPS7 | ribosomal protein S7 | - |

| Binding partners of KIAA1462 by LC-MS | | The Human Protein Atlas (Version 10.0) |
|---|---|---|
| gene | description | subcellular location |
| RPS9 | ribosomal protein S9 | - |
| SYNCRIP | synaptotagmin binding, cytoplasmic RNA interacting protein | - |
| SYNPO | synaptopodin | nucleus, cytoplasm, cytoskeleton (actin filaments) |
| TCP1 | t-complex 1 | nucleus, cytoplasm, plasma membrane, Golgi apparatus, cell junctions |
| TJP1 | tight junction protein 1 | cell junctions, cytoplasm, Golgi apparatus |
| TJP2 | tight junction protein 2 | plasma membrane, cytoplasm, cell junctions |
| TOM1 | target of myb 1 (chicken) | cytoplasm, centrosome |
| TOM1L2 | target of myb 1-like 2 (chicken) | nucleus |
| TPM1 | tropomyosin 1 (alpha) | cytoplasm, cytoskeleton (actin filaments) |
| VDAC1 | voltage-dependent anion channel 1 | - |
| XRCC6 | X-ray repair complementing defective repair in Chinese hamster cells 6 | - |
| ZYX | zyxin | cytoplasm, focal adhesions |

Left and middle column shows the precipitated proteins with KIAA1462 antibody identified by liquid chromatography-mass spectrometry (LC-MS). The subcellular location of the proteins - as presented in the right column - was derived from The Human Protein Atlas (Version 10.0).
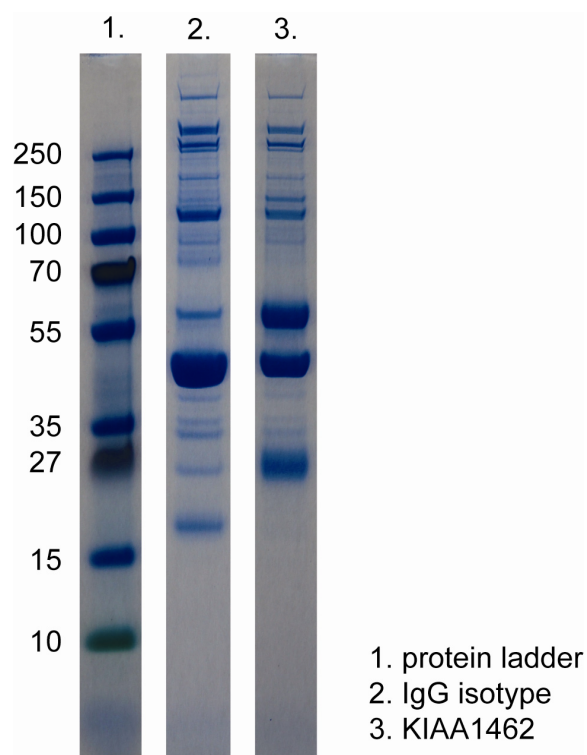
**Figure 8. Candidate binding partners of KIAA1462 identified by LC-MS.** Protein complexes were immunoprecipitated using Dynabeads® magnetic beads coated with IgG isotype or KIAA1462 antibody and separated on 12.5% SDS-PAGE gel, followed by Coomassie blue staining. Liquid chromatography-mass spectrometry (LC-MS) was used to identify the precipitated proteins with IgG isotype antibody (lane 2) or KIAA1462 antibody (lane 3).

Previously, it has been demonstrated that CTNND1 modulates RhoA activity.[17] Therefore, KIAA1462 may influence RhoA activity via CTNND1. To verify this, activated RhoA levels (RhoA-GTP) were measured. This showed that KIAA1462 depletion impaired RhoA activity (Figure 9C-E). Combined, these data indicate that KIAA1462 modulates RhoA activity via CTNND1 interaction.
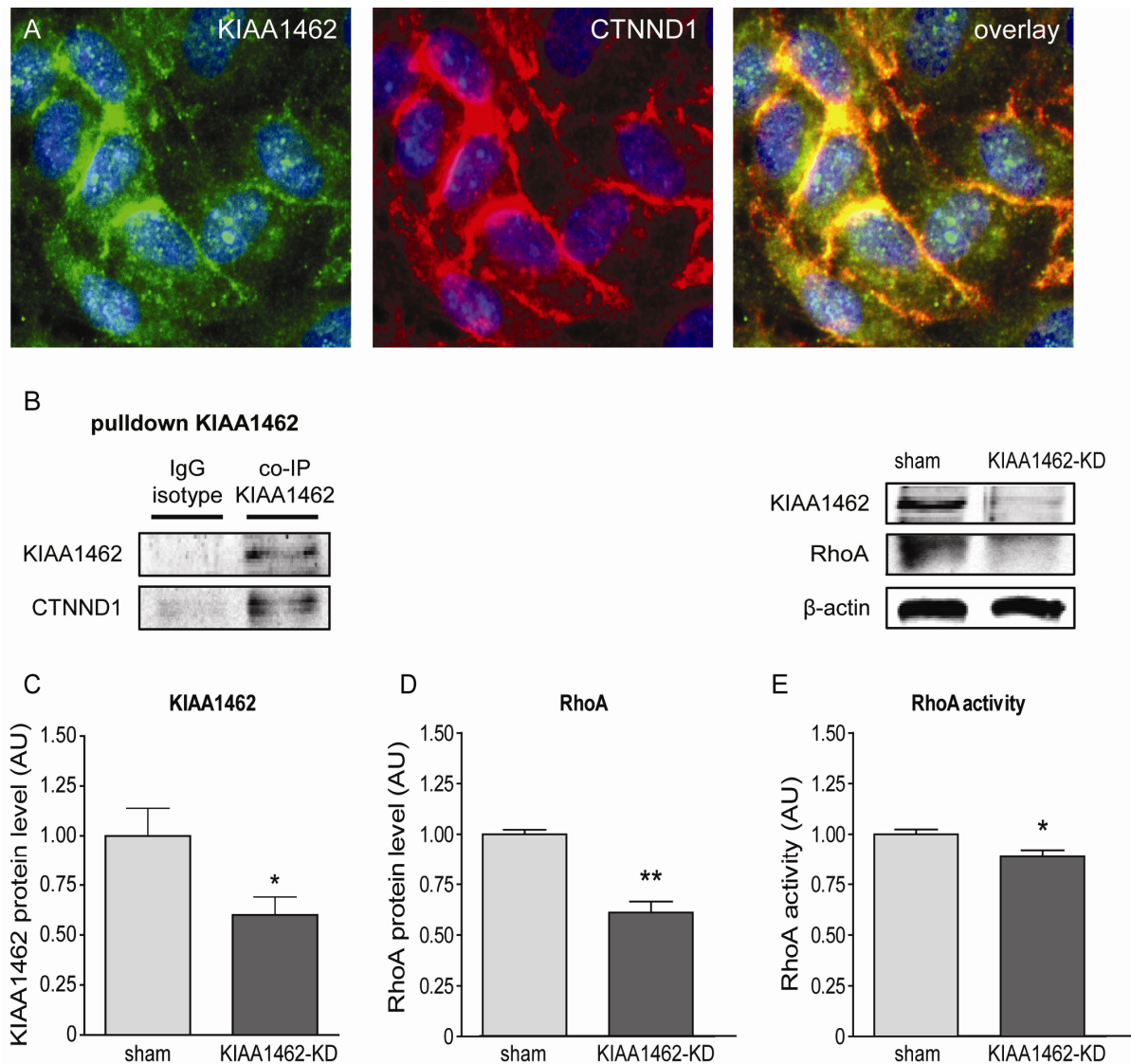
**Figure 9. KIAA1462 binds CTNND1 and modulates RhoA activity.** (**A**) KIAA1462 co-localise with CTNND1 in HUVECs, as demonstrated by immunofluorescent staining. KIAA1462 (green), CTNND1 (red), co-localised area (yellow) and nuclei (blue) (n = 3). (**B**) Immunoprecipitation of KIAA1462 in HUVECs showed an effective pull down of KIAA1462 (upper panel) and co-immunoprecipitation of CTNND1 (lower panel). Immunoprecipitation using a rat IgG isotype control showed no effective pull down of KIAA1462 or CTNND1 (representative picture for n = 3). (**C, D**) Western blot analysis of HUVECs transfected with KIAA1462 targeting siRNA (KIAA1462-KD) showed a decline in (**C**) KIAA1462 and (**D**) RhoA protein levels. (**E**) KIAA1462-KD in HUVECs resulted in a decrease in RhoA-GTP levels as shown by GAP-assay measurements (n = 3; mean ± SEM).

## RhoA activity affects G1–S-phase transition

Activated RhoA promotes G1–S-phase transition and cell proliferation via ROCK phosphorylation, or regulation of SKP2 gene transcription and Rb phosphorylation.[11-13] Western blot analysis demonstrated that indeed both downstream signalling cascades were affected (Figure 10A, B, E, F); knockdown of KIAA1462 decreased signal transduction via ROCK2 by downregulation of ROCK2 phosphorylation (Figure 10A, B). On the other hand, knockdown of KIAA1462 also diminishing the expression of ubiquitin ligase SKP2, illustrated by a decline in mRNA levels measured by qPCR analysis (Figure 10C, D). Finally, Rb was less phosphorylated (Figure 10E, F). Overall, these data demonstrate that KIAA1462 regulates G1–S-phase transition via downstream signalling of RhoA.
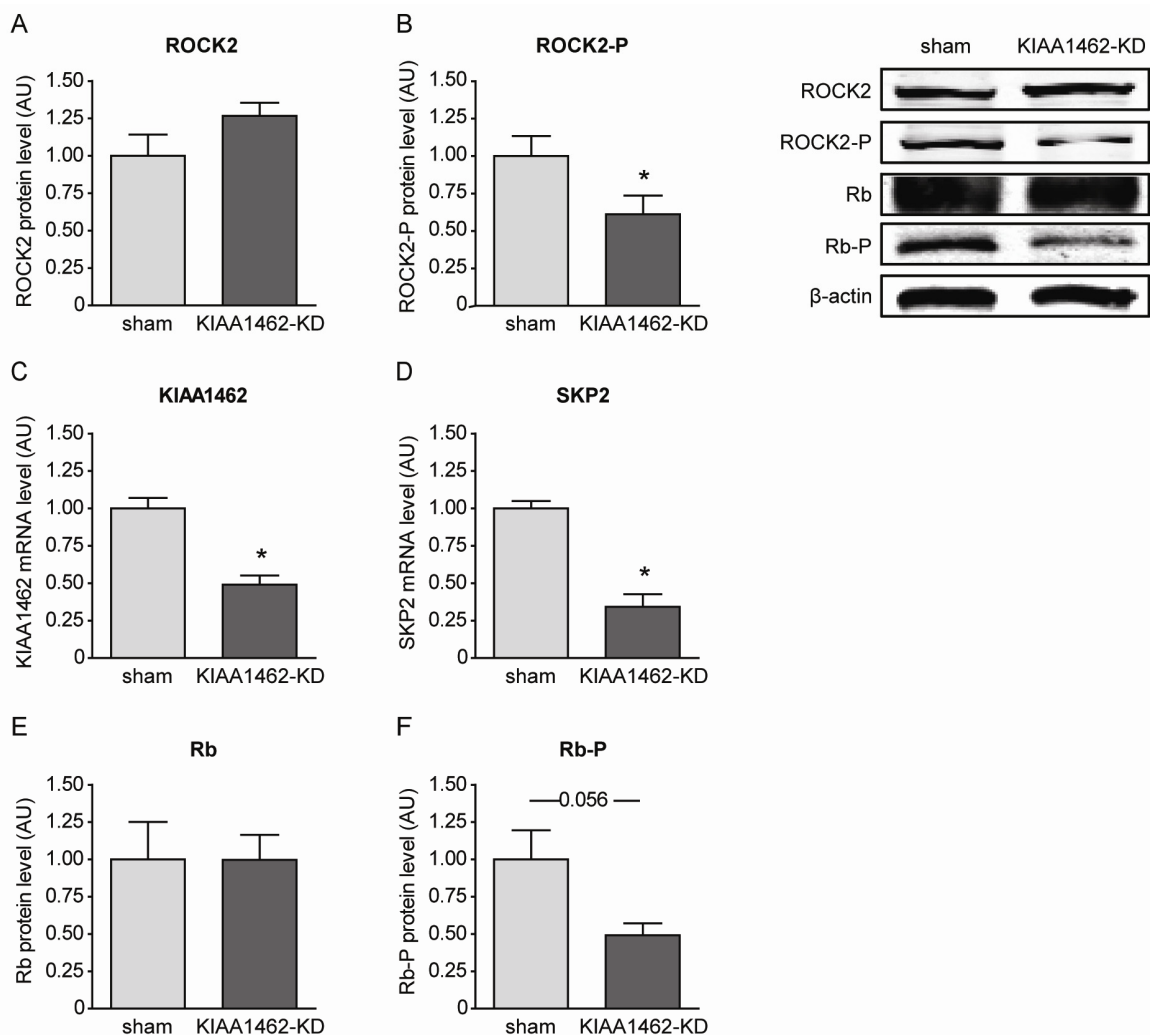


**Figure 10. KIAA1462 affects the downstream effectors of RhoA.** (**A, B, E, F**) Western blot analysis of HUVECs transfected with KIAA1462 targeting siRNA (KIAA1462-KD) showed a limited activation of the downstream effectors of RhoA-GTP, including: (**B**) ROCK2-P and (**F**) Rb-P, whereas (**A**) ROCK2 and (**E**) Rb were not affected. (**C, D**) qPCR analysis of KIAA1462-KD in HUVECs showed a reduction in expression levels of (**C**) KIAA1462 and (**D**) SKP2 (n = 3; mean ± SEM).

**Knockdown of KIAA1462 in zebrafish arrests gastrulation at 80-90% epiboly**

In zebrafish, changes in signal transduction via ROCK or SKP2/Rb could greatly effect embryonic development.[18,19] To determine the effect of KIAA1462 knockdown, zebrafish embryos were injected with an ATG Loc100001168 targeting MO and compared with uninjected controls.

Silencing of KIAA1462 expression resulted in an arrest of embryonic development between shield stage and 90% epiboly (84% of the injected embryos, n = 200). This effect on zebrafish embryogenesis indicates that KIAA1462 also *in vivo* modulates the downstream signalling cascades of RhoA.

**9430020K01Rik-knockout mice exhibits suppressed blood vessel formation in the retina and heart tissue**

To confirm the *in vitro* and *in vivo* findings of 9430020K01Rik silencing, we generated a C57BL/6.9430020K01Rik*tm1(KOMP)Mbp/MCL*-knockout mouse line (Figure 11A). Validation of adequate 9430020K01Rik knockout was achieved by PCR, using toe biopsies from 9430020K01Rik-knockout mice and non-transgenic controls. Figure 11B showed DNA fragments of wild-type and knockout alleles.
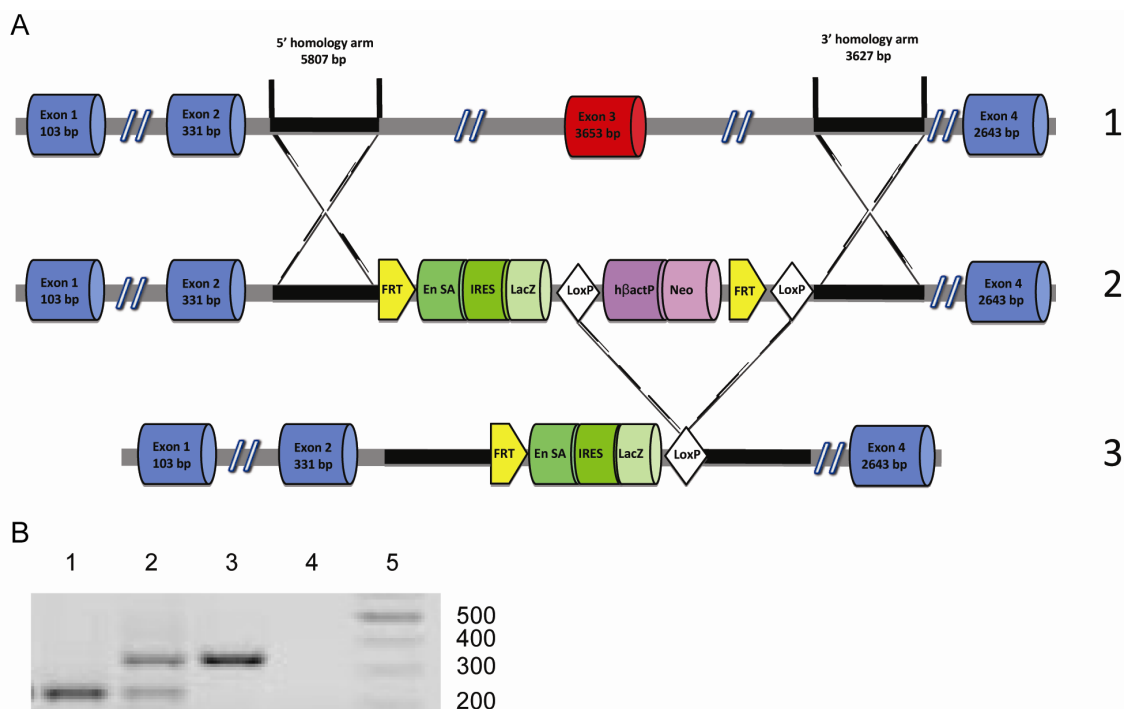


**Figure 11. Vascular development in 9430020K01Rik-knockout mice.** (**A**) 9430020K01Rik alleles, distances are not drawn to scale: 1. wild-type allele, 2. out-of-frame exon 3 is replaced with a LacZ reporter gene and Neomycin selection marker, and 3. Neomycin marker is removed to generate the C57BL/6.9430020K01Rik*tm1(KOMP)Mbp/MCL*-knockout mouse line. (**B**) PCR analysis to discriminate between wild-type and knockout (post-Cre) alleles: 1. wild-type, 2. heterozygote, 3. knockout, 4. blanco (H$_2$O), and 5. DNA ladder.

Knockout of 9430020K01Rik affected the outgrowth of the vasculature toward the retinal borders in the same way due to 9430020K01Rik silencing by intra-ocular injection of si-9430020K01Rik (Figure 11C). Assessment and quantification of the number of vascular branches, the total number of vessels and the total tubule length after visualisation of the vasculature by isolectin GS-IB$_4$ staining, showed a reduction in the total number of junctions and the total number of vessels between 9430020K01Rik-knockout mice and wild-type littermates (controls), while there was no difference observed in the total tubule length (Figure 11D-F).
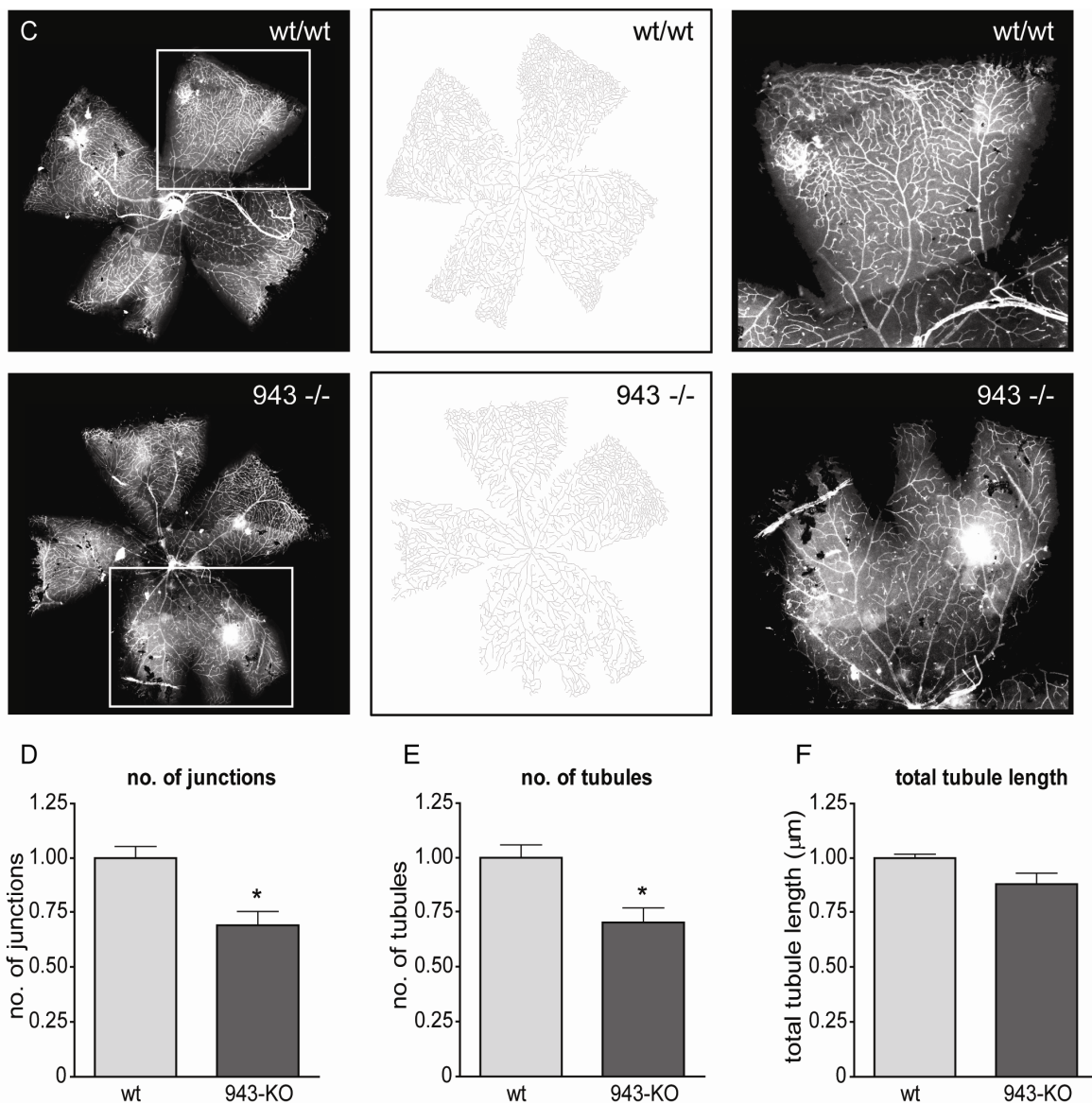


(**C**) Retinas stained with isolectin GS-IB$_4$. (**D-F**) Quantification by means of the dimensions of the vascular network showed a reduction in the total number of junctions and the total number of vessels in 9430020K01Rik-knockout mice (943-KO): (**D**) number of junctions, (**E**) number of tubules and (**F**) total tubule length (n = 3; mean ± SEM).

Immunohistochemistry studies on sections from heart tissue - taken from 9430020K01Rik-knockout mice or wild-type littermates - using isolectin GS-IB$_4$, demonstrated a reduction of capillary density in heart tissue of 9430020K01Rik-knockout mice compared with wild-type controls (Figure 11G). These data confirm an essential role of 9430020K01Rik in vessel outgrowth during vascular development.
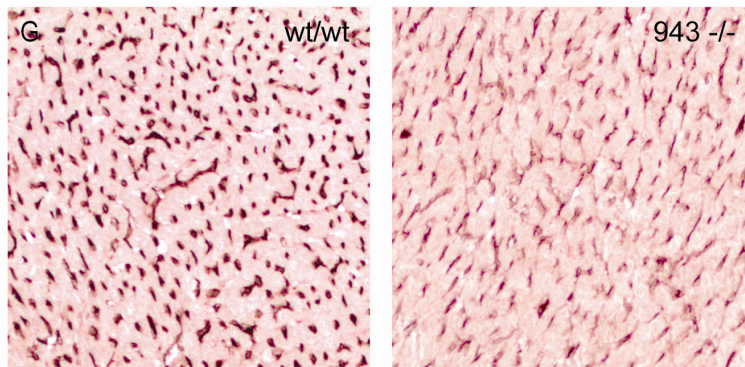


(**G**) Heart tissue stained with isolectin GS-IB$_4$ showed a reduction in capillary density in 9430020K01Rik-knockout mice compared with wild-type littermates (representative picture for n = 3).

## *Discussion*

In this study we demonstrated that 9430020K01Rik (KIAA1462) regulates vessel outgrowth during vascular development in mice. Knockout of 9430020K01Rik in mice resulted in diminished blood vessel formation in the developing retinal vasculature and reduced capillary density in heart tissue. Functional knockdown of Loc100001168 in zebrafish arrested gastrulation at 80-90% epiboly.

*In vitro*, we demonstrated that loss of KIAA1462 lead to decreased RhoA activation, which resulted in diminished G1–S-phase transition during cell cycle progression. Co-immunoprecipitation identified CTNND1 as binding partner of KIAA1462. Further evaluation of KIAA1462 signalling demonstrated an important role for KIAA1462 in RhoA-mediated cell cycle progression; KIAA1462 mediates RhoA activation via CTNND1 binding, and downstream signalling via the ROCK2 and Rb cascades. Knockdown of KIAA1462 significantly decreased RhoA-induced EC proliferation.

The KIAA1462 gene encodes a 148 kDa protein without any known domains, but contains a proline-rich region. Although proline often plays a purely structural role in proteins, it has a high non-specific binding ability because it functions as a strong hydrogen bond acceptor. Proline-rich regions are often involved in the formation of multi-molecular complexes.[20] Previously, it has been shown that KIAA1462 is as a component of the VE-

cadherin junctional complex in cultured ECs.[14] Clustering of VE-cadherin at the cell-cell borders promotes complex formation of multiple proteins, including; signalling, regulatory and scaffold proteins. One of these proteins that interacts with VE-cadherin is CTNND1 which acts as a regulator of Rho-GTPases and its downstream targets, including ROCK.[21,22] ROCK activity is associated with endothelial dysfunction which is one of the main causes of CAD.[8,23] In addition, genome-wide association studies have detected a missense variant (p.S1002T) in the KIAA1462 gene which increases the risk of CAD by 15%.[9,10] Based on the high expression level of KIAA1462 in the EC subset, we hypothesised that KIAA1462 was also involved in the angiogenic process. Here, we show that indeed KIAA1462 acts as a potent regulator of EC proliferation by interaction with CTNND1, modifying RhoA activity during vascular growth.

In our study, KIAA1462 was co-localised with CTTND1 at the plasma membrane of ECs. Additional co-immunoprecipitation studies showed that KIAA1462 and CTNND1 also indeed formed a protein complex. CTNND1 belongs to a subfamily of armadillo proteins and is a component of the VE-cadherin complex in adherens junctions.[24-27] Likewise, CTNND1 binding to VE-cadherin was verified (data not shown). Beside the structural role of CTNND1 in cell-cell contacts, it also modulates nuclear transcription and regulates the activation of Rho-GTPases - especially RhoA - and its downstream signalling cascades.[22,28] The ability of CTNND1 to stabilise cadherin complexes at the plasma membrane and to regulate the activity of RhoA, depends on the subcellular localisation of CTNND1. Previous work has indicated that CTNND1 exists in an equilibrium between two states; bound to cadherins or free in the cytoplasm.[17] Soluble, cytoplasmic CTNND1 inhibits the exchange of GDP with GTP of RhoA, downregulating RhoA activity.[29] Our data clearly show that KIAA1462 is involved in RhoA activation and that KIAA1462 binds CTNND1 in the VE-cadherin junctional complex. We propose that KIAA1462 plays an important role in the equilibrium of CTNND1 by stabilising the interaction of CTNND1 with VE-cadherin at the plasma membrane, lowering the fraction of soluble, cytoplasmic CTNND1 which results in an increase of RhoA activity.

RhoA influences cell morphogenesis through remodelling of the cytoskeleton and regulates in this way cell proliferation in late G1-phase.[11,30] Downstream effectors of RhoA includes the ROCK family protein kinases and the mammalian homolog of *Drosophila* diaphanous (mDia) family of formins. Except interphase, formins also exert their effects during embryonic development.[31] Previous studies show that diaphanous-related formin 2 (zDia2) is required for cellular movements during epiboly and convergent extension in zebrafish gastrulation. MO-induced knockdown of zDia2 in zebrafish is characterised by late epiboly arrest at 80-90% epiboly and mild convergent extension defects.[18,32] Inhibition of ROCK also leads to abnormal cytokinesis and epiboly in zebrafish.[19] We found in zebrafish a similar phenotype like zDia2 and ROCK after MO blocking of Loc100001168.

Our data show that KIAA1462 acts in the same pathway as the ROCK family protein kinases and zDia2.

zDia2 has a high sequence homology with mDia which shuttles between the cytoplasm and nucleus.[33] Here, it promotes the ubiquitin ligase SKP2 expression.[18] When expressed, SKP2 ubiquitylates the cell cycle inhibitor p27$^{Kip1}$ and regulates its degradation. p27$^{Kip1}$ is an inhibitor of the cyclin D1-CDK4 complex, which phosphorylates the Rb protein in late G1.[13,34] In line with these findings, our data demonstrate that loss of KIAA1462 inhibited SKP2 expression, which was associated with a decrease in Rb phosphorylation.

ROCK family protein kinases - the other downstream effector of RhoA - can be subdivided in two isoforms: ROCK1 and ROCK2.[35-37] Our data clearly show that loss of KIAA1462 lead to diminished ROCK2 activation. ROCK2 is highly expressed in the heart and brain, and plays a strong role in capillary development.[38-41] Our data confirmed these findings, since 9430020K01Rik knockout in mice diminished capillary density in heart tissue. These findings further proof that KIAA1462 regulates both downstream cascades of RhoA and finally in this way EC proliferation (Figure 12).

In conclusion, here we have identified 9430020K01Rik (KIAA1462) as a new regulator of EC proliferation during angiogenesis by binding to CTNND1 in the VE-cadherin junctional complex at the plasma membrane of ECs, followed by activation of the RhoA-mediated ROCK2 and Rb signalling pathway, which ultimately lead to G1–S-phase transition that promotes EC proliferation and vessel outgrowth. To our knowledge, this study is the first report of the function of 9430020K01Rik (KIAA1462) in ECs during normal embryonic and postnatal blood vessel formation. As mentioned before, ROCK family protein kinases can be subdivided in two isoforms. Since ROCK1 and ROCK2 functions in a redundant manner, loss of ROCK2 activity can be compensated by ROCK1. Activation of ROCK1 in bone marrow-derived macrophages is critical to the development of early atherosclerosis by mediating foam cell formation and macrophage chemotaxis.[37,40,42] In line with these findings, the missense variant (p.S1002T) in the KIAA1462 gene could result in ROCK2-compensated activation by ROCK1, leading to a severed development of atherosclerosis, increasing the risk of CAD. Additional molecular and population based research is needed to provide further evidence fore the role of KIAA1462 in the development of atherosclerosis and CAD.
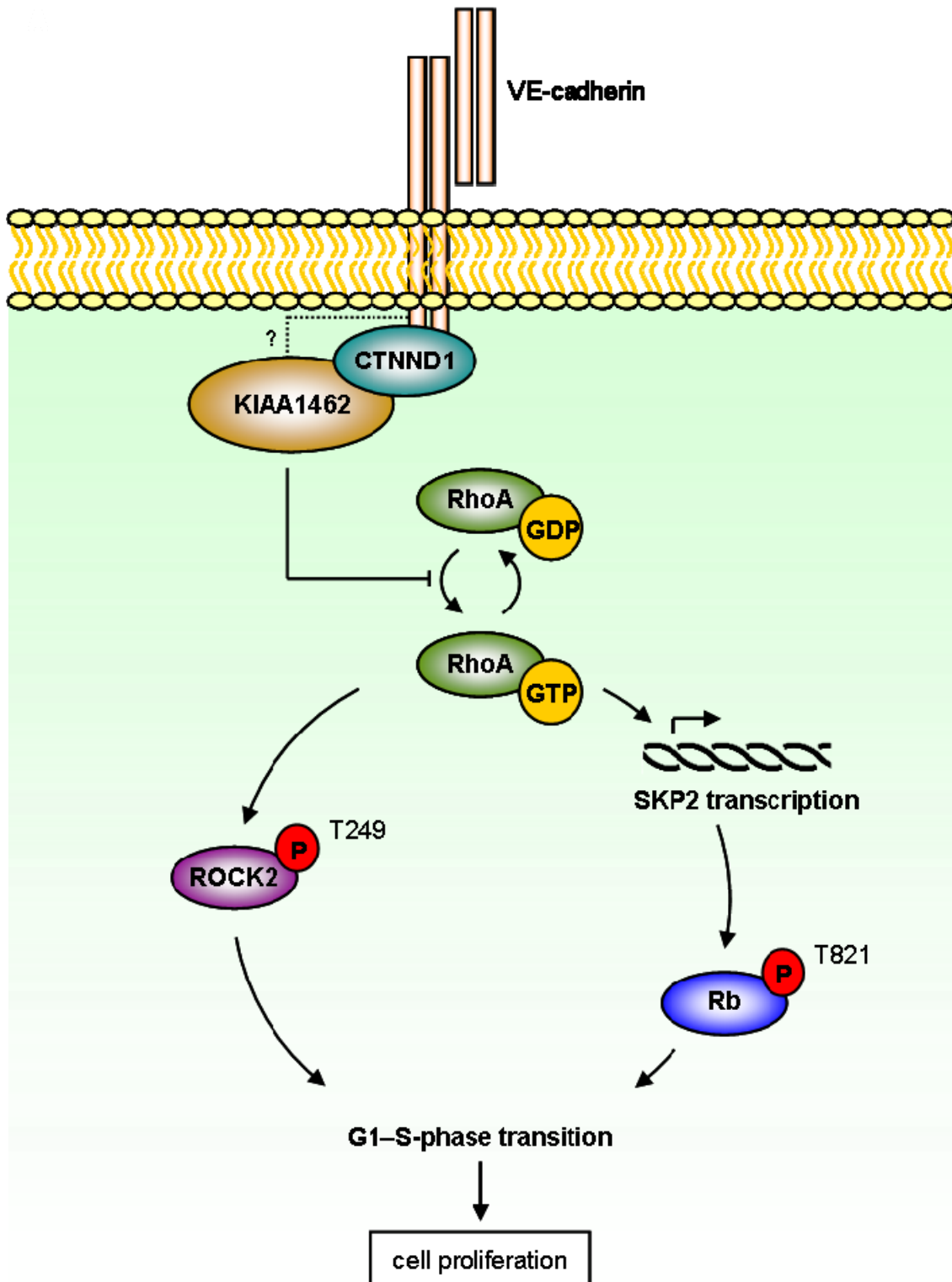
**Figure 12. Molecular pathway of KIAA1462 during angiogenesis.** KIAA1462 regulates endothelial cell proliferation by its interaction with CTNND1 in the VE-cadherin junctional complex at the plasma membrane of endothelial cells, limiting the amount of free CTNND1 in the cytoplasm. Because of this RhoA activity increases, which results in downstream activation of ROCK2 and Rb. These proteins modulate cell proliferation by stimulating G1–S-phase transition.

# *References*

1. Boehm M, Nabel EG. The cell cycle and cardiovascular diseases. *Prog Cell Cycle Res.* 2003;5:19-30.
2. Liu WF, Nelson CM, Tan JL, Chen CS. Cadherins, RhoA, and Rac1 are differentially required for stretch-mediated proliferation in endothelial versus smooth muscle cells. *Circ Res.* 2007;101(5):e44-e52.
3. Shimokawa H, Takeshita A. Rho-kinase is an important therapeutic target in cardiovascular medicine. *Arterioscler Thromb Vasc Biol.* 2005;25(9):1767-1775.
4. Libby P. Inflammation in atherosclerosis. *Nature.* 2002;420(6917):868-874.
5. Ross R. Atherosclerosis - an inflammatory disease. *N Engl J Med.* 1999;340(2):115-126.
6. Wallez Y, Huber P. Endothelial adherens and tight junctions in vascular homeostasis, inflammation and angiogenesis. *Biochim Biophys Acta.* 2008;1778(3):794-809.
7. Carmeliet P, Lampugnani MG, Moons L, Breviario F, Compernolle V, Bono F, Balconi G, Spagnuolo R, Oosthuyse B, Dewerchin M, Zanetti A, Angellilo A, Mattot V, Nuyens D, Lutgens E, Clotman F, de Ruiter MC, Gittenberger-de Groot A, Poelmann R, Lupu F, Herbert JM, Collen D, Dejana E. Targeted deficiency or cytosolic truncation of the VE-cadherin gene in mice impairs VEGF-mediated endothelial survival and angiogenesis. *Cell.* 1999;98(2):147-157.
8. Marzilli M, Merz CN, Boden WE, Bonow RO, Capozza PG, Chilian WM, DeMaria AN, Guarini G, Huqi A, Morrone D, Patel MR, Weintraub WS. Obstructive coronary atherosclerosis and ischemic heart disease: an elusive link! *J Am Coll Cardiol.* 2012;60(11):951-956.
9. Coronary Artery Disease (C4D) Genetics Consortium. A genome-wide association study in Europeans and South Asians identifies five new loci for coronary artery disease. *Nat genet.* 2011;43(4):339-344.
10. Erdmann J, Willenborg C, Nahrstaedt J, Preuss M, König IR, Baumert J, Linsel-Nitschke P, Gieger C, Tennstedt S, Belcredi P, Aherrahrou Z, Klopp N, Loley C, Stark K, Hengstenberg C, Bruse P, Freyer J, Wagner AK, Medack A, Lieb W, Grosshennig A, Sager HB, Reinhardt A, Schäfer A, Schreiber S, El Mokhtari NE, Raaz-Schrauder D, Illig T, Garlichs CD, Ekici AB, Reis A, Schrezenmeir J, Rubin D, Ziegler A, Wichmann HE, Doering A, Meisinger C, Meitinger T, Peters A, Schunkert H. Genome-wide association study identifies a new locus for coronary artery disease on chromosome 10p11.23. *Eur Heart J.* 2011;32(2):158-168.
11. Wozniak MA, Chen CS. Mechanotransduction in development: a growing role for contractility. *Nat Rev Mol Cell Biol.* 2009;10(1):34-43.

12. Pirone DM, Liu WF, Ruiz SA, Gao L, Raghavan S, Lemmon CA, Romer LH, Chen CS. An inhibitory role for FAK in regulating proliferation: a link between limited adhesion and RhoA-ROCK signalling. *J Cell Biol.* 2006;174(2):277-288.

13. Mammoto A, Huang S, Moore K, Oh P, Ingber DE. Role of RhoA, mDia and ROCK in cell shape-dependent control of the SKP2-p27Kip1 pathway and the G1/S transition. *J Biol Chem.* 2004;279(25):26323-26330.

14. Akashi M, Higashi T, Masuda S, Komori T, Furuse M. A coronary artery disease-associated gene product, JCAD/KIAA1462, is a novel component of endothelial cell-cell junctions. *Biochem Biophys Res Commun.* 2011;413(2):224-229.

15. Nasevicius A, Ekker SC. Effective targeted gene 'knockdown' in zebrafish. *Nat Genet.* 2000;26(2):216-220.

16. Dekkers DH, Bezstarosti K, Gurusamy N, Luijk K, Verhoeven AJ, Rijkers EJ, Demmers JA, Lamers JM, Maulik N, Das DK. Identification by a differential proteomic approach of the induced stress and redox proteins by resveratrol in the normal and diabetic rat heart. *J Cell Mol Med.* 2008;12(5A):1677-1689.

17. Noren NK, Liu BP, Burridge K, Kreft B. p120 catenin regulates the actin cytoskeleton via Rho family GTPases. *J Cell Biol.* 2000;150(3):567-580.

18. Lai SL, Chan TH, Lin MJ, Huang WP, Lou SW, Lee SJ. Diaphanous-related formin 2 and profilin I are required for gastrulation cell movements. *PLoS One.* 2008;3(10):e3439.

19. Lai SL, Chang CN, Wang PJ, Lee SJ. Rho mediates cytokinesis and epiboly via ROCK in zebrafish. *Mol Reprod Dev.* 2005;71(2):186-196.

20. Williamson MP. The structure and function of proline-rich regions in proteins. *Biochem J.* 1994;297(Pt 2):249-260.

21. Dejana E, Orsenigo F, Lampugnani MG. The role of adherens junctions and VE-cadherin in the control of vascular permeability. *J Cell Sci.* 2008;121(Pt 13):2115-2122.

22. Anastasiadis PZ, Reynolds AB. Regulation of Rho-GTPases by p120-catenin. *Curr Opin Cell Biol.* 2001;13(5):604-610.

23. Zhou Q, Liao JK. Rho-kinase: an important mediator of atherosclerosis and vascular disease. *Curr Pharm Des.* 2009;15(27):3108-3115.

24. Soto E, Yanagisawa M, Marlow LA, Copland JA, Perez EA, Anastasiadis PZ. p120 catenin induces opposing effects on tumour cell growth depending on E-cadherin expression. *J Cell Biol.* 2008;183(4):737-749.

25. Keil R, Wolf A, Hüttelmaier S, Hatzfeld M. Beyond regulation of cell adhesion: local control of RhoA at the cleavage furrow by the p0071 catenin. *Cell Cycle.* 2007;6(2):122-127.

26. Hatzfeld M. The p120 family of cell adhesion molecules. *Eur J Cell Biol.* 2005;84(2-3):205-214.

27. Yap AS, Niessen CM, Gumbiner BM. The juxtamembrane region of the cadherin cytoplasmic tail supports lateral clustering, adhesive strengthening and interaction with p120ctn. *J Cell Biol.* 1998;141(3):779-789.

28. Pieters T, van Roy F, van Hengel J. Functions of p120ctn isoforms in cell-cell adhesion and intracellular signalling. *Front Biosci (Landmark Ed).* 2012;17:1669-1694.

29. Anastasiadis PZ, Moon SY, Thoreson MA, Mariner DJ, Crawford HC, Zheng Y, Reynolds AB. Inhibition of RhoA by p120 catenin. *Nat Cell Biol.* 2000;2(9):637-644.

30. Narumiya S, Yasuda S. Rho-GTPases in animal cell mitosis. *Curr Opin Cell Biol.* 2006;18(2):199-205.

31. Wallar BJ, Alberts AS. The formins: active scaffolds that remodel the cytoskeleton. *Trends Cell Biol.* 2003;13(8):435-446.

32. Lepage SE, Bruce AE. Zebrafish epiboly: mechanics and mechanisms. *Int J Dev Biol.* 2010;54(8-9):1213-1228.

33. Miki T, Okawa K, Sekimoto T, Yoneda Y, Watanabe S, Ishizaki T, Narumiya S. mDia2 shuttles between the nucleus and the cytoplasm through the importin-{alpha}/{beta}- and CRM1-mediated nuclear transport mechanism. *J Biol Chem.* 2009;284(9):5753-5762.

34. Huang S, Chen CS, Ingber DE. Control of cyclin D1, p27Kip1 and cell cycle progression in human capillary endothelial cells by cell shape and cytoskeleton tension. *Mol Biol Cell.* 1998;9(11):3179-3193.

35. Leung T, Manser E, Tan L, Lim L. A novel serine/threonine kinase binding the Ras-related RhoA-GTPase which translocates the kinase to peripheral membranes. *J Biol Chem.* 1995;270(49):29051-29054.

36. Nakagawa O, Fujisawa K, Ishizaki T, Saito Y, Nakao K, Narumiya S. ROCK1 and ROCK2, two isoforms of Rho-associated coiled-coil forming protein serine/threonine kinase in mice. *FEBS Lett.* 1996;392(2):189-193.

37. Loirand G, Guérin P, Pacaud P. Rho-kinases in cardiovascular physiology and pathophysiology. *Circ Res.* 2006;98(3):322-334.

38. Street CA, Bryan BA. Rho-kinase proteins - pleiotropic modulators of cell survival and apoptosis. *Anticancer Res.* 2011;31(11):3645-3657.

39. Bryan BA, Dennstedt E, Mitchell DC, Walshe TE, Noma K, Loureiro R, Saint-Geniez M, Campaigniac JP, Liao JK, D'Amore PA. RhoA/ROCK signalling is essential for multiple aspects of VEGF-mediated angiogenesis. *FASEB J.* 2010;24(9):3186-3195.

40. Nunes KP, Rigsby CS, Webb RC. RhoA/Rho-kinase and vascular diseases: what is the link? *Cell Mol Life Sci.* 2010;67(22):3823-3836.

41. Wei L, Roberts W, Wang L, Yamada M, Zhang S, Zhao Z, Rivkees SA, Schwartz RJ, Imanaka-Yoshida K. Rho-kinases play an obligatory role in vertebrate embryonic organogenesis. *Development.* 2001;128(15):2953-2962.

42. Wang HW, Liu PY, Oyama N, Rikitake Y, Kitamoto S, Gitlin J, Liao JK, Boisvert WA. Deficiency of ROCK1 in bone marrow-derived cells protects against atherosclerosis in LDLR-/- mice. *FASEB J.* 2008;22(10):3561-3570.

# Chapter 3

## Klf7 regulates endothelial cell proliferation and differentiation in angiogenesis

R.A. Haasdijk, D. Tempel, P.E. Bürgisser, E.H.M. van de Kamp
L.A.J. Blonden, C. Cheng, H.J. Duckers

## *Abstract*

**Objective** - Cell cycle withdrawal is necessary for transition from an undetermined to a restricted endothelial cell fate. Krüppel-like factors are involved in the expression of cell cycle regulatory proteins. Here, we demonstrate an essential role for Krüppel-like factor 7 (Klf7) in the regulation of endothelial cell proliferation and differentiation during vascular development.

**Methods and Results** - *In vitro* analysis of gene function in endothelial cells showed that Klf7 affects $p21^{Cip1/Waf1}$ activity. Overexpression of Klf7 stimulated $p21^{Cip1/Waf1}$, leading to diminished G1–S-phase transition which finally resulted in decreased cell proliferation.

**Conclusion** - We conclude that Klf7 is crucial for the regulation of endothelial cell proliferation and differentiation via modulation of $p21^{Cip1/Waf1}$ activity during vascular development.

## *Introduction*

During vascular development angioblasts differentiate into endothelial cells (EC).[1] Transition from an undetermined to a restricted EC fate depends on the time of withdrawal from the cell cycle.[2] Cell cycle progression is regulated by many different proteins, including cyclins, cyclin-dependent kinases (CDK) and CDK inhibitors. In particular, the CDK inhibitor $p21^{Cip1/Waf1}$ plays an important role in cell cycle control: $p21^{Cip1/Waf1}$-mediated G1-arrest allow cell cycle withdrawal and cell differentiation.[3-5] Increased $p21^{Cip1/Waf1}$ expression also induce genes associated with senescence and age-related conditions such as atherosclerosis and Alzheimer disease.[6,7] The expression of cell cycle regulatory proteins is controlled by several transcription factors, which can be divided according to the structural motif that contacts the DNA - one such motif is the zinc finger.[8] This motif is found by Krüppel-like factors (Klf) which contain three highly conserved $Cys_2$-$His_2$ zinc fingers at the carboxyl terminus of the protein and enable Klfs to bind GC-rich promoters.[9-11] Klfs function as activator, repressor or both of a large variety of genes.[12] Previous studies have demonstrated that the Klf family play important roles in cell proliferation, differentiation and apoptosis in several different organ systems during embryonic development, adult life and cancer-related angiogenesis.[13-15] One such Klf family member is Krüppel-like factor 7 (Klf7), also known as ubiquitously Klf (UKLF) because of its widely expression in adult tissue, in particular the nervous system where it has an essential role in neurite outgrowth and survival.[2,16-18] After that, it has also been demonstrated that Klf7 is specifically expressed in vascular ECs.[14,18] In spite of this, our knowledge of the role of Klf7 in EC function remains limited. In this study, we have identified a particular role for Klf7 in blood vessel development.

Recently, we have carried out a genome-wide microarray analysis in search of genes involved in the regulation of new vessel formation. Gene expression profiles of isolated Flk1-positive angioblasts during murine embryonic development were compared with the profiles of Flk1-negative cells. One of the genes that was identified as a new potential regulator of vascular development was Klf7. The Klf7 gene encodes a ~34 kDa protein which contains three domains: at the carboxyl terminus a DNA binding domain made of three zinc fingers separated by TGEKP(Y/F)X spacers, at the central part a nuclear localisation signal (NLS), a leucine-zipper motif and a hydrophobic serine-rich region functioning as a protein interaction domain, and at the amino terminus an acidic transactivation domain.[13,18] However, the basic biological function of Klf7 in angiogenesis remains fully unknown.

In this study, we sought to characterise the function of Klf7 in ECs during blood vessel formation *in vitro* using primary cell cultures. Our data show that Klf7 plays an important role in the regulation of EC proliferation. Overexpression of Klf7 led to diminished G1–S-

phase transition. Further *in vitro* studies demonstrate that Klf7 stimulates p21$^{Cip1/Waf1}$ activity. Together, these findings contribute to the basic understanding of how Klf7 plays an important role in EC proliferation during vascular development.

## *Methods*

This study was carried out in accordance with the Council of Europe Convention (ETS123)/Directive (86/609/EEC) for the protection of vertebrate animals used for experimental and other scientific purposes and with the approval of the National and Local Animal Care Committee.

### Mice

Plugged FVB/N mice (*Mus musculus*) were ordered at Harlan (Indianapolis, USA). They were maintained under standard husbandry conditions.

### Isolation of Flk1-positive and Flk1-negative cells from mouse embryos

From eight to sixteen days post-fertilisation (dpf), embryos were collected from plugged FVB/N mice and homogenised. Cells were stained with PE-conjugated anti-mouse Flk1 antibody 1:50 (555308; BD, Breda, The Netherlands). Hoechst (Sigma-Aldrich, Zwijndrecht, The Netherlands) was used to select dead cells. Flk1-positive/Hoechst-negative cells and Flk1-negative/Hoechst-negative cells were sorted on a BD FACSCanto$^{TM}$ (Breda, The Netherlands). Isolation of mRNA was carried out using the RNeasy Mini Kit from Qiagen (Venlo, The Netherlands).

### Microarray analysis

Double stranded cDNA was generated from 5 μg mRNA. Biotin-labelled RNA was synthesised using the BioArray$^{TM}$ HighYield$^{TM}$ RNA Transcript Labeling Kit from ENZO Life Sciences (Raamsdonksveer, The Netherlands). After clean-up and fragmentation, approximately 20 μg of labelled cRNA was hybridised to the GeneChip$^{®}$ Mouse Genome 430 2.0 Array (Affymetrix, Santa Clara, USA). Rosetta Resolver$^{®}$ (Rosetta Biosoftware, Cambridge, USA) was used to get quantile normalised raw data from the arrays. These data were merged into OmniViz$^{®}$ (BioWisdom, Cambridge, UK) and a threshold minimum for intensities was set at 30. Fold differences were calculated from log averages determined by the different experimental conditions.

## Cell cultures

Primary cultures of human umbilical vein endothelial cells (HUVEC) were cultured in EBM®-2 medium supplemented with a commercial BulletKit, 10% foetal calf serum (FCS) and 1% penicillin/streptomycin (Lonza, Breda, The Netherlands). Primary aorta-derived human vascular smooth muscle cells (vSMC) were cultured in SmGM®-2 medium supplemented with a commercial BulletKit, 10% FCS and 1% penicillin/streptomycin (Lonza, Breda, The Netherlands). HeLa and sarcoma cells were cultured in Dulbecco's modified Eagle's medium (DMEM) supplemented with 10% FCS (Cambrex, Wiesbaden, Germany). Cells were cultured at 37°C in 5% $CO_2$. Passages three to six were used throughout the study.

## Immunofluorescence

HUVECs were grown in gelatin-coated 48-wells. After 24 hours, the cells were fixed in 4% formaldehyde and permeabilised with 0.2% Triton® X-100. Cells were incubated overnight at 4°C with Klf7 antibody 1:125 (HPA030490; Sigma-Aldrich, Zwijndrecht, The Netherlands). For the detection of the primary antibody, Alexa Fluor® 488 1:100 (Invitrogen, Bleiswijk, The Netherlands) was used. Actin filaments were stained with rhodamin-phalloidin 1:40 (R415; Invitrogen, Bleiswijk, The Netherlands). The nucleus was stained with 4,6-diamidino-2-phenylindole (DAPI) in Vectashield® mounting medium (H-1200; Vector Laboratories, Burlingame, USA). Cells were visualised with a fluorescence microscope (Axiovert S100; Carl Zeiss, Sliedrecht, The Netherlands).

## Klf7 adenovirus-induced overexpression

HUVECs were cultured in EBM®-2 medium supplemented with a commercial BulletKit and infected with Klf7 adenovirus (pAd-Klf7) (MOI 50) or sham adenovirus (MOI 50) as control. Overexpression of Klf7 was validated by qPCR analysis and Western blot two days post-infection using the following human primers: 5'-GAC AGC TAC ACA GCC GTC AA-3' (forward) and 5'-AGC TGA GAG CAG CCT TCT TG-3' (reverse) for Klf7 (Biolegio, Nijmegen, The Netherlands), and anti-human Klf7 antibody 1:125 (HPA030490; Sigma-Aldrich, Zwijndrecht, The Netherlands). Beta-actin primers 5'-TCC CTG GAG AAG AGC TAC GA-3' (forward) and 5'-AGC ACT GTG TTG GCG TAC AG-3' (reverse) (Biolegio, Nijmegen, The Netherlands) were used as housekeeping gene, while beta-actin antibody 1:500 (ab8229; Abcam, Cambridge, UK) was used as a loading control.

## 2D matrigel network-formation assay

To induce network-formation, HUVECs - infected with sham adenovirus or pAd-Klf7 - were cultured on a 2D Matrigel™ matrix (BD, Breda, The Netherlands). The tubules were stained by Calcein-AM (BD, Breda, The Netherlands) after 24 hours of network-formation. Each condition was assessed by fluorescence microscopy (Axiovert S100; Carl Zeiss,

Sliedrecht, The Netherlands). Image analysis of number of junctions, tubules and total tubule length was carried out using Angiosys Image Analysis Software 1.0 (TCS CellWorks, Buckingham, UK).

**Cell proliferation assay**

EC proliferation *in vitro* was evaluated by culturing HUVECs - infected with sham adenovirus or pAd-Klf7 - in gelatin-coated 6-wells and counting them at different time points.

In brief, 50,000 cells were seeded and incubated in EBM®-2 medium supplemented with 0.2% FCS for 4 hours to synchronise the cell cycle. Thereafter, HUVECs were trypsinised after 0, 8, 24 and 48 hours, and counted with a Bürker-Türk. At all time points the amount of cells was expressed as percentage, whereas time point zero the amount of cells was expressed as 100%.

**Cell cycle assay**

For cell cycle experiments, HUVECs - infected with sham adenovirus or pAd-Klf7 - were trypsinised and fixed in 70% ice-cold ethanol overnight at 4°C. After being washed in phosphate-buffered saline (PBS), the cells were resuspended in 300 µl PBS containing 69 µM propidium iodide (PI), 37 mM sodium citrate and 200 µg RNase. Cell cycle profile was measured on a BD FACSCanto™ (Breda, The Netherlands).

**Apoptosis assay**

To induce apoptosis, HUVECs - 24 hours post-infection - were serum starved for 4 hours and replenished with EBM®-2 medium supplemented with a commercial BulletKit for 24 hours. The cells were then harvested and resuspended in FACS buffer containing Annexin V and PI (BD, Breda, The Netherlands). After 15 minutes incubation at room temperature, Binding Buffer (BD, Breda, The Netherlands) was added before the cells were analysed on a BD FACSCanto™ (Breda, The Netherlands). Gating was set to exclude cell doublets and cell clumps.

**Western blot**

To determine whether overexpression of Klf7 interfered with cellular processes, Western blot analysis was carried out using HUVEC protein lysates. At 72 hours post-infection, HUVECs were serum starved for 4 hours and replenished with EBM®-2 medium supplemented with a commercial BulletKit for 30 minutes. Cells were lysed in NP40 Cell Lysis Buffer (Invitrogen, Bleiswijk, The Netherlands) and analysed on a 12.5% SDS-PAGE gel, followed by immunoblotting using anti-human antibodies against Klf7 1:125 (HPA030490; Sigma-Aldrich, Zwijndrecht, The Netherlands) and p21$^{Cip1/Waf1}$ 1:500 (sc-

469; Santa Cruz Biotechnology, Heidelberg, Germany). Beta-actin antibody 1:500 (ab8229; Abcam, Cambridge, UK) was used as a loading control. Protein bands were visualised by the Odyssey® Infrared Imaging System and analysed by Odyssey 3.0 software (LI-COR Biotechnology, Cambridge, UK).

**Statistical analysis**

Data were reported as mean ± standard error of the mean (SEM). Statistical significance was evaluated using a Student's *t*-test and was accepted at $P < 0.05$ (* $P < 0.05$, ** $P < 0.01$ in the figures).

# *Results*

**Expression of Klf7 is upregulated during mouse embryogenesis**

To identify new genes involved in angiogenesis, a genome-wide microarray analysis was carried out followed by validation of the results by qPCR. Gene expression profiles of Flk1-positive angioblasts at various stages of murine embryonic development were compared with the profiles of Flk1-negative cells. Klf7 was upregulated in Flk1-positive angioblasts from 8 to 16 dpf. Expression levels were highest upregulated around 9 dpf, which coincides with the period of early angiogenesis in murine development and suggests a potential role of Klf7 in blood vessel formation (Figure 1).
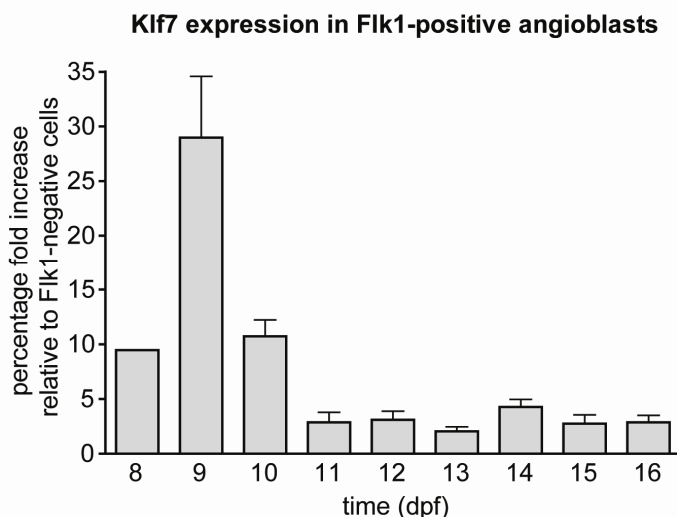


**Figure 1. Klf7 is upregulated in Flk1-positive angioblasts during mouse development.** Endogenous expression level of Klf7 in Flk1-positive angioblasts during murine embryonic development from 8 to 16 days post-fertilisation (dpf) compared with Flk1-negative cells as analysed by qPCR. The expression level of Klf7 in Flk1-negative cells was arbitrarily set to one (n = 4; mean ± SEM). The highest upregulation was detected around day 9, which coincides with the period of early angiogenesis in murine development.

**Klf7 is highly expressed in cultured endothelial cells**

To validate the endothelial expression of Klf7 in cultured cells, we determined the expression level of the Klf7 human orthologue in a number of different cell types. In a comparison between HUVECs, vSMCs, HeLa and sarcoma cells, the highest mRNA expression level of Klf7 was observed in HUVECs (Figure 2A). Intracellular immunofluorescent detection of Klf7 in HUVECs demonstrated that the protein was mainly located in the Golgi apparatus (Figure 2B).
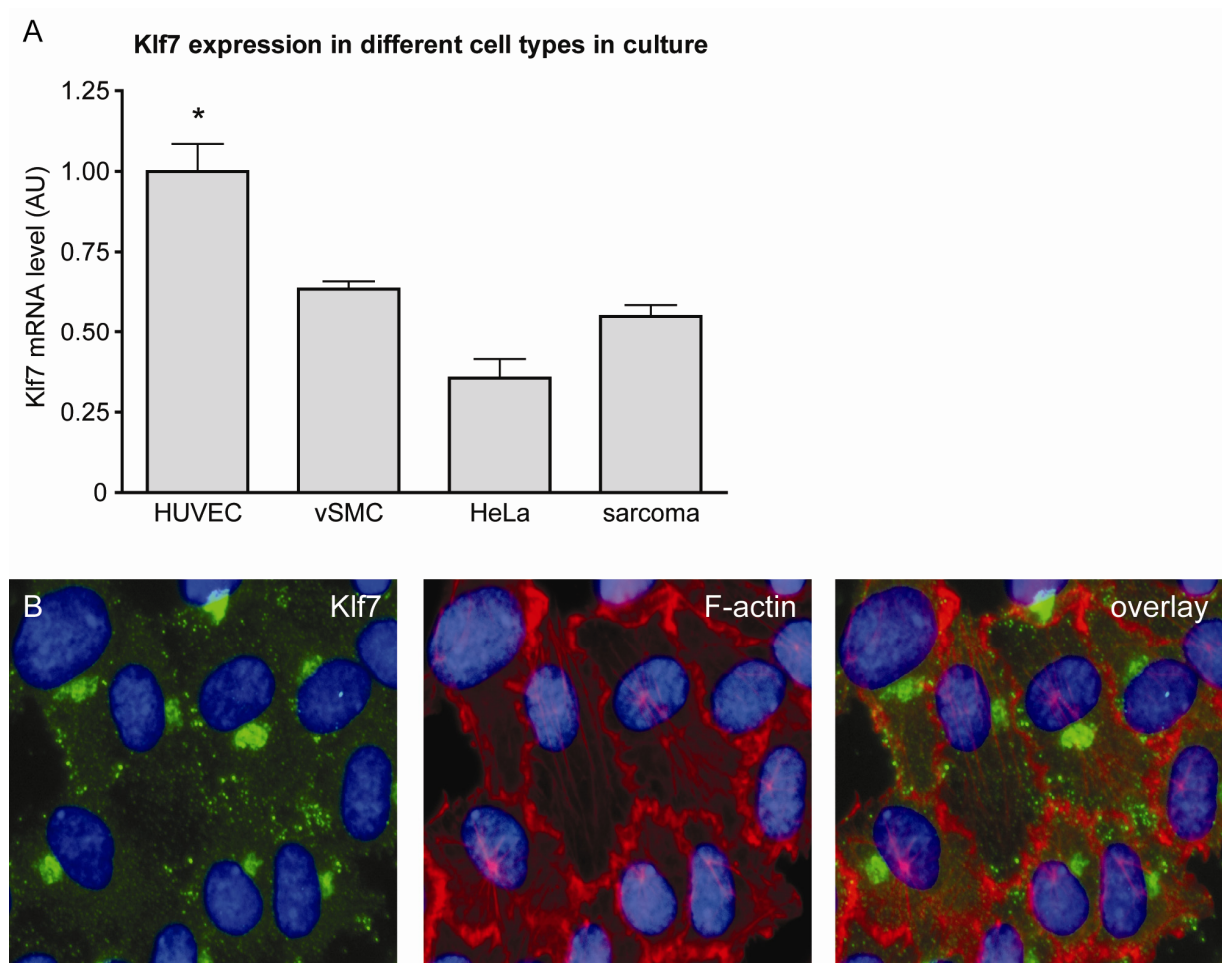


**Figure 2. Klf7 expression in different cell types in culture.** (**A**) Klf7 was highly expressed in HUVEC compared with vSMC, HeLa and sarcoma cells, as demonstrated by qPCR analysis (n = 3; mean ± SEM). (**B**) Klf7 was mainly located in the Golgi apparatus, as demonstrated by immunofluorescent staining. Klf7 (green), F-actin (red), co-localised area (yellow) and nuclei (blue) (n = 3).

**Overexpression of Klf7 inhibits vascular network-formation *in vitro***

To further assess the function of Klf7 in cultured ECs, overexpression of Klf7 in HUVECs was induced by infection of pAd-Klf7 and compared with sham adenovirus infected and uninfected controls. In pAd-Klf7 infected cells, endogenous Klf7 expression was significantly higher than in the control cultures on both mRNA (Figure 3A) and protein level (Figure 3B).
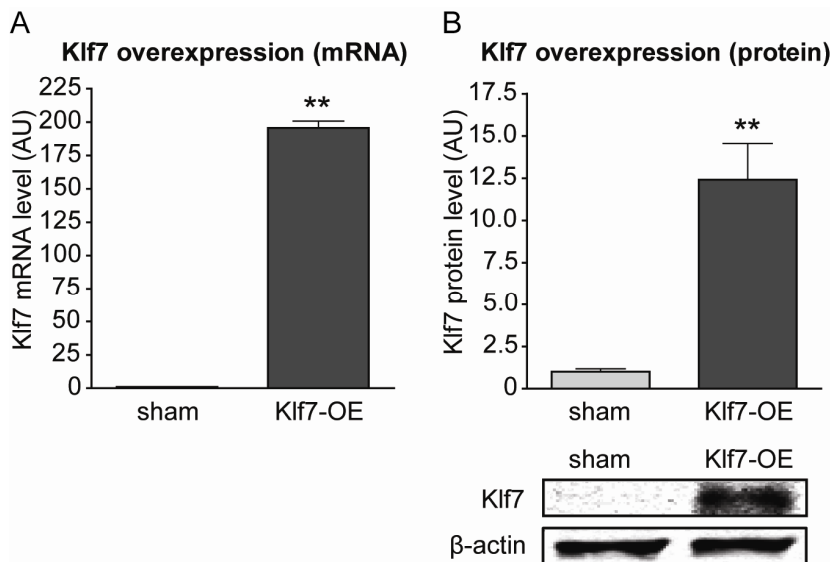


**Figure 3. Adenovirus-mediated overexpression of Klf7 in cultured endothelial cells.** (**A**) qPCR analysis of HUVECs infected with Klf7 adenovirus (Klf7-OE) showed an increase in mRNA expression levels of Klf7. (**B**) Western blot analysis of Klf7-OE in HUVECs showed an increase in protein expression levels of Klf7 (n = 5; mean ± SEM).

To investigate the effect of Klf7 overexpression on vascular network-formation, *in vitro* network-formation experiments with HUVECs were carried out. Overexpression of Klf7 had an inhibitory effect on the number of junctions and capillary tubules when compared with cultures infected with equivalent MOI of sham adenovirus or uninfected controls (Figure 4A-D). These data indicate that Klf7 has an essential role in vascular network-formation. The process of vessel growth is determined by many different factors. One of these is cell proliferation.
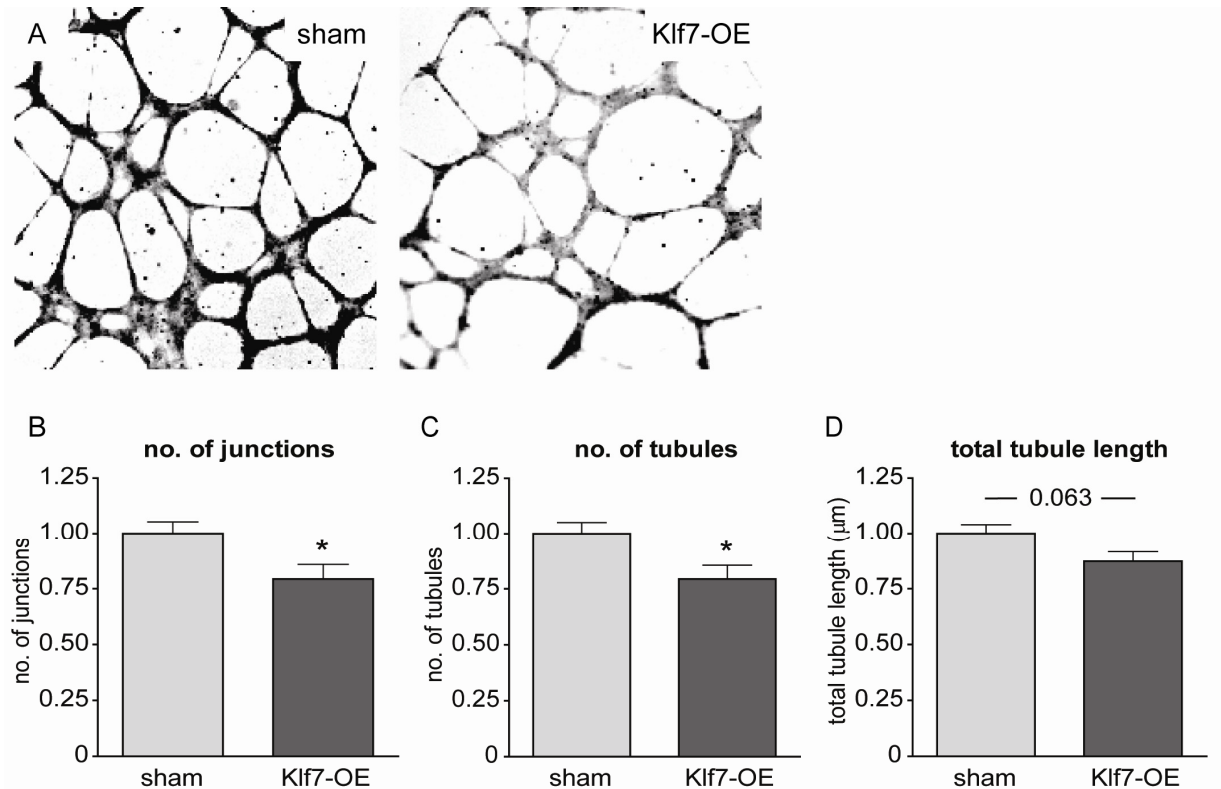
**Figure 4. Klf7 overexpression in cultured endothelial cells impairs vascular network-formation.** (**A**) Assessment of network-formation capacity for Klf7-overexpressed HUVECs (Klf7-OE) in a 2D matrigel experiment. Tubules were stained by Calcein-AM uptake. (**B-D**) Quantification of the vascular network showed a delay in network-formation in Klf7-OE HUVECs: (**B**) number of junctions, (**C**) number of tubules and (**D**) total tubule length (n = 5; mean ± SEM).

## Klf7 overexpression in HUVECs reduces cell proliferation through a blockade of G1–S-phase transition

To determine the effect of Klf7 on cell proliferation *in vitro*, a proliferation assay was carried out. Cell proliferation was reduced after overexpression of Klf7 in HUVECs (Figure 5A). Sufficient cell cycle progression is necessary for proliferation. We therefore assessed the effect of Klf7 overexpression on the cell cycle. Flow cytometric analysis of PI demonstrated that overexpression of Klf7 in HUVECs blocks the G1–S-phase transition (Figure 5B-D). In addition, an increase of apoptosis was observed in pAd-Klf7 infected cells compared with sham adenovirus infected and uninfected controls (Figure 5E-G). Together, these data suggest that Klf7 regulates cell proliferation by G1–S-phase transition.
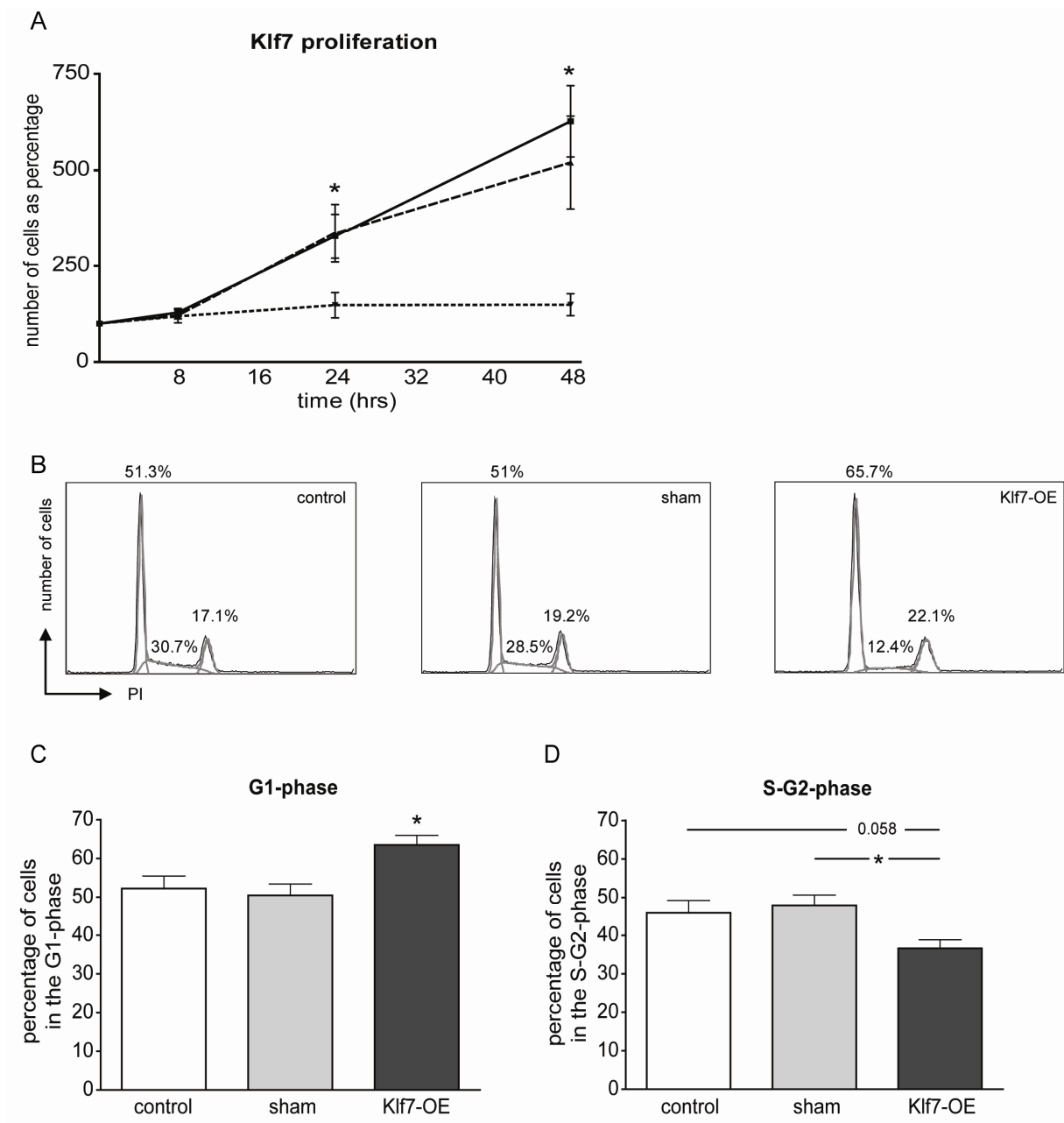
**Figure 5. Klf7 regulates cell proliferation through G1–S-phase transition.** (**A**) Averaged curves of cell proliferation of HUVECs. ——— : control, – – – : sham adenovirus, ········ : pAd-Klf7. (**B**) Representative flow cytometric analysis of HUVECs. (**C-D**) Quantification of the G1 and S–G2-phase of the cell cycle in HUVECs showed a blockade in G1–S-phase transition after Klf7 overexpression (Klf7-OE), as analysed by flow cytometry: (**C**) G1-phase and (**D**) S–G2-phase.
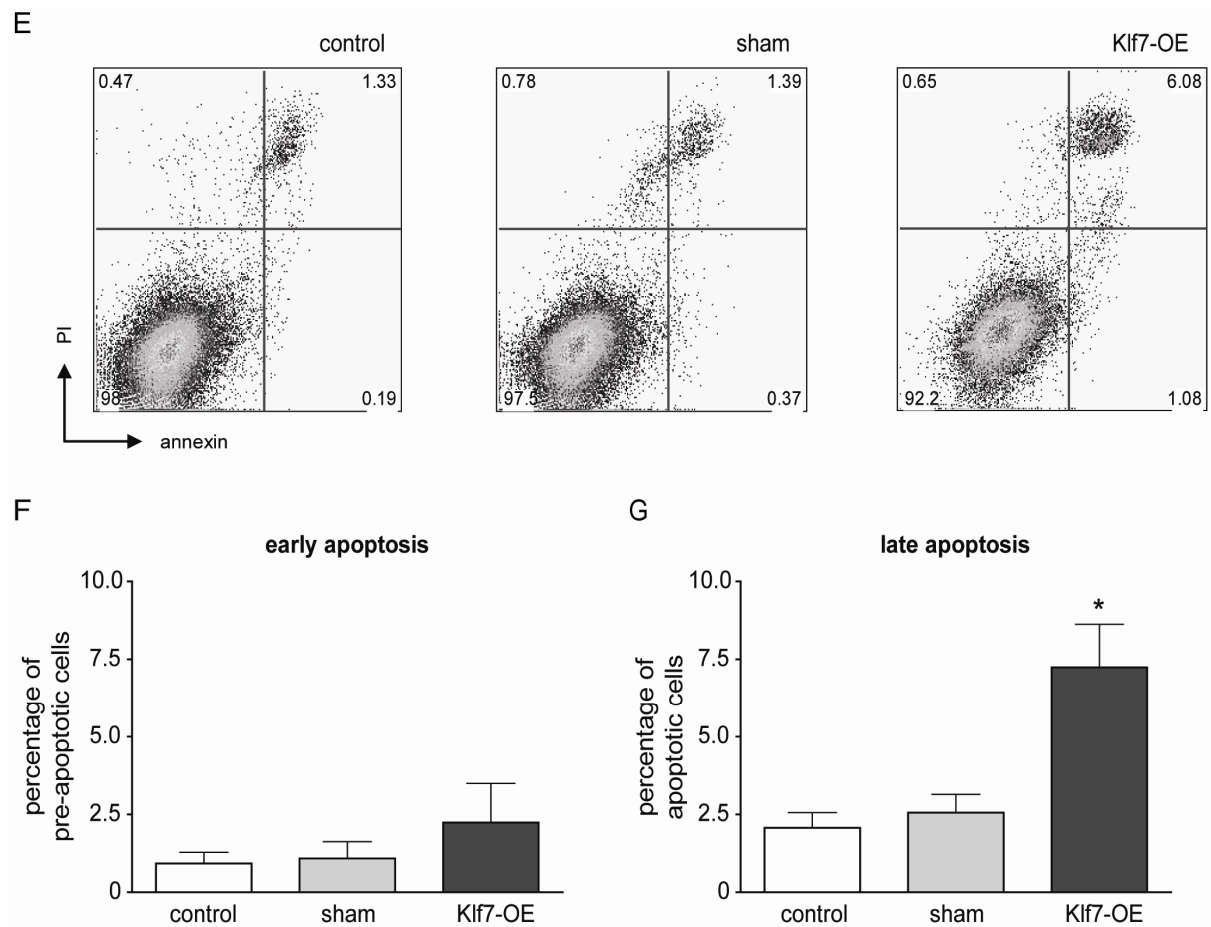
(**E**) Representative flow cytometric analysis of HUVECs. (**F-G**) Quantification of early and late apoptosis in HUVECs showed an increase of apoptosis after Klf7-OE, as analysed by flow cytometry: (**F**) early apoptosis and (**G**) late apoptosis (n = 4; mean ± SEM).

## Klf7 regulates p21$^{Cip1/Waf1}$ activity

Cell cycle progression is controlled by many different proteins, including cyclins, CDKs and CDK inhibitors.[3,5] Western blot analysis demonstrated that the downstream signalling cascade of Klf7 was affected (Figure 6A, B); overexpression of Klf7 (Figure 6A) increased signal transduction via p21$^{Cip1/Waf1}$ by upregulation of p21$^{Cip1/Waf1}$ protein levels (Figure 6B). These data demonstrate that Klf7 regulates G1–S-phase transition via p21$^{Cip1/Waf1}$.
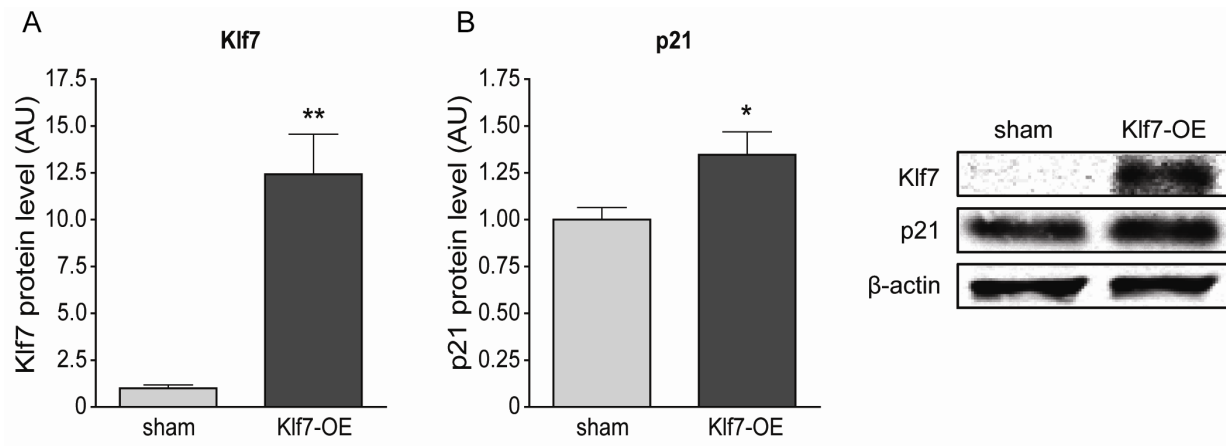
**Figure 6. Klf7 stimulates p21<sup>Cip1/Waf1</sup> activity.** Western blot analysis of (**A**) HUVECs infected with Klf7 adenovirus (Klf7-OE) showed an increased activation of (**B**) p21<sup>Cip1/Waf1</sup> (n = 5; mean ± SEM).

## *Discussion*

In this study we demonstrated that Klf7 regulates EC proliferation during *in vitro* vascular network-formation. Overexpression of Klf7 led to diminished G1–S-phase transition during cell cycle progression.

We demonstrated that Klf 7 was upregulated at various stages of murine embryonic development. Klf-like gene products were also identified before in lower vertebrate and invertebrate organisms, in which they control blood vessel formation, erythroid differentiation and epidermal development during embryogenesis.[19,20] In zebrafish, Klf7 is mainly expressed in neuronal tissue, including the olfactory vesicle, cranial ganglia, and neurons in the marginal zone and ganglion cell layer of the retina (*www.zfin.org*). Further reports indicate that Klf7 is an important regulator of axon regeneration in zebrafish.[21] In our study, knockdown of Klf7 in the developing zebrafish with morpholino (MO) injections resulted in no obvious defects (data not shown). Unlike a vascular expression pattern and/or vascular phenotype for Klf7 in zebrafish wasn't found, a role for Klf7 in vascular development can't be excluded. It is known that Klf family members have developed independently in different species, thus direct functional analogies by comparison of mammalian and non-mammalian Klf proteins may be unreliable.[9] In addition, it has been reported that Klf7 was highly expressed throughout the brain and kidney during murine embryogenesis, whereas in adult life Klf7 expression was more restricted to the cerebellum and spinal cord.[2,17,18] During murine development, Klf7 mRNA accumulate at embryonic day (E)9.5 in the central and peripheral nervous system and reach its maximum around E11.5-13.5 - the period of synaptogenesis.[2] In isolated endothelial precursor cells, we found

a maximum of Klf7 expression around E9.0 which corresponds with the period of angiogenesis. Also in cultured ECs Klf7 was highly expressed. Based on the period and specific expression of Klf7 in the EC subset, we hypothesised that Klf7 may play a functional role in blood vessel formation. Indeed, overexpression of Klf7 in a vascular network-formation assay resulted in less capillary tubule formation and branching.

To obtain more insight in the molecular mechanism by which Klf7 affect vascular growth, we analysed PI by flow cytometry, demonstrating that overexpression of Klf7 in HUVECs blocks the G1–S-phase transition. Further evaluation of the downstream pathway of Klf7 identified p21$^{Cip1/Waf1}$ as a downstream effector of Klf7. It was previously reported in 293T cells that Klf7 binds to the proximal promoter of this CDK inhibitor.[22] Overexpression of Klf7 *in vitro* and *in vivo* in different cell types resulted in a decrease in DNA synthesis, induction of p21$^{Cip1/Waf1}$ and inhibition of cyclin D1, which leads to a G1-arrest and induce terminal differentiation or maintenance of a quiescent phenotype.[2,4,17,18,22,23] Together, these findings provide further proof that Klf7 has a critical role in the decision between EC proliferation and cell cycle arrest/differentiation (Figure 7).

p21$^{Cip1/Waf1}$ plays also additional roles outside of the nucleus.[3,24] Previously, it has been demonstrated that p21$^{Cip1/Waf1}$ is involved in the regulation of actin cytoskeleton dynamics through inhibition of the Rho-ROCK-LIMK pathway and in this way promote neurite outgrowth.[3,17,25,26] Thereafter, p21$^{Cip1/Waf1}$ also counteract the apoptotic process in human HepG2 hepatoma cells by binding pro-caspase 3 and blocks its activation, thus protecting cells against apoptosis.[7] Followed on G1-arrest, we found *in vitro* an increase in apoptosis after Klf7 overexpression. Reports suggest that prolonged G1-arrest can activate death-promoting factors, thus in this way probably by-passing the suspected protective effect of increased p21$^{Cip1/Waf1}$ levels.[27]

To bind GC-rich promoters, Klf7 has to be transported to the nucleus.[18] Reports indicate that shuttling of Klf7 is directed by MoKA - a co-activator of Klf7. MoKA and Klf7 were co-expressed in cells that withdraw from the cell cycle. High levels of MoKA were found in the brain, branchial arches and limbs around E10.5 during murine embryogenesis, and low levels in all adult tissues.[22] We detected Klf7 in the Golgi apparatus where most of the Klf proteins are modified by phosphorylation and glycosylation to generate function specificity.[18] Co-immunoprecipitation identified MoKA as a possible binding partner of Klf7 in cultured ECs, but MoKA was also pulled down by the isotype control (data not shown). The different developmental stages in which Klf7 (maximum around E9.0) and MoKA (maximum around E10.5) were transcribed could suggest an independent involvement of the two proteins in different regulatory pathways in ECs. The ability of MoKA to bind Klf7 can also depend on the cellular context in which both proteins can be find, for example *in vitro* or *in vivo* conditions, or primary versus established cells.[9,11,18]
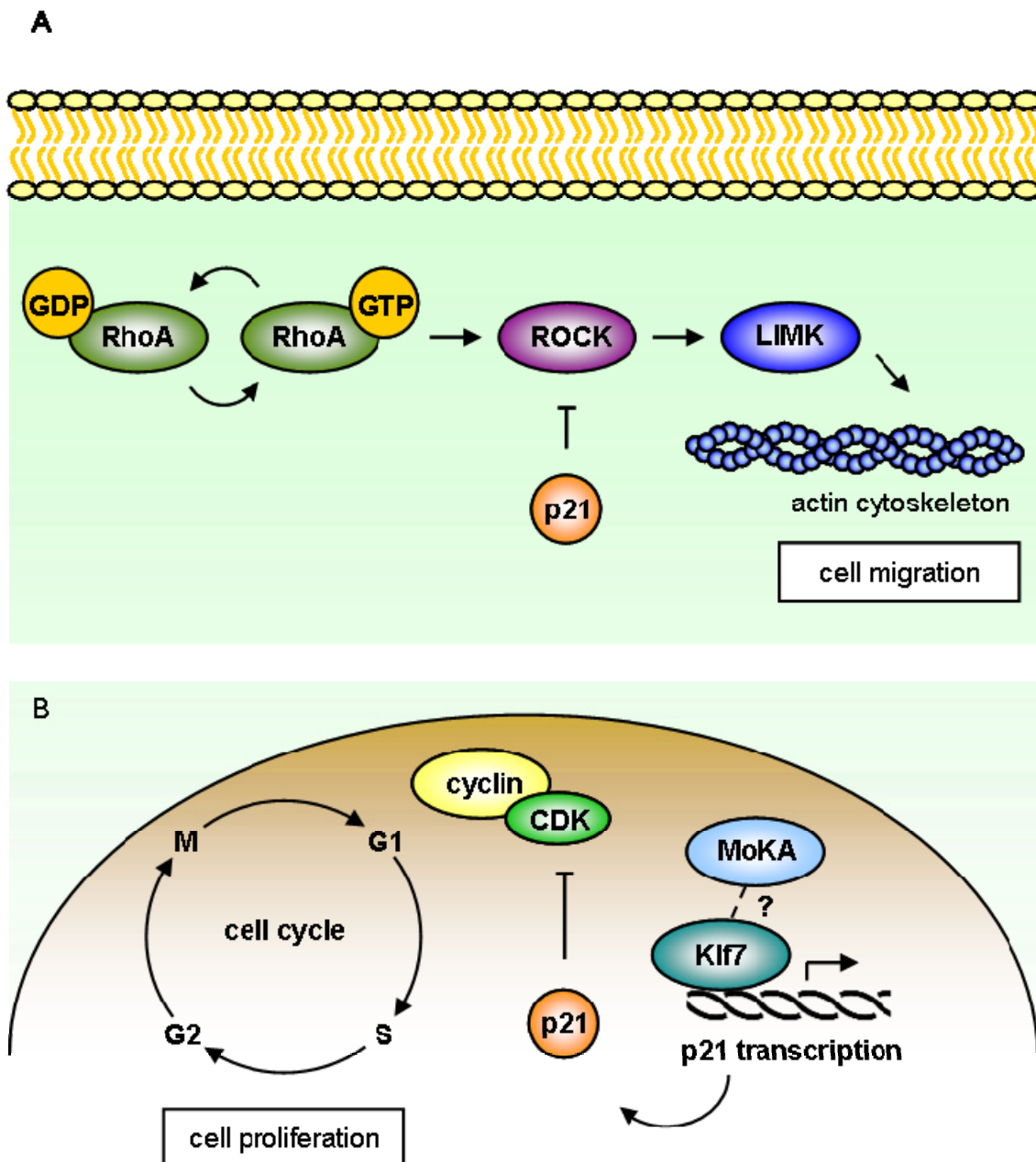
**Figure 7. Molecular pathway of Klf7 during angiogenesis.** (**A**) Hypothetical: outside of the nucleus, p21$^{Cip1/Waf1}$ regulates actin cytoskeleton dynamics through inhibition of the Rho-ROCK-LIMK pathway and in this way endothelial cell migration. Klf7 possibly influence this process indirectly. (**B**) Klf7 regulates endothelial cell proliferation by activating p21$^{Cip1/Waf1}$ transcription and activity which results in diminished cell proliferation by inhibiting G1–S-phase transition. MoKA possibly binds Klf7 as co-activator.

In conclusion, here we have identified Klf7 as a new regulator of EC proliferation and differentiation in vascular development by downstream activation of p21$^{Cip1/Waf1}$, which leads to G1-arrest and ultimately to cell cycle withdrawal. To our knowledge, this study is the first report of the function of Klf7 in ECs during normal embryonic and postnatal blood vessel formation. Interestingly, three other Klf family members - Klf2, Klf4 and Klf6 - are also expressed in vascular ECs.[28-31] Klf6 is closely related to Klf7 and show overlapping functions in cell differentiation.[2,18] Loss of Klf6 is associated with impaired haematopoiesis, while overexpression enhance the haematopoietic potential of embryonic stem cells.[32,33] Based on our findings, Klf7 and Klf6 might be involved also much earlier in embryogenesis at the moment when haemangioblasts differentiate into haematopoietic stem cells and angioblasts. Additional research is needed to provide further evidence for this potential role in primitive vascular plexus formation.

## *References*

1. Conway EM, Collen D, Carmeliet P. Molecular mechanisms of blood vessel growth. *Cardiovasc Res.* 2001;49(3):507-521.
2. Laub F, Aldabe R, Friedrich V Jr, Ohnishi S, Yoshida T, Ramirez F. Developmental expression of mouse Krüppel-like transcription factor Klf7 suggests a potential role in neurogenesis. *Dev Biol.* 2001;233(2):305-318.
3. Denicourt C, Dowdy SF. Cip/Kip proteins: more than just CDKs inhibitors. *Genes Dev.* 2004;18(8):851-855.
4. Gartel AL, Tyner AL. Transcriptional regulation of the p21Cip1/Waf1 gene. *Exp Cell Res.* 1999;246(2):280-289.
5. Morgan DO. Principles of CDK regulation. *Nature.* 1995;374(6518):131-134.
6. Chang BD, Watanabe K, Broude EV, Fang J, Poole JC, Kalinichenko TV, Roninson IB. Effects of p21Cip1/Waf1/Sdi1 on cellular gene expression: implications for carcinogenesis, senescence and age-related diseases. *Proc Natl Acad Sci U S A.* 2000;97(8):4291-4296.
7. Dotto GP. p21Cip1/Waf1: more than a break to the cell cycle? *Biochim Biophys Acta.* 2000;1471(1):M43-M56.
8. Mitchell PJ, Tjian R. Transcriptional regulation in mammalian cells by sequence-specific DNA binding proteins. *Science.* 1989;245(4916):371-378.
9. Bieker JJ. Krüppel-like factors: three fingers in many pies. *J Biol Chem.* 2001;276(37):34355-34358.
10. Philipsen S, Suske G. A tale of three fingers: the family of mammalian Sp/XKLF transcription factors. *Nucleic Acids Res.* 1999;27(15):2991-3000.

11. Turner J, Crossley M. Mammalian Krüppel-like transcription factors: more than just a pretty finger. *Trends Biochem Sci.* 1999;24(6):236-240.

12. Suske G, Bruford E, Philipsen S. Mammalian Sp/KLF transcription factors: bring in the family. *Genomics.* 2005;85(5):551-556.

13. Kaczynski J, Cook T, Urrutia R. Sp1- and Krüppel-like transcription factors. *Genome Biol.* 2003;4(2):206.

14. Black AR, Black JD, Azizkhan-Clifford J. Sp1 and Krüppel-like factor family of transcription factors in cell growth regulation and cancer. *J Cell Physiol.* 2001;188(2):143-160.

15. Dang DT, Pevsner J, Yang VW. The biology of the mammalian Krüppel-like family of transcription factors. *Int J Biochem Cell Biol.* 2000;32(11-12):1103-1121.

16. Kajimura D, Dragomir C, Ramirez F, Laub F. Identification of genes regulated by transcription factor Klf7 in differentiating olfactory sensory neurons. *Gene.* 2007;388(1-2):34-42.

17. Laub F, Lei L, Sumiyoshi H, Kajimura D, Dragomir C, Smaldone S, Puche AC, Petros TJ, Mason C, Parada LF, Ramirez F. Transcription factor Klf7 is important for neuronal morphogenesis in selected regions of the nervous system. *Mol Cell Biol.* 2005;25(13):5699-5711.

18. Matsumoto N, Laub F, Aldabe R, Zhang W, Ramirez F, Yoshida T, Terada M. Cloning the cDNA for a new human zinc finger protein defines a group of closely related Krüppel-like transcription factors. *J Biol Chem.* 1998;273(43):28229-28237.

19. Huber TL, Perkins AC, Deconinck AE, Chan FY, Mead PE, Zon LI. Neptune, a Krüppel-like transcription factor that participates in primitive erythropoiesis in Xenopus. *Curr Biol.* 2001;11(18):1456-1461.

20. Oates AC, Pratt SJ, Vail B, Yan YI, Ho RK, Johnson SL, Postlethwait JH, Zon LI. The zebrafish Klf gene family. *Blood.* 2001;98(6):1792-1801.

21. Veldman MB, Bemben MA, Thompson RC, Goldman D. Gene expression analysis of zebrafish retinal ganglion cells during optic nerve regeneration identifies Klf6a and Klf7a as important regulators of axon regeneration. *Dev Biol.* 2007;312(2):596-612.

22. Smaldone S, Laub F, Else C, Dragomir C, Ramirez F. Identification of MoKA, a novel F-box protein that modulates Krüppel-like transcription factor 7 activity. *Mol Cell Biol.* 2004;24(3):1058-1069.

23. Harper JW, Adami GR, Wei N, Keyomarsi K, Elledge SJ. The p21 Cdk-interacting protein Cip1 is a potent inhibitor of G1 cyclin-dependent kinases. *Cell.* 1993;75(4):805-816.

24. Coqueret O. New roles for p21 and p27 cell-cycle inhibitors: a function for each cell compartment? *Trends Cell Biol.* 2003;13(2):65-70.

25. Lee S, Helfman DM. Cytoplasmic p21Cip1 is involved in Ras-induced inhibition of the ROCK/LIMK/cofilin pathway. *J Biol Chem.* 2004;279(3):1885-1891.

26. Tanaka H, Yamashita T, Asada M, Mizutani S, Yoshikawa H, Tohyama M. Cytoplasmic p21Cip1/Waf1 regulates neurite remodelling by inhibiting Rho-kinase activity. *J Cell Biol.* 2002;158(2):321-329.

27. Tentner AR, Lee MJ, Ostheimer GJ, Samson LD, Lauffenburger DA, Yaffe MB. Combined experimental and computational analysis of DNA damage signalling reveals context-dependent roles for Erk in apoptosis and G1/S-arrest after genotoxic stress. *Mol Syst Biol.* 2012;8:568.

28. Atkins GB, Jain MK. Role of Krüppel-like transcription factors in endothelial biology. *Circ Res.* 2007;100(12):1686-1695.

29. Kojima S, Hayashi S, Shimokado K, Suzuki Y, Shimada J, Crippa MP, Friedman SL. Transcriptional activation of urokinase by the Krüppel-like factor Zf9/COPEB activates latent TGF-beta1 in vascular endothelial cells. *Blood.* 2000;95(4):1309-1316.

30. Yet SF, McA'Nulty MM, Folta SC, Yen HW, Yoshizumi M, Hsieh CM, Layne MD, Chin MT, Wang H, Perrella MA, Jain MK, Lee ME. Human EZF, a Krüppel-like zinc finger protein, is expressed in vascular endothelial cells and contains transcriptional activation and repression domains. *J Biol Chem.* 1998;273(2):1026-1031.

31. Kuo CT, Veselits ML, Barton KP, Lu MM, Clendenin C, Leiden JM. The LKLF transcription factor is required for normal tunica media formation and blood vessel stabilisation during murine embryogenesis. *Genes Dev.* 1997;11(22):2996-3006.

32. Schuettpelz LG, Gopalan PK, Giuste FO, Romine MP, van Os R, Link DC. Krüppel-like factor 7 overexpression suppresses haematopoietic stem and progenitor cell function. *Blood.* 2012;120(15):2981-2989.

33. Matsumoto N, Kubo A, Liu H, Akita K, Laub F, Ramirez F, Keller G, Friedman SL. Developmental regulation of yolk sac haematopoiesis by Krüppel-like factor 6. *Blood.* 2006;107(4):1357-1365.

# Chapter 4

## Tagln2 is essential for endothelial cell migration in angiogenesis

R.A. Haasdijk, C. Cheng, D. Tempel, R.L.J.M. Herpers, P.E. Bürgisser
E.H.M. van de Kamp, L.A.J. Blonden, S. Schulte-Merker, H.J. Duckers

## *Abstract*

**Objective** - Actin-binding proteins are involved in the migratory properties of hepatocellular carcinoma cells. However, the function of these proteins in endothelial cells (EC) requires further definition. Using a microarray screen for angiogenesis-associated genes during embryogenesis, we identified Transgelin 2 (Tagln2) as a new angiopotent factor with an undefined biological function. Here, we investigate the contribution of Tagln2 to EC migration during vascular development.

**Methods and Results** - Verification by *in situ* hybridisation in zebrafish demonstrated that Tagln2 is predominantly expressed in ECs. Knockdown of Tagln2 in zebrafish embryos resulted in ectopic sprouting of intersegmental vessels. In line with this finding, knockdown of Tagln2 in a murine retina model enhanced vascular outgrowth. Studies in human ECs verified the advantageous effect of Tagln2 downregulation on EC migration *in vitro* and identified Tagln2 as a new mediator of VEGF receptor 2 (VEGFR-2) synthesis.

**Conclusion** - Tagln2 is a crucial regulator of EC migration and VEGFR-2 turnover, both requirements for angiogenesis.

## *Introduction*

Migratory properties of endothelial cells (EC) are essential for vascular outgrowth during angiogenesis. One of the main factors that determines cell motility is the flexibility of the actin cytoskeleton. Microtubule dynamics contribute to the formation of protrusions - or lamellipodia - at the leading edge of the cell promoting directed migration, while on the other hand stress fibres are important for contraction of the cell body allowing forward progression.[1-3] Different proteins have been identified in the regulation of actin polymerisation, including profilin, cofilin and the Arp2/3 complex. All these proteins bind to the actin cytoskeleton and influence actin dynamics.[4-7] The tumour suppressor protein Transgelin 2 (Tagln2) - a Cdc2-related serine/threonine protein kinase - is also an actin-binding protein. In hepatocellular carcinoma cells, Tagln2 has an inhibitory effect on cell motility through its suppressive effect on actin polymerisation and stress fibre formation. The actin binding affinity of Tagln2 is controlled by PFTK1 through phosphorylation of Tagln2 serine residues. Reduction of PFTK1 expression in HKCI-4 cells affects the phospho-serine status of Tagln2 and results in accumulation of the total amount of Tagln2 protein. Unphosphorylated Tagln2 shows more physical interaction with actin, which leads to actin depolymerisation and a general reduction in migration. In contrast, Tagln2 downregulation in PFTK1-depleted cells rescues actin stress fibre formation.[8] Tagln2 is not only highly expressed in hepatocellular carcinoma cells, but also in other types of tumour cells and it is a well known marker of differentiated smooth muscle cells. Next to it, Tagln2 is expressed in ECs too, suggesting a possible involvement in EC function.[9-11] In spite of this, our knowledge of the role of Tagln2 in ECs remains limited. In this study, we have sought to characterise the basic biological function of Tagln2 in ECs during blood vessel formation *in vitro* using primary cell cultures and *in vivo* in zebrafish and murine vascular development.

Recently, we identified Tagln2 as a new potential regulator of angiogenesis from a genome-wide microarray analysis in search of genes involved in the regulation of new vessel formation. Gene expression profiles of isolated Flk1-positive angioblasts during murine embryonic development were compared with the profiles of Flk1-negative cells. Subsequently, our data show that Tagln2 plays an important role in the regulation of EC migration during angiogenesis. *In vivo*, a loss of Tagln2 led to ectopic sprouting of intersegmental vessels (ISV) in developing zebrafish, whereas an increased outgrowth of the vasculature was detected during postnatal vascular retinal development in mice. Further *in vitro* studies demonstrate that silencing of Tagln2 stimulated EC migration and enhanced VEGF receptor 2 (VEGFR-2) synthesis. Together, these findings contribute to the basic understanding of how Tagln2 plays an important role in the basic regulation of EC migration during vascular development.

## *Methods*

This study was carried out in accordance with the Council of Europe Convention (ETS123)/Directive (86/609/EEC) for the protection of vertebrate animals used for experimental and other scientific purposes and with the approval of the National and Local Animal Care Committee.

**Zebrafish**

Zebrafish (*Danio rerio*) were maintained under standard laboratory conditions. The transgenic zebrafish line used was Tg(Kdrl:eGFP)[s843].[12]

**Whole-mount *in situ* hybridisation**

Template DNA for probe generation was obtained by direct amplification of the target gene from genomic DNA. The reverse primer was tagged with a T3 RNA polymerase promoter tail to allow direct *in vitro* transcription and generation of antisense probes after PCR purification. Antisense RNA probes of Tagln2 were generated by *in vitro* transcription using the digoxigenin RNA Labeling Mix from Roche (Woerden, The Netherlands). *In situ* hybridisation was carried out as previously described.[13] The following zebrafish primers were used: 5'-TTT AAT GGG CAT TTA TTG AG-3' (forward) and 5'-GGA TCC ATT AAC CCT CAC TAA AGG GAA CAG TGT GAG ACA AAG GAA GC-3' (reverse) (Biolegio, Nijmegen, The Netherlands).

**Morpholino injection**

Morpholinos (MO) against Tagln2 were obtained from Gene Tools (Philomath, USA) and resuspended in Milli-Q water containing 0.2% phenol red. Different doses of the MO were injected into single-cell stage zebrafish embryos as previously described.[14] MO knockdown efficiency was tested by reverse transcriptase PCR. The following zebrafish MOs were used: 5'-GGA CGG ACC TTT ATT TGC CAT TTT G-3' (MO Tagln2-ATG) and 5'-AAC TGA TTG CGG TGA CTT ACA CAT C-3' (MO Tagln2-splice).

**Mice**

Plugged FVB/N mice (*Mus musculus*) were ordered at Harlan (Indianapolis, USA). C57BL/6J mice were obtained from laboratory stock. They were maintained under standard husbandry conditions.

**Isolation of Flk1-positive and Flk1-negative cells from mouse embryos**

From eight to sixteen days post-fertilisation (dpf), embryos were collected from plugged FVB/N mice and homogenised. Cells were stained with PE-conjugated anti-mouse Flk1

antibody 1:50 (555308; BD, Breda, The Netherlands). Hoechst (Sigma-Aldrich, Zwijndrecht, The Netherlands) was used to select dead cells. Flk1-positive/Hoechst-negative cells and Flk1-negative/Hoechst-negative cells were sorted on a BD FACSCanto™ (Breda, The Netherlands). Isolation of mRNA was carried out using the RNeasy Mini Kit from Qiagen (Venlo, The Netherlands).

## Microarray analysis

Double stranded cDNA was generated from 5 µg mRNA. Biotin-labelled RNA was synthesised using the BioArray™ HighYield™ RNA Transcript Labeling Kit from ENZO Life Sciences (Raamsdonksveer, The Netherlands). After clean-up and fragmentation, approximately 20 µg of labelled cRNA was hybridised to the GeneChip® Mouse Genome 430 2.0 Array (Affymetrix, Santa Clara, USA). Rosetta Resolver® (Rosetta Biosoftware, Cambridge, USA) was used to get quantile normalised raw data from the arrays. These data were merged into OmniViz® (BioWisdom, Cambridge, UK) and a threshold minimum for intensities was set at 30. Fold differences were calculated from log averages determined by the different experimental conditions.

## Mouse model of retinal vascularisation

Two-day old C57BL/6J mice pups were anesthetised by placement on ice. One microlitre of Tagln2 targeting siRNA (si-Tagln2) (1.33 µg/µl) was injected into the left eye using a 33-Gauge needle (World Precision Instruments, Berlin, Germany). As a control, one microlitre of scrambled non-targeting siRNA (si-sham) (1.33 µg/µl) was injected into the right eye. siRNA was obtained from Thermo Fisher Scientific (Breda, The Netherlands). The following mix of mouse si-Tagln2 was used: 5'-CAU GAA UGG UUA AUA UAU A-3' – 5'-CGA GUU UGC UGA UUU UAA A-3' – 5'-GCA GGG ACU UAA UUU AUA G-3' – 5'-UGU GCA AGC UUA UUA AUU C-3'. Mice pups were killed five days after intra-ocular injection. The retinas were stained with Alexa Fluor® 488-conjugated isolectin GS-IB$_4$ 1:200 (I21411; Invitrogen, Bleiswijk, The Netherlands) before assessment under a fluorescence microscope (Axiovert S100; Carl Zeiss, Sliedrecht, The Netherlands). Image analysis of the number of junctions, tubules and total tubule length was carried out using Angiosys Image Analysis Software 1.0 (TCS CellWorks, Buckingham, UK). Validation of adequate Tagln2 knockdown in the retina (two days after intra-ocular injection) was achieved by quantitative real time PCR using the following mouse primers: 5'-GTC TGG AAG ATG TCC GTG GT-3' (forward) and 5'-CTT CCA GAA GTG GCT CAA GG-3' (reverse) (Biolegio, Nijmegen, The Netherlands).

## Cell cultures

Primary cultures of human umbilical vein endothelial cells (HUVEC) were cultured in EBM®-2 medium supplemented with a commercial BulletKit, 10% foetal calf serum (FCS)

and 1% penicillin/streptomycin (Lonza, Breda, The Netherlands). Cells were cultured at 37°C in 5% $CO_2$. Passages three to six were used throughout the study.

**Immunofluorescence**

HUVECs - transfected with si-sham or si-Tagln2 - were grown in gelatin-coated 48-wells. After 24 hours, the cells were fixed in 4% formaldehyde and permeabilised with 0.2% Triton® X-100. Cells were incubated overnight at 4°C with Tagln2 antibody 1:200 (HPA001925; Sigma-Aldrich, Zwijndrecht, The Netherlands). For the detection of the primary antibody Alexa Fluor® 488 1:100 (Invitrogen, Bleiswijk, The Netherlands) was used. Actin filaments were stained with rhodamin-phalloidin 1:40 (R415; Invitrogen, Bleiswijk, The Netherlands). The nucleus was stained with 4,6-diamidino-2-phenylindole (DAPI) in Vectashield® mounting medium (H-1200; Vector Laboratories, Burlingame, USA). Cells were visualised with a fluorescence microscope (Axiovert S100; Carl Zeiss, Sliedrecht, The Netherlands).

**Targeted siRNA knockdown**

HUVECs were grown to 60-70% confluence and DharmaFECT1 Transfection Reagent was used to transfect 5 ng siRNA (Thermo Fisher Scientific, Breda, The Netherlands). The following mix of human si-Tagln2 was used: 5'-GCU CAU UAA UGC ACU GUA C-3' – 5'-GGC AGU AGC CCG AGA UGA U-3' – 5'-GCA AGA ACG UGA UCG GGU U-3' – 5'-GAA CAU GGC CUG UGU GCA G-3'. Si-sham was used as a control. Knockdown of Tagln2 was validated by quantitative real time PCR analysis and Western blot two days post-transfection using the following human primers: 5'-CCC TGA CAG AAA GGA GCT TG-3' (forward) and 5'-CGG AAC TTC TCG GAT AAC CA-3' (reverse) (Biolegio, Nijmegen, The Netherlands), and anti-human Tagln2 antibody 1:500 (HPA001925; Sigma-Aldrich, Zwijndrecht, The Netherlands). Beta-actin primers 5'-TCC CTG GAG AAG AGC TAC GA-3' (forward) and 5'-AGC ACT GTG TTG GCG TAC AG-3' (reverse) (Biolegio, Nijmegen, The Netherlands) were used as housekeeping gene, while beta-actin antibody 1:500 (ab8229; Abcam, Cambridge, UK) was used as a loading control.

For Tagln - a family member of Tagln2 - the following human primers were used: 5'-AAC AGC CTG TAC CCT GAT GG-3' (forward) and 5'-AGT GCC CAT CAT TCT TGG TC-3' (reverse) (Biolegio, Nijmegen, The Netherlands).

**Tagln2 adenovirus-induced overexpression**

HUVECs were cultured in EBM®-2 medium supplemented with a commercial BulletKit and infected with Tagln2 adenovirus (pAd-Tagln2) (MOI 50) or sham adenovirus (pAd-sham) (MOI 50) as control. Overexpression of Tagln2 was validated by quantitative real time PCR analysis and Western blot two days post-infection.

## 2D matrigel network-formation assay

To induce network-formation, HUVECs - transfected with si-sham or si-Tagln2 - were cultured on a 2D Matrigel$^{TM}$ matrix (BD, Breda, The Netherlands). The tubules were stained by Calcein-AM (BD, Breda, The Netherlands) after 24 hours of network-formation. Each condition was assessed by fluorescence microscopy (Axiovert S100; Carl Zeiss, Sliedrecht, The Netherlands). Image analysis of the number of junctions, tubules and total tubule length was carried out using Angiosys Image Analysis Software 1.0 (TCS CellWorks, Buckingham, UK).

## Migration assay

EC migration *in vitro* was evaluated by culturing HUVECs into wells with cell free areas created by micro-plug barriers. Migration distance was determined 18 hours after the micro-plug barriers were removed as previously described.[15]

In brief, cell free areas were created by inserting flexible micro-plugs (AMS Biotechnology, Germany) in gelatin-coated 96-wells. HUVECs were harvested with Accutase (Lonza, Breda, The Netherlands) 24 hours after transfection with si-sham/pAd-sham or si-Tagln2/pAd-Tagln2, and 50,000 cells were seeded per well in 100 μl EBM$^{®}$-2 medium supplemented with a commercial BulletKit (Lonza, Breda, The Netherlands). After 24 hours of incubation, the micro-plug barriers were removed before refreshing the medium. Cells were stained by Calcein-AM (BD, Breda, The Netherlands) after 18 hours of migration. Each condition was assessed by fluorescence microscopy (Axiovert S100; Carl Zeiss, Sliedrecht, The Netherlands). Migratory distance was determined using Axio Vision Software (Carl Zeiss, Sliedrecht, The Netherlands).

## Expression of VEGFR-2

In HUVECs - transfected with si-sham or si-Tagln2 - the expression of VEGFR-2 was determined by qPCR analysis two days post-transfection using the following human primers: 5'-AGC GAT GGC CTC TTC TGT AA-3' (forward) and 5'-ACA CGA CTC CAT GTT GGT CA-3' (reverse) for VEGFR-2 (Biolegio, Nijmegen, The Netherlands). Beta-actin primers 5'-TCC CTG GAG AAG AGC TAC GA-3' (forward) and 5'-AGC ACT GTG TTG GCG TAC AG-3' (reverse) (Biolegio, Nijmegen, The Netherlands) were used as housekeeping gene.

## Statistical analysis

Data were reported as mean ± standard error of the mean (SEM). Statistical significance was evaluated using a Student's *t*-test and was accepted at $P < 0.05$ (* $P < 0.05$, ** $P < 0.01$ in the figures).

## *Results*

### Expression of Tagln2 is upregulated during mouse embryogenesis

To identify new genes involved in angiogenesis, a genome-wide microarray analysis was carried out followed by validation of the results by qPCR. Gene expression profiles of Flk1-positive angioblasts at various stages of murine embryonic development were compared with the profiles of Flk1-negative cells. Tagln2 was upregulated in Flk1-positive angioblasts from 8 to 16 dpf. Expression levels were highest upregulated around 10 dpf, which coincides with the period of angiogenesis in murine development and suggests a potential role of Tagln2 in blood vessel formation (Figure 1).
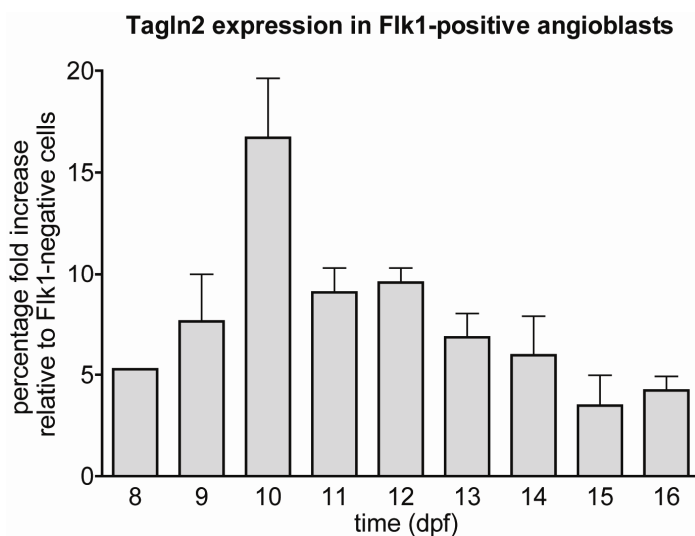


**Figure 1. Tagln2 is upregulated in Flk1-positive angioblasts during mouse development.** Endogenous expression level of Tagln2 in Flk1-positive angioblasts during murine embryonic development from 8 to 16 days post-fertilisation (dpf) compared with Flk1-negative cells as analysed by qPCR. The expression level of Tagln2 in Flk1-negative cells was arbitrarily set to one (n = 4; mean ± SEM). The highest upregulation was detected around day 10, which coincides with the period of angiogenesis in murine development.

### Tagln2 is expressed in the developing vasculature in zebrafish

To validate Tagln2 expression in the developing vascular network, we examined embryonic expression of the Tagln2 (SM22α-a) zebrafish orthologue by whole-mount *in situ* hybridisation. Tagln2 transcripts were localised in the main axial vessels - dorsal aorta and posterior cardinal vein - and ISVs at 26 hours post-fertilisation (hpf) (Figure 2A).

## Knockdown of Tagln2 in zebrafish results in ectopic sprouting of intersegmental vessels

To assess the function of Tagln2 *in vivo*, the gene was silenced in developing zebrafish of the Tg(Kdrl:eGFP)[s843] line, using MO-knockdown technology. Adequate targeting of Tagln2 was verified using RT-PCR analysis. Silencing of Tagln2 resulted in no obvious defects of vascular development during the first four days after fertilisation. However, at 5-6 dpf reduced vascularisation of the gills and hyperplasticity of the ISVs were observed in the injected embryos (Figure 2B).
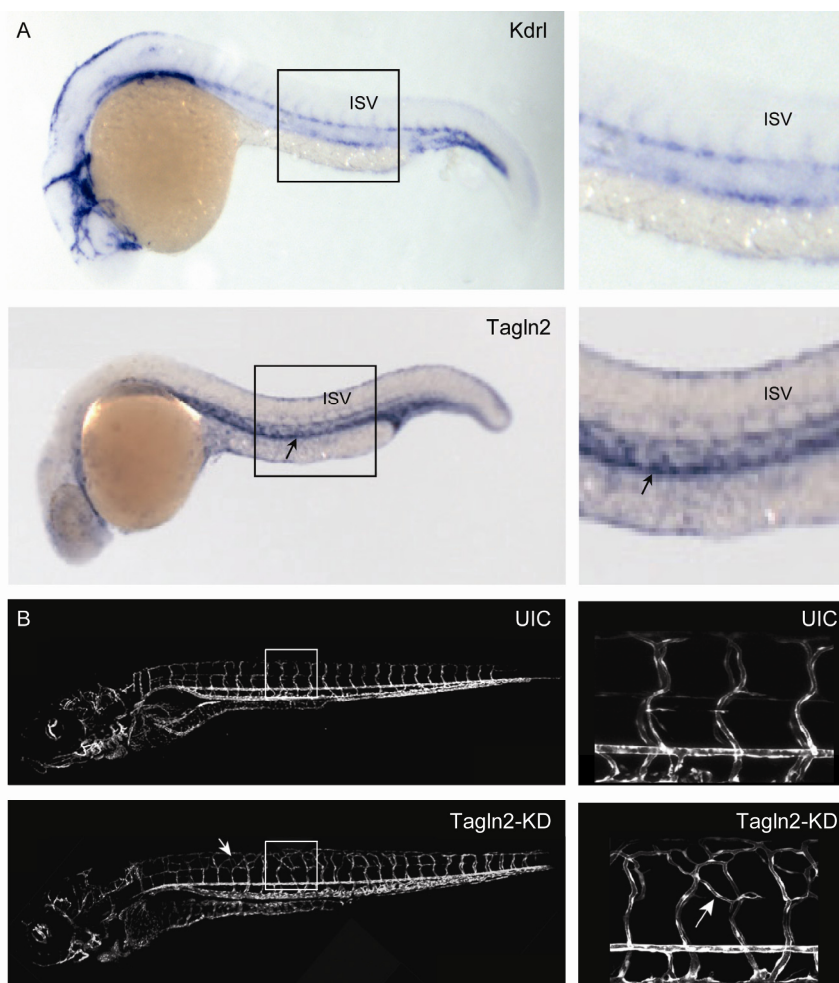


**Figure 2. Morpholino-induced knockdown of Tagln2 in zebrafish results in ectopic sprouting of intersegmental vessels.** (**A**) Whole-mount *in situ* hybridisation of Kdrl (upper panel) or Tagln2 (lower panel) in zebrafish larvae at 26 hours post-fertilisation (hpf), lateral view, anterior is to the left. Compared with Kdrl - endothelial specific -, Tagln2 transcripts were localised in the developing vascular network, including main axial vessels - dorsal aorta and posterior cardinal vein - (black arrow) and intersegmental vessels (ISV). (**B**) Tg(Kdrl:eGFP)[s843] embryos at 6 dpf, lateral view, anterior is to the left. Ectopic sprouting of ISVs (white arrow) was observed between the Tagln2 morpholino injected (Tagln2-KD) embryos and the uninjected control (UIC) embryos.

**Tagln2 knockdown in the developing retinal vasculature of neonatal mice promotes vascular outgrowth**

To further validate the findings in the zebrafish, Tagln2 function was studied during the development of the retinal vasculature of neonatal mice. Tagln2 knockdown was induced in the first week of retinal vascular development by intra-ocular injection of a siRNA pool composed of four different Tagln2 targeting siRNA sequences in two-day old wild-type C57BL/6J mouse pups and compared with controls injected with a scrambled non-targeting siRNA pool. Efficient knockdown of Tagln2 was observed two days after intra-ocular injection (Figure 3).
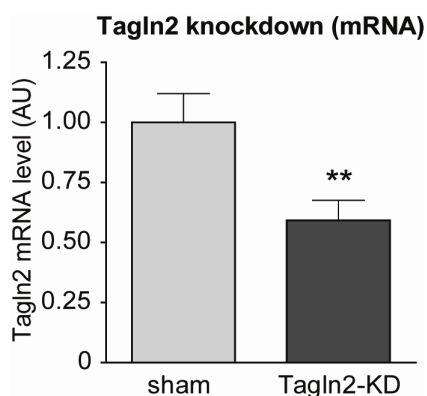


**Figure 3. Tagln2 depletion in the developing retinal vasculature of neonatal mice after siRNA targeting.** Endogenous expression level of Tagln2 in the retina after intra-ocular injection of Tagln2 targeting siRNA (Tagln2-KD) showed a reduction in expression levels of Tagln2 as analysed by qPCR (n = 10; mean ± SEM).

Like in the developing zebrafish, loss of Tagln2 expression had no primarily effect on vascular network-formation (Figure 4A). Assessment and quantification of the number of vascular branches, the total number of vessels and the total tubule length after visualisation of the vasculature by isolectin GS-IB$_4$ staining, identified no differences between si-Tagln2 and si-sham injected eyes five days after intra-ocular injection (Figure 4B-D). However, the outgrowth of the angiogenic front toward the retinal border reached significantly further in si-Tagln2 injected eyes than in si-sham injected eyes (Figure 4E, F). Combined, these data point towards an essential possible role for Tagln2 in EC migration during blood vessel development.
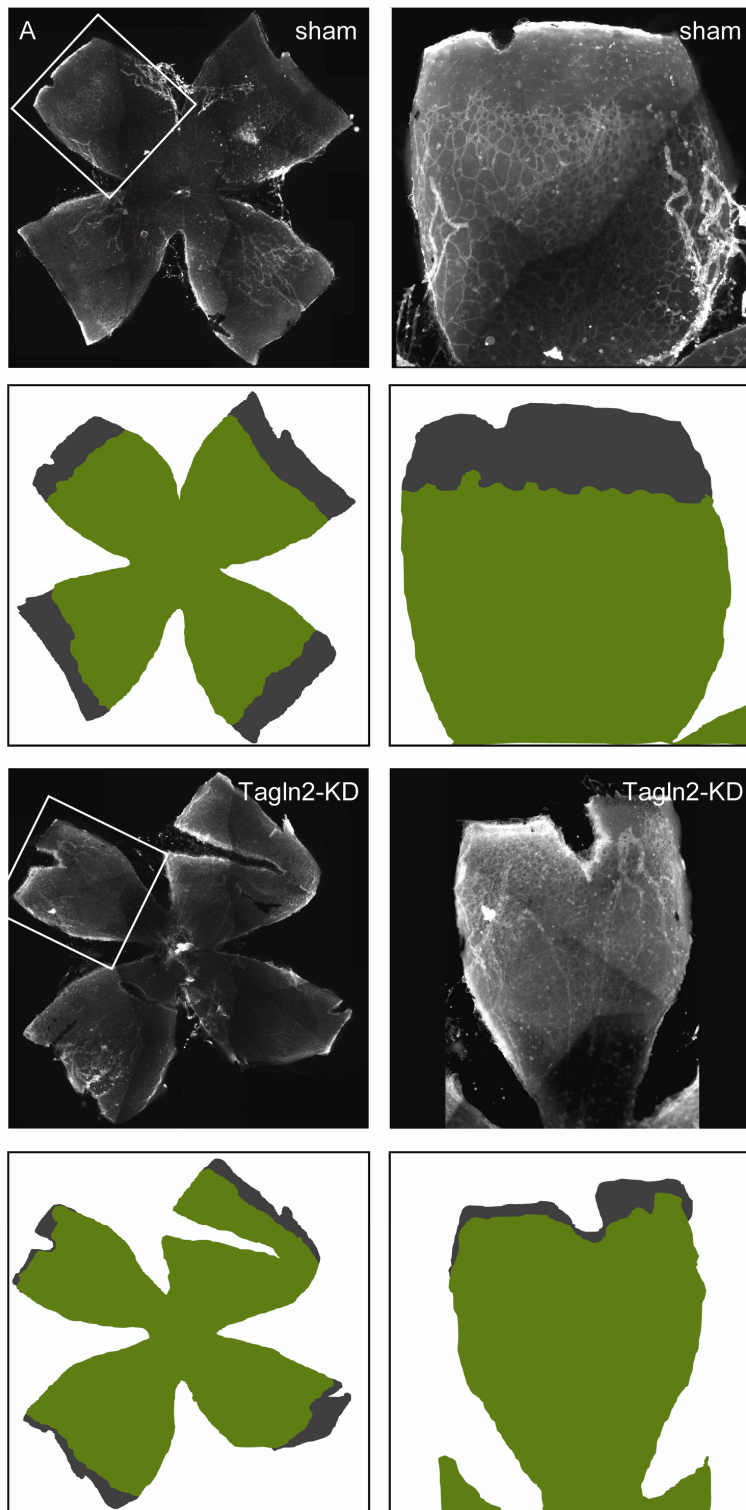
**Figure 4. Tagln2 depletion during murine retinal vascular development results in increased vascular outgrowth toward the retinal border.** (**A**) Whole-mount en-face staining of Tagln2 targeting siRNA (Tagln2-KD) versus scrambled non-targeting siRNA (sham) injected retinas. Isolectin GS-IB$_4$-FITC was used to visualise the retinal vasculature (green in the schematic representation of the retina, whereas dark gray shows the avascularised area).
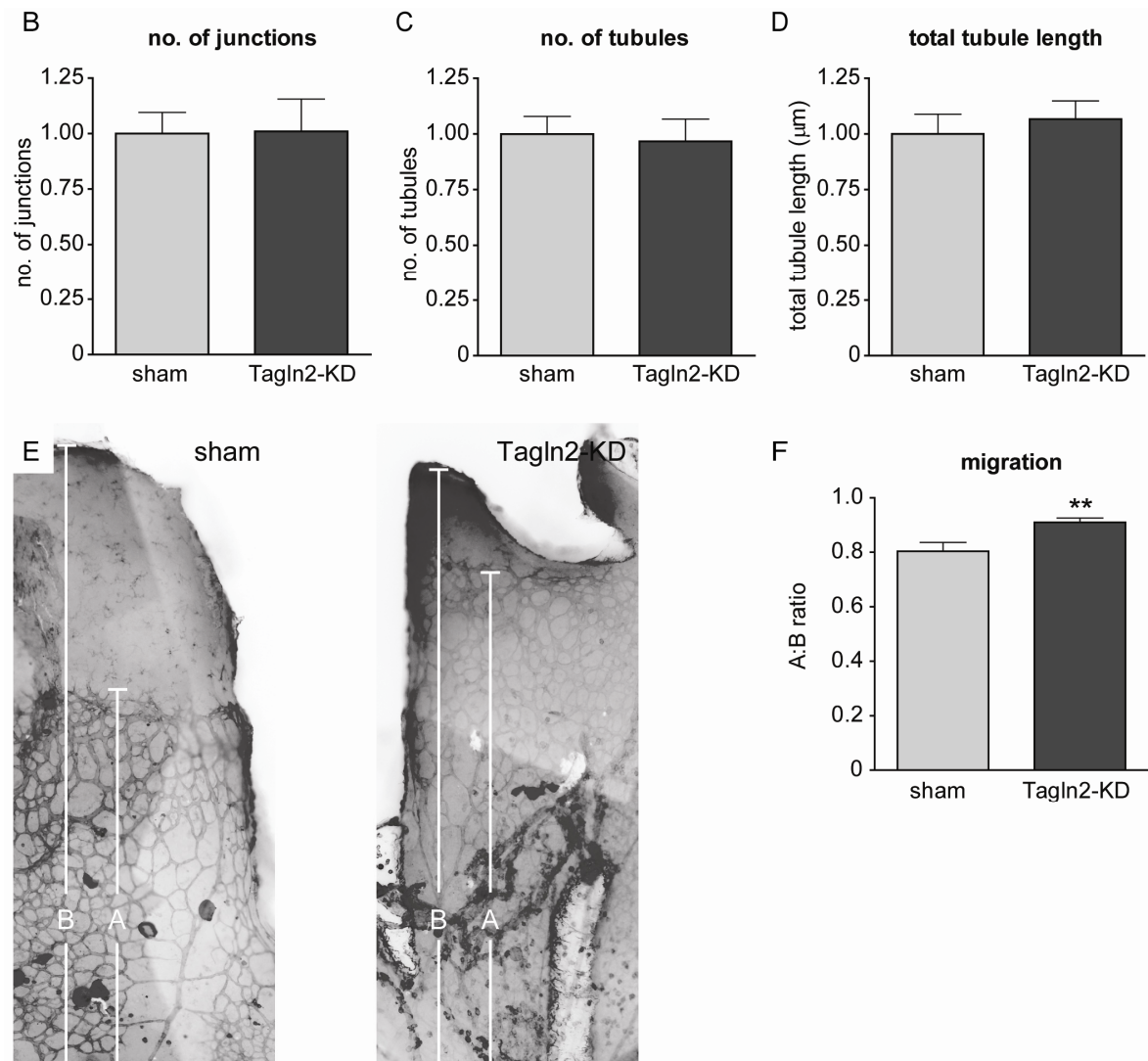
(**B-D**) Quantification by means of the dimensions of the vascular network showed no obvious defects after Tagln2-KD: (**B**) number of junctions, (**C**) number of tubules and (**D**) total tubule length remain unaffected. (**E**) Retinas stained with isolectin GS-IB$_4$ (endothelial cells, dark gray) demonstrate an increased vascular outgrowth toward the retinal border in the Tagln2-KD injected group. (**F**) Quantification of retinal vascular outgrowth expressed as the A:B ratio, where A is the distance from the optic disc to the border of the vascular network and B the distance from the optic disc to the retinal border, showed a 13% increase in Tagln2-KD versus sham injected retinas (n = 10; mean ± SEM).

## Tagln2 depletion promotes vascular network-formation and enhances endothelial cell migration *in vitro*

To clarify the molecular mechanism underlying the increased vascular outgrowth, we moved to *in vitro* assays to define Tagln2 function in vascular cells. Tagln2 mRNA expression was observed in HUVECs (data not shown). Intracellular immunofluorescent detection of Tagln2 in HUVECs demonstrated that the protein was mainly located near the

actin cytoskeleton and protein expression disappeared after Tagln2 knockdown (Figure 5A).
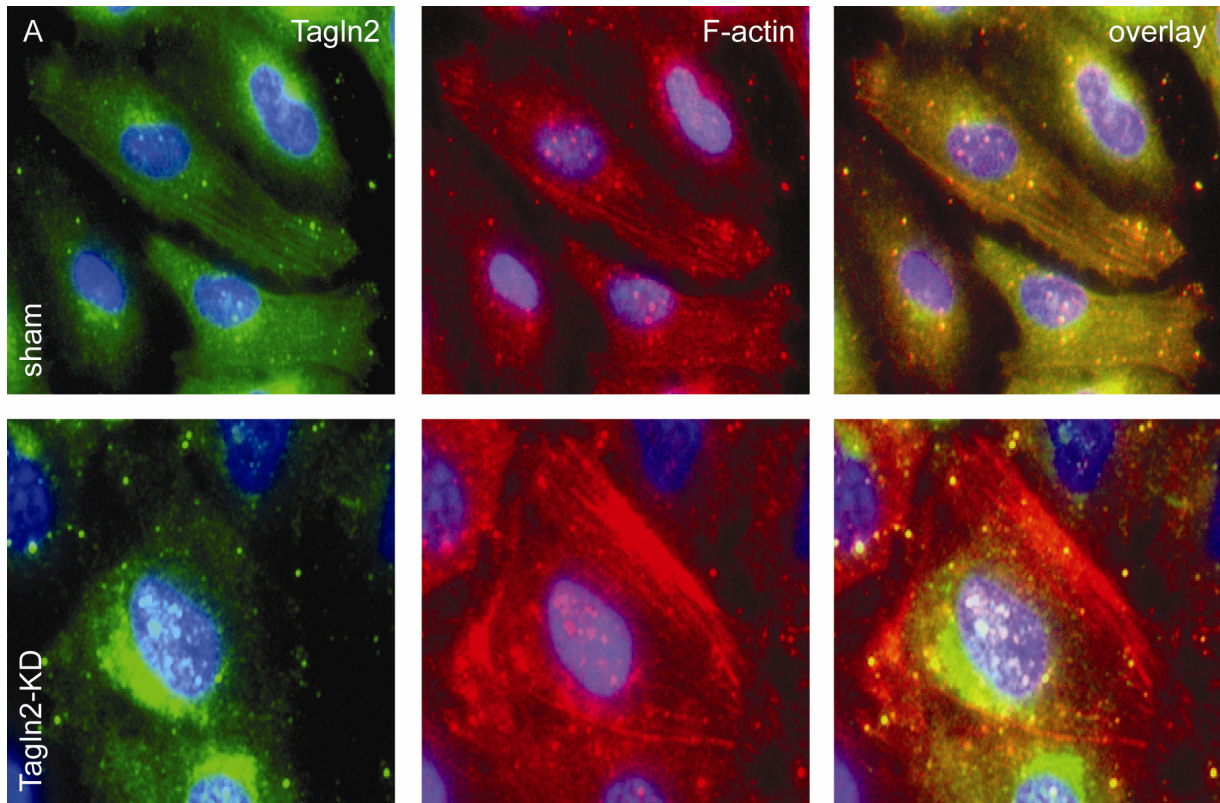


**Figure 5. Tagln2 knockdown in cultured endothelial cells promotes cell migration.** (**A**) Tagln2 was mainly located near the actin cytoskeleton, as demonstrated by immunofluorescent staining, with lack of signal in Tagln2-silenced ECs (Tagln2-KD). Tagln2 (green), F-actin (red), co-localised area (yellow) and nuclei (blue) (n = 3).

Whereas loss of Tagln2 did not affect network-formation *in vivo*, siRNA-mediated knockdown of Tagln2 in HUVECs affected network-formation in a stimulatory manner in a standard 2D matrigel analysis - as indicated by an increase in the number of junctions, capillary tubules and total tubule length - when compared with cultures transfected with equimolar of scrambled non-targeting siRNA and untransfected controls (Figure 5B-E).
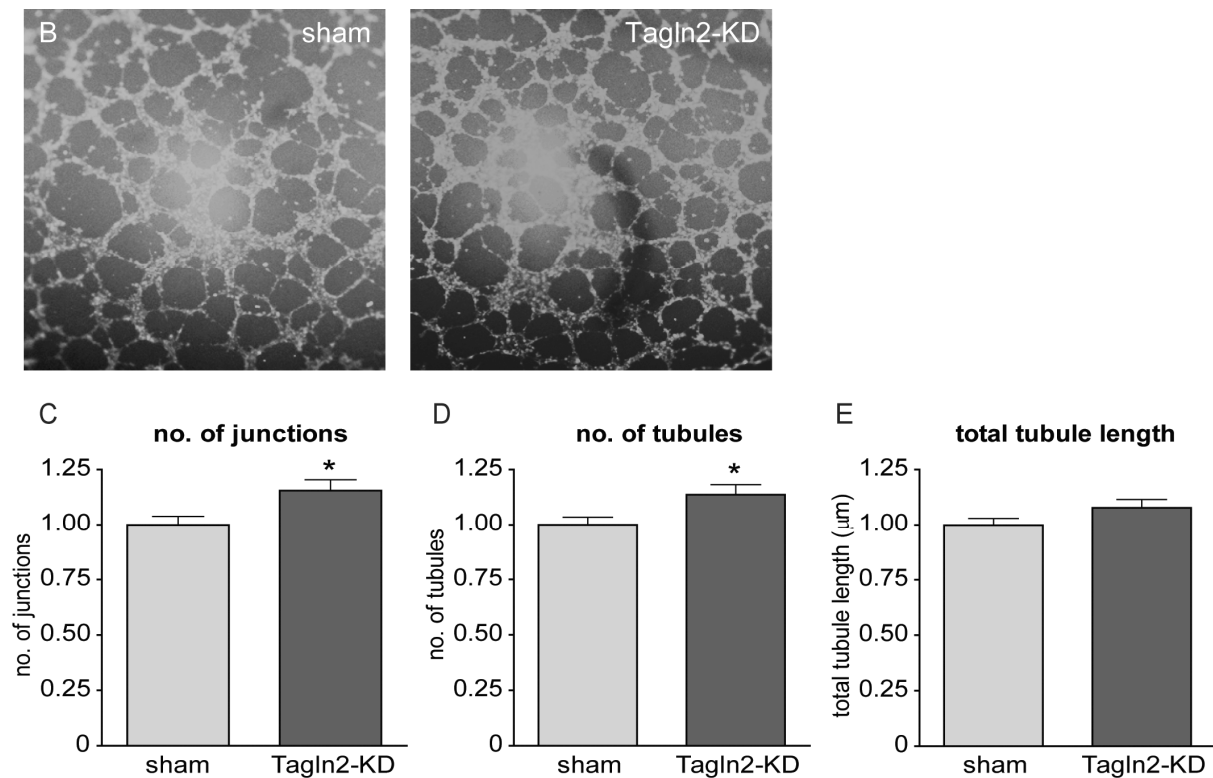
(**B**) Assessment of network-formation capacity in Tagln2-KD HUVECs in a 2D matrigel experiment. Tubules were stained by Calcein-AM uptake. (**C-E**) Quantification of the vascular network showed enhanced vascular branching in Tagln2-KD HUVECs: (**C**) number of junctions, (**D**) number of tubules and (**E**) total tubule length (n = 12; mean ± SEM).

Adequate knockdown of the target gene was validated on both mRNA and protein level, and did not affect the expression of the family member Tagln (Figure 6A-C). A migration assay was carried out to determine the effect of Tagln2 on migration in HUVECs. Similar to the *in vivo* findings, migration was significantly increased in Tagln2-depleted HUVECs (Figure 5F). In contrast, HUVECs transfected with an adenoviral plasmid expressing human Tagln2 cDNA showed the opposite effect with a significant decline in migration as compared with sham adenovirus-treated controls (Figure 5G, Tagln2 overexpression validation is shown in Figure 6D, E). The speed of migration is influenced by the rate of VEGFR-2 turnover.[16] qPCR analysis showed that Tagln2 depletion increased VEGFR-2 synthesis, implying increased rates of receptor turnover (Figure 5H). Combined, these findings demonstrate that Tagln2 contributes to angiogenesis involving EC migration, possibly by affecting VEGFR-2 turnover.
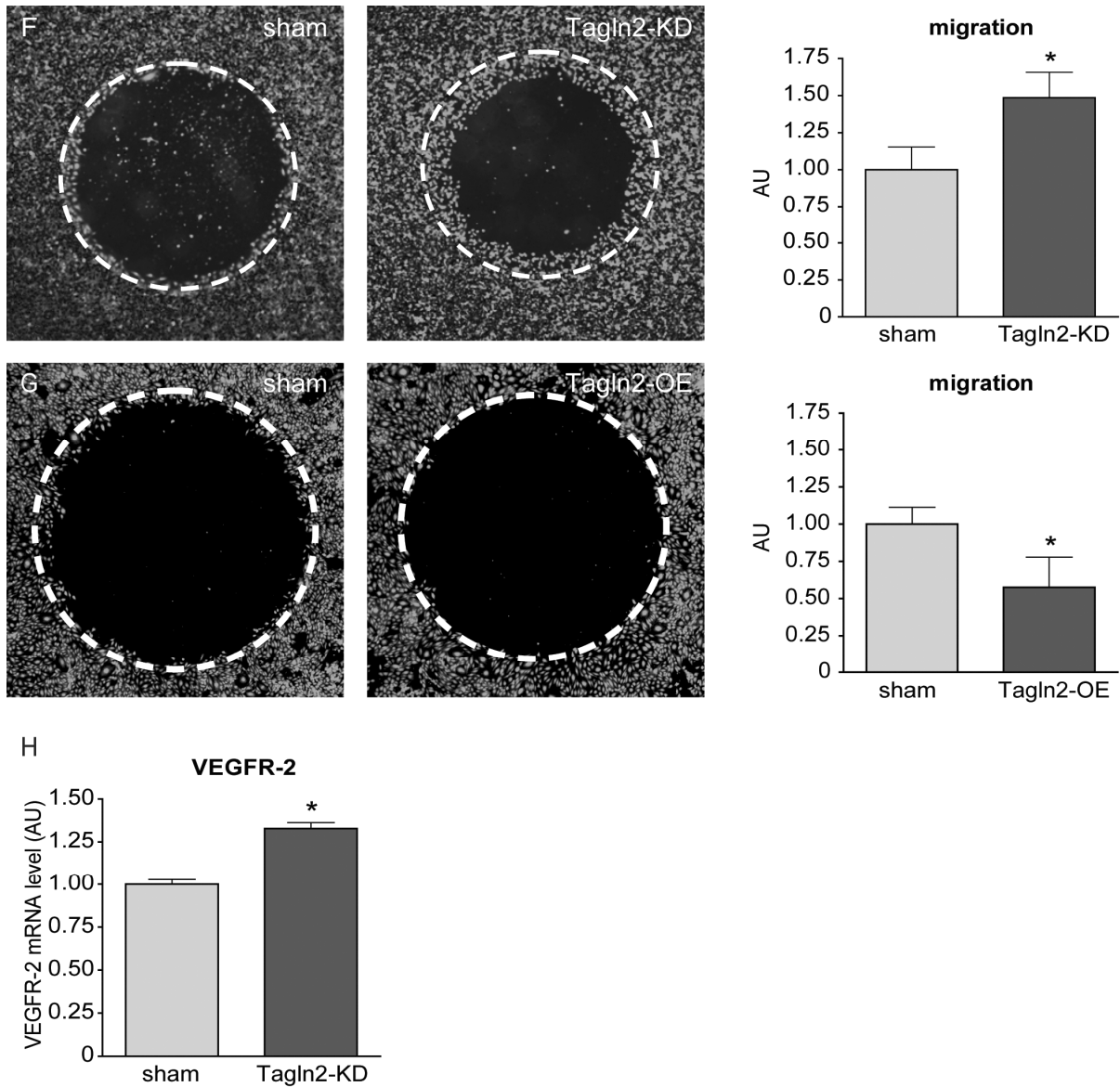
(**F, G**) Migration assay in which the white circle indicates the original cell-free area created by micro-plug barriers. Bar graph indicates the percentage of cell coverage of the cell-cleared area for the different groups after 18 hours of migration. Measurement of the migratory distance of ECs *in vitro* showed (**F**) enhanced migration of Tagln2-KD HUVECs versus sham (n = 7; mean ± SEM), while (**G**) Tagln2 overexpression (Tagln2-OE) showed a diminished migration of Tagln2-OE HUVECs versus sham (n = 4; mean ± SEM). (**H**) qPCR analysis of Tagln2-KD in HUVECs showed an increase in expression level of VEGFR-2 versus sham (n = 3; mean ± SEM).
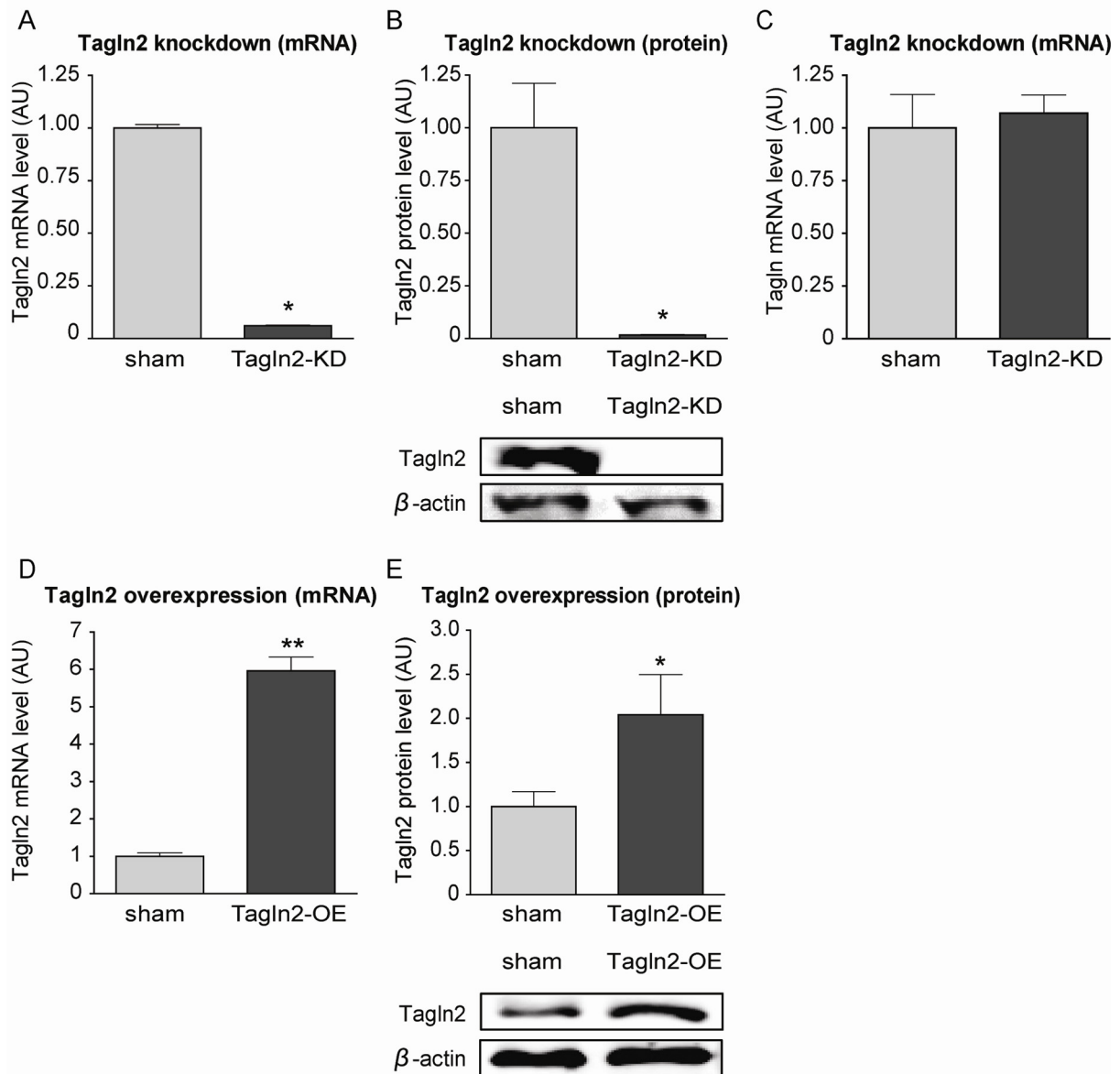
**Figure 6. siRNA-mediated knockdown and adenovirus-mediated overexpression of Tagln2 in cultured endothelial cells.** (**A**) qPCR analysis of HUVECs transfected with Tagln2 targeting siRNA (Tagln2-KD) showed a reduction in expression levels of Tagln2. (**B**) Western blot analysis of Tagln2-KD in HUVECs also showed a reduction in expression levels of Tagln2. (**C**) The expression levels of Tagln were not affected after Tagln2-KD in HUVECs as analysed by qPCR. (**D**) Overexpression of Tagln2 (Tagln2-OE) enhances Tagln2 expression levels as analysed by qPCR and (**E**) Western blot (n = 3; mean ± SEM).

## Discussion

In this study we have identified Tagln2 as a potent angiogenic regulator during embryonic and postnatal vascular development. We showed that Tagln2 was upregulated in the developing murine embryo in Flk1-positive angioblasts compared with Flk1-negative cells, while whole-mount *in situ* hybridisation in developing zebrafish larvae validated the predominant vascular expression of Tagln2. Furthermore, we demonstrated that Tagln2 is essential for EC migration during blood vessel formation in zebrafish and mice. Knockdown of Tagln2 in zebrafish and in the developing retinal vasculature of neonatal mice resulted in ectopic vessel formation and enhanced EC migration. *In vitro*, Tagln2 controls network-formation and EC migration.

The Tagln2 gene is one of the 72 genes in the human genome that encodes a calponin homology actin-binding domain or CH domain - a superfamily of actin-binding domains found in both cytoskeletal and signal transduction proteins.[17] At protein level, Tagln2 has a high homology (65%) with its family member Tagln - also known as SM22α - which is an early marker of differentiated smooth muscle cells.[8,11] The expression of SM22α is regulated by the transforming growth factor (TGF)-β signalling pathway, which is involved in mural cell recruitment during stabilisation of the newly formed vessel branches as a result of angiogenic sprouting.[18] During murine embryogenesis SM22α is mainly expressed in vascular smooth muscle cells (vSMC) and cardiac myocytes around embryonic day (E)9.5, the same period as Tagln2 expression.[19] Like Tagln2, SM22α acts as a tumour suppressor gene and inhibits the expression of matrix metalloproteinase 9 (MMP9).[20,21] MMPs are involved in the breakdown of the extracellular matrix (ECM) in physiological conditions such as angiogenic sprouting, or in disease processes like metastasis.[22-24] Based on the high homology of the SM22α and the Tagln2 protein, and the overlapping time period of expression during murine embryogenesis, we speculate that Tagln2 may be involved in early vessel stabilisation during angiogenesis.

In our study, knockdown of Tagln2 in zebrafish was characterised by ectopic sprouting of the ISVs, indicating a defect in EC migration or vessel stabilisation. ISVs develop via migration and division of ECs from the dorsal aorta and the cardinal vein, and are guided by attractive and repulsive signals from the external environment. Once these new branches touch other sprouts, they establish connections and the sprouting vessels fuse at the most dorsal region of the trunk to form the dorsal longitudinal anastomotic vessel (DLAV), followed by further vessel stabilisation.[25-29] Ectopic branching can be due to prolonged angiogenic sprouting behaviour of the ECs within the ISVs. Normally, the endothelium of neovessels become quiescent after tip cell fusion by VE-cadherin stabilisation, deposition of ECM components, mural cell recruitment and downregulation of the VEGFR-2 signalling pathway.[4,30-32] Several mutants have been identified in zebrafish that display a

similar ectopic branching phenotype of the ISVs that is similar to the Tagln2 MO-induced silenced zebrafish, including stl (= microsomal triglyceride transfer protein) and cdh5 (= VE-cadherin) mutants, and those with defects in the Dll4-Notch signalling pathway (rbpsuh, dll4, inhibition of γ-secretase).[25,27,33-37] All of these genes are involved directly or indirectly in tip cell formation, migration or vessel stabilisation. However, our data clearly show that ectopic sprouting of the ISVs took place at a later stage of development - around 5-6 dpf when the circulatory system has developed normally - which corresponds mostly with the stl mutant phenotype.[33] The stl gene encodes the microsomal triglyceride transfer protein (mtp). Via apolipoprotein B (ApoB) synthesis, mtp modulates VEGF receptor 1 (VEGFR-1) expression - a decoy receptor for VEGF with an inhibitory role in angiogenesis.[4,25,33] Loss of VEGFR-1 in zebrafish resembles the phenotype of stl mutants.[33] Thus, stl mutants show an indirect stimulatory effect on VEGFR-2 signalling. In cultured ECs, we demonstrated that Tagln2 depletion resulted in a direct stimulatory effect on the VEGFR-2 signalling pathway by increasing VEGFR-2 synthesis, which reflects enhanced VEGFR-2 turnover, which may inhibit EC transition from active - migratory, proliferative and pro-sprouting - into quiescence. In line with our findings on the effect of Tagln2 silencing on EC migration, high rates of VEGFR-2 turnover are indeed associated with migratory cells.[16] In addition, previous reports of direct or indirect stimulation of the VEGFR-2 signalling in mice show ectopic angiogenic sprouting due to lack of vessel stabilisation as a consequence of impaired cell-cell adhesion or less mural cell recruitment.[30,38,39] Sphingosine-1-phosphate receptor 1 (S1PR1) knockout mice exhibit increased formation of ectopic vessel branches with retained pericyte coverage at a relatively late developmental stage when vascular stabilisation is essential. S1PR1 signalling is involved in vascular stabilisation through inhibition of the VEGFR-2 signalling pathway, protecting blood vessels against prolonged angiogenic behaviour.[30] Our data clearly show that Tagln2 knockdown stimulated EC migration in retinal vascular development of mice, possibly due to a prolonged turnover of VEGFR-2 and subsequent angiogenic behaviour of newly formed blood vessels. Unless the outgrowth of the vascular network toward the retinal border was more extensive after Tagln2 knockdown compared with controls, the total tubule length was unchanged. This could be due to earlier remodelling of the vascular network in si-Tagln2 injected eyes, as a consequence of reaching the retinal border much earlier compared with controls.

EC migration is encouraged by actin polymerisation and lamellipodia formation which stimulates random formation of cell-cell contacts, reflected *in vitro* by an increase in the number of branching points during a 2D matrigel network-formation assay.[1,40,41] In accordance with these previous findings, we found that downregulation of the total amount of Tagln2 - including the active form - resulted in an increased number of branching points of *in vitro* network-formation, potentially as a result of increased lamellipodia formation

due to less actin depolymerisation by Tagln2 (Figure 7). These findings further provide supportive data that Tagln2 regulates EC migration by modulation of the actin cytoskeleton.
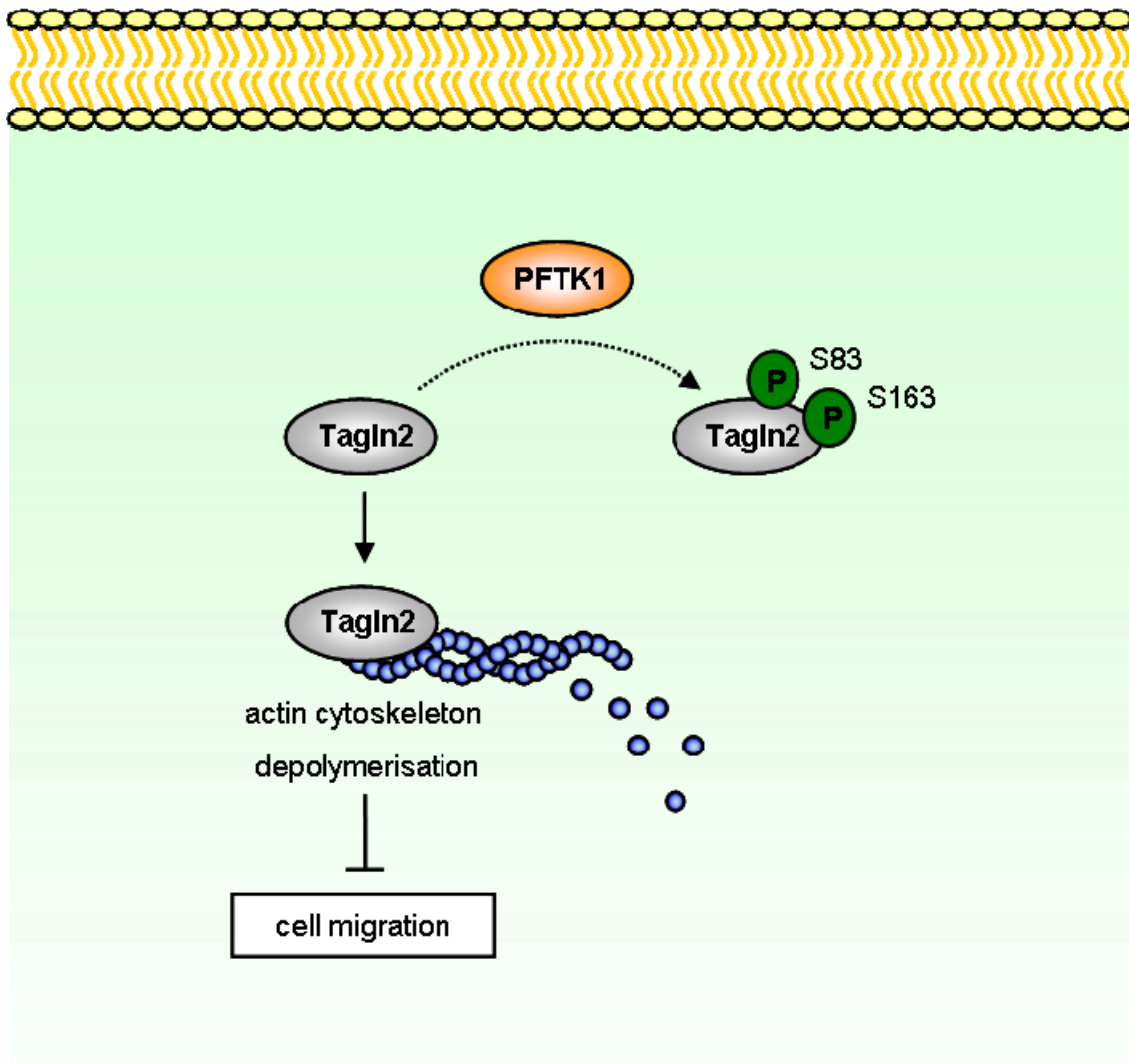


**Figure 7. Molecular pathway of Tagln2 during angiogenesis.** Active Tagln2 depolymerise the actin cytoskeleton, inhibiting lamellipodia formation, which is associated with less cell migration.

In conclusion, here we have identified Tagln2 as a new regulator of EC migration and vessel stabilisation in vascular development by stimulating actin depolymerisation and negatively regulating VEGFR-2 turnover, which leads to a quiescent phenotype of the ECs. To our knowledge, this study is the first report of the biological function of Tagln2 in ECs during normal embryonic and postnatal blood vessel formation. As mentioned before, the

effect of Tagln2 on cell motility has also been described in carcinoma cells.[8-10] In line with these findings, the gene may also be an interesting research target for the development of new therapeutics in the treatment of cancer metastasis in which both cancer cell spreading and tumour vascularisation are decisive factors in disease progression.

## *References*

1. Aman A, Piotrowski T. Cell migration during morphogenesis. *Dev Biol.* 2010;341(1):20-33.
2. Lamalice L, Le Boeuf F, Huot J. Endothelial cell migration during angiogenesis. *Circ Res.* 2007;100(6):782-794.
3. Garrett TA, Van Buul JD, Burridge K. VEGF-induced Rac1 activation in endothelial cells is regulated by the guanine nucleotide exchange factor Vav2. *Exp Cell Res.* 2007;313(15):3285-3297.
4. Galan Moya EM, Le Guelte A, Gavard J. PAKing up to the endothelium. *Cell Signal.* 2009;21(12):1727-1737.
5. Horowitz A, Simons M. Branching morphogenesis. *Circ Res.* 2008;103(8):784-795.
6. Heasman SJ, Ridley AJ. Mammalian Rho-GTPases: new insights into their functions from *in vivo* studies. *Nat Rev Mol Cell Biol.* 2008;9(9):690-701.
7. Dickson BJ. Rho-GTPases in growth cone guidance. *Curr Opin Neurobiol.* 2001;11(1):103-110.
8. Leung WK, Ching AK, Chan AW, Poon TC, Mian H, Wong AS, To KF, Wong N. A novel interplay between oncogenic PFTK1 protein kinase and tumour suppressor Tagln2 in the control of liver cancer cell motility. *Oncogene.* 2011;30(44):4464-4475.
9. Yoshida A, Okamoto N, Tozawa-Ono A, Koizumi H, Kiguchi K, Ishizuka B, Kumai T, Suzuki N. Proteomic analysis of differential protein expression by brain metastases of gynaecological malignancies. *Hum Cell.* 2013;26(2):56-66.
10. Elsner M, Rauser S, Maier S, Schöne C, Balluff B, Meding S, Jung G, Nipp M, Sarioglu H, Maccarrone G, Aichler M, Feuchtinger A, Langer R, Jütting U, Feith M, Küster B, Ueffing M, Zitzelsberger H, Höfler H, Walch A. MALDI imaging-mass spectrometry reveals COX7A2, Tagln2 and S100-A10 as novel prognostic markers in Barrett's adenocarcinoma. *J Proteomics.* 2012;75(15):4693-4704.
11. Stanier P, Abu-Hayyeh S, Murdoch JN, Eddleston J, Copp AJ. Paralogous SM22alpha (Tagln) genes map to mouse chromosomes 1 and 9: further evidence for a paralogous relationship. *Genomics.* 1998;51(1):144-147.

12. Jin SW, Beis D, Mitchell T, Chen JN, Stainier DY. Cellular and molecular analyses of vascular tube and lumen formation in zebrafish. *Development.* 2005;132(23):5199-5209.

13. Gjini E, Hekking LH, Küchler A, Saharinen P, Wienholds E, Post JA, Alitalo K, Schulte-Merker S. Zebrafish Tie-2 shares a redundant role with Tie-1 in heart development and regulates vessel integrity. *Dis Model Mech.* 2011;4(1):57-66.

14. Nasevicius A, Ekker SC. Effective targeted gene 'knockdown' in zebrafish. *Nat Genet.* 2000;26(2):216-220.

15. Cheng C, Haasdijk RA, Tempel D, den Dekker WK, Chrifi I, Blonden LA, van de Kamp EH, de Boer M, Bürgisser PE, Noordeloos A, Rens JA, ten Hagen TL, Duckers HJ. PDGF-induced migration of vascular smooth muscle cells is inhibited by haem oxygenase-1 via VEGFR-2 upregulation and subsequent assembly of inactive VEGFR-2/PDGFR-β heterodimers. *Arterioscler Thromb Vasc Biol.* 2012;32(5):1289-1298.

16. Nakayama M, Nakayama A, van Lessen M, Yamamoto H, Hoffmann S, Drexler HC, Itoh N, Hirose T, Breier G, Vestweber D, Cooper JA, Ohno S, Kaibuchi K, Adams RH. Spatial regulation of VEGF receptor endocytosis in angiogenesis. *Nat Cell Biol.* 2013;15(3):249-260.

17. Castresana J, Saraste M. Does Vav bind to F-actin through a CH domain? *FEBS Lett.* 1995;374(2):149-151.

18. Qiu P, Ritchie RP, Fu Z, Cao D, Cumming J, Miano JM, Wang DZ, Li HJ, Li L. Myocardin enhances Smad3-mediated transforming growth factor-beta1 signalling in a CArG box-independent manner: Smad-binding element is an important cis element for SM22alpha transcription *in vivo*. *Circ Res.* 2005;97(10):983-991.

19. Lepore JJ, Cheng L, Min Lu M, Mericko PA, Morrisey EE, Parmacek MS. High-efficiency somatic mutagenesis in smooth muscle cells and cardiac myocytes in SM22alpha-Cre transgenic mice. *Genesis.* 2005;41(4):179-184.

20. Gimona M, Grashoff C, Kopp P. Oktoberfest for adhesion structures. *EMBO Rep.* 2005;6(10):922-926.

21. Gimona M, Kaverina I, Resch GP, Vignal E, Burgstaller G. Calponin repeats regulate actin filament stability and formation of podosomes in smooth muscle cells. *Mol Biol Cell.* 2003;14(6):2482-2491.

22. Arroyo AG, Iruela-Arispe ML. Extracellular matrix, inflammation and the angiogenic response. *Cardiovasc Res.* 2010;86(2):226-235.

23. Nyberg P, Xie L, Kalluri R. Endogenous inhibitors of angiogenesis. *Cancer Res.* 2005;65(10):3967-3979.

24. Carmeliet P. Angiogenesis in health and disease. *Nat Med.* 2003;9(6):653-660.

25. Ellertsdóttir E, Lenard A, Blum Y, Krudewig A, Herwig L, Affolter M, Belting HG. Vascular morphogenesis in the zebrafish embryo. *Dev Biol.* 2010;341(1):56-65.

26. Blum Y, Belting HG, Ellertsdóttir E, Herwig L, Lüders F, Affolter M. Complex cell rearrangements during intersegmental vessel sprouting and vessel fusion in the zebrafish embryo. *Dev Biol.* 2008;316(2):312-322.

27. Roca C, Adams RH. Regulation of vascular morphogenesis by Notch signalling. *Genes Dev.* 2007;21(20):2511-2524.

28. Suchting S, Bicknell R, Eichmann A. Neuronal clues to vascular guidance. *Exp Cell Res.* 2006;312(5):668-675.

29. Zhong TP. Zebrafish genetics and formation of embryonic vasculature. *Curr Top Dev Biol.* 2005;71:53-81.

30. Gaengel K, Niaudet C, Hagikura K, Laviña B, Muhl L, Hofmann JJ, Ebarasi L, Nyström S, Rymo S, Chen LL, Pang MF, Jin Y, Raschperger E, Roswall P, Schulte D, Benedito R, Larsson J, Hellström M, Fuxe J, Uhlén P, Adams R, Jakobsson L, Majumdar A, Vestweber D, Uv A, Betsholtz C. The sphingosine-1-phosphate receptor S1PR1 restricts sprouting angiogenesis by regulating the interplay between VE-cadherin and VEGFR-2. *Dev Cell.* 2012;23(3):587-599.

31. Abraham S, Yeo M, Montero-Balaguer M, Paterson H, Dejana E, Marshall CJ, Mavria G. VE-cadherin-mediated cell-cell interaction suppresses sprouting via signalling to MLC2 phosphorylation. *Curr Biol.* 2009;19(8):668-674.

32. Grazia Lampugnani M, Zanetti A, Corada M, Takahashi T, Balconi G, Breviario F, Orsenigo F, Cattelino A, Kemler R, Daniel TO, Dejana E. Contact inhibition of VEGF-induced proliferation requires vascular endothelial cadherin, beta-catenin and the phosphatase DEP-1/CD148. *J Cell Biol.* 2003;161(4):793-804.

33. Avraham-Davidi I, Ely Y, Pham VN, Castranova D, Grunspan M, Malkinson G, Gibbs-Bar L, Mayseless O, Allmog G, Lo B, Warren CM, Chen TT, Ungos J, Kidd K, Shaw K, Rogachev I, Wan W, Murphy PM, Farber SA, Carmel L, Shelness GS, Iruela-Arispe ML, Weinstein BM, Yaniv K. ApoB-containing lipoproteins regulate angiogenesis by modulating expression of VEGF receptor 1. *Nat Med.* 2012;18(6):967-973.

34. Montero-Balaguer M, Swirsding K, Orsenigo F, Cotelli F, Mione M, Dejana E. Stable vascular connections and remodelling require full expression of VE-cadherin in zebrafish embryos. *PLoS One.* 2009;4(6):e5772.

35. Hogan BM, Herpers R, Witte M, Heloterä H, Alitalo K, Duckers HJ, Schulte-Merker S. Vegfc/Flt4 signalling is suppressed by Dll4 in developing zebrafish intersegmental arteries. *Development.* 2009;136(23):4001-4009.

36. Siekmann AF, Lawson ND. Notch signalling limits angiogenic cell behaviour in developing zebrafish arteries. *Nature.* 2007;445(7129):781-784.

37. Habeck H, Odenthal J, Walderich B, Maischein H, Schulte-Merker S; Tübingen 2000 screen consortium. Analysis of a zebrafish VEGF receptor mutant reveals specific disruption of angiogenesis. *Curr Biol.* 2002;12(16):1405-1412.

38. Gavard J, Gutkind JS. VEGF controls endothelial cell permeability by promoting the beta-arrestin-dependent endocytosis of VE-cadherin. *Nat Cell Biol.* 2006;8(11):1223-1234.

39. Lee MJ, Thangada S, Claffey KP, Ancellin N, Liu CH, Kluk M, Volpi M, Sha'afi RI, Hla T. Vascular endothelial cell adherens junction assembly and morphogenesis induced by sphingosine-1-phosphate. *Cell.* 1999;99(3):301-312.

40. Michaelis UR, Chavakis E, Kruse C, Jungblut B, Kaluza D, Wandzioch K, Manavski Y, Heide H, Santoni MJ, Potente M, Eble JA, Borg JP, Brandes RP. The polarity protein Scrib is essential for directed endothelial cell migration. *Circ Res.* 2013;112(6):924-934.

41. Franco CA, Li Z. SRF in angiogenesis: branching the vascular system. *Cell Adh Migr.* 2009;3(3):264-267.

# Chapter 5

# Thsd1:
# a new regulator of
# endothelial barrier function
# in vascular development
# and advanced atherosclerosis

R.A. Haasdijk*, W.K. den Dekker*

D. Tempel[§], R. Szulcek[§], F.L. Bos[§], D.M.A. Hermkens[§]

I. Chrifi, M.M. Brandt, E.H.M. van de Kamp, L.A.J. Blonden, J. van Bezu, J.C. Sluimer

E.A.L. Biessen, G.P. van Nieuw Amerongen, S. Schulte-Merker, C. Cheng, H.J. Duckers

*, § contributed equally

## *Abstract*

**Objective** - Impairment of the endothelial barrier leads to haemorrhaging and is involved in vascular-related disease, including atherosclerosis. The mechanism that regulates vascular integrity is complex and requires further definition. Using a microarray screen for angiogenesis-associated genes during embryogenesis, we identified Thrombospondin type I domain 1 (Thsd1) as a new angiopotent factor with an undefined biological function. Here, we investigate the contribution of Thsd1 to vascular integrity.

**Methods and Results** - Verification by *in situ* hybridisation in zebrafish demonstrates that Thsd1 is predominantly expressed in endothelial cells (EC). Knockdown of Thsd1 in zebrafish embryos and in a murine retina model induced severe haemorrhaging. Vascular growth remained unaffected, despite a decline in vascular integrity. Studies in human ECs verified the deleterious effect of Thsd1 silencing on endothelial barrier function and identified Thsd1 as a new binding partner of the CRT-LRP1 complex. Thsd1 activates downstream signalling of LRP1 via FAK-PI3K, leading to Rac1-mediated actin cytoskeleton interaction with cell-cell junctions. In human carotid endarteriectomy specimens, Thsd1 expression increases in ECs in advanced atherosclerotic lesions with intraplaque haemorrhaging compared with stable lesions, implying involvement of Thsd1 in neovascular bleeding. In a murine atherosclerosis model, Thsd1 overexpression decreased plaque vulnerability by attenuating vascular leakage, while Thsd1 knockdown aggravated haemorrhaging, again independent of vascular growth. Pro-atherogenic factors - including low oxygen and TNFα - decrease Thsd1 expression, whereas anti-atherogenic IL-10 increases mRNA expression of protective Thsd1.

**Conclusion** - Thsd1 is a crucial regulator of endothelial barrier function during vascular development and in the pathobiology of haemorrhaging-prone neovascular growth in atherosclerosis.

## Introduction

The vascular endothelium functions as a selective barrier for protein and fluid exchange between the blood stream and the surrounding tissues. The integrity of the vascular endothelium is actively controlled by dynamic interaction between the actin cytoskeleton, cell-cell junctions and cell-matrix focal adhesions.[1] Although physical contacts between endothelial cells (EC) are present during the earliest phases of vasculogenesis and angiogenesis, a functional vascular barrier is only established after the neovessels have undergone critical rearrangements at the molecular level of the actin cytoskeleton and cell-cell junction sites. This maturation of the endothelial barrier is stringently controlled by members of the Rho family of GTPases.[2-5] In particular, Rac1 plays a vital role in maintaining vascular barrier function: Rac1-mediated adaptation of the actin cytoskeleton strengthens the VE-cadherin/actin cytoskeleton bonds, which are crucial for the formation of stable endothelial cell-cell junctions.[6-9] Disruption of this Rac1 regulatory pathway leads to endothelial barrier dysfunction and loss of vascular integrity, and is implicated to be an important contributing factor to the onset and progression of vascular-related diseases such as diabetic retinopathy and atherosclerosis.[1,10] In atherosclerosis, dysfunction of the endothelium on top of the fibrous cap triggers extravasation of inflammatory cells that contribute to lesion growth. As atherosclerosis progresses, plaques become characterised by neovascular growth of vessels which are phenotypically immature, defined by lack of endothelial barrier function and increased susceptibility to rupture.[11] Although previous studies have demonstrated the importance of endothelial barrier function in vascular development and disease, our knowledge of the molecular mechanisms that orchestrate the basic - Rac1-mediated - principles of regulation remains limited, in particular in the light of vascular-related pathologies. In this study, we have identified a new gene with a high level of endothelial expression that is a potent regulator of endothelial barrier integrity.

Recently, we have carried out a genome-wide microarray analysis in search for genes involved in the regulation of new vessel formation. Gene expression profiles of isolated Flk1-positive angioblasts during murine embryonic development were compared with the profiles of Flk1-negative cells. One of the genes that was identified as a new potential regulator of vascular development was Thrombospondin type I domain 1 (Thsd1). Although Thsd1 was previously described as a marker of haematopoietic stem cells and ECs[12], the basic biological function of Thsd1 in angiogenesis *in vitro* and *in vivo* remains fully unknown.

Here, we sought to characterise the function of Thsd1 in ECs during blood vessel formation *in vitro* using primary cell cultures and *in vivo* in zebrafish and murine vascular development. Our data show that Thsd1 plays an important role in establishing and preserving the endothelial barrier function during angiogenesis *in vivo*, as loss of Thsd1 led

to vessel disruption and severe haemorrhaging. Silencing of Thsd1 led to vessel rupture of the cranial vasculature in developing zebrafish, whereas extensive haemorrhaging was detected during postnatal retinal vascular development in mice. This loss of endothelial integrity was unrelated to the angiogenic potential of the ECs, since no difference in vascular growth was observed. Further *in vitro* studies demonstrate that Thsd1 activates the calreticulin (CRT) - low density lipoprotein receptor-related protein 1 (LRP1) signalling pathway by complex formation with CRT. Loss of this complex interferes with actin cytoskeleton modulation - a process shown to be regulated by Rac1 - leading to loss of endothelial barrier function by limiting VE-cadherin/actin cytoskeleton interaction. These findings points toward an important role for Thsd1 in the basic regulation of vascular barrier function. In addition, a strong increase in Thsd1 endothelial expression was observed in the neovasculature of advanced human atherosclerotic lesions, suggesting a possible Thsd1-mediated feed-back mechanism to counteract loss of vascular integrity of intimal neovessels. Evaluation of Thsd1 function in a well-validated flow-based murine vulnerable plaque model, clearly demonstrated that siRNA-mediated silencing of endogenous Thsd1 further compromised neovascular integrity and worsened intraplaque haemorrhaging, whereas overexpression of Thsd1 improved endothelial barrier function and significantly reduced vascular bleeding. These *in vivo* studies identify Thsd1 as a vital factor in the formation and conservation of intimal neovessel integrity in advanced atherosclerosis. Loss of Thsd1 function results in extensive intraplaque haemorrhaging and amplifies the inflamed state of the plaque lesion, leading to a further decline of vulnerable plaque stability. Considering the potent vascular stabilising function of the gene, Thsd1 might be an interesting target for the development of therapeutics in the treatment of vascular pathologies in which endothelial barrier function is affected.

## *Methods*

A more detailed description of materials and methods is available in the Data Supplement (*online*). Summarised descriptions of the different techniques used in this study are supplied below.

This study was carried out in accordance with the Council of Europe Convention (ETS123)/Directive (86/609/EEC) for the protection of vertebrate animals used for experimental and other scientific purposes and with the approval of the National and Local Animal Care Committee.

## Zebrafish

Zebrafish (*Danio rerio*) were maintained under standard laboratory conditions. The transgenic zebrafish lines used were Tg(Fli1:eGFP)[y1] and Tg(Kdrl:eGFP x Gata1:dsRed)[y1].

## Whole-mount *in situ* hybridisation

As template for *in vitro* transcription, a Thsd1 cDNA fragment of at least 250 bp was used to ensure probe specificity. Antisense RNA probes of Thsd1 were generated by *in vitro* transcription using the digoxigenin RNA Labeling Mix from Roche (Woerden, The Netherlands). *In situ* hybridisation was carried out as previously described.[13]

## *o*-Dianisidine staining

Erythrocytes were stained by incubating embryos in a solution containing *o*-Dianisidine (Sigma-Aldrich, Zwijndrecht, The Netherlands) as previously described.[13]

## Mice

Plugged FVB/N mice (*Mus musculus*) were ordered at Harlan (Indianapolis, USA). C57BL/6.ApoE-knockout mice were obtained from The Jackson Laboratory (Bar Harbor, USA). C57BL/6J mice were obtained from laboratory stock. They were maintained under standard husbandry conditions.

## Mouse model of retinal vascularisation

Two-day old C57BL/6J mice pups were anesthetised by placement on ice. Thsd1 targeting siRNA (si-Thsd1) was injected into the left eye. As a control, scrambled non-targeting siRNA (si-sham) was injected into the right eye. Mice pups were killed five days after intra-ocular injection. The retinas were stained with Alexa Fluor® 488-conjugated isolectin GS-IB$_4$ (Invitrogen, Bleiswijk, The Netherlands) before assessment under a fluorescence microscope (Axiovert S100; Carl Zeiss, Sliedrecht, The Netherlands). To rescue the phenotype caused by Thsd1 knockdown, another group of two-day old C57BL/6J mice pups were treated by intra-ocular injection of si-Thsd1 in both eyes as described, combined with or without Rac1 activator (CN02-A, 0.25 U/ml; Cytoskeleton, Denver, USA).

## TER-119 staining

Retinas were incubated with TER-119 antibody (Novus Biologicals, Cambridge, UK) to stain erythrocytes.

## ApoE-knockout mice vulnerable plaque model

Ten-week old female ApoE-knockout mice were put on a Western diet containing 15% (w/w) cacao and 0.25% (w/w) cholesterol (Arie Blok, Woerden, The Netherlands). Two weeks after start of the Western diet, mice were operated and a tapered cast was surgically

inserted around the right common carotid artery. Nine weeks after cast placement, mice were re-operated and either adenovirus expressing murine Thsd1 (pAd-Thsd1) or si-Thsd1, or sham virus (pAd-sham) or si-sham was placed around the right common carotid artery. Mice were killed three days after re-operation. One hour before killing, FITC-labelled Dextran (Sigma-Aldrich, Zwijndrecht, The Netherlands) was intravenously injected. Next, the carotid artery was flushed, taken out, snap frozen in liquid nitrogen, and stored at -80ºC until immunohistological staining.

**Thsd1 and CD31 expression in human carotid endarterectomy specimens**

Human carotid endarterectomy specimens were collected and processed by the Experimental Vascular Pathology group (Maastricht UMC+, The Netherlands). From all samples, three randomly taken regions were studied for Thsd1 and CD31 - an endothelial cell marker - expression. For every region the Thsd1:CD31 ratio was determined. The average of these three regions was used as final Thsd1:CD31 ratio for that sample. All samples were stained with antibodies against Thsd1 (Sigma-Aldrich, Zwijndrecht, The Netherlands) and CD31 (DakoCytomation, Glostrup, Denmark). An horseradish peroxidase (HRP)-labelled secondary antibody in combination with nickel-3,3'-diaminobenzidine (N-DAB) (Sigma-Aldrich, Zwijndrecht, The Netherlands) was used to visualise the signal.

**Cell cultures**

Primary cultures of human umbilical vein endothelial cells (HUVEC) were cultured in EBM®-2 medium supplemented with a commercial BulletKit, 10% foetal calf serum (FCS) and 1% penicillin/streptomycin (Lonza, Breda, The Netherlands). Primary aorta-derived human vascular smooth muscle cells (vSMC) were cultured in SmGM®-2 medium supplemented with a commercial BulletKit, 10% FCS and 1% penicillin/streptomycin (Lonza, Breda, The Netherlands). HeLa and sarcoma cells were cultured in Dulbecco's modified Eagle's medium (DMEM) supplemented with 10% FCS (Cambrex, Wiesbaden, Germany). Cells were cultured at 37°C in 5% $CO_2$. Passages three to six were used throughout the study.

**2D matrigel network-formation assay**

To induce network-formation, HUVECs - transfected with si-sham or si-Thsd1 - were cultured on a 2D Matrigel™ matrix (BD, Breda, The Netherlands). The tubules were stained by Calcein-AM (BD, Breda, The Netherlands) after 24 hours of network-formation. Each condition was assessed by fluorescence microscopy (Axiovert S100; Carl Zeiss, Sliedrecht, The Netherlands). Image analysis of the number of junctions, tubules and total tubule length was carried out using Angiosys Image Analysis Software 1.0 (TCS CellWorks, Buckingham, UK).

**Transwell permeability assay and ECIS measurements**

Endothelial barrier function *in vitro* was evaluated by culturing HUVECs on porous filters and measuring the passage of HRP as previously described.[14,15]

For electric cell-substrate impedance sensing (ECIS) measurements, cells were seeded on gelatin-coated ECIS arrays, each with 8 wells with 10 gold electrodes per well (Applied BioPhysics, Troy, USA). Experiments were carried out following standard protocols as previously described.[16]

**Co-immunoprecipitation**

Protein complexes were immunoprecipitated using Dynabeads® magnetic beads from Invitrogen (Bleiswijk, The Netherlands) according to the instruction manual and analysed using a 12.5% SDS-PAGE gel, followed by immunoblotting using anti-human antibodies against Thsd1 (Sigma-Aldrich, Zwijndrecht, The Netherlands), CD36 (Hycult Biotech, Uden, The Netherlands), CRT (Thermo Fisher Scientific, Breda, The Netherlands) and LRP1 that recognises the heavy chain of the protein (Abcam, Cambridge, UK).

**Western blot**

To determine whether knockdown of Thsd1 interfered with cellular processes, Western blot analysis was carried out using HUVEC protein lysates. At 72 hours post-transfection, HUVECs were serum starved for 4 hours and replenished with EBM®-2 medium supplemented with a commercial BulletKit, with or without Rac1 activator (CN02-A, 0.05 U/ml; Cytoskeleton, Denver, USA) for 30 minutes. Cells were lysed in NP40 Cell Lysis Buffer (Invitrogen, Bleiswijk, The Netherlands) and analysed on a 12.5% SDS-PAGE gel, followed by immunoblotting using anti-human antibodies against focal adhesion kinase (FAK), phosphorylated-FAK (Y397) (FAK-P) (Abcam, Cambridge, UK), phosphatidylinositol 3-kinase p85α (PI3K) (Cell Signaling Technology, Leiden, The Netherlands), phosphorylated-PI3K p85α (Y508) (PI3K-P) (Santa Cruz Biotechnology, Heidelberg, Germany) and Rac1 (Abcam, Cambridge, UK). Beta-actin antibody (Abcam, Cambridge, UK) was used as a loading control. Protein bands were visualised by the Odyssey® Infrared Imaging System and analysed by Odyssey 3.0 software (LI-COR Biotechnology, Cambridge, UK).

**Rac1 activation assay**

Rac1 activity was measured using the G-LISA® Rac Activation Assay Biochem Kit™ from Cytoskeleton (Denver, USA) according to the instruction manual.

**Statistical analysis**

Data were reported as mean ± standard error of the mean (SEM). Statistical significance was evaluated using a Student's *t*-test and was accepted at *P* < 0.05 (* *P* < 0.05, ** *P* < 0.01 in the figures).

## *Results*

**Vascular specific expression of Thsd1 during mouse and zebrafish development**

To identify new genes involved in angiogenesis, a genome-wide microarray analysis was carried out followed by validation of the results by qPCR. Gene expression profiles of Flk1-positive angioblasts at various stages of murine embryonic development were compared with the profiles of Flk1-negative cells. Thsd1 was upregulated in Flk1-positive angioblasts from 8 to 16 days post-fertilisation (dpf). Expression levels were highest upregulated around 8 to 11 dpf, which coincides with the period of early angiogenesis in murine development and suggests a potential role of Thsd1 in blood vessel formation (Figure 1A).
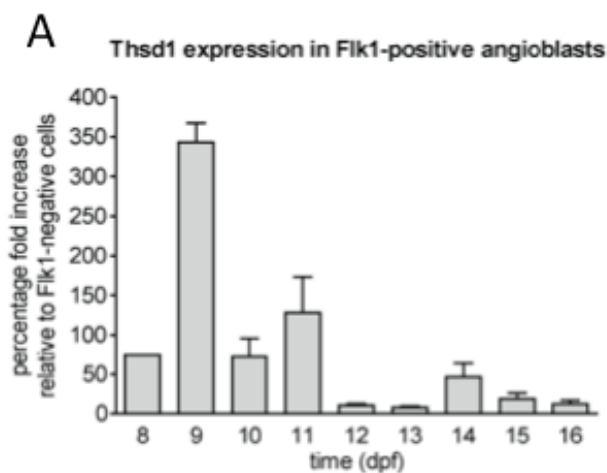


**Figure 1. Vascular specific expression of Thsd1 during mouse and zebrafish development.** (**A**) Endogenous expression level of Thsd1 in Flk1-positive angioblasts during murine embryonic development from 8 to 16 days post-fertilisation (dpf) compared with Flk1-negative cells as analysed by qPCR. The expression level of Thsd1 in Flk1-negative cells was arbitrarily set to one (n = 4; mean ± SEM). The highest upregulation was detected around day 8 to 11, which coincides with the period of early angiogenesis in murine development.

Further evidence of a vascular-related expression profile for Thsd1 was provided by examining the gene in developing zebrafish larvae by whole-mount *in situ* hybridisation: expression of the Thsd1 zebrafish orthologue was detected in the main axial vessels - dorsal aorta and posterior cardinal vein - and head vessels at 26 hours post-fertilisation (hpf). In addition, Thsd1 expression was also detected in the caudal and midcerebral veins (MCeV), and in the somites (Figure 1B).
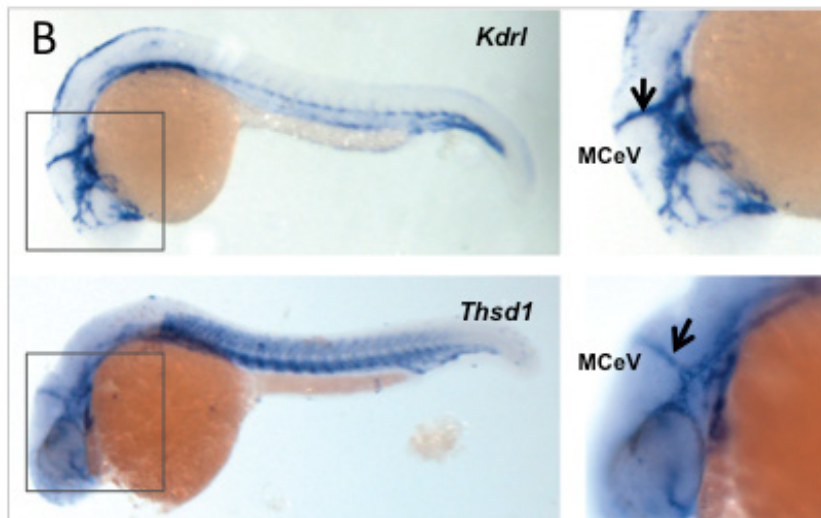


(**B**) Whole-mount *in situ* hybridisation comparison of endothelial specific Kdrl (upper panel) with Thsd1 (lower panel) in zebrafish at 26 hours post-fertilisation (hpf), lateral view, anterior is to the left. Like Kdrl, Thsd1 transcripts were localised in the developing vascular network, including the main axial vessels - dorsal aorta and posterior cardinal vein - and cerebral vasculature (black arrow), as well as in the caudal and midcerebral veins (MCeV). In addition, expression of Thsd1 in the somites was observed. Right hand panel shows high magnification images of the head region.

## Knockdown of Thsd1 in zebrafish induces haemorrhaging of cerebral vessels

For functional evaluation of Thsd1 *in vivo*, the gene was silenced in developing zebrafish larvae of the transgenic zebrafish lines Tg(Fli1:eGFP)[y1] and Tg(Kdrl:eGFP x Gata1:dsRed)[y1], using morpholino (MO)-knockdown technology. Adequate targeting of Thsd1 was verified by qPCR analysis (Supplemental figure 1, *online*). Silencing of Thsd1 had no effect on vascular growth, and macroscopic evaluation showed no obvious defects in the general vasculature (Figure 1C). However, time-lapse studies carried out during the first 48 hpf identified severe and frequent haemorrhaging in the cranial region - a known predilection site for vascular haemorrhaging in zebrafish[13, 17-21] - that was observed in 24% of the injected embryos (n = 195). Haemorrhaging occurred as a sudden rupture of blood vessels, implying intrinsic weakness and lack of integrity of the neovascular barrier (Figure 1D, E). Cerebral haemorrhaging was further confirmed by an *o*-Dianisidine staining of

iron/haem in red blood cells in Thsd1-silenced wild-type zebrafish. Thsd1 silencing resulted in large areas of accumulated blood in the head of the zebrafish larvae compared with uninjected controls (Figure 1F). This phenotype was consistently observed in the Thsd1-silenced zebrafish after injections of different MO concentrations (Figure 1G).
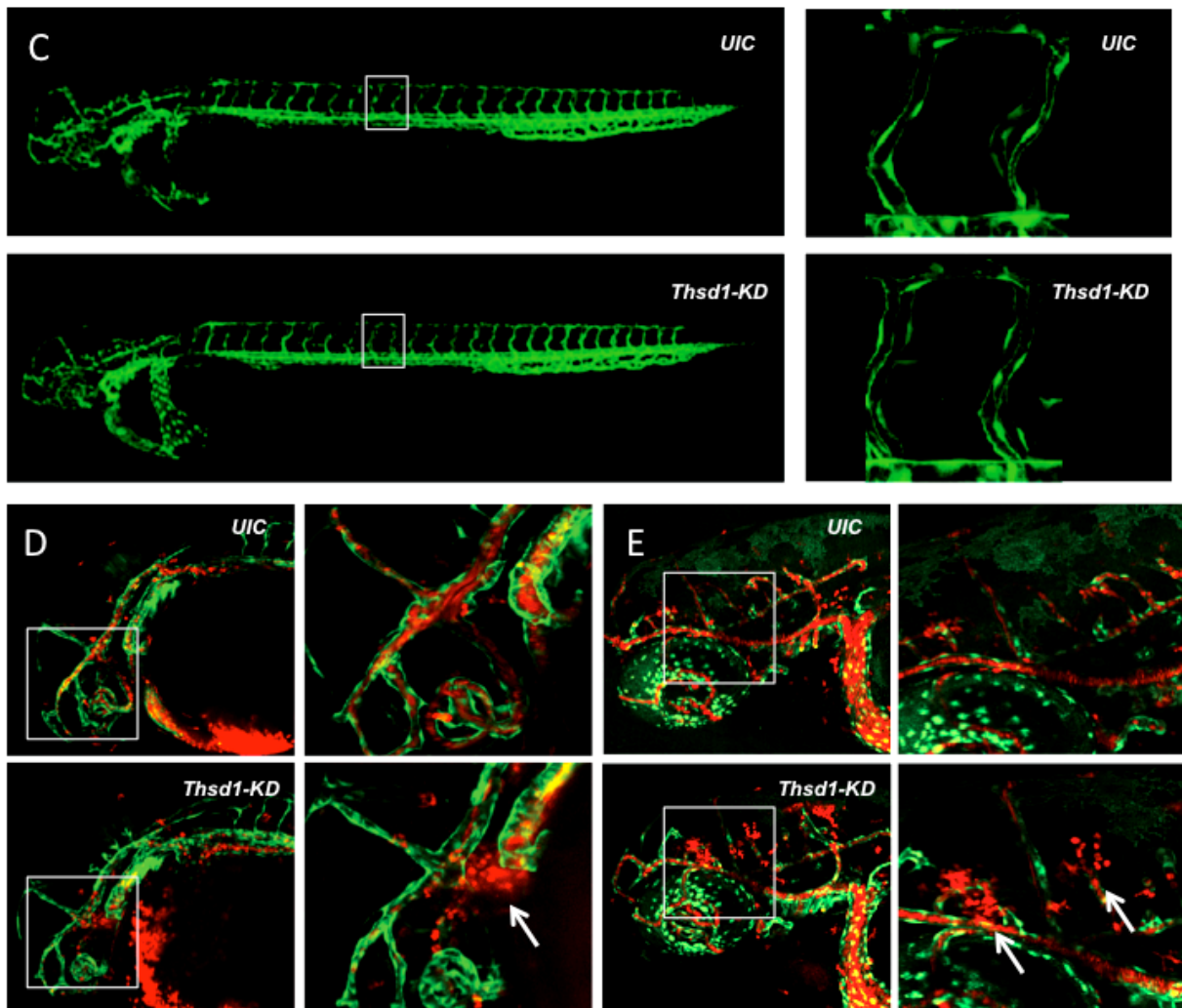


**Morpholino-induced knockdown of Thsd1 in zebrafish results in acute cerebral haemorrhages without affecting vascular growth.** (**C**) Tg(Fli1:eGFP)[y1] embryos at 26 hpf, lateral view, anterior is to the left. No apparent morphological abnormalities in the trunk or cerebral vasculature were observed between the Thsd1 targeting morpholino-injected (Thsd1-KD) embryos and the uninjected control (UIC) embryos. Right hand panel shows high magnification images of intersegmental outgrowth in the trunk region. (**D, E**) Tg(Kdrl:eGFP x Gata1:dsRed)[y1] Thsd1-KD embryos around (**D**) 28 hpf and (**E**) 2 dpf, lateral view, anterior is to the left. Endothelial cells (Kdrl:eGFP-positive, green) and erythrocytes (Gata1:dsRed-positive, red). Right hand panel shows high magnification images of the head region. Extensive and frequent haemorrhages were detected in the head region (white arrow).
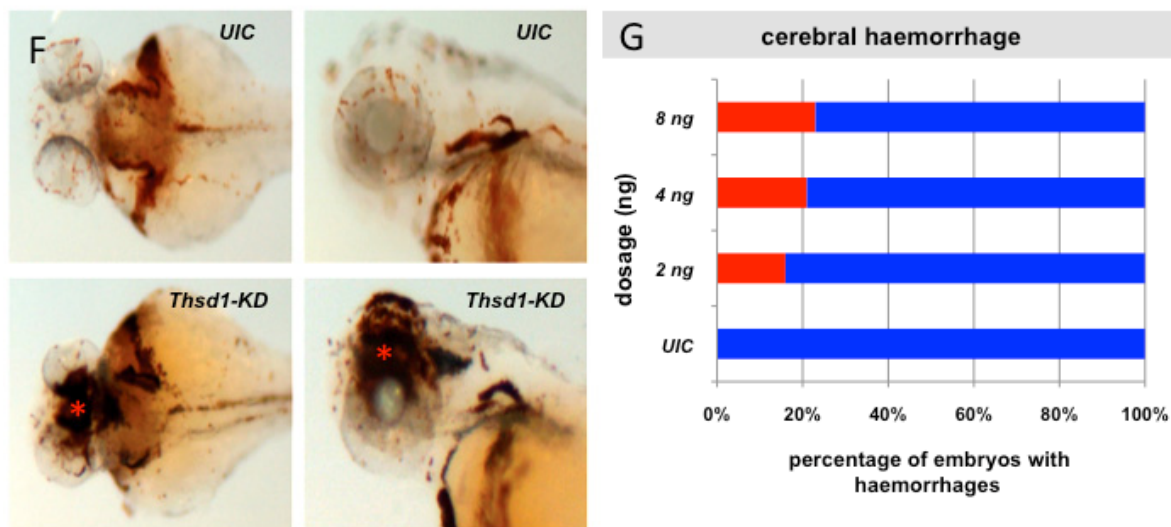
(**F**) *o*-Dianisidine stained embryos around 26-28 hpf, top view (left) lateral view (right), anterior is to the left. Areas of accumulated blood (red asterisk) in the head region were observed in Thsd1-KD embryos. (**G**) Morpholino dose-response increase in the percentage of zebrafish with the cerebral haemorrhage phenotype (red bar) compared with the wild-type phenotype (no cerebral haemorrhaging, blue bar).

## Thsd1 knockdown in the developing retinal vasculature of neonatal mice promotes vascular haemorrhages

To further validate the findings in the zebrafish, Thsd1 function was studied during the development of the retinal vasculature of neonatal mice. To determine the optimal moment of Thsd1 knockdown, Thsd1 mRNA expression in the murine retina was evaluated during postnatal development by qPCR analysis. Thsd1 mRNA levels were adjusted to CD31 mRNA levels to compensate for changes in percentage of ECs. High expression levels of Thsd1 were observed from 3 to 9 days post-partum, which corresponds with the period of plexus formation and vascular remodelling (Figure 2A). Based on these findings, Thsd1 knockdown was induced in the first week of retinal vascular development by intra-ocular injection of a siRNA pool composed of four different Thsd1 targeting siRNA sequences in two-day old wild-type C57BL/6J mouse pups and compared with controls injected with a scrambled non-targeting siRNA pool. Efficient knockdown of Thsd1 was observed two days after intra-ocular injection (Supplemental figure 2, *online*). Assessment and quantification of the number of vascular branches, the total number of vessels and the total tubule length after visualisation of the vasculature by isolectin GS-IB$_4$ staining, showed no difference between si-Thsd1 and si-sham injected eyes five days after intra-ocular injection (Figure 2B-E, whole retina image provided in Supplemental figure 3A, *online*).
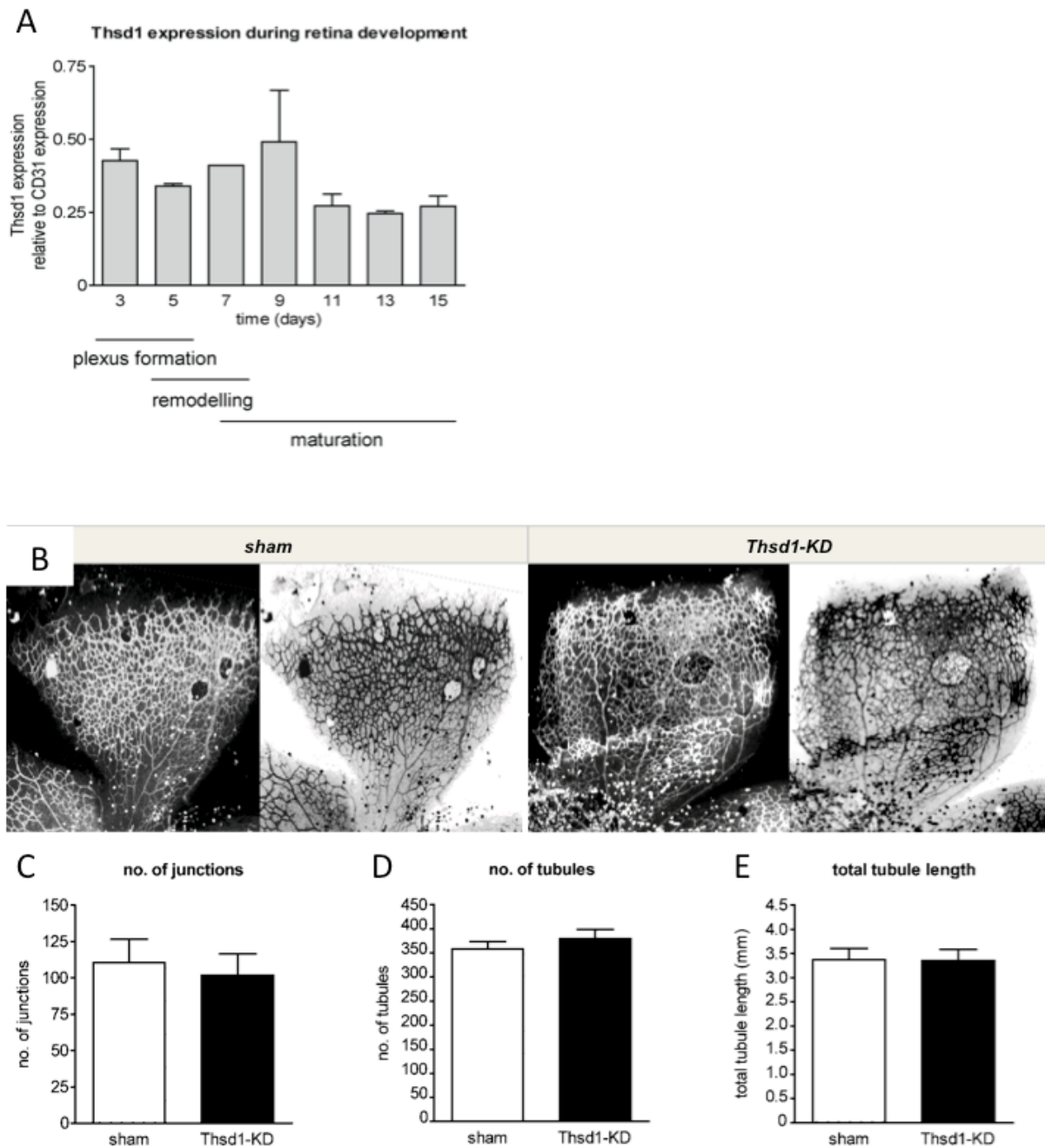
**Figure 2. Thsd1 depletion during murine retinal vascular development results in vascular haemorrhaging without affecting vascular growth.** (**A**) Endogenous expression level of Thsd1 in the developing retinal vasculature of neonatal mice from 3 to 15 days after birth compared with CD31 expression in the retina (n = 3; mean ± SEM). Thsd1 is highly expressed from day 3 to 9, which coincides with the period of plexus formation and remodelling. (**B**) Retinas stained with isolectin GS-IB$_4$. Left hand image shows black and white micrograph, right hand image shows the inverse image. (**C-E**) Quantification by means of the dimensions of the vascular network showed no morphological defects after Thsd1 knockdown (Thsd1-KD): (**C**) number of junctions, (**D**) number of tubules and (**E**) total tubule length.

However, double-staining of retinas with isolectin GS-IB₄ (ECs, green) and TER-119 antibody (erythrocytes, red) showed a significant higher frequency of haemorrhaging and larger areas of bleeding in the si-Thsd1 injected eyes, whereas retinal haemorrhaging was hardly observed in si-sham injected controls (Figure 2F, G, whole retina image provided in Supplemental figure 3B, *online*). Thus, like in the developing zebrafish, loss of Thsd1 expression had no effect on vascular growth, but had resulted in a vasculature highly susceptible to vascular haemorrhaging. Combined, these data has identified a role for Thsd1 in establishing vascular integrity during blood vessel development.
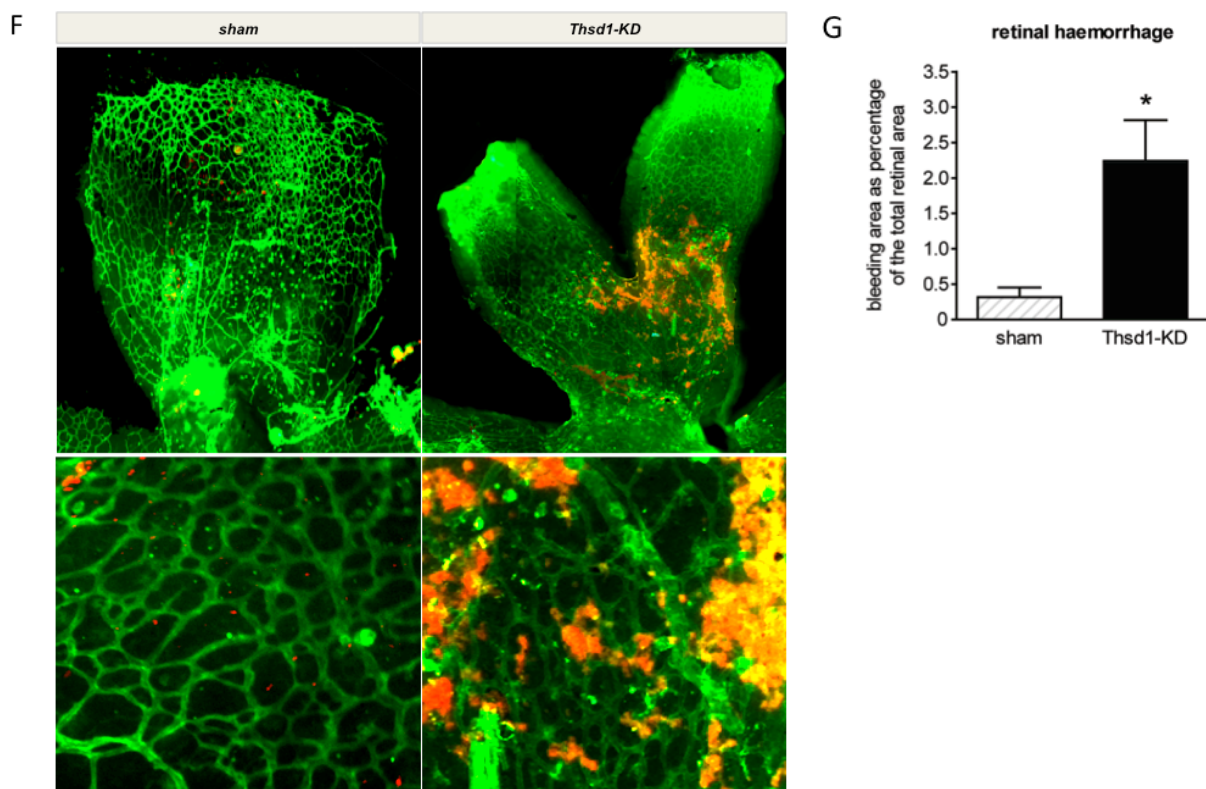


In contrast, double-staining of retinas with isolectin GS-IB₄ (endothelial cells, green) and TER-119 (erythrocytes, red) demonstrated severe and frequent vascular haemorrhaging in the Thsd1-KD group: (**F**) Thsd1-KD induced significantly larger areas of extravascular TER-119 erythrocytes accumulation. Upper panel shows low magnification and lower panel shows high magnification micrographs. (**G**) Quantification of retinal haemorrhage with the bleeding area expressed as percentage of the total retinal area showed a 600% increase in Thsd1-KD versus sham retinas (n = 10; mean ± SEM).

## Thsd1 controls endothelial barrier function *in vitro*

To clarify the molecular mechanism underlying the impaired endothelial integrity, we moved to *in vitro* assays to define Thsd1 function in vascular cells. The expression level of Thsd1 was evaluated in different cell types. On comparing HUVECs, vSMCs, HeLa and

sarcoma cells, the highest mRNA expression level of Thsd1 was observed in HUVECs (Figure 3A). In line with previous *in vivo* findings, siRNA-mediated knockdown of Thsd1 in HUVECs did not affect network-formation in a standard 2D matrigel network-formation assay (as indicated by the number of junctions, capillary tubules or total tubule length) when compared with cultures transfected with equimolar of si-sham or untransfected controls (Figure 3B-E). Adequate knockdown of the target gene was validated on both mRNA and protein level, and did not affect the expression of the family member Thrombospondin 1 (Supplemental figure 4A-C, *online*).
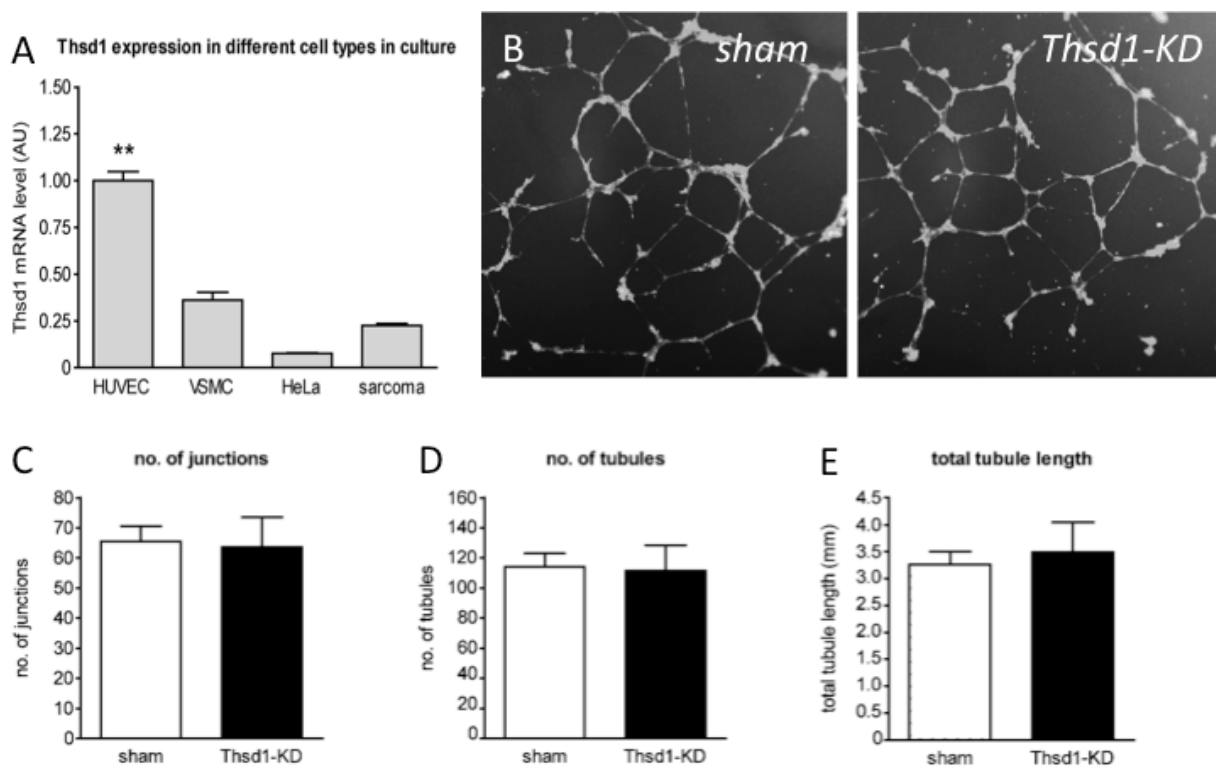


**Figure 3. Thsd1 knockdown in cultured endothelial cells impairs endothelial integrity.** (**A**) Thsd1 was highly expressed in HUVEC compared with vSMC, HeLa and sarcoma cells, as demonstrated by qPCR analysis. (**B**) Assessment of network-formation capacity for Thsd1-silenced ECs (Thsd1-KD) in a 2D matrigel experiment. Tubules were stained by Calcein-AM uptake. (**C-E**) Quantification of the vascular network showed no morphological changes in Thsd1-KD HUVECs: (**C**) number of junctions, (**D**) number of tubules and (**E**) total tubule length (n = 3; mean ± SEM).

A Transwell permeability assay - measuring HRP passage - was carried out to determine the effect of Thsd1 on the endothelial barrier function in HUVECs. Like the *in vivo* findings, endothelial barrier function was significantly decreased in Thsd1-depleted HUVECs as suggested by increased permeability for HRP (Figure 3F). Further evaluation of endothelial barrier function by ECIS measurements showed that Thsd1 silencing in

HUVEC monolayers severely impeded the build-up of endothelial electric resistance compared with sham treated groups, thus verifying a decline in effective cell junction formation (Figure 3G).
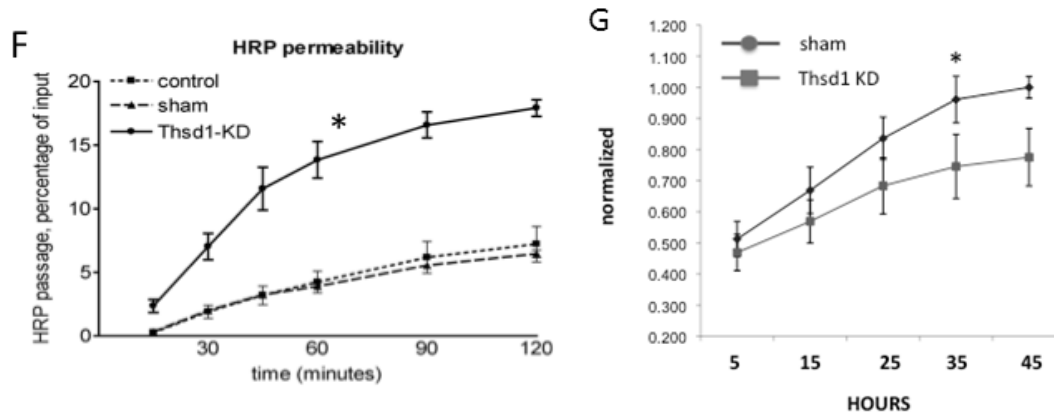


(**F**) Measurement of endothelial barrier function *in vitro*. Passage of horseradish peroxidase (HRP) over a confluent monolayer of HUVECs during thrombin (1 U/ml) stimulation for the different conditions showed significant increased HRP permeability after Thsd1 silencing (n = 3; mean ± SEM). (**G**) ECIS measurement of sham or Thsd1-KD HUVEC monolayers showed a delay in electric resistance build-up as a result of Thsd1 inhibition (n = 3; mean ± SEM).

### Thsd1 mediates cell-cell interaction via CRT-LRP1 downstream signalling regulation of Rac1

Previous reports indicated that Thrombospondin 1 mediates EC apoptosis via CD36 binding and signalling.[22-24] To evaluate if Thsd1, like its family member, may mediate vascular barrier function via this apoptosis pathway, co-immunoprecipitation analysis was carried out to identify the binding partners of Thsd1. No binding between Thsd1 and CD36 was detected in HUVECs (Supplemental figure 5A, *online*). In addition, no effect was observed on early or late apoptosis in si-Thsd1 transfected cells compared with si-sham transfected and untransfected controls (Supplemental figure 5B-D, *online*). Thus, these data indicate that Thsd1 operates via a separate, CD36-independent pathway.

Based on the homology in protein domains between Thsd1 and Thrombospondin 1, the CRT-LRP1 complex may provide a potential binding target for Thsd1. Co-immunoprecipitation analysis confirmed that Thsd1 and CRT could indeed form a protein complex. Likewise, CRT binding to LRP1 was verified (Figure 4A, B, additional controls in Supplemental figure 6, *online*). In addition, separation of the cytosolic and cell-membrane fraction demonstrated that Thsd1 was present in both compartments (Figure 4D). Co-immunoprecipitation analysis of the different fractions clearly showed that cell-

membrane bound Thsd1 could directly bind to CRT located in the same compartment, although Thsd1 binding to CRT in the cytosol also takes place (Figure 4D).
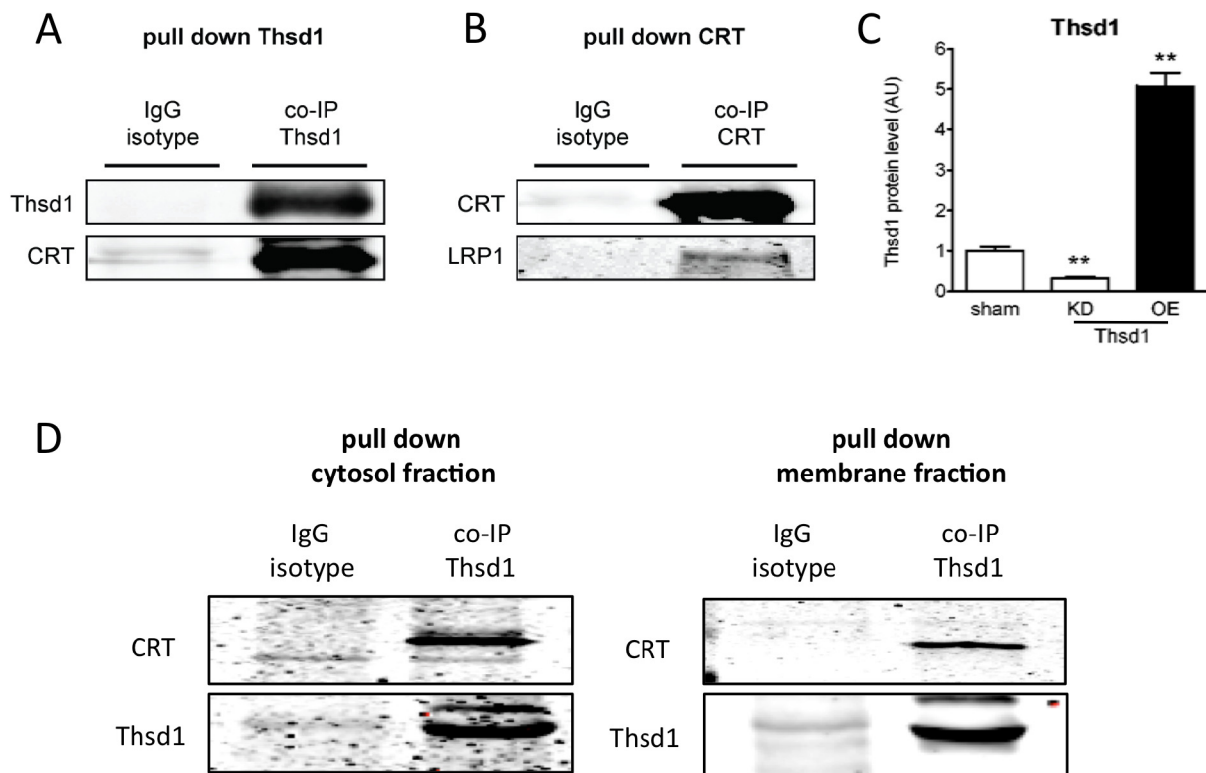


**Figure 4. Thsd1 binds the CRT-LRP1 complex and induces actin cytoskeleton modulation via Rac1 activation.** (**A**) Immunoprecipitation of Thsd1 in HUVECs showed an effective pull down of Thsd1 (upper panel) and co-immunoprecipitation of CRT (lower panel). Immunoprecipitation using a mouse IgG isotype control showed no effective pull down of Thsd1 or CRT. (**B**) Immunoprecipitation of CRT in HUVECs showed an effective pull down of CRT (upper panel) and co-immunoprecipitation of LRP1 (lower panel). Immunoprecipitation using a mouse IgG isotype control showed no effective pull down of CRT or LRP1. (**C**) Western blot analysis of Thsd1 level in HUVECs transfected with Thsd1 targeting siRNA (Thsd1-KD) or HUVECs infected with an adenovirus expressing human Thsd1 (Thsd1-OE). (**D**) Co-immunoprecipitation of Thsd1 using IgG capture antibody directed against Thsd1 compared with IgG isotype control on the isolation beads in the membrane and cytosol fraction showed that Thsd1 binding to CRT takes place in the cell membrane fraction and cytosol fraction (shown are representative results of n = 2).

Western blot analysis further demonstrated that the downstream signalling cascade of CRT-LRP1 was regulated by Thsd1 (Figure 4C-K): knockdown of Thsd1 (Figure 4C, Thsd1 overexpression validation is shown in Supplemental figure 3D, E, *online*) decreased signal transduction via FAK by downregulation of FAK protein and FAK phosphorylation (Figure 4E, H), while PI3K phosphorylation was diminished (Figure 4F, I). Further downstream, Thsd1 silencing inhibited PI3K-mediated Rac1 activation, demonstrated by a decline in

Rac1-GTP levels, while total Rac1 protein levels remained unaffected (Figure 4G, J). These findings are further strengthened by the effect of Thsd1 overexpression: HUVECs infected with an adenovirus expressing human Thsd1, showed opposite effects with increased FAK phosphorylation and Rac1 activation compared with sham virus treated controls (Figure 4C-K). A LRP1 blocking study with RAP (Receptor Associated Protein) was carried out to verify direct Thsd1 involvement in CRT-LPR1 signalling. Indeed, RAP treatment blocked Rac1 activation in Thsd1 overexpressing HUVECs, indicating that LRP1 activation via Thsd1-CRT complex formation is relevant for Thsd1 signalling via Rac1 (Figure 4L).
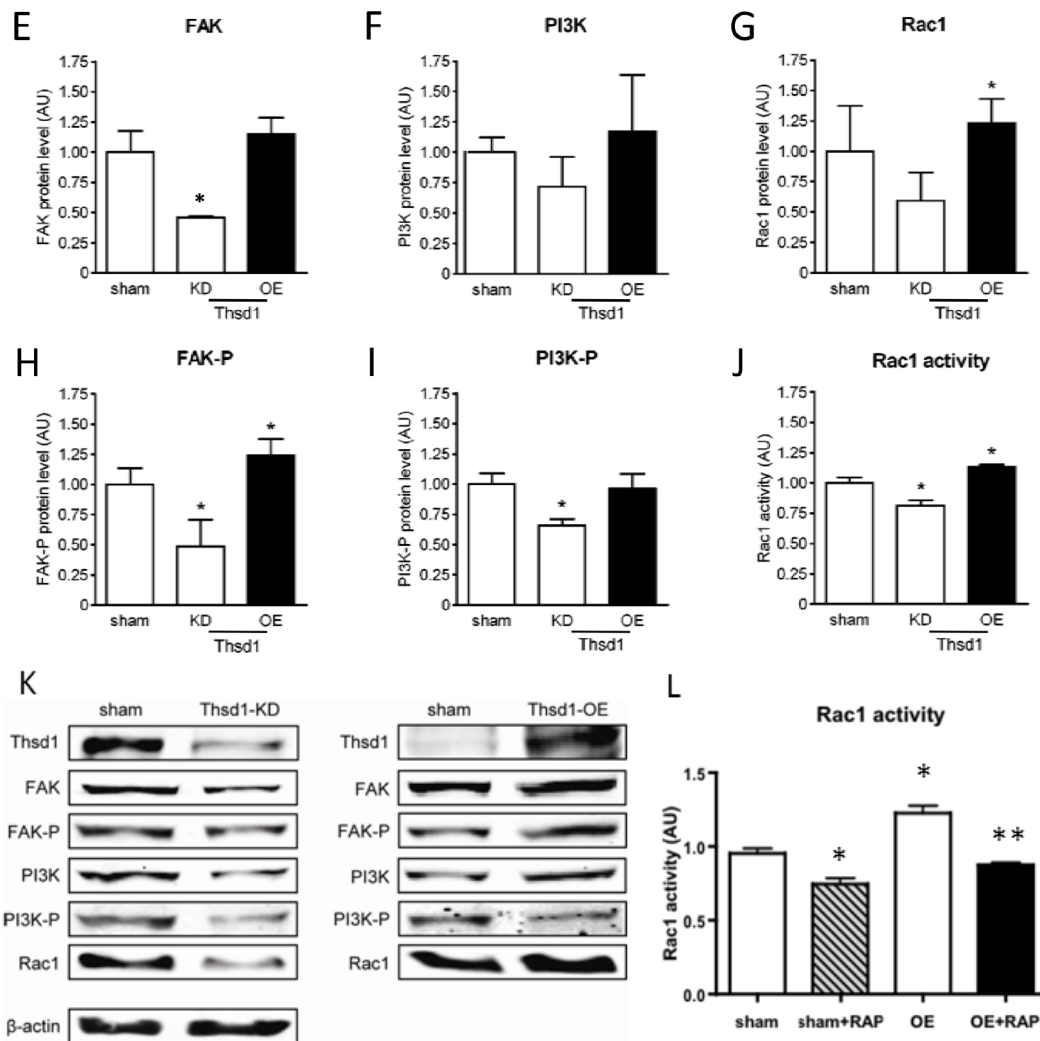


(**E-K**) Western blot analysis of CRT-LRP1 downstream targets in Thsd1-KD or Thsd1-OE conditions: Thsd1-KD downregulated (**E**) FAK, (**H**) FAK-P and (**I**) PI3K-P, whereas (**F**) PI3K and (**G**) Rac1 were not affected. Thsd1-OE enhanced (**H**) FAK-P and (**G**) Rac1, whereas (**E**) FAK, (**F**) PI3K and (**I**) PI3K-P remained unaffected. (**J**) Thsd1-KD in HUVECs showed a decline in Rac1-GTP levels measured by GEF-assays, while Thsd1-OE resulted in an increase in Rac1-GTP levels. (**L**) Pre-incubation with 50 µg/ml RAP (Receptor Associated Protein) before Rac1 activation with high serum medium limited the effect of Thsd1-OE on Rac1 activation (n = 4; mean ± SEM).

Rac1 is an important mediator of endothelial barrier function as it enforces cell-cell and cell-matrix interaction via regulation of the actin cytoskeleton.[7-9] To study the Rac1-mediated function of Thsd1 in actin dynamics, si-Thsd1, si-sham and control ECs were evaluated in an adhesion assay in which cells were seeded on a collagen-coated surface. Cell spreading and actin filaments distribution was evaluated at different time points after cell seeding (Figure 4M, Supplemental figure 7A, *online*). Quantification and stratification of cell size showed that Thsd1 knockdown induced a trend towards a decrease in the number of large cells ($>1500$ nm$^2$) compared with si-sham transfected controls (Figure 4N).
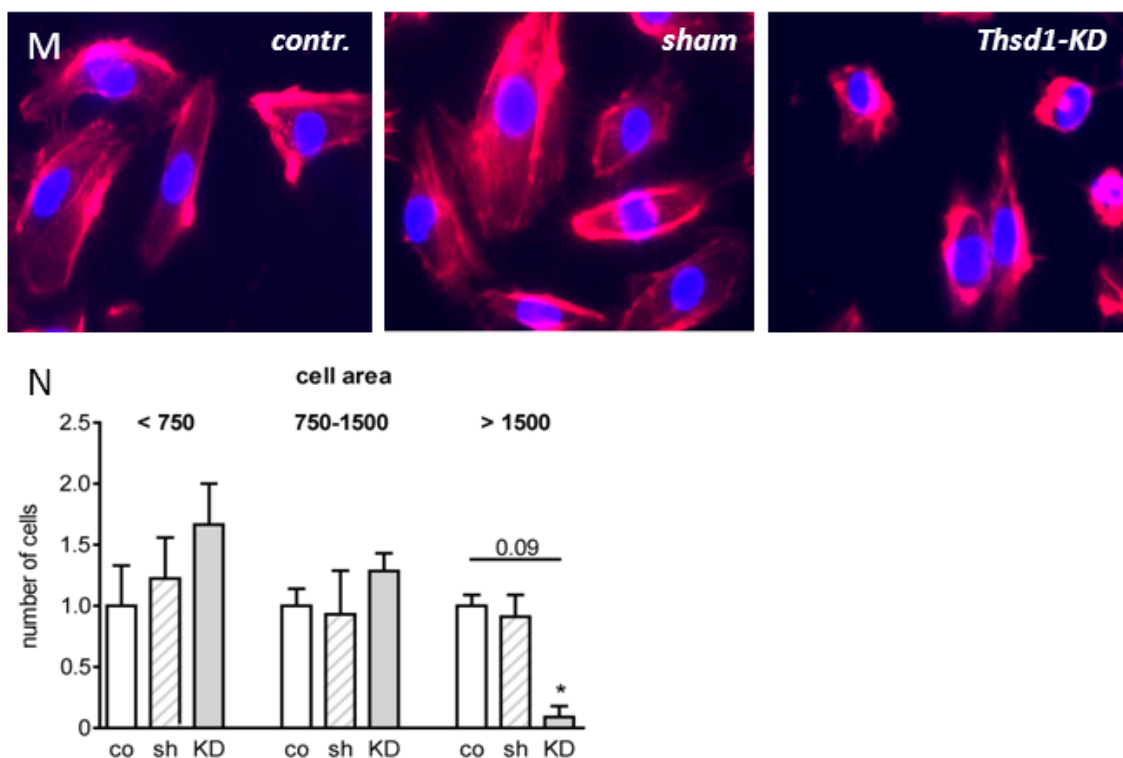


**Rac1 activity affects actin cytoskeleton dynamics during cell spreading.** Actin mobility was assessed in a cell spreading assay. (**M**) 30 minutes after cell seeding, Thsd1-KD showed a delay in actin cytoskeleton spreading compared with scrambled non-targeting siRNA (sham) transfected and untransfected controls (contr). F-actin fibres (red) and nuclei (blue). (**N**) Quantification of the cell/actin surface area showed a decrease in the number of large cells ($>1500$ nm$^2$) in Thsd1-KD HUVECs (KD) compared with scrambled non-targeting siRNA (sh) transfected and untransfected controls (co) (n = 3; mean ± SEM).

This decline in cell size and thus spreading efficiency was associated with a defect in cell-extracellular matrix interaction: paxillin and vinculin visualisation of focal adhesion sites showed a significant decline of focal adhesion capping at stress fibre ends in Thsd1-silenced cells compared with control conditions at different time points after cell seeding (Supplemental figure 7B, *online*). Loss of association between VE-cadherin and the actin

cytoskeleton at cell-cell junction sites promotes endothelial and vascular permeability.[6] Therefore, the effect of Thsd1 knockdown was assessed on VE-cadherin/actin cytoskeleton association in a confluent HUVEC monolayer. Knockdown of Thsd1 in HUVECs reduced co-localisation of VE-cadherin with the actin cytoskeleton compared with sham transfected and untransfected controls (Figure 4O). Taken together, these data indicate that Thsd1 modulates cell-cell interaction via a signalling mechanism that involves CRT-LRP1, FAK, PI3K and Rac1-mediated regulation of the endothelial actin cytoskeleton.
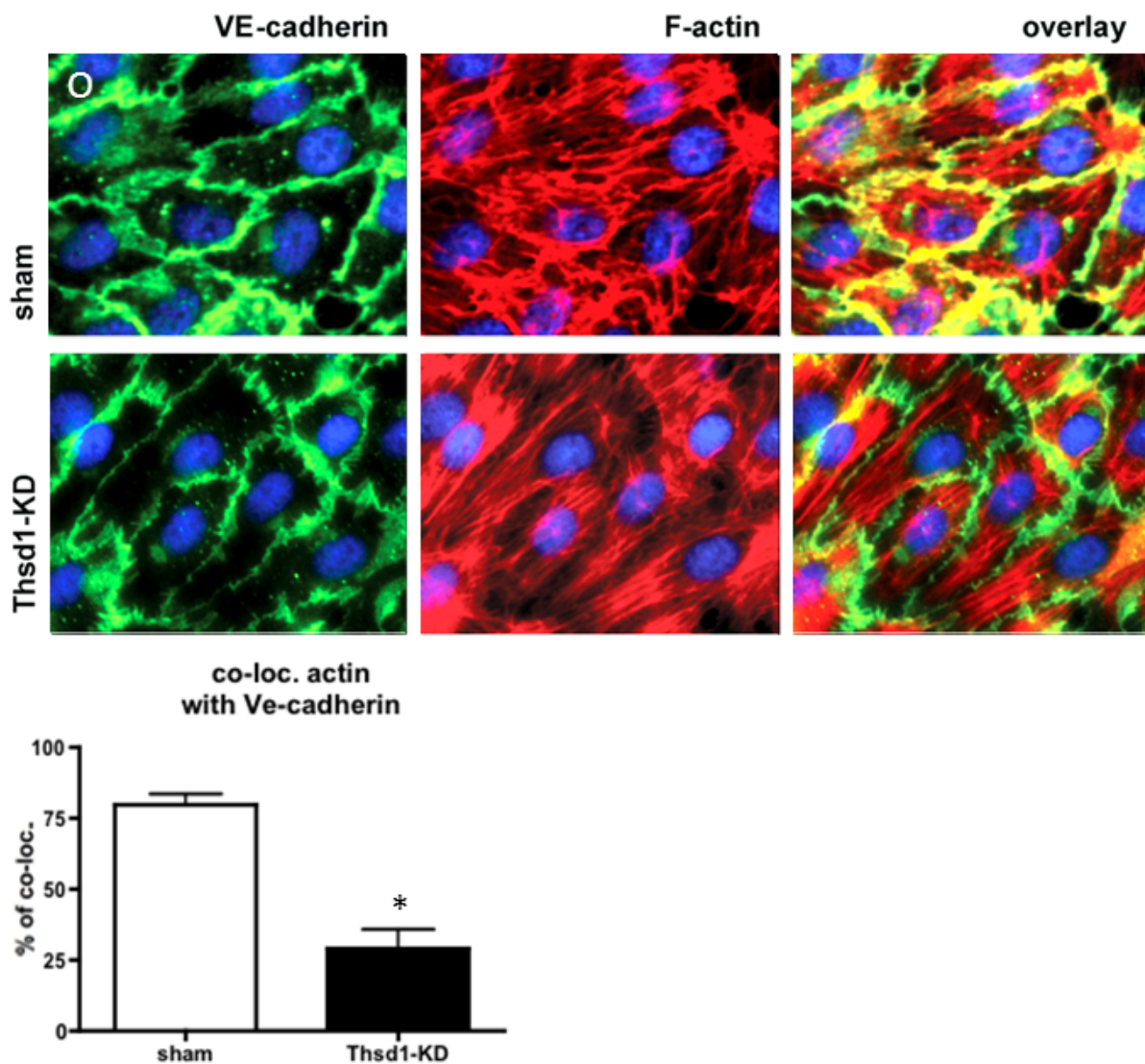


(**O**) Thsd1-KD reduced co-localisation of VE-cadherin with the actin cytoskeleton at the cell-cell junctions, as demonstrated by intracellular immunofluorescent staining. VE-cadherin (green), F-actin (red), co-localised area (yellow) and nuclei (blue). Quantification of the percentage of actin filaments that are co-localised with VE-cadherin are shown in the lower graph (n = 3; mean ± SEM).

## Rac1 activation prevents loss of endothelial barrier function induced by Thsd1 knockdown

Our experiments points toward a Rac1-mediated loss of endothelial integrity in response to Thsd1 silencing. To validate whether this Thsd1-induced modulation of Rac1 activity is crucial for this process, si-Thsd1 transfected HUVECs were treated with a pharmaceutical activator for Rac1 in the Transwell permeability assay *in vitro*. Rac1 stimulation rescued endothelial permeability after Thsd1 knockdown (Figure 4P), thus confirming that Thsd1-induced loss of endothelial permeability in cultured cells was indeed mediated via Rac1 inhibition. To further validate these *in vitro* findings, a phenotype rescue experiment was carried out in the murine retina model: Thsd1 was silenced in combination with treatment with the Rac1 activator and compared with controls that had been treated with intra-ocular injection of si-Thsd1 only. In line with our *in vitro* findings, Rac1 activation reversed the effects of Thsd1 silencing with a significant reduction in the extend of vascular haemorrhaging (Figure 4Q). Combined, these data provide evidence that Thsd1 regulates endothelial permeability via Rac1 activation.
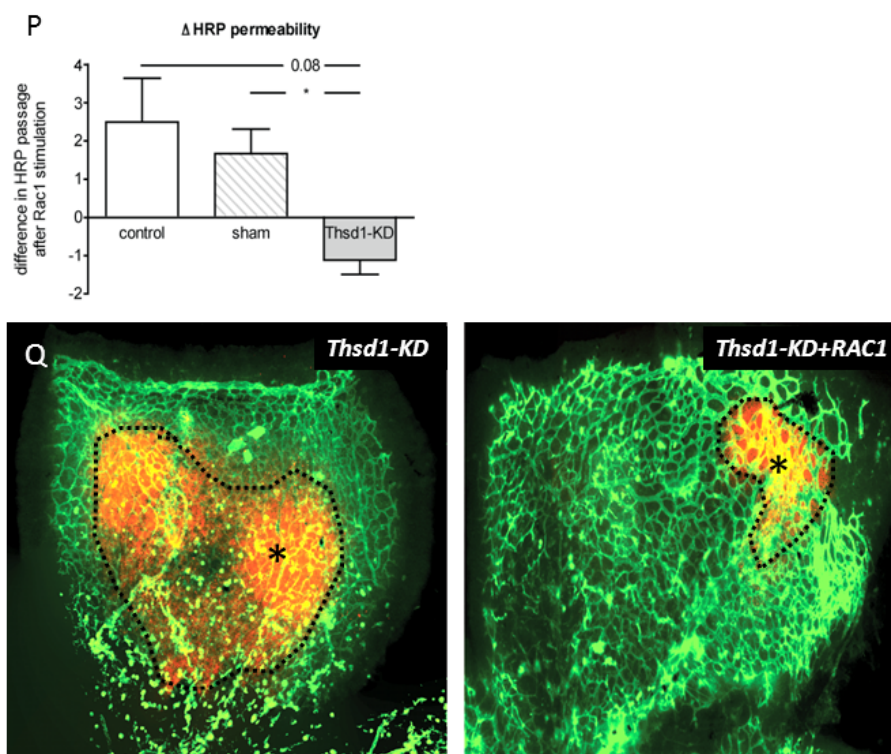


**Rac1 stimulation rescues impaired endothelial integrity in Thsd1-depleted cells.** (**P**) Measurement of endothelial barrier function *in vitro*. Differences in HRP passage in Rac1-stimulated HUVEC monolayers compared with no Rac1 activation after 120 minutes of HRP passage are shown. Control, sham and Thsd1-KD conditions without Rac1 activation were set to zero. Graphs indicate changes in HRP passage in response to Rac1 activation in the different groups ($n = 3$; mean $\pm$ SEM). (**Q**) Representative pictures of double-stained retinas with isolectin GS-IB$_4$ (endothelial cells, green) and TER-119 (erythrocytes, red). Rac1 stimulation reduced area size of extravascular TER-119 erythrocytes accumulation (dotted area marked by an asterisk) after Thsd1-KD ($n = 5$).

## Thsd1 correlates with neovascular intraplaque haemorrhaging and increased plaque vulnerability

Intimal neovascular growth of highly permeable vessels with compromised vascular integrity is an important contributor to atherosclerotic lesion progression and plaque destabilisation. Previous reports demonstrated an association between changes in expression levels of VE-cadherin and loss of endothelial cell-cell contacts in plaque neovessels with intimal extravasation of blood-derived cells[25], while increased Rac1 activation was correlated to lesion advancement[26], suggesting an involvement of these molecular regulators of cell-cell barrier function.
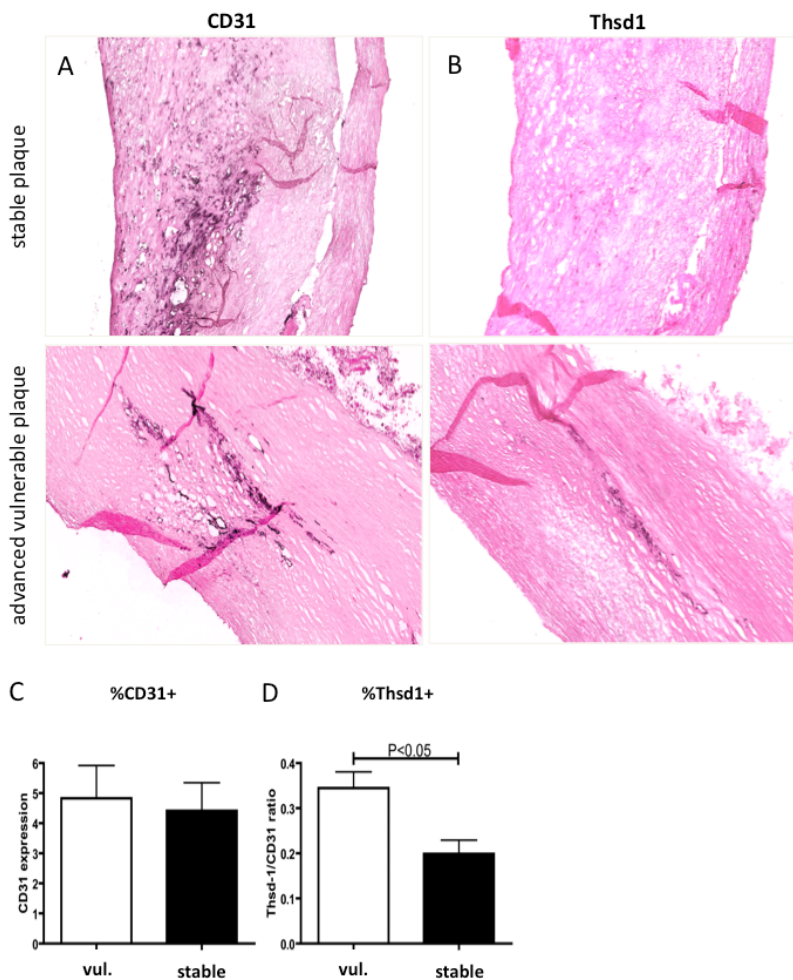


**Figure 5. Thsd1 correlates with neovascular intraplaque haemorrhaging and increased plaque vulnerability.** Representative sections of carotid endarteriectomy specimens stained for (**A**) CD31 and (**B**) Thsd1. Specimens were divided in stable plaque (upper row) and advanced vulnerable plaque lesions with intraplaque haemorrhage (lower row). (**C**) Quantification of CD31 expression in stable plaque (stable) and vulnerable plaque (vul) with intraplaque haemorrhage. No significant difference in CD31 expression between the two groups was observed. (**D**) Quantification of Thsd1:CD31 ratio in stable plaque and vulnerable plaque with intraplaque haemorrhage. Thsd1:CD31 ratio was significantly increased in vulnerable plaque specimens with intraplaque haemorrhage (n = 5; mean ± SEM).

135

Next, we investigated the possible role of Thsd1 in the pathobiology of the compromised neovasculature in advanced atherosclerotic lesions. A correlation study was carried out in human atherosclerotic plaques that were obtained from patients with symptomatic carotid artery disease. Plaques were divided into stable plaques and advanced plaques vulnerable to rupture with pathological evidence of intraplaque haemorrhage. Thsd1 and CD31 expression was determined by immunohistological staining (Figure 5A, B). The ratio of CD31-positive ECs expressing Thsd1 was significantly increased in vulnerable plaques with intraplaque haemorrhage compared with stable plaques, 0.34 ± 0.04% versus 0.20 ± 0.03% of the total intimal area (Figure 5D). This was independent of the degree of vascularisation, as there was no difference in CD31 expression between stable plaques and vulnerable plaques with intraplaque haemorrhage, 4.8 ± 1.1% versus 4.4 ± 0.9% of the total intimal area (Figure 5C). These results points toward a possible role for Thsd1 in endothelial barrier dysfunction in advanced atherosclerotic lesions that are vulnerable to rupture.

**Thsd1 attenuates intraplaque haemorrhage and plaque destabilisation without affecting neovascular growth**

Our previous *in vivo* and *in vitro* findings indicate that Thsd1 is a beneficial factor for maintaining endothelial barrier function. Here, we hypothesised that Thsd1 overexpression may reduce vascular bleeding in vulnerable plaque. The effect of Thsd1 overexpression was assessed in our ApoE-knockout mice vulnerable plaque model. Peri-adventitial infection of an adenovirus expressing murine Thsd1 in the carotid artery resulted in a significant increase in Thsd1 mRNA expression compared with infection with a sham virus (Supplemental figure 8, *online*). Endogenous Thsd1 expression in the carotid arteries of non-treated ApoE-knockout mice was significantly increased in response to 1 week of feeding of a high cholesterol, high fat diet (Supplemental figure 8, *online*). Overexpression of Thsd1 induced clear attenuation of the plaque phenotype at 9 weeks after flow-alteration and atherosclerosis induction, indicated by a significant 75% decrease in neovascular leakage, as measured by Dextran-FITC extravasation in pAd-Thsd1 treated murine carotid arteries compared with pAd-sham treated controls (Figure 6A, B). This observation was also validated by TER-119 immunohistological staining of perivascular accumulation of erythrocytes (Figure 6A, C). A reduction in vascular leakage was also detected in the plaque adventitial area, where Thsd1 reduced Dextran-FITC leakage with 75% as observed by whole-mount visualisation by confocal microscopy (Figure 6D). These effects were independent of intimal neovascular growth, as no changes in numbers of CD31-positive cells were observed (Figure 6E, F). Coincided with improved neovascular integrity, a 40% reduction in intraplaque macrophages accumulation in the Thsd1 overexpression group was observed (Figure 6G, H), whereas intraplaque lipid accumulation remained unaffected (Figure 6I, J). This reduction in percentage of intraplaque macrophages did not affect lesion

size as measured by intima:media ratio (Figure 6K, L). However, necrotic core area was significantly decreased (Figure 6M). Together, these data clearly demonstrate that Thsd1 overexpression is capable to restore compromised endothelial barrier function in vulnerable plaque.
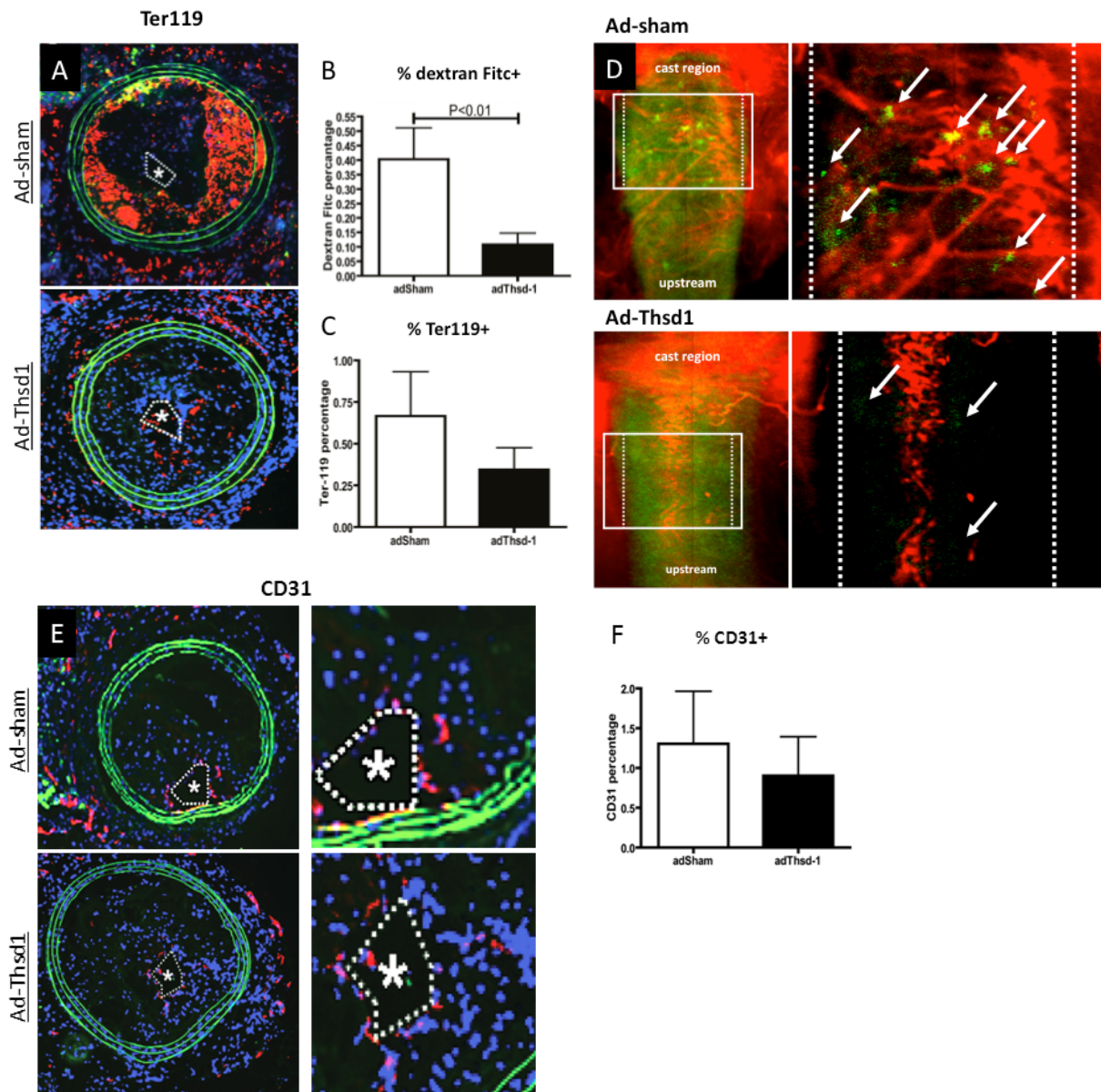


**Figure 6. Overexpression of Thsd1 attenuates intraplaque haemorrhaging and stabilises plaque phenotype in an ApoE-knockout mice vulnerable plaque model.** (**A**) Representative sections of pAd-sham and pAd-Thsd1 treated advanced murine lesions stained for TER-119. Quantification of (**B**) the percentage Dextran-FITC-positive area and (**C**) the percentage TER-119-positive area. (**D**) Whole-mount immunostaining of the adventitial vasculature with isolectin GS-IB$_4$ (endothelial cells, red) with detection of Dextran-FITC perivascular leakage (green, indicated by arrows) in the upstream (atherosclerotic) carotid region from the flow device. Dotted lines indicate vessel boundaries (n = 6). (**E**) Representative sections of pAd-sham and pAd-Thsd1 treated advanced murine lesions stained for CD31. (**F**) Quantification of the percentage CD31-positive area.
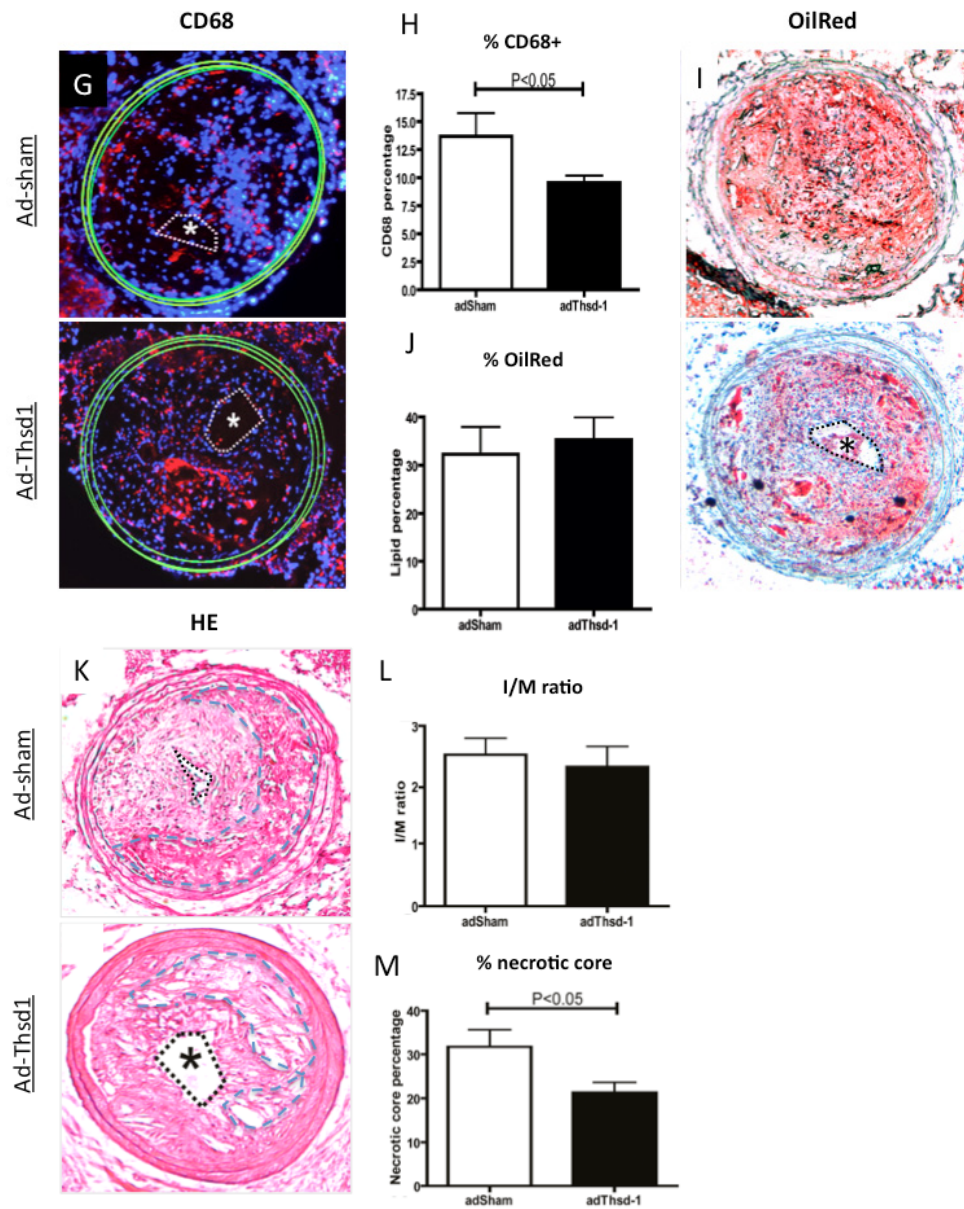
(**G**) Representative sections of pAd-sham and pAd-Thsd1 treated advanced murine lesions stained for CD68. (**H**) Quantification of the percentage CD68-positive area. (**I**) Representative sections of pAd-sham and pAd-Thsd1 treated advanced murine lesions stained for lipids. (**J**) Quantification of the percentage Oilred O-positive area. (**K**) Representative haematoxylin and eosin staining of pAd-sham and pAd-Thsd1 treated advanced murine lesions. (**L**) Quantification of the intima:media (I:M) ratio and (**M**) the percentage necrotic core area. For all micrographs, lumen areas are indicated by dotted lines (white) marked by an asterisk. Necrotic core areas are indicated by dotted lines in blue. For **A**, **E** and **G**: elastin fibres (green), DAPI (blue), Ter119, CD31 and CD68 (red) (n = 10; mean ± SEM).

**siRNA-mediated silencing of Thsd1 aggravates vascular leakage in murine vulnerable plaque**

The protective function of Thsd1 in the vasculature of vulnerable plaque is also validated by a Thsd1 knockdown experiment in the same ApoE-knockout mice vulnerable plaque model: Thsd1 knockdown of the atherosclerotic carotid arteries was achieved by siRNA-mediated silencing as shown by qPCR analysis (Supplemental figure 8, *online*). In line with previous results, Thsd1 knockdown in the ApoE-knockout mice vulnerable plaque model severely aggravated vascular leakage, shown by a 2000% increase in Dextran-FITC perivascular leakage (Figure 7A, B) and a 500% increase in intimal extravascular accumulation of TER-119-positive erythrocytes (Figure 7C). Like in the Thsd1 overexpression condition, no effect of Thsd1 knockdown on intimal neovascular growth was observed, as no difference in CD31-positive cells was detected (Figure 7D, E). However, Thsd1 knockdown did not affect intraplaque macrophage or lipid accumulation (Figure 7F, G). Lesion and necrotic core size also remained unaffected (Figure 7H, I).
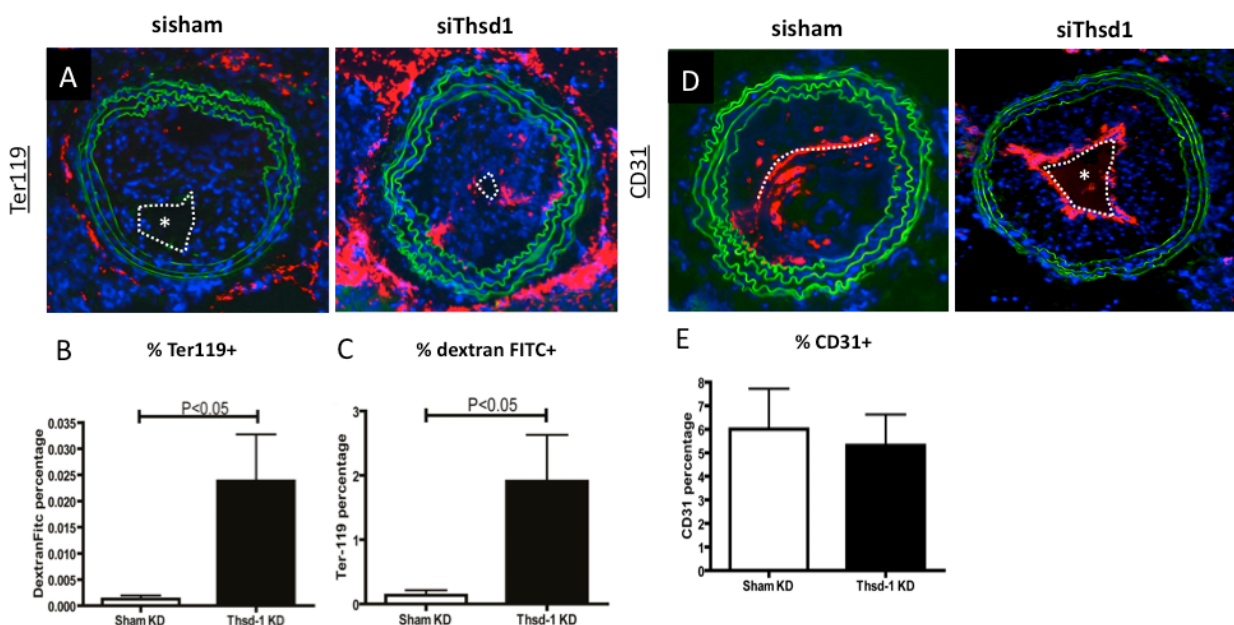


**Figure 7. Thsd1 knockdown severely aggravates intraplaque haemorrhaging in murine vulnerable plaque.** (**A**) Representative sections of si-sham and si-Thsd1 treated advanced murine lesions stained for TER-119. (**B**) Quantification of the percentage Dextran-FITC-positive area and (**C**) the percentage TER-119-positive area. (**D**) Representative sections of si-sham and si-Thsd1 treated advanced murine lesions stained for CD31. (**E**) Quantification of the percentage CD31-positive area.
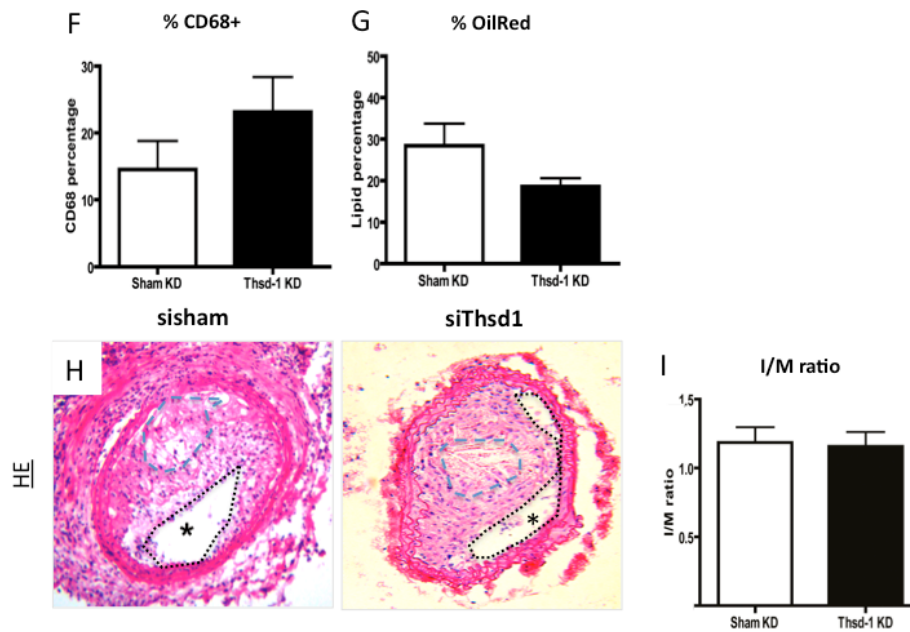
Quantification of (**F**) the percentage CD68-positive area and (**G**) the percentage Oilred O-positive area. (**H**) Representative haematoxylin and eosin staining of si-sham and si-Thsd1 treated advanced murine lesions. (**I**) Quantification of the intima:media (I:M) ratio. For all micrographs, lumen areas are indicated by dotted lines (white) marked by an asterisk. Necrotic core areas are indicated by dotted lines in blue. For **A** and **D**: elastin fibres (green), DAPI (blue), TER-119 and CD31 (red) (n = 10; mean ± SEM).

## Pro-atherogenic and anti-atherogenic stimuli determine Thsd1 mRNA expression in HUVECs

Combined, the results of our ApoE-knockout mice vulnerable plaque model clearly demonstrate that Thsd1 attenuates vascular haemorrhaging and plaque destabilisation by enhancing intimal neovascular integrity. To further characterise the influence of atherogenic triggers on Thsd1 expression in atherosclerosis, we assessed the effect of two well-known pro-atherogenic stimuli - low oxygen and the pro-inflammatory cytokine TNFα - and one anti-atherogenic stimulus - the anti-inflammatory cytokine IL-10 - on Thsd1 expression in HUVECs.

HUVECs were exposed to low oxygen (3% $O_2$) conditions for 4 days and compared with normal oxygen (20% $O_2$) cultures. From day 1, a steady decrease in Thsd1 mRNA level was observed compared with normal oxygen controls. On day 3 and 4, Thsd1 mRNA expression was significantly decreased in HUVECs exposed to low oxygen (Figure 7J). Likewise, stimulation with different concentrations of the pro-atherogenic cytokine TNFα also decreased Thsd1 mRNA expression in HUVECs (Figure 7K).

In contrast, the anti-atherogenic cytokine IL-10 triggered a rise in Thsd1 mRNA expression (Figure 7L). Thus, the anti-atherogenic and pro-atherogenic factors that are abundant in the micro-environment of advanced atherosclerotic lesions determine the expression level of cell-cell barrier function protective Thsd1.
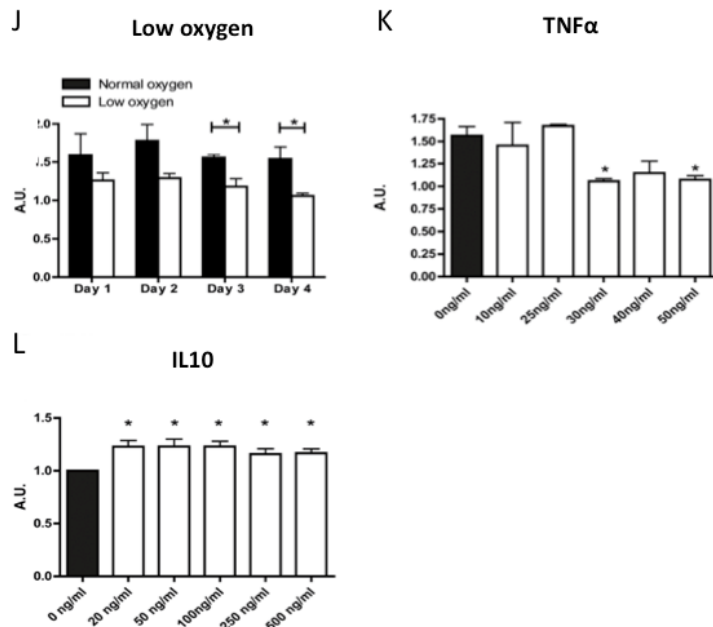


**Pro-atherogenic and anti-atherogenic stimuli determine Thsd1 mRNA expression.** Response of endogenous Thsd1 mRNA expression levels in HUVECs to pro-atherogenic stimuli, including: (**J**) low (3% $O_2$) and normal (20% $O_2$) oxygen conditions over time, and (**K**) different concentrations of TNFα. Response of endogenous Thsd1 mRNA expression levels in HUVECs to an anti-atherogenic stimulus, concerning: (**L**) IL-10. Thsd1 mRNA expression in endothelial cells was diminished by pro-atherogenic stimuli, while an anti-atherogenic stimulus increased Thsd1 mRNA expression (n = 4; mean ± SEM).

## *Discussion*

In this study we identified Thsd1 as a potent angiogenic regulator during embryonic and postnatal vascular development. We showed that Thsd1 was upregulated in the developing murine embryo in Flk1-positive angioblasts compared with Flk1-negative cells, while whole-mount *in situ* hybridisation in developing zebrafish larvae validated the predominant vascular expression of Thsd1. The thrombospondin type I domain (TSP1) in the Thsd1 protein shares a high homology (98%) with the TSP1 domain of Thrombospondin 1, a gene known for its anti-angiogenic properties.[23,27] Reports indicate that upregulation of the zebrafish Thrombospondin 1 orthologue by mRNA injection of Eleven-Nineteen Lysine-

rich Leukaemia (ELL) - a transcription factor of Thrombospondin 1 - resulted in multiple vascular haemorrhaging.[28] Unlike Thrombospondin 1, the basic function of Thsd1 in vascular development was until now, still largely unknown. Based on the specific expression of Thsd1 in the EC subset, we hypothesised that Thsd1 may play a functional role in angiogenesis. Indeed, knockdown of Thsd1 in the developing zebrafish with MO injections resulted in frequent and severe haemorrhaging in the head region.

Coinciding with this finding, the cranial region was also the location of high Thsd1 expression in the cerebral vasculature during early development. In addition, multiple previous studies have suggested that the cranial vasculature may be a predilection site for vascular rupture in the zebrafish model.[13,17,21] Several zebrafish mutants have been identified that display a very similar vascular haemorrhaging phenotype, including heg1, ccm1, ccm2 and ccm3.[17,29,30] Like Thsd1, these genes appear to be involved directly or indirectly in Rac1 activation and RhoA degradation.[31] Little is known about the biochemical and physical properties of Thsd1. Previously, it has been demonstrated that the Thsd1 gene is located between FLJ11712 and C13orf9 within 13q14.3 and has three transcripts (splice variants) of which isoform 1 and 2 are single-pass type I membrane proteins, while isoform 3 is secreted extracellular into the blood plasma. Thsd1 is a glycoprotein of 852 amino acids (94,584 Da) synthesised by many cells and contains a TSP1 domain, which has been found in a number of proteins involved in the complement pathway, as well as in extracellular matrix proteins.[32-34]

Our studies indicate that whereas the vascular integrity seemed to be affected by Thsd1 silencing, the vascular cerebral network appeared to remain intact. This distinct phenotype was once again observed when Thsd1 was silenced in a murine retina model for angiogenesis[35], in which Thsd1 knockdown with siRNA resulted in vascular haemorrhages, independent of changes in vascular macrostructures such as outgrowth of the vasculature towards the border and total number of vessels. To obtain more insight in the molecular mechanisms by which Thsd1 affect vascular integrity without affecting vascular growth, we studied the function of Thsd1 in HUVEC in a number of *in vitro* assays. Cultured monolayers of Thsd1-silenced HUVECs reacted in line with the observed phenotype *in vivo*, demonstrating that cell-cell barrier function was diminished in a Transwell permeability assay. On the other hand, network-formation remained unaffected as shown by a 2D matrigel network-formation assay. Further evaluation of the binding partners and downstream pathways of Thsd1 identified CRT of the CRT-LRP1 complex as a direct downstream effector of Thsd1, and clarified that Thsd1 modulates cell-cell barrier function via a Rac1-actin cytoskeleton-mediated pathway in which FAK-PI3K signalling is involved. It has to be noted that LRP1 immunoblotting of Thsd1 pull down lysates shows only a very weak LRP1 band (data not shown), as LRP1 can be detected as a clear band in CRT pull down samples. These findings imply that LRP1 is not directly associated to Thsd1, but forms a complex with Thsd1 via the intermediate adaptor function of CRT.

Rac1 activity is crucial for the process of cell spreading, as it decreases cell contractility via actomyosin suppression and counteracts RhoA-induced actin stress fibre formation.[35] In addition, activation of Rac1 has been reported to preserve cell-cell junction formation and thereby endothelial barrier function.[36,37] Here, our data clearly show that Thsd1 is involved in Rac1 activation and that Thsd1 knockdown diminished adaptation of the actin cytoskeleton of ECs during cell adhesion.

It was previously reported that cells with impaired interaction between the actin cytoskeleton and cell-cell junction sites were able to proceed through the early phase of *in vitro* network-formation, while in the later phases of angiogenesis increased rigidity of the actin cytoskeleton resulted in loss of endothelial barrier function.[38] In the later phase of vascular development, the maturation of newly formed vessels in response to biological and biomechanical cues - such as pericyte stimulation and blood flow - are characterised by the transition of 'pro-angiogenic' ECs into the quiescent phalanx cell phenotype. Acquisition of this phalanx cell phenotype includes strengthening of the cell-cell junctions mediated by VE-cadherin, and involves modulation in junction complex assembly, restriction of VEGFR-2 signalling and actin cytoskeleton reorganisation.[39] In the light of the findings reported in this study, Thsd1 silencing may therefore compromise vascular integrity by inhibiting Rac1 modulation of the actin cytoskeleton in late angiogenesis during this transition into the quiescent phalanx cell phase. Indeed, qPCR evaluation of co-cultures of HUVECs with human brain-derived pericytes in a duo-chamber system that enables direct reciprocal contact, showed that Thsd1 expression was significantly induced by pericyte stimulation (preliminary data, not shown). However, further evaluation of typical neovessel stabilising or mural cell - pericytes or vSMCs - recruitment factors, including Ang1 and 2, Tie2, PDGF-β, PDGFR-2, VEGF-A and VEGFR-2, showed no changes in response to Thsd1 silencing (preliminary data, now shown). Additional studies are needed to clarify the potential role of Thsd1 in neovessel stabilisation. Rac1 activation is regulated by FAK.[40] Previously, it has been demonstrated that Thrombospondin 1 binds to CRT, leading to stabilisation of the CRT-LRP1 complex at the cell surface resulting in downstream activation of FAK.[41] As Thsd1 shares a similar domain with Thrombospondin 1, we hypothesised that Thsd1 could likewise bind to CRT. Our data confirmed complex formation of Thsd1 and CRT. In addition, the downstream activation of the CRT-LRP1/FAK signalling cascade was verified *in vitro* and *in vivo*. We further demonstrated that PI3K activation, downstream of FAK, was inhibited by Thsd1 knockdown. Previously, it was demonstrated that PI3K is involved in the regulation of vessel integrity during embryonic development and tumour neovascularisation. Loss of PI3K led to depolarisation or junction disassembly, which resulted in weak cell-cell junctions, leakage and structural failure.[42] Overexpression of PI3K promotes Rac1 activity.[43] In line with these findings, our data demonstrate that loss of Thsd1 inhibited FAK-PI3K signalling, which was associated

with a decrease in Rac1 activity. These findings provide further proof that Thsd1 regulates vessel integrity by a Rac1-mediated pathway (Figure 8).



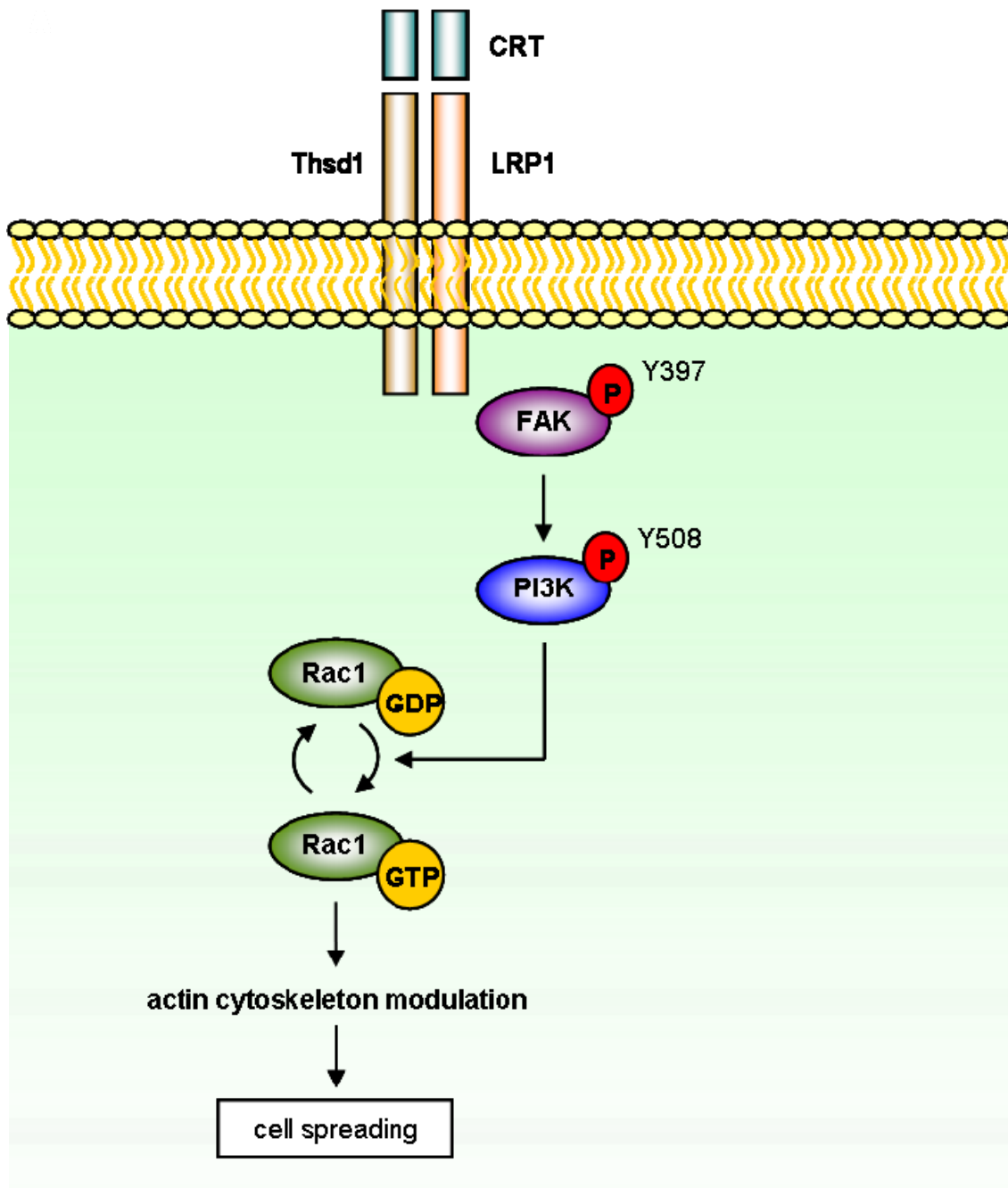**Figure 8. Molecular pathway of Thsd1 during angiogenesis.** Thsd1 maintains vascular integrity by its interaction with CRT at the cell surface, stabilising the CRT-LRP1 complex. Complex stabilisation results in downstream activation of FAK and PI3K, which increases Rac1-GTP levels. Rac1 regulates cell spreading by actin cytoskeleton modulation and maintains endothelial integrity by strengthening VE-cadherin/actin bonds.

As endothelial cell-cell barrier function and neovascular integrity play important roles in progression and destabilisation of rupture prone atherosclerotic lesions, we aimed to evaluate the function of Thsd1 in this widespread vascular-related disease. Advanced atherosclerotic lesions in humans are characterised by intimal growth of a neovasculature with apparent compromised integrity. Immunopathological assessment of human carotid endarterectomy specimens demonstrated that Thsd1 expression was significantly increased in advanced vulnerable lesions with intraplaque haemorrhaging compared with stable plaques, suggesting a compensatory upregulation of Thsd1 to maintain vascular integrity in the intimal neovascular endothelium. This idea of a Thsd1-involved feedback mechanism in order to preserve cell-cell barrier function was validated by our Thsd1 gain- and loss-of-function studies in the ApoE-knockout mice vulnerable plaque model: Thsd1 overexpression led to less intraplaque haemorrhaging as measured by a lower percentage of intraplaque erythrocytes and a decrease in intraplaque Dextran-FITC leakage.

Methia *et al* previously showed that ApoE-knockout mice on a high cholesterol diet exhibited dramatic blood-brain barrier defects. ApoE consists of three isoforms, ApoE2, ApoE3 and ApoE4. It was further demonstrated that ApoE4 is a major risk factor for Alzheimer's disease.[43] Interestingly, Nishitsuji *et al*[44] could proof that the effect of ApoE on blood-brain barrier leakage was isoform dependant as ApoE4-knockin mice showed a more severely compromised blood-brain barrier function than ApoE3-knockin mice. Later, Bell *et al*[45] showed that ApoE, ApoE3 and ApoE4 regulate blood-brain barrier permeability via the CypA-NFκB-MMP9 pathway. ApoE and ApoE3 are both known to suppress CypA-NFκB-MMP9 activation via LRP1. In contrast, the working mechanism of ApoE4 is LRP1-independent of MMP9.

Potentially, the LRP1-mediated inhibition of CypA-NFκB-MMP9 signalling could represent a second mechanism via which Thsd1 regulates vascular permeability: Thsd1 may activate LRP1 leading to decreased CypA levels and subsequently less nuclear NFκB translocation and MMP9 activation, thus contributing to endothelial integrity. Although it has been shown that Thrombospondin 1 influences MMP9 activity, it has not yet been shown that this pathway also acts via LRP1. Additional studies are needed to further elucidate the contribution of Thsd1 function to vascular integrity via MMP9 activation.

There is emerging evidence that intraplaque haemorrhaging plays an important role in plaque progression towards a vulnerable plaque.[46,47] Furthermore, intraplaque haemorrhaging is correlated with plaque rupture and predicted future cardiovascular events and outcome in cardiovascular patients.[48,49] Intraplaque haemorrhage is the result from extravasation of erythrocytes from newly formed vessels. Neovascularisation - driven by intraplaque hypoxia[50] - results in the formation of immature and fragile vessels under influence of VEGF-A. These immature and fragile vessels have a greater vascular permeability resulting in the extravasation of leucocytes and erythrocytes, leading to an increase in inflammatory response, expansion of the necrotic core and intraplaque

haemorrhaging. Stabilisation of these so-called leaky vessels might prevent plaque destabilisation and formation of a vulnerable plaque.[10] Remarkably, macrophage accumulation and necrotic core size were in decline after Thsd1 was overexpressed in our ApoE-knockout mice vulnerable plaque model. This indicates that as Thsd1 attenuates endothelial dysfunction in atherosclerosis, the beneficial effects of improved neovascular integrity in the lesion also slowdown plaque progression. Overall, Thsd1 overexpression led to a more stable plaque phenotype compared with sham treated animals, an effect that was independent of neovascular growth as there was no difference in percentage of adventitial or intimal endothelial structures. A limitation of these overexpression studies is that pAd-Thsd1 virus infection could not be achieved selectively and overexpression of Thsd1 in non-ECs may contribute to the observed findings. However, by carrying out Thsd1 loss-of-function studies in the same ApoE-knockout mice vulnerable plaque model, the essential role of Thsd1 in the regulation of vascular integrity and attenuation of atherosclerosis progression could be confirmed: in contrast to Thsd1 overexpression, Thsd1 knockdown led to a significant increase in intraplaque erythrocyte and Dextran-FITC perivascular leakage without affecting neovascular growth.

In conclusion, here we have identified Thsd1 as a new regulator of vascular integrity in vascular development and advanced vascular disease. To our knowledge, this study is the first report of the biological function of Thsd1 in ECs during normal embryonic and postnatal blood vessel formation. In advanced atherosclerotic lesions, Thsd1 is involved in maintaining cell-cell barrier function in the intraplaque neovasculature and protects the plaque from extensive haemorrhaging and further disease progression. In the light of our findings of the basic and pathobiological function of Thsd1, the gene may be considered an interesting research target for the development of new diagnostics and therapeutics in the treatment of atherosclerosis and other vascular-related diseases in which the pathophysiology entails loss of blood vessel integrity.

## *References*

1. Klaassen I, van Noorden CJ, Schlingemann RO. Molecular basis of the inner blood-retinal barrier and its breakdown in diabetic macular oedema and other pathological conditions. *Prog Retin Eye Res.* 2013;34:19-48.
2. Vandenbroucke E, Mehta D, Minshall R, Malik AB. Regulation of endothelial junctional permeability. *Ann N Y Acad Sci.* 2008;1123:134-145.
3. Tian X, Tian Y, Sarich N, Wu T, Birukova AA. Novel role of stathmin in microtubule-dependent control of endothelial permeability. *FASEB J.* 2012;26(9):3862-3874.

4. Spindler V, Schlegel N, Waschke J. Role of GTPases in control of microvascular permeability. *Cardiovasc Res.* 2010;87(2):243-253.

5. Broman MT, Mehta D, Malik AB. Cdc42 regulates the restoration of endothelial adherens junctions and permeability. *Trends Cardiovasc Med.* 2007;17(5):151-156.

6. Kim SH, Cho YR, Kim HJ, Oh JS, Ahn EK, Ko HJ, Hwang BJ, Lee SJ, Cho Y, Kim YK, Stetler-Stevenson WG, Seo DW. Antagonism of VEGF-A-induced increase in vascular permeability by an integrin α3β1-Shp-1-cAMP/PKA pathway. *Blood.* 2012;120(24):4892-4902.

7. Huveneers S, Oldenburg J, Spanjaard E, van der Krogt G, Grigoriev I, Akhmanova A, Rehmann H, de Rooij J. Vinculin associates with endothelial VE-cadherin junctions to control force-dependent remodelling. *J Cell Biol.* 2012;196(5):641-652.

8. Hoang MV, Nagy JA, Senger DR. Active Rac1 improves pathologic VEGF neovessel architecture and reduces vascular leak: mechanistic similarities with angiopoietin 1. *Blood.* 2011;117(5):1751-1760.

9. Kraemer A, Goodwin M, Verma S, Yap AS, Ali RG. Rac is a dominant regulator of cadherin-directed actin assembly that is activated by adhesive ligation independently of Tiam1. *Am J Physiol Cell Physiol.* 2007;292(3):C1061-C1069.

10. Jain RK, Finn AV, Kolodgie FD, Gold HK, Virmani R. Anti-angiogenic therapy for normalisation of atherosclerotic plaque vasculature: a potential strategy for plaque stabilisation. *Nat Clin Pract Cardiovasc Med.* 2007;4(9):491-502.

11. Sluimer JC, Daemen MJ. Novel concepts in atherogenesis: angiogenesis and hypoxia in atherosclerosis. *J Pathol.* 2009;218(1):7-29.

12. Takayanagi S, Hiroyama T, Yamazaki S, Nakajima T, Morita Y, Usui J, Eto K, Motohashi T, Shiomi K, Keino-Masu K, Masu M, Oike Y, Mori S, Yoshida N, Iwama A, Nakauchi H. Genetic marking of haematopoietic stem and endothelial cells: identification of the Tmtsp gene encoding a novel cell surface protein with the thrombospondin 1 domain. *Blood.* 2006;107(11):4317-4325.

13. Gjini E, Hekking LH, Küchler A, Saharinen P, Wienholds E, Post JA, Alitalo K, Schulte-Merker S. Zebrafish Tie2 shares a redundant role with Tie1 in heart development and regulates vessel integrity. *Dis Model Mech.* 2011;4(1):57-66.

14. van der Heijden M, van Nieuw Amerongen GP, van Bezu J, Paul MA, Groeneveld AB, van Hinsbergh VW. Opposing effects of the angiopoietins on the thrombin-induced permeability of human pulmonary microvascular endothelial cells. *PLoS One.* 2011;6(8):e23448.

15. van Nieuw Amerongen GP, Vermeer MA, Nègre-Aminou P, Lankelma J, Emeis JJ, van Hinsbergh VW. Simvastatin improves disturbed endothelial barrier function. *Circulation.* 2000;102(23):2803-2809.

16. Aman J, van Bezu J, Damanafshan A, Huveneers S, Eringa EC, Vogel SM, Groeneveld AB, Vonk Noordegraaf A, van Hinsbergh VW, van Nieuw Amerongen GP. Effective treatment of oedema and endothelial barrier dysfunction with imatinib. *Circulation.* 2012;126(23):2728-2738.

17. Kleaveland B, Zheng X, Liu JJ, Blum Y, Tung JJ, Zou Z, Sweeney SM, Chen M, Guo L, Lu MM, Zhou D, Kitajewski J, Affolter M, Ginsberg MH, Kahn ML. Regulation of cardiovascular development and integrity by the heart of glass-cerebral cavernous malformation protein pathway. *Nat Med.* 2009;15(2):169-176.

18. Montero-Balaguer M, Swirsding K, Orsenigo F, Cotelli F, Mione M, Dejana E. Stable vascular connections and remodelling require full expression of VE-cadherin in zebrafish embryos. *PLoS One.* 2009;4(6):e5772.

19. Gore AV, Lampugnani MG, Dye L, Dejana E, Weinstein BM. Combinatorial interaction between CCM pathway genes precipitates haemorrhagic stroke. *Dis Model Mech.* 2008;1(4-5):275-281.

20. Liu J, Fraser SD, Faloon PW, Rollins EL, Vom Berg J, Starovic-Subota O, Laliberte AL, Chen JN, Serluca FC, Childs SJ. A betaPix Pak2a signalling pathway regulates cerebral vascular stability in zebrafish. *Proc Natl Acad Sci U S A.* 2007;104(35):13990-13995.

21. Buchner DA, Su F, Yamaoka JS, Kamei M, Shavit JA, Barthel LK, McGee B, Amigo JD, Kim S, Hanosh AW, Jagadeeswaran P, Goldman D, Lawson ND, Raymond PA, Weinstein BM, Ginsburg D, Lyons SE. Pak2a mutations cause cerebral haemorrhage in redhead zebrafish. *Proc Natl Acad Sci U S A.* 2007;104(35):13996-14001.

22. Kwon HB, Choi YK, Lim JJ, Kwon SH, Her S, Kim HJ, Lim KJ, Ahn JC, Kim YM, Bae MK, Park JA, Jeong CH, Mochizuki N, Kim KW. AKAP12 regulates vascular integrity in zebrafish. *Exp Mol Med.* 2012;44(3):225-235.

23. Armstrong LC, Bornstein P. Thrombospondins 1 and 2 function as inhibitors of angiogenesis. *Matrix Biol.* 2003;22(1):63-71.

24. Dawson DW, Pearce SF, Zhong R, Silverstein RL, Frazier WA, Bouck NP. CD36 mediates the *in vitro* inhibitory effects of thrombospondin 1 on endothelial cells. *J Cell Biol.* 1997;138(3):707-717.

25. Bobryshev YV, Cherian SM, Inder SJ, Lord RS. Neovascular expression of VE-cadherin in human atherosclerotic arteries and its relation to intimal inflammation. *Cardiovasc Res.* 1999;43(4):1003-1017.

26. Ohkawara H, Ishibashi T, Shiomi M, Sugimoto K, Uekita H, Kamioka M, Takuwa Y, Teramoto T, Maruyama Y, Takeishi Y. RhoA and Rac1 changes in the atherosclerotic lesions of WHHLMI rabbits. *J Atheroscler Thromb.* 2009;16(6):846-856.

27. Good DJ, Polverini PJ, Rastinejad F, Le Beau MM, Lemons RS, Frazier WA, Bouck NP. A tumour suppressor-dependent inhibitor of angiogenesis is immunologically and functionally indistinguishable from a fragment of thrombospondin. *Proc Natl Acad Sci U S A.* 1990;87(17):6624-6628.

28. Zhou J, Feng X, Ban B, Liu J, Wang Z, Xiao W. Elongation factor ELL (Eleven-Nineteen Lysine-rich Leukaemia) acts as a transcription factor for direct thrombospondin 1 regulation. *J Biol Chem.* 2009;284(28):19142-19152.

29. Voss K, Stahl S, Hogan BM, Reinders J, Schleider E, Schulte-Merker S, Felbor U. Functional analyses of human and zebrafish 18-amino acid in-frame deletion pave the way for domain mapping of the cerebral cavernous malformation 3 protein. *Hum Mutat.* 2009;30(6):1003-1011.

30. Stainier DY, Fouquet B, Chen JN, Warren KS, Weinstein BM, Meiler SE, Mohideen MA, Neuhauss SC, Solnica-Krezel L, Schier AF, Zwartkruis F, Stemple DL, Malicki J, Driever W, Fishman MC. Mutations affecting the formation and function of the cardiovascular system in the zebrafish embryo. *Development.* 1996;123:285-292.

31. Faurobert E, Albiges-Rizo C. Recent insights into cerebral cavernous malformations: a complex jigsaw puzzle under construction. *FEBS J.* 2010;277(5):1084-1096.

32. Ko JM, Chan PL, Yau WL, Chan HK, Chan KC, Yu ZY, Kwong FM, Miller LD, Liu ET, Yang LC, Lo PH, Stanbridge EJ, Tang JC, Srivastava G, Tsao SW, Law S, Lung ML. Monochromosome transfer and microarray analysis identify a critical tumour-suppressive region mapping to chromosome 13q14 and Thsd1 in oesophageal carcinoma. *Mol Cancer Res.* 2008;6(4):592-603.

33. Dunham A, Matthews LH, Burton J, Ashurst JL, Howe KL, Ashcroft KJ, Beare BM, Burford DC, Hunt SE, Griffiths-Jones S, Jones MC, Keenan SJ, Oliver K, Scott CE, Ainscough R, Almeida JP, Ambrose KD, Andrews DT, Ashwell RI, Babbage AK, Bagguley CL, Bailey J, Bannerjee R, Barlow KF, Bates K, Beasley H, Bird CP, Bray-Allen S, Brown AJ, Brown JY, Burrill W, Carder C, Carter NP, Chapman JC, Clamp ME, Clark SY, Clarke G, Clee CM, Clegg SC, Cobley V, Collins JE, Corby N, Coville GJ, Deloukas P, Dhami P, Dunham I, Dunn M, Earthrowl ME, Ellington AG, Faulkner L, Frankish AG, Frankland J, French L, Garner P, Garnett J, Gilbert JG, Gilson CJ, Ghori J, Grafham DV, Gribble SM, Griffiths C, Hall RE, Hammond S, Harley JL, Hart EA, Heath PD, Howden PJ, Huckle EJ, Hunt PJ, Hunt AR, Johnson C, Johnson D, Kay M, Kimberley AM, King A, Laird GK, Langford CJ, Lawlor S, Leongamornlert DA, Lloyd DM, Lloyd C, Loveland JE, Lovell J, Martin S, Mashreghi-Mohammadi M, McLaren SJ, McMurray A, Milne S, Moore MJ, Nickerson T, Palmer SA, Pearce AV, Peck AI, Pelan S, Phillimore B, Porter KM, Rice CM, Searle S, Sehra HK, Shownkeen R, Skuce CD, Smith M, Steward CA, Sycamore N, Tester J, Thomas DW, Tracey A, Tromans A, Tubby B, Wall M, Wallis JM, West AP, Whitehead SL, Willey DL, Wilming L, Wray PW, Wright MW, Young L, Coulson A, Durbin R, Hubbard T,

Sulston JE, Beck S, Bentley DR, Rogers J, Ross MT. The DNA sequence and analysis of human chromosome 13. *Nature.* 2004;428(6982):522-528.

34. Ota T, Suzuki Y, Nishikawa T, Otsuki T, Sugiyama T, Irie R, Wakamatsu A, Hayashi K, Sato H, Nagai K, Kimura K, Makita H, Sekine M, Obayashi M, Nishi T, Shibahara T, Tanaka T, Ishii S, Yamamoto J, Saito K, Kawai Y, Isono Y, Nakamura Y, Nagahari K, Murakami K, Yasuda T, Iwayanagi T, Wagatsuma M, Shiratori A, Sudo H, Hosoiri T, Kaku Y, Kodaira H, Kondo H, Sugawara M, Takahashi M, Kanda K, Yokoi T, Furuya T, Kikkawa E, Omura Y, Abe K, Kamihara K, Katsuta N, Sato K, Tanikawa M, Yamazaki M, Ninomiya K, Ishibashi T, Yamashita H, Murakawa K, Fujimori K, Tanai H, Kimata M, Watanabe M, Hiraoka S, Chiba Y, Ishida S, Ono Y, Takiguchi S, Watanabe S, Yosida M, Hotuta T, Kusano J, Kanehori K, Takahashi-Fujii A, Hara H, Tanase TO, Nomura Y, Togiya S, Komai F, Hara R, Takeuchi K, Arita M, Imose N, Musashino K, Yuuki H, Oshima A, Sasaki N, Aotsuka S, Yoshikawa Y, Matsunawa H, Ichihara T, Shiohata N, Sano S, Moriya S, Momiyama H, Satoh N, Takami S, Terashima Y, Suzuki O, Nakagawa S, Senoh A, Mizoguchi H, Goto Y, Shimizu F, Wakebe H, Hishigaki H, Watanabe T, Sugiyama A, Takemoto M, Kawakami B, Yamazaki M, Watanabe K, Kumagai A, Itakura S, Fukuzumi Y, Fujimori Y, Komiyama M, Tashiro H, Tanigami A, Fujiwara T, Ono T, Yamada K, Fujii Y, Ozaki K, Hirao M, Ohmori Y, Kawabata A, Hikiji T, Kobatake N, Inagaki H, Ikema Y, Okamoto S, Okitani R, Kawakami T, Noguchi S, Itoh T, Shigeta K, Senba T, Matsumura K, Nakajima Y, Mizuno T, Morinaga M, Sasaki M, Togashi T, Oyama M, Hata H, Watanabe M, Komatsu T, Mizushima-Sugano J, Satoh T, Shirai Y, Takahashi Y, Nakagawa K, Okumura K, Nagase T, Nomura N, Kikuchi H, Masuho Y, Yamashita R, Nakai K, Yada T, Nakamura Y, Ohara O, Isogai T, Sugano S. Complete sequencing and characterisation of 21,243 full-length human cDNAs. *Nat Genet.* 2004;36(1):40-45.

35. Stahl A, Connor KM, Sapieha P, Chen J, Dennison RJ, Krah NM, Seaward MR, Willett KL, Aderman CM, Guerin KI, Hua J, Löfqvist C, Hellström A, Smith LE. The mouse retina as an angiogenesis model. *Invest Ophthalmol Vis Sci.* 2010;51(6):2813-2826.

36. Waschke J, Burger S, Curry FR, Drenckhahn D, Adamson RH. Activation of Rac1 and Cdc42 stabilises the microvascular endothelial barrier. *Histochem Cell Biol.* 2006;125(4):397-406.

37. Wójciak-Stothard B, Potempa S, Eichholtz T, Ridley AJ. Rho and Rac but not Cdc42 regulate endothelial cell permeability. *J Cell Sci.* 2001;114(Pt 7):1343-1355.

38. Chervin-Pétinot A, Courçon M, Almagro S, Nicolas A, Grichine A, Grunwald D, Prandini MH, Huber P, Gulino-Debrac D. Epithelial protein lost in neoplasm (EPLIN) interacts with α-catenin and actin filaments in endothelial cells and stabilises vascular capillary network *in vitro*. *J Biol Chem.* 2012;287(10):7556-7572.

39. Potente M, Gerhardt H, Carmeliet P. Basic and therapeutic aspects of angiogenesis. *Cell.* 2011;146(6):873-887.

40. Tomar A, Schlaepfer DD. Focal adhesion kinase: switching between GAPs and GEFs in the regulation of cell motility. *Curr Opin Cell Biol.* 2009;21(5):676-683.

41. Orr AW, Pallero MA, Xiong WC, Murphy-Ullrich JE. Thrombospondin induces RhoA inactivation through FAK-dependent signalling to stimulate focal adhesion disassembly. *J Biol Chem.* 2004;279(47):48983-48992.

42. Yuan TL, Choi HS, Matsui A, Benes C, Lifshits E, Luo J, Frangioni JV, Cantley LC. Class 1A PI3K regulates vessel integrity during development and tumourigenesis. *Proc Natl Acad Sci U S A.* 2008;105(28):9739-9744.

43. Corder EH, Saunders AM, Strittmatter WJ, Schmechel DE, Gaskell PC, Small GW, Roses AD, Haines JL, Pericak-Vance MA. Gene dose of apolipoprotein E type 4 allele and the risk of Alzheimer's disease in late onset families. *Science.* 1993;261(5123):921-923.

44. Nishitsuji K, Hosono T, Nakamura T, Bu G, Michikawa M. Apolipoprotein E regulates the integrity of tight junctions in an isoform-dependent manner in an *in vitro* blood-brain barrier model. *J Biol Chem.* 2011;286(20):17536-17542.

45. Bell RD, Winkler EA, Singh I, Sagare AP, Deane R, Wu Z, Holtzman DM, Betsholtz C, Armulik A, Sallstrom J, Berk BC, Zlokovic BV. Apolipoprotein E controls cerebrovascular integrity via cyclophilin A. *Nature.* 2012;485(7399):512-516.

46. Kolodgie FD, Gold HK, Burke AP, Fowler DR, Kruth HS, Weber DK, Farb A, Guerrero LJ, Hayase M, Kutys R, Narula J, Finn AV, Virmani R. Intraplaque haemorrhage and progression of coronary atheroma. *N Engl J Med.* 2003;349(24):2316-2325.

47. Michel JB, Virmani R, Arbustini E, Pasterkamp G. Intraplaque haemorrhages as the trigger of plaque vulnerability. *Eur Heart J.* 2011;32(16):1977-1985, 1985a, 1985b, 1985c.

48. Altaf N, MacSweeney ST, Gladman J, Auer DP. Carotid intraplaque haemorrhage predicts recurrent symptoms in patients with high-grade carotid stenosis. *Stroke.* 2007;38(5):1633-1635.

49. Hellings WE, Peeters W, Moll FL, Piers SR, van Setten J, van der Spek PJ, de Vries JP, Seldenrijk KA, de Bruin PC, Vink A, Velema E, de Kleijn DP, Pasterkamp G. Composition of carotid atherosclerotic plaque is associated with cardiovascular outcome: a prognostic study. *Circulation.* 2010;121(17):1941-1950.

50. Moreno PR, Purushothaman KR, Sirol M, Levy AP, Fuster V. Neovascularisation in human atherosclerosis. *Circulation.* 2006;113(18):2245-2252.

# Chapter 6

# Cerebral cavernous malformations: from molecular pathogenesis to genetic counselling and clinical management

R.A. Haasdijk, C. Cheng, A.J. Maat-Kievit, H.J. Duckers

## *Abstract*

Cerebral cavernous (or capillary-venous) malformations (CCM) have a prevalence of about 0.1-0.5% in the general population. Genes mutated in CCM encode proteins that modulate junction formation between vascular endothelial cells. Mutations lead to the development of abnormal vascular structures. In this article, we review the clinical features, molecular and genetic basis of the disease, and management.

## Introduction

Cerebral cavernous (or capillary-venous) malformations (CCM; OMIM no. 116860) are vascular malformations with a prevalence of 0.1-0.5% in the general population, with a familial incidence close to 20%.[1-3] CCM may occur sporadically, but most of the time it has an autosomal dominant inheritance pattern with variable expression and incomplete penetrance.[2-6] At least three genes have been associated with CCM: k-rev interaction trapped protein 1 (KRIT1) (CCM1; OMIM *604214), MGC4607 (CCM2; OMIM #603284), and programmed cell death 10 (PDCD10) (CCM3; OMIM #603285). These genes encode proteins that are involved in junction formation between vascular endothelial cells. Mutations in the CCM genes, which are in general loss-of-function mutations, lead to the development of abnormal vascular structures characterised by thin-walled, dilated blood vessels with gaps between the endothelial cells.[1,7]

The underlying genetic mechanism in CCM is partially understood. Second-site genetic mutations have been proposed as one of the possible molecular mechanisms.[1,8]

A total of 9% of individuals were symptomatic before age 10 years, 62-72% between 10 and 40 years, and 19% after age 40 years.[9,10] Up to 25% of individuals with CCM remain symptom free throughout their lives.[11] This percentage may be an underestimate because many asymptomatic persons go unrecognised. Otten *et al*[12] reported an absence of symptoms in 90% of individuals with CCM ascertained in autopsy. Approximately 50-75% of persons with CCM become symptomatic. Affected individuals most often present with seizures (40-70%), focal neurologic deficits (35-50%), non-specific headaches (10-30%) and cerebral haemorrhage (41%).[9,11,13,14] In the most recent study, Denier *et al*[15] found seizures in 55%, focal neurological deficits in 9%, non-specific headaches in 4% and cerebral haemorrhage in 32%.

In most cases, cavernous malformations (or cavernomas) are located within the brain, but in a small proportion of patients with familial CCM, cavernomas may also be observed in the spinal cord, retina, skin or liver.[2,3,16] Retinal cavernomas occur in about 5% of patients with familial CCM. They are unilateral, generally stable and asymptomatic, and can be diagnosed by routine fundoscopy.[2,17] Cutaneous vascular malformations are seen in 9% of familial CCM patients. Three distinct major phenotypes were identified: hyperkeratotic cutaneous capillary-venous malformations (39%), strongly associated with a KRIT1 mutation. Second, capillary malformations (34%) and finally, venous malformations (21%) mostly seen in patients with a PDCD10 mutation. Patients with a Malcavernin mutation are possibly less prone for cutaneous vascular malformations.[2,16,18]

## *Molecular and genetic basis of CCMs*

### Mutated genes and new loci

To date, three genes have been associated with the pathogenesis of CCM, including KRIT1 - also known as CCM1 - located on chromosome 7q11.2-21,[19,20] Malcavernin, murine OSM-osmosensing scaffold for MEKK3 (MGC4607) - also known as CCM2 - on chromosome 7p13[19,21] and PDCD10 - also known as CCM3 -, originally identified as TF-1 cell apoptosis-related gene-15 (TFAR15) on chromosome 3q26.1 (Table 1).[19,22,23] In addition, there is at least one further - as yet unspecified - gene that can cause CCM, which has been mapped to chromosome 3q26.3-27.2. Gianfrancesco *et al*[25] reported the zona pellucida-like domain containing 1 gene as possible candidate. This gene is also located on the long arm of chromosome three centromeric of PDCD10.[3,24-26]

**Table 1. CCM protein interactions.**

| Ligand | Interacted protein | Possible function |
|---|---|---|
| KRIT1 (CCM1) | Rap1a<br>ICAP1α<br>Malcavernin<br>HEG1 receptor<br>Junctional proteins<br>(plus end of ) Microtubules | Tumour suppressor gene<br>Cell adhesion<br>Cell spreading<br>Direction of endothelial cell migration |
| Malcavernin (CCM2) | KRIT1<br>PDCD10<br>Rac1<br>Kinases involved in the p38<br>MAPK signalling cascade | Sequester KRIT1 to the cytosol<br>Lumen formation<br>Vascular permeability<br>Migration |
| PDCD10 (CCM3) | Malcavernin<br>STK24<br>STK25<br>Mst4 | Apoptosis<br>Direction of endothelial cell migration |

CCM: cerebral cavernous (or capillary-venous) malformations, HEG1: heart of glass 1 receptor, ICAP1α: α isoform of the β₁-integrin regulator integrin cytoplasmic adaptor protein 1, KRIT1: k-rev interaction trapped protein 1, PDCD10: programmed cell death 10, STK24/25: serine/threonine protein kinase.

## Distribution and frequency of gene mutations

Close to 100 mutations (88 germline mutations) have been identified in the KRIT1 gene, representing about 40-53% of the CCM families. Mutations in the MGC4607 gene may account for 15-20% of familial CCM cases.[3,7,26-28] The only missense mutation in the MGC4607 gene reported so far, is a leucine to arginine substitution at amino acid 198 (L198R), located in the phosphotyrosine-binding domain (PTB) of Malcavernin.[29] Approximately 10-40% of CCM families have been linked to the PDCD10 gene.[26,28] With a single exception, mutations in the PDCD10 gene are either truncating or large genomic deletions of the entire gene. The only known in-frame deletion of PDCD10 is located in exon 5, encompassing amino acids L33-K50, encoding the serine/threonine kinase binding and phosphorylation domain.[22,23,30] In about 22% of CCM cases with multiple lesions no mutation is detected in the three CCM genes.[26] Although *de novo* mutations have been reported for all three CCM genes, they appear to be more common in the PDCD10 gene.[2,31]

The proportion of familial cases has been estimated approximately at 20% in the general population, and estimated to be as high as 50% in Hispanic-American patients of Mexican descent. These families are all apparently related to the same founder mutation (Q455X) in the KRIT1 gene.[2,3,5]

## Genotype-phenotype relationship

CCM is an autosomal dominant disorder with a clinical penetrance of 88% in CCM1 families, 100% in CCM2 and 63% in CCM3 families.[2,32]

Different explanations have been provided for the molecular pathogenesis of lesion formation in CCM. First, a Knudsonian two-hit mechanism might be involved. According to this mechanism, CCM formation would require a complete loss of the two alleles of a given CCM gene within affected cells. Loss of one of the alleles (first hit) would be the result of a germline mutation, whereas loss of the second allele (or second hit) will occur somatically. In this view, familial CCM exhibits an autosomal dominant mode of inheritance, but is likely recessive at the cellular level.[2,27,33] On the basis of animal, as well as human studies, evidence grows for the two-hit mechanism. For example, in Ccm heterozygous mice, homozygous knockout for Msh2, penetrance of CCM lesions has been increased. Even so, in surgically resected mature lesions from CCM patients, mutations have been found in both alleles.[34] Second, haploinsufficiency may also be an explanation in CCM pathophysiology. In this case, the patient has only a single functional copy of one of the CCM genes, due to mutational inactivation of the other. The single functional copy of the gene, however, does not result in sufficient protein for, for example, an adequate functional junction formation between endothelial cells, which in turn leads to the development of abnormal vascular structures. Third, paradominant inheritance might explain several CCM features. In paradominant inheritance, heterozygous individuals carrying a 'paradominant' mutation are phenotypically normal, but the trait only becomes

manifest when a somatic mutation occurs during embryogenesis, giving rise to loss of heterozygosity and formation of a mutant cell population that is homozygous for the mutation. In addition, a second hit may be caused by environmental factors. The exposure of CCM mutated, presensitised microvascular regions to oxidative stress generated by endothelial nitric oxide synthase uncoupling and reactive oxygen species formation could lead to perivascular astrocytosis.[35-37] The localised nature and the number of lesions (usually a single one in sporadic cases versus multiple lesions in familial cases), as well as the age of first presentation of the phenotype being earlier in familial cases and fits in this type of inheritance. Finally, trans-heterozygosity - in which a patient has synergistic mutations in different genes of the CCM pathway (for example a germline mutation in the KRIT1 gene with an additional somatic mutation in the MGC4607 or PDCD10 gene) - might also explain intrafamilial clinical variability. Indeed, it has been shown that a decrease in the KRIT1, MGC4607 or PDCD10 gene alone caused little or no effect independently, but when combined, resulted in very high incidence of intracranial haemorrhage.[1,3,27,38]

## *Biology of CCMs*

### **Protein function and expression pattern**

The KRIT1 gene contains 20 exons of which 16 encode a 736 amino acid protein containing three NPxY/F motifs and three ankyrin repeat domains at the N-terminus, and one C-terminal band 4.1 ezrin radixin moesin domain (FERM) found in exons 14-20 (Figure 1).[1,2,27,39-41] The NPxY/F motifs may be involved in dimerisation either intramolecular folding of the KRIT1 protein, resulting in a closed and open conformation of KRIT1.[41] After that, the first NPxY/F motif interacts with the α-isoform of the $\beta_1$-integrin regulator integrin cytoplasmic adaptor protein 1 (ICAP1α). ICAP1α is a 200 amino acid protein containing a PTB domain and even as KRIT1 a nuclear localisation signal motif in the N-terminus. There is evidence that both KRIT1 and ICAP1α can translocate into the nucleus, where they could cooperate in regulating gene expression. In particular, an open/closed conformation switch regulates KRIT1 nucleocytoplasmic shuttling and molecular interactions.[40,41] The ankyrin repeats in KRIT1 are thought to be involved in protein-protein interaction and have been found in many proteins. No partner interacting with KRIT1 ankyrin repeats has yet been found.[27,39,41] The FERM domain in KRIT1 is composed of three subdomains, F1-F3, arranged in cloverleaf shape. The F3 subdomain has a PTB-like domain, which recognises the NPxY/F motif on the cytoplasmic tail of transmembrane receptors. Rap1a is also bind by the FERM domain, suggesting that KRIT1 may function as a scaffold for transmembrane receptors and Rap1a.[27,29,39,41]

The MGC4607 gene contains 10 exons encoding Malcavernin, a 444 amino acid protein containing a PTB domain similar to that of ICAP1α. Malcavernin binds KRIT1 by the PTB domain and inhibits in this way nuclear translocation of the KRIT1-ICAP1α complex.[2,7,21,41]

The PDCD10 gene contains seven exons encoding a 212 amino acid protein containing a dimerisation domain at the N-terminus and a C-terminal focal adhesion targeting-homology domain with a highly conserved HP1 surface.[42] Previous studies suggested also the presence of an N-terminal serine/threonine kinase binding and phosphorylation domain, which binds proteins of the germinal centre kinase III family (STK24, STK25 and Mst4).[2,30,43-46] The dimerisation domain mediates dimerisation of PDCD10. The Fat-homology domain is important for stabilisation of the expressed PDCD10 protein and interacts with the PTB domain of Malcavernin and paxillin LD motifs.[42] PDCD10 also binds Ptdlns(3,4,5)P3 and functions in this way in the (PI3k-)PIP$_3$-PDPK1-Akt signalling pathway.[23,47] He *et al* suggested that the C-terminus of PDCD10 could be important in the stabilisation of VEGFR-2 signalling, which is crucial for vascular development.[23,48]
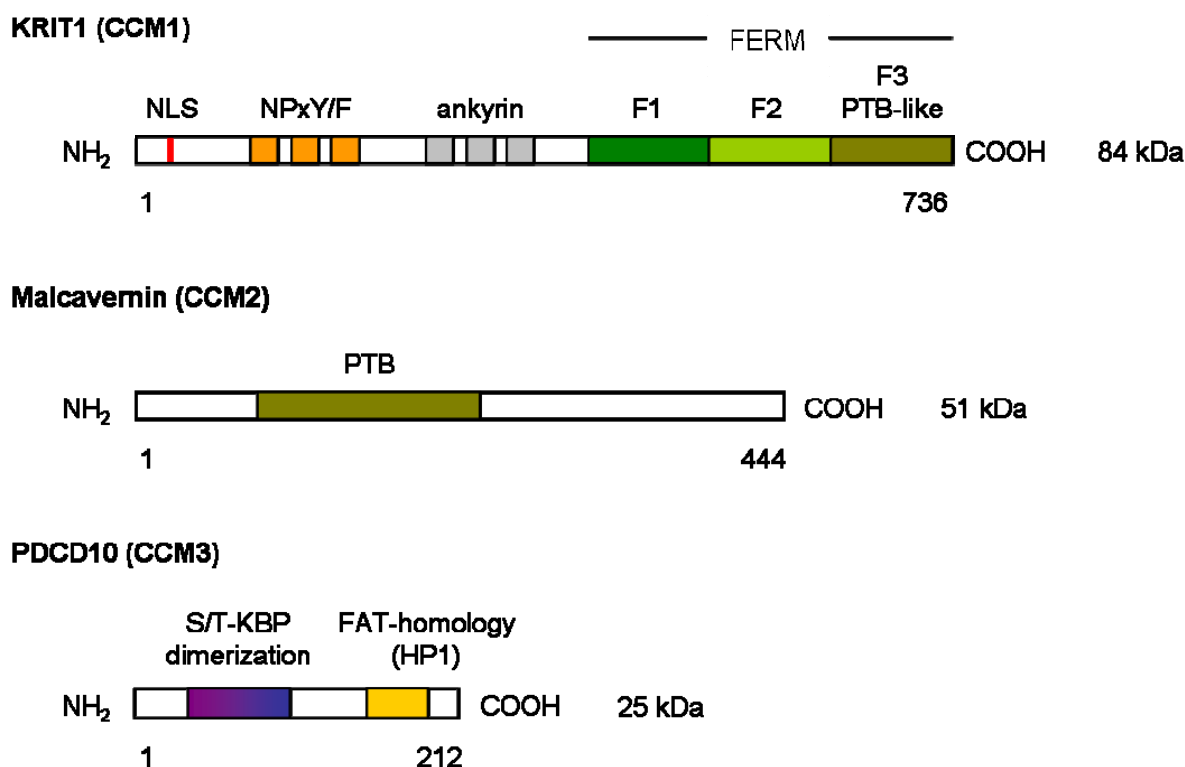


**Figure 1. Functional domains of CCM proteins.** Ankyrin: protein-protein interaction domain, FERM: four-point one ezrin radixin moesin domain, NLS: nuclear localisation signal, NPxY/F: ICAP1α - Malcavernin binding site, PTB: phosphotyrosine-binding domain, S/T-KBP: serine/threonine kinase binding and phosphorylation domain.

Despite the vascular nature of CCM, *in situ* hybridisation studies have shown KRIT1 mRNA and protein expression in astrocytes, neurons and various epithelial cells. KRIT1 protein was also detected in vascular endothelial cells during early angiogenesis, localised in the cell-cell junctions.[3,49] Guzeloglu-Kayisli *et al*[50] demonstrate that KRIT1 is also present in endothelial cells and cells involved in the formation of the blood-brain barrier, which implicates an important role for KRIT1 in intercellular communication and adherence. MGC4607 mRNA expression has been detected in neurons and astrocytes, as well as in cerebral vessels. PDCD10 mRNA is expressed in neuronal cells at adult stages, but also during embryogenesis.[3,51]

Additional, neural expression of KRIT1, MGC4607 and PDCD10 imply that vascular malformations in CCM could also result from a defect in signalling between endothelial and neural cells, but it is still unclear whether the primary defect is of vascular or neuronal origin.[3] In spite of this, most research has been focused on endothelial cells.

**Histology**

The vessel wall in CCM is characterised by less and abnormal junction formation between endothelial cells. After that, the expression of intercellular junction proteins is increased to compensate for the loose of cell contacts. Another characteristic of CCM is the lack of subendothelial support in the vessel wall of CCM made visible by decline in the presence of perivascular supporting cells (pericytes) and deposition of a basal lamina with disorganised collagen bundles. In addition, the formation of microgaps at the interendothelial junction sites was observed using scanning electron microscopy.[52,53] Zhao *et al*[54] suggested that CCM may develop as a result of irregular organisation of endothelial cells, as a consequence of an increased proliferation and migration potential of these cells. In line with this hypothesis, increased migratory and proliferatory endothelial cell function would indeed require reduced cell-cell contact and reduced presence of pericytes.

## *Molecular pathogenesis of CCMs*

At the molecular level CCM proteins regulate cell-cell adhesion (Figure 2A), cell polarity and most likely cell adhesion to the extracellular matrix (Figure 2B).[1,46,55]

**Cell-cell adhesion**

Initiation and maintenance of cell-cell adhesion require the assembly of adherens junctions. The formation of these adherens junctions is stimulated by Rap1a, which forms a complex with KRIT1. Rap1a recruits KRIT1 to the plasma membrane, where it binds to the heart of glass 1 (HEG1) receptor to form a ternary complex of HEG1, KRIT1 and

Malcavernin.[19,41,56] HEG1 is a transmembrane protein, expressed specifically in the endothelium and endocardium. No binding ligand for HEG1 is currently known, although it has been suggested in previous studies that HEG1 may be involved in the Wnt/β-catenin signalling, possibly by binding KRIT1.[41,57-59] KRIT1 binds β-catenin and stimulate the association of β-catenin with vascular endothelial-cadherin, required for adherens junction formation.[60] KRIT1 may also function as a tumour suppressor gene; KRIT1-β-catenin binding prevents β-catenin translocation to the nucleus where displacement of the transcriptional repressor Groucho from T-cell factor proteins by β-catenin would activate Wnt target gene expression.[55,61,62] However, β-catenin activity in the nucleus is also vital for the blood-brain barrier, as many regulatory proteins involved in its development are under Wnt/β-catenin control.[41,62]

## Cell polarity

Adherens junctions also promote tight junction assembly. This takes place by the formation of a ternary complex of KRIT1, AF6/afadin and claudin 5.[55,63] Tight junctions may function as a physical barrier along the cell surface. As a consequence of asymmetrical distribution of proteins and lipids across this barrier, cell polarisation takes place.[41,64] Cell polarity is important in the process of lumen formation.[41] Except tight junction formation, cell polarity is also established through a reshaping of the intracellular cytoskeleton organisation. This is regulated by ROCK, a RhoA effector. Crose *et al*[65] showed that Malcavernin regulates RhoA protein level. Malcavernin binding of Smurf1 increases Smurf1-mediated degradation of RhoA. After that, Borikova *et al*[66] also showed that KRIT1 and PDCD10 in addition to Malcavernin are required for the regulation of RhoA protein levels. KRIT1 is a negative regulator of RhoA activity. The functional mechanism of KRIT1 is not yet totally known. In contrast, some aspects of PDCD10 inhibition of RhoA activation has been elucidated, as PDCD10 acts by stabilisation of germinal centre kinase III proteins and subsequent activation of moesin, a RhoA inhibitor.[67-69] Loss of the CCM proteins results in an increase of RhoA activity and changes in regulation of ROCK and the cytoskeleton rigidity.

## Cell adhesion to the extracellular matrix

$β_1$-integrin, essential for the control of the intracellular cytoskeleton organisation, regulates endothelial cell adhesion to the extracellular matrix.[39,70] It is proposed that $β_1$-integrin signal to Cdc42 and Rac1.[41,71,72] Both are required for the induction of vacuole and lumen formation in vascular endothelial cells.[39,43,73,74] In addition, $β_1$-integrin also promotes blood vessel maturation by stimulating the adhesion of mural cells to endothelial cells.[41] $β_1$-integrin function is inhibited by binding of ICAP1α. KRIT1 competes with $β_1$-integrin for binding to ICAP1α, suggesting that KRIT1 may regulate the ICAP1α inhibitory effect on $β_1$-integrin.[7,27-29,39,41]
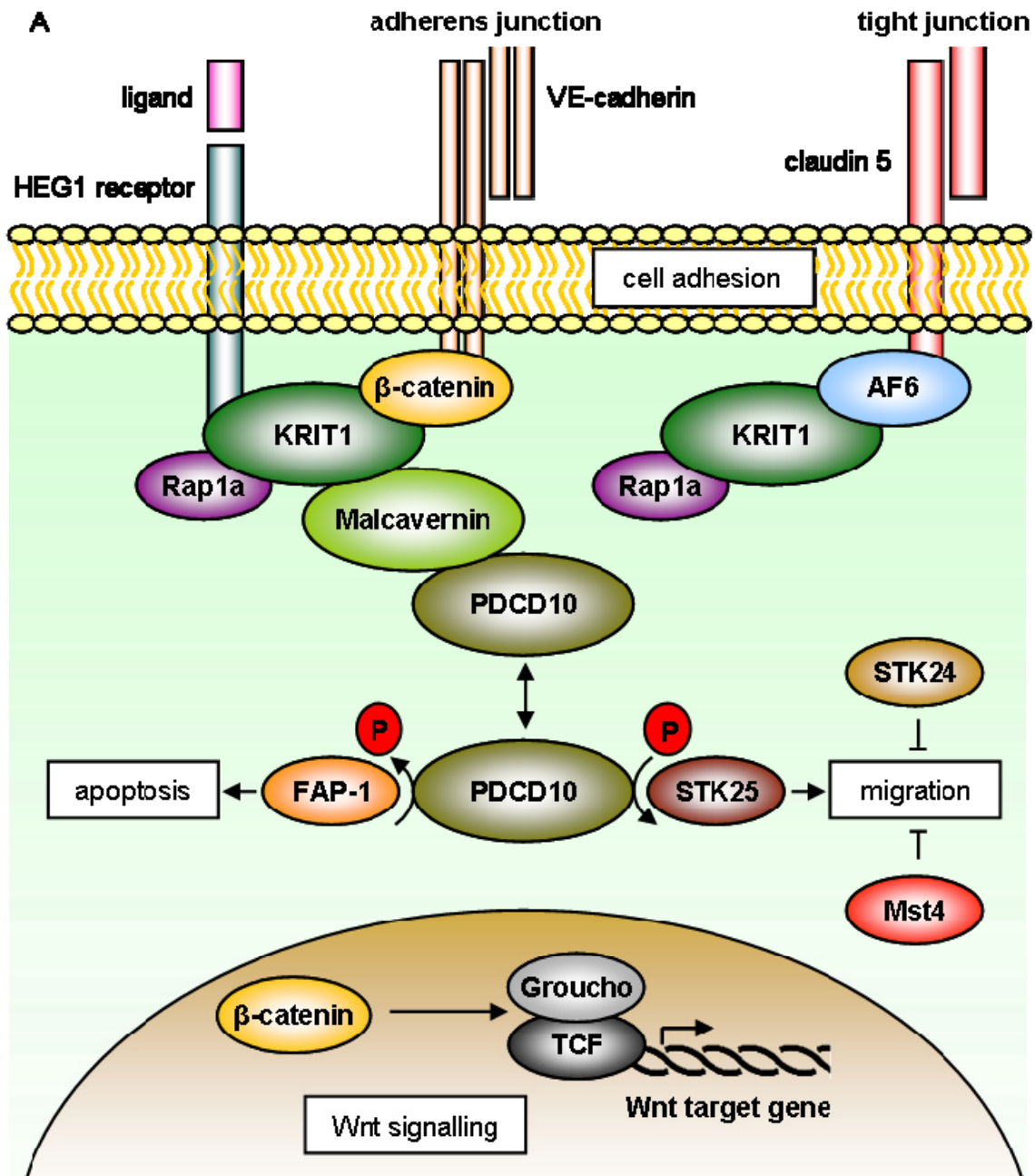
**Figure 2. Integrin signalling pathway.** (**A**) Cell-cell adhesion. HEG1 receptor: heart of glass type 1 receptor, KRIT1: k-rev interaction trapped protein 1, PDCD10: programmed cell death 10, STK24/25: serine/threonine protein kinase, TCF: T-cell factor protein. ( ⊢⎯⎯⊣ ) inhibition, ( ⎯⎯▶ ) stimulation, ( ◀⎯▶ ) interaction.
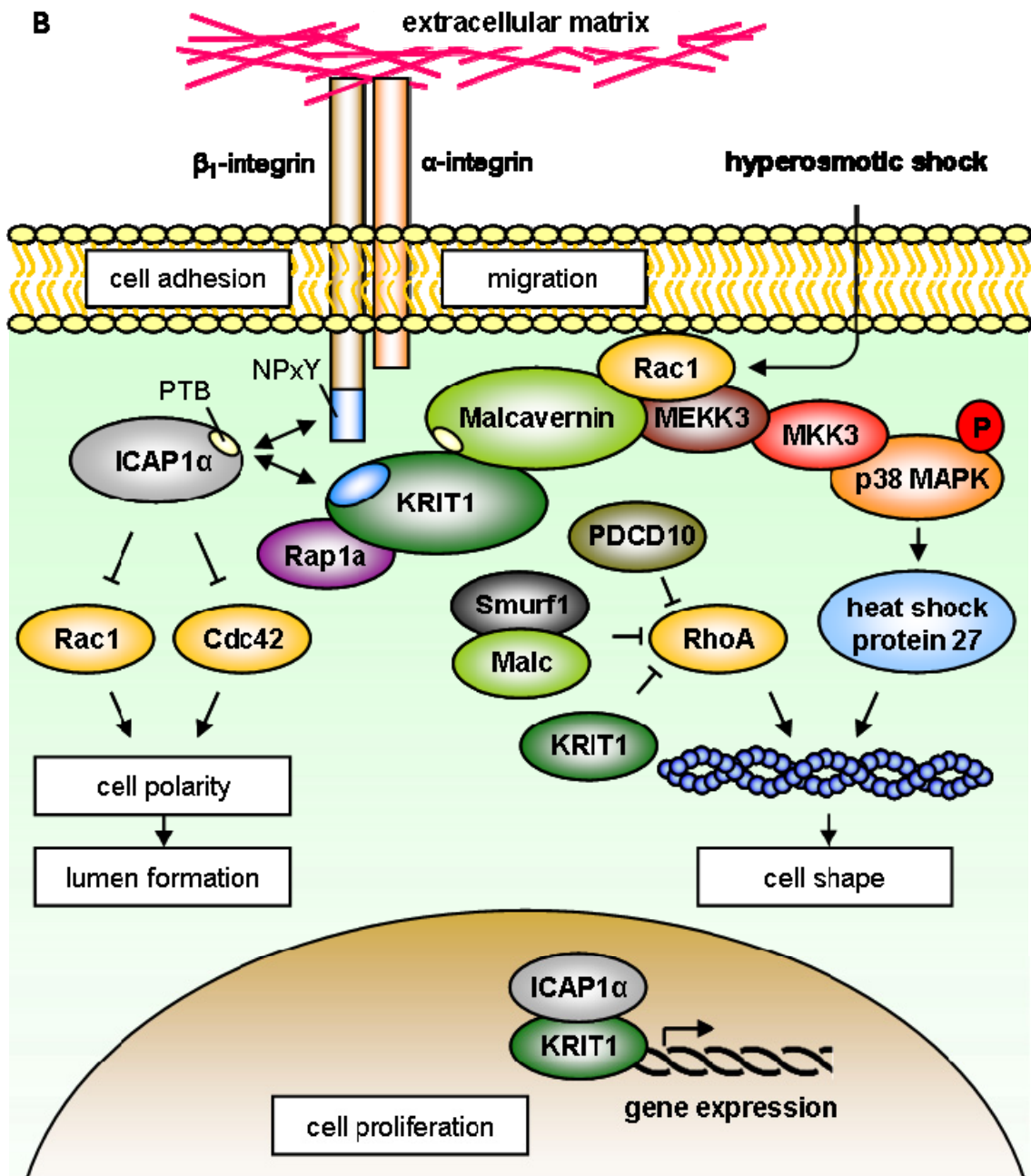
(**B**) Cell-extracellular matrix adhesion. ICAP1α: α isoform of the β$_1$-integrin regulator integrin cytoplasmic adaptor protein 1, KRIT1: k-rev interaction trapped protein 1, PDCD10: programmed cell death 10, PTB: phosphotyrosine-binding domain. ( ———|) inhibition, ( ——▶) stimulation, ( ◀——▶) interaction.

Cell adhesion to the extracellular matrix induces formation of focal adhesion sites in which plaque proteins - such as vinculin and paxillin - provide a bridge between β-integrins and the actin cytoskeleton. Subsequent activation of signalling cascades, regulated by focal adhesion kinase, promote actin cytoskeleton plasticity.[75] Malcavernin has been shown to be capable to regulate actin cytoskeleton plasticity. In response to hyperosmotic shock, restoration of cell volume and cell shape is regulated by the p38 MAPK signalling cascade, controlled by Malcavernin. Malcavernin acts as a scaffold protein for Rac1 and the upstream kinases MEKK3 and MKK3. The p38 MAPK signalling pathway leads to the activation of heat shock protein 27, which in turn activates actin polymerisation and stabilisation.[29,41,55,73,76]

## *Clinical management of CCMs*

**Genetic counselling and molecular diagnosis**
To estimate the genetic risk of CCM, three key points are essential (Figure 3)[3]:

- a detailed three-generation family tree with specific enquiry about seizures, cerebral haemorrhages, focal neurological deficits and (recurrent) headaches
- MRI of the brain to differentiate between solitary or multiple CCM lesions
- age of onset

Genetic testing for KRIT1, MGC4607 and PDCD10 can confirm the clinical diagnosis in patients, and enables predictive and prenatal testing.

The yield of mutation screening in CCM depends on family history. If only a single lesion can be detected, familial transmission is extremely rare. In contrast, sporadic cases with multiple cerebral lesions are most likely to have a genetic cause and need to be considered as familial cases. In these cases, genetic screening of all three CCM genes is indicated. The sensitivity of this screen is estimated to be 57%; therefore, the patient should be aware that a negative test does not exclude a genetic cause.[2,3] The explanation for a negative test may be a somatic mosaicism of a *de novo* mutation during gestation, which is not always detectable in DNA extracted from peripheral mononuclear blood cells. Also additional mutations outside the CCM coding exons may account for altered transcription of CCM associated proteins and fail to be detected by conventional gene mapping techniques.[2]

In familial cases, sensitivity of genetic screening of all three CCM genes in a CCM proband with an affected relative is 96%. Once the mutation has been identified in a proband, sensitivity of screening of the relatives of this particular patient is 100%.[2] Genetic counselling is important to help patients and relatives to come to an informed choice.

When mutation screening is negative, predictive testing of relatives is not an option, which precludes the need for a magnetic resonance imaging (MRI). When mutation screening is positive, an additional MRI would be recommended. Although the sensitivity of MRI is very high, MRI as an initial screening test does not exclude a predisposition for CCM, as the disease may be in its latent phase, devoid of CNS lesions.[2,27]

Predictive testing of minors should not be performed, given the possible psychological and socio-economic consequences of genetic testing, late onset, and reduced penetrance.[2]
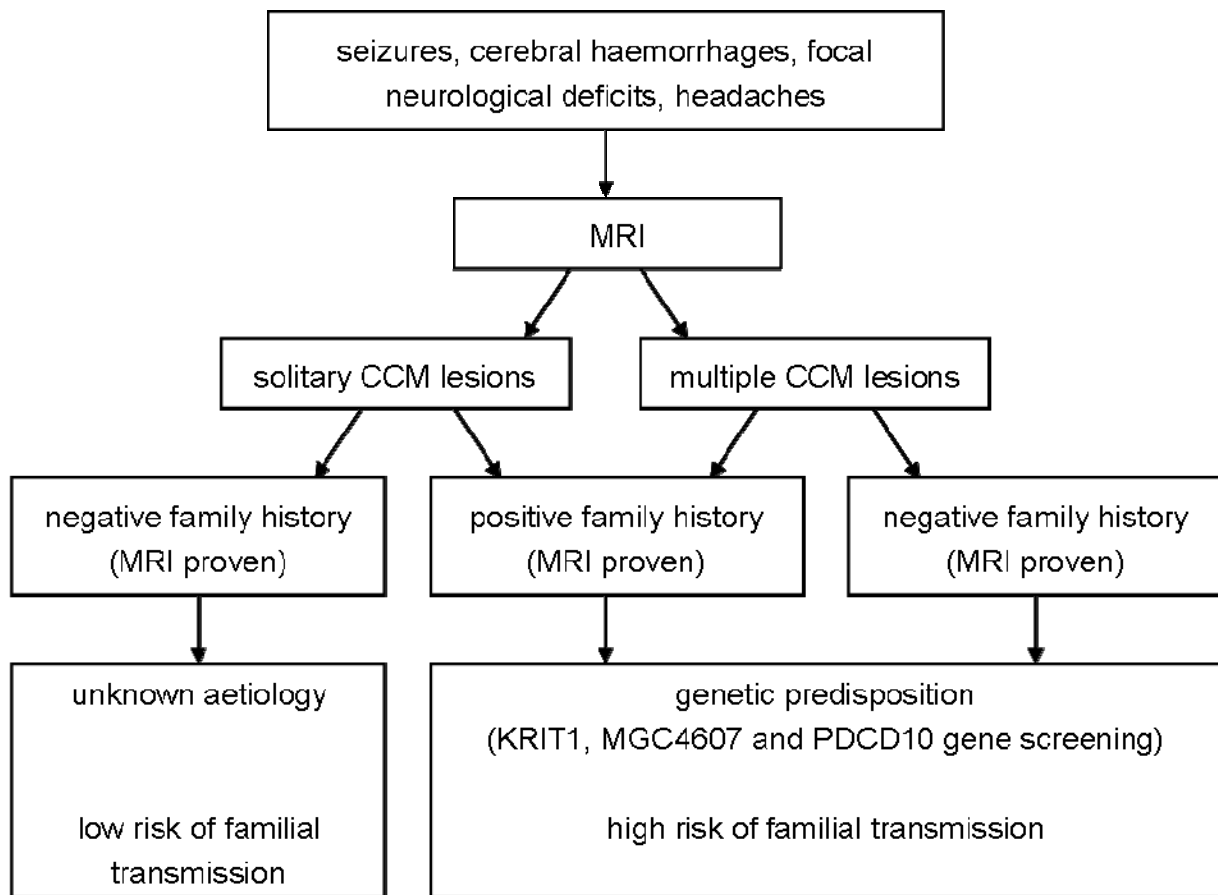


**Figure 3. Scheme for work-up of CCM patients at clinical presentation.** Most patients (50-80%) with CCM are sporadic without a known family history of CCM. Solitary CCM lesions may be found in 8-19% of familial cases and roughly 75% of sporadic cases. Multiple lesions are indicative of familial forms of CCM.[27]

**Prenatal diagnosis and pregnancy**

Prenatal diagnosis or pre-implantation genetic diagnosis is technically feasible in known familial mutations. Decisions about termination of pregnancy in case of familial mutation detection in a foetus might be difficult, because of reduced penetrance and late onset of symptoms. There is no contra-indication for pregnancy and normal delivery in patients with identified small lesions, without recent clinical signs of haemorrhage. Large lesions or recent symptomatic haemorrhages are a relative contra-indication for pregnancy. In case of pregnancy, caesarean section should then be considered.[2,27]

**Clinical management of CCMs**

Clinical monitoring of CCM depends on the presence of clinical manifestations. In asymptomatic individuals with an increased risk of CCM, a MRI analysis every 1 or 2 years should be considered. In our hospital MRI will be performed in carriers or at-risk persons. Only if neurological problems arise or increase, MRI will be repeated. The indication for surgery should be discussed individually with the patient in an experienced neurosurgical centre. Thereby, patients clinical course in combination with MRI characteristics of the CCM lesion, such as localisation, size or new haemorrhage, are important factors for the decision of surgery. In case of deep-seated or brainstem lesions, surgery is associated with a morbidity rate of 30-70% and a mortality rate of 2%. Stereotactic radiosurgery for these lesions remains controversial.[77-79]

Medical treatment consists of inhibition of RhoA by simvastatin, or its effector protein ROCK by fasudil. Also cyclic adenosine monophosphate-elevating drugs should be considered. All of them stabilise CCM lesions by improving vascular integrity.[66,79-82] Preventing progression of CCM lesions could be reached by sorafenib - an anti-angiogenic drug - targeting VEGF receptors and ERK signalling, which is enhanced in the endothelium of CCM lesions.[83,84] Treatment with antiplatelet drugs should be avoided, whereas anticoagulation with coumadin derivatives is contra-indicated.[2,19,53]

**Prognosis of CCMs**

The long-term prognosis of familial CCM is not well known, but the available data suggest that it is quite favourable after (surgical) treatment.

MRI identified new lesions appear at a rate of 0.2-0.4 lesions per patient year. The new onset seizure rate is 2.4% per patient year and the haemorrhage rate is 3.1%.[2,3,10,27,85]

## Conclusion

The pathogenesis of CCM remains to date incompletely clarified. One theory is a perturbed relationship between adhesion and migration of endothelial precursor cells during the formation of the primary vascular plexus. Initiation, guidance and termination of migration are precisely regulated by interaction with the extracellular matrix and neighbouring cells. Adhesion and migration are linked by the CCM pathway proteins. CCM complex components function as bridging molecules between junctional and cytoplasmic proteins. Loss-of-function of one of the CCM proteins leads to a decrease in adhesion. This theory is mainly based on research carried out in endothelial cells. Additional studies to the effect of interaction between neural and endothelial cells are necessary, as it remains unclear whether the primary defect of CCM is of vascular or neuronal origin.

## References

1. Gore AV, Lampugnani MG, Dye L, Dejana E, Weinstein BM. Combinatorial interaction between CCM pathway genes precipitates haemorrhagic stroke. *Dis Model Mech.* 2008;1(4-5):275-281.
2. Labauge P, Denier C, Bergametti F, Tournier-Lasserve E. Genetics of cavernous angiomas. *Lancet Neurol.* 2007;6(3):237-244.
3. Revencu N, Vikkula M. Cerebral cavernous malformation: new molecular and clinical insights. *J Med Genet.* 2006;43(9):716-721.
4. Dashti SR, Hoffer A, Hu YC, Selman WR. Molecular genetics of familial cerebral cavernous malformations. *Neurosurg Focus.* 2006;21(1):e2.
5. Rigamonti D, Hadley MN, Drayer BP, Johnson PC, Hoenig-Rigamonti K, Knight JT, Spetzler RF. Cerebral cavernous malformations. Incidence and familial occurrence. *N Eng J Med.* 1988;319(6):343-347.
6. Felbor U, Sure U, Grimm T, Bertalanffy H. Genetics of cerebral angioma. *Zentralbl Neurochir.* 2006;67(3):110-116.
7. Brouillard P, Vikkula M. Genetic causes of vascular malformations. *Hum Mol Genet.* 2007;16(Spec No. 2):R140-R149.
8. Gault J, Shenkar R, Recksiek P, Awad IA. Bi-allelic somatic and germline CCM1 truncating mutations in a cerebral cavernous malformation lesion. *Stroke.* 2005;36(4):872-874.
9. Brunereau L, Labauge P, Tournier-Lasserve E, Laberge S, Levy C, Houtteville JP. Familial form of intracranial cavernous angioma: MR imaging findings in 51 families. French Society of Neurosurgery. *Radiology.* 2000;214(1):209-216.

10. Labauge P, Brunereau L, Laberge S, Houtteville JP. Prospective follow-up of 33 asymptomatic patients with familial cerebral cavernous malformations. *Neurology.* 2001;57(10):1825-1828.

11. Siegel AM. Familial cavernous angioma: an unknown, known disease. *Acta Neurol Scand.* 1998;98(6):369-371.

12. Otten P, Pizzolato GP, Rilliet B, Berney J. [131 cases of cavernous angioma (cavernomas) of the CNS, discovered by retrospective analysis of 24,535 autopsies]. *Neurochirurgie.* 1989;35(2):82-83, 128-131.

13. Zabramski JM, Wascher TM, Spetzler RF, Johnson B, Golfinos J, Drayer BP, Brown B, Rigamonti D, Brown G. The natural history of familial cavernous malformations: results of an ongoing study. *J Neurosurg.* 1994;80(3):422-432.

14. Rigamonti D, Drayer BP, Johnson PC, Hadley MN, Zabramski J, Spetzler RF. The MRI appearance of cavernous malformations (angiomas). *J Neurosurg.* 1987;67(4):518-524.

15. Denier C, Labauge P, Brunereau L, Cavé-Riant F, Marchelli F, Arnoult M, Cecillon M, Maciazek J, Joutel A, Tournier-Lasserve E; Société Française de Neurochirurgie; Société de Neurochirurgie de Langue Française. Clinical features of cerebral cavernous malformations patients with KRIT1 mutations. *Ann Neurol.* 2004;55(2):213-220.

16. Eerola I, Plate KH, Spiegel R, Boon LM, Mulliken JB, Vikkula M. KRIT1 is mutated in hyperkeratotic cutaneous capillary-venous malformation associated with cerebral capillary malformation. *Hum Mol Genet.* 2000;9(9):1351-1355.

17. Labauge P, Krivosic V, Denier C, Tournier-Lasserve E, Gaudric A. Frequency of retinal cavernomas in 60 patients with familial cerebral cavernomas: a clinical and genetic study. *Arch Ophthalmol.* 2006;124(6):885-886.

18. Sirvente J, Enjolras O, Wassef M, Tournier-Lasserve E, Labauge P. Frequency and phenotypes of cutaneous vascular malformations in a consecutive series of 417 patients with familial cerebral cavernous malformations. *J Eur Dermatol Venereol.* 2009;23(9):1066-1072.

19. Kleaveland B, Zheng X, Liu JJ, Blum Y, Tung JJ, Zou Z, Sweeney SM, Chen M, Guo L, Lu MM, Zhou D, Kitajewski J, Affolter M, Ginsberg MH, Kahn ML. Regulation of cardiovascular development and integrity by the heart of glass-cerebral cavernous malformation protein pathway. *Nat Med.* 2009;15(2):169-176.

20. Laberge-le Couteulx S, Jung HH, Labauge P, Houtteville JP, Lescoat C, Cecillon M, Marechal E, Joutel A, Bach JF, Tournier-Lasserve E. Truncating mutations in CCM1, encoding KRIT1, cause hereditary cavernous angiomas. *Nat Genet.* 1999;23(2):189-193.

21. Liquori CL, Berg MJ, Siegel AM, Huang E, Zawistowski JS, Stoffer T, Verlaan D, Balogun F, Hughes L, Leedom TP, Plummer NW, Cannella M, Maglione V, Squitieri F, Johnson EW, Rouleau GA, Ptacek L, Marchuk DA. Mutations in a gene encoding a novel protein containing a phosphotyrosine-binding domain cause type 2 cerebral cavernous malformations. *Am J Hum Genet.* 2003;73(6):1459-1464.

22. Bergametti F, Denier C, Labauge P, Arnoult M, Boetto S, Clanet M, Coubes P, Echenne B, Ibrahim R, Irthum B, Jacquet G, Lonjon M, Moreau JJ, Neau JP, Parker F, Tremoulet M, Tournier-Lasserve E; Société Française de Neurochirurgie. Mutations within the programmed cell death 10 gene cause cerebral cavernous malformations. *Am J Hum Genet.* 2005;76(1):42-51.

23. Dibble CF, Horst JA, Malone MH, Park K, Temple B, Cheeseman H, Barbaro JR, Johnson GL, Bencharit S. Defining the functional domain of programmed cell death 10 through its interactions with phosphatidylinositol-3,4,5-triphosphate. *PLoS One.* 2010;5(7):e11740.

24. Liquori CL, Berg MJ, Squitieri F, Ottenbacher M, Sorlie M, Leedom TP, Cannella M, Maglione V, Ptacek L, Johnson EW, Marchuk DA. Low frequency of PDCD10 mutations in a panel of CCM3 probands: potential for a fourth CCM locus. *Hum Mutat.* 2006;27(1):118.

25. Gianfrancesco F, Esposito T, Penco S, Maglione V, Liquori CL, Patrosso MC, Zuffardi O, Ciccodicola A, Marchuk DA, Squitieri F. ZPLD1 gene is disrupted in a patient with balanced translocation that exhibits cerebral cavernous malformations. *Neuroscience.* 2008;155(2):345-349.

26. Riant F, Bergametti F, Ayrignac X, Boulday G, Tournier-Lasserve E. Recent insights into cerebral cavernous malformations: the molecular genetics of CCM. *FEBS J.* 2010;277(5):1070-1075.

27. Gault J, Sarin H, Awadallah NA, Shenkar R, Awad IA. Pathobiology of human cerebrovascular malformations: basic mechanisms and clinical relevance. *Neurosurgery.* 2004;55(1):1-16; discussion 16-17.

28. Wang QK. Update on the molecular genetics of vascular anomalies. *Lymphat Res Biol.* 2005;3(4):226-233.

29. Plummer NW, Zawistowski JS, Marchuk DA. Genetics of cerebral cavernous malformations. *Curr Neurol Neurosci Rep.* 2005;5(5):391-396.

30. Voss K, Stahl S, Hogan BM, Reinders J, Schleider E, Schulte-Merker S, Felbor U. Functional analyses of human and zebrafish 18-amino acid in-frame deletion pave the way for domain mapping of the cerebral cavernous malformation 3 protein. *Hum Mutat.* 2009;30(6):1003-1011.

31. Denier C, Labauge P, Bergametti F, Marchelli F, Riant F, Arnoult M, Maciazek J, Vicaut E, Brunereau L, Tournier-Lasserve E; Société Française de Neurochirurgie. Genotype-phenotype correlations in cerebral cavernous malformations patients. *Ann Neurol.* 2006;60(5):550-556.

32. Craig HD, Günel M, Cepeda O, Johnson EW, Ptacek L, Steinberg GK, Ogilvy CS, Berg MJ, Crawford SC, Scott RM, Steichen-Gersdorf E, Sabroe R, Kennedy CT, Mettler G, Beis MJ, Fryer A, Awad IA, Lifton RP. Multilocus linkage identifies two new loci for a mendelian form of stroke, cerebral cavernous malformation, at 7p15-13 and 3q25.2-27. *Hum Mol Genet.* 1998;7(12):1851-1858.

33. Akers AL, Johnson E, Steinberg GK, Zabramski JM, Marchuk DA. Bi-allelic somatic and germline mutations in cerebral cavernous malformations (CCMs): evidence for a two-hit mechanism of CCM pathogenesis. *Hum Mol Genet.* 2009;18(5):919-930.

34. McDonald DA, Shenkar R, Shi C, Stockton RA, Akers AL, Kucherlapati MH, Kucherlapati R, Brainer J, Ginsberg MH, Awad IA, Marchuk DA. A novel mouse model of cerebral cavernous malformations based on the two-hit mutation hypothesis recapitulates the human disease. *Hum Mol Genet.* 2011;20(2):211-222.

35. Goitre L, Balzac F, Degani S, Degan P, Marchi S, Pinton P, Retta SF. KRIT1 regulates the homeostasis of intracellular reactive oxygen species. *PLoS One.* 2010;5(7):e11786.

36. Belik J, Jerkic M, McIntyre BA, Pan J, Leen J, Yu LX, Henkelman RM, Toporsian M, Letarte M. Age-dependent endothelial nitric oxide synthase uncoupling in pulmonary arteries of endoglin heterozygous mice. *Am J Physiol Lung Cell Mol Physiol.* 2009;297(6):L1170-L1178.

37. Louvi A, Chen L, Two AM, Zhang H, Min W, Günel M. Loss of cerebral cavernous malformation 3 (CCM3) in neuroglia leads to CCM and vascular pathology. *Proc Natl Acad Sci U S A.* 2011;108(9):3737-3742.

38. Knudson AG. Two genetic hits (more or less) to cancer. *Nat Rev Cancer.* 2001;1(2):157-162.

39. Marchuk DA, Srinivasan S, Squire TL, Zawistowski JS. Vascular morphogenesis: tales of two syndromes. *Hum Mol Genet.* 2003;12(Spec No. 1):R97-R112.

40. Francalanci F, Avolio M, De Luca E, Longo D, Menchise V, Guazzi P, Sgrò F, Marino M, Goitre L, Balzac F, Trabalzini L, Retta SF. Structural and functional differences between KRIT1A and KRIT1B isoforms: a framework for understanding CCM pathogenesis. *Exp Cell Res.* 2009;315(2):285-303.

41. Faurobert E, Albiges-Rizo C. Recent insights into cerebral cavernous malformations: a complex jigsaw puzzle under construction. *FEBS J.* 2010;277(5):1084-1096.

42. Li X, Zhang R, Zhang H, He Y, Ji W, Min W, Boggon TJ. Crystal structure of CCM3, a cerebral cavernous malformation protein critical for vascular integrity. *J Biol Chem.* 2010;285(31):24099-24107.

43. Huang CY, Wu YM, Hsu CY, Lee WS, Lai MD, Lu TJ, Huang CL, Leu TH, Shih HM, Fang HI, Robinson DR, Kung HJ, Yuan CJ. Caspase activation of mammalian sterile 20-like kinase 3 (Mst3). Nuclear translocation and induction of apoptosis. *J Biol Chem.* 2002;277(37):34367-34374.

44. Lu TJ, Lai WY, Huang CY, Hsieh WJ, Yu JS, Hsieh YJ, Chang WT, Leu TH, Chang WC, Chuang WJ, Tang MJ, Chen TY, Lu TL, Lai MD. Inhibition of cell migration by autophosphorylated mammalian sterile 20-like kinase 3 (Mst3) involves paxillin and protein-tyrosine phosphatase-PEST. *J Biol Chem.* 2006;281(50):38405-38417.

45. Ma X, Zhao H, Shan J, Long F, Chen Y, Chen Y, Zhang Y, Han X, Ma D. PDCD10 interacts with Ste20-related kinase Mst4 to promote cell growth and transformation via modulation of the ERK pathway. *Mol Biol Cell.* 2007;18(6):1965-1978.

46. Voss K, Stahl S, Schleider E, Ullrich S, Nickel J, Mueller TD, Felbor U. CCM3 interacts with CCM2 indicating common pathogenesis for cerebral cavernous malformations. *Neurogenetics.* 2007;8(4):249-256.

47. Schleider E, Stahl S, Wüstehube J, Walter U, Fischer A, Felbor U. Evidence for anti-angiogenic and pro-survival functions of the cerebral cavernous malformation protein 3. *Neurogenetics.* 2011;12(1):83-86.

48. He Y, Zhang H, Yu L, Günel M, Boggon TJ, Chen H, Min W. Stabilisation of VEGFR-2 signalling by cerebral cavernous malformation 3 is critical for vascular development. *Sci Signal.* 2010;3(116):ra26.

49. Denier C, Gasc JM, Chapon F, Domenga V, Lescoat C, Joutel A, Tournier-Lasserve E. KRIT1/cerebral cavernous malformation 1 mRNA is preferentially expressed in neurons and epithelial cells in embryo and adult. *Mech Dev.* 2002;117(1-2):363-367.

50. Guzeloglu-Kayisli O, Amankulor NM, Voorhees J, Luleci G, Lifton RP, Günel M. KRIT1/cerebral cavernous malformation 1 protein localises to vascular endothelium, astrocytes and pyramidal cells of the adult human cerebral cortex. *Neurosurgery.* 2004;54(4):943-949.

51. Petit N, Blécon A, Denier C, Tournier-Lasserve E. Patterns of expression of the three cerebral cavernous malformation (CCM) genes during embryonic and postnatal brain development. *Gene Expr Patterns.* 2006;6(5):495-503.

52. Wong JH, Awad IA, Kim JH. Ultrastructural pathological features of cerebrovascular malformations: a preliminary report. *Neurosurgery.* 2000;46(6):1454-1459.

53. Burkhardt JK, Schmidt D, Schoenauer R, Brokopp C, Agarkova I, Bozinov O, Bertalanffy H, Hoerstrup SP. Upregulation of transmembrane endothelial junction proteins in human cerebral cavernous malformations. *Neurosurg Focus.* 2010;29(3):E3.

54. Zhao Y, Tan YZ, Zhou LF, Wang HJ, Mao Y. Morphological observation and *in vitro* angiogenesis assay of endothelial cells isolated from human cerebral cavernous malformations. *Stroke.* 2007;38(4):1313-1319.

55. Dejana E, Tournier-Lasserve E, Weinstein BM. The control of vascular integrity by endothelial cell junctions: molecular basis and pathological implications. *Dev Cell.* 2009;16(2):209-221.

56. Whitehead KJ, Plummer NW, Adams JA, Marchuk DA, Li DY. CCM1 is required for arterial morphogenesis: implications for the aetiology of human cavernous malformations. *Development.* 2004;131(6):1437-1448.

57. Huang L, Ren J, Chen D, Li Y, Kharbanda S, Kufe D. MUC1 cytoplasmic domain co-activates Wnt target gene transcription and confers transformation. *Cancer Biol Ther.* 2003;2(6):702-706.

58. Lang T, Hansson GC, Samuelsson T. An inventory of mucin genes in the chicken genome shows that the mucin domain of MUC13 is encoded by multiple exons and that ovomucin is part of a locus of related gel-forming mucins. *BMC Genomics.* 2006;7:197.

59. Udhayakumar G, Jayanthi V, Devaraj N, Devaraj H. Interaction of MUC1 with beta-catenin modulates the Wnt target gene cyclin D1 in *H. pylori*-induced gastric cancer. *Mol Carcinog.* 2007;46(9):807-817.

60. Glading AJ, Ginsberg MH. Rap1 and its effector KRIT1/CCM1 regulate beta-catenin signalling. *Dis Model Mech.* 2010;3(1-2):73-83.

61. Clevers H. Wnt/beta-catenin signalling in development and disease. *Cell.* 2006;127(3):469-480.

62. Liebner S, Corada M, Bangsow T, Babbage J, Taddei A, Czupalla CJ, Reis M, Felici A, Wolburg H, Fruttiger M, Taketo MM, von Melchner H, Plate KH, Gerhardt H, Dejana E. Wnt/beta-catenin signalling controls development of the blood-brain barrier. *J Cell Biol.* 2008;183(3):409-417.

63. González-Mariscal L, Tapia R, Chamorro D. Crosstalk of tight junction components with signalling pathways. *Biochim Biophys Acta.* 2008;1778(3):729-756.

64. Lampugnani MG, Orsenigo F, Rudini N, Maddaluno L, Boulday G, Chapon F, Dejana E. CCM1 regulates vascular-lumen organisation by inducing endothelial polarity. *J Cell Sci.* 2010;123(Pt 7):1073-1080.

65. Crose LE, Hilder TL, Sciaky N, Johnson GL. Cerebral cavernous malformation 2 protein promotes smad ubiquitin regulatory factor 1-mediated RhoA degradation in endothelial cells. *J Biol Chem.* 2009;284(20):13301-13305.

66. Borikova AL, Dibble CF, Sciaky N, Welch CM, Abell AN, Bencharit S, Johnson GL. Rho-kinase inhibition rescues the endothelial cell cerebral cavernous malformation phenotype. *J Biol Chem.* 2010;285(16):11760-11764.

67. Zheng X, Xu C, Di Lorenzo A, Kleaveland B, Zou Z, Seiler C, Chen M, Cheng L, Xiao J, He J, Pack MA, Sessa WC, Kahn ML. CCM3 signalling through sterile 20-like kinases plays an essential role during zebrafish cardiovascular development and cerebral cavernous malformations. *J Clin Invest.* 2010;120(8):2795-2804.

68. Preisinger C, Short B, De Corte V, Bruyneel E, Haas A, Kopajtich R, Gettemans J, Barr FA. YSK1 is activated by the Golgi matrix protein GM130 and plays a role in cell migration through its substrate 14-3-3zeta. *J Cell Biol.* 2004;164(7):1009-1020.

69. Fidalgo M, Fraile M, Pires A, Force T, Pombo C, Zalvide J. CCM3/PDCD10 stabilises GCKIII proteins to promote Golgi assembly and cell orientation. *J Cell Sci.* 2010;123(Pt 8):1274-1284.

70. Rupp PA, Little CD. Integrins in vascular development. *Circ Res.* 2001;89(7):566-572.

71. Bayless KJ, Davis GE. The Cdc42 and Rac1 GTPases are required for capillary lumen formation in three-dimensional extracellular matrices. *J Cell Sci.* 2002;115(Pt 6):1123-1136.

72. Iruela-Arispe ML, Davis GE. Cellular and molecular mechanisms of vascular lumen formation. *Dev Cell.* 2009;16(2):222-231.

73. Whitehead KJ, Chan AC, Navankasattusas S, Koh W, London NR, Ling J, Mayo AH, Drakos SG, Jones CA, Zhu W, Marchuk DA, Davis GE, Li DY. The cerebral cavernous malformation signalling pathway promotes vascular integrity via Rho-GTPases. *Nat Med.* 2009;15(2):177-184.

74. Liu H, Rigamonti D, Badr A, Zhang J. CCM1 regulates microvascular morphogenesis during angiogenesis. *J Vasc Res.* 2011;48(2):130-140.

75. Harburger DS, Calderwood DA. Integrin signalling at a glance. *J Cell Sci.* 2009;122(Pt 2):159-163.

76. Mudgett JS, Ding J, Guh-Siesel L, Chartrain NA, Yang L, Gopal S, Shen MM. Essential role for p38alpha mitogen-activated protein kinase in placental angiogenesis. *Proc Natl Acad Sci U S A.* 2000;97(19):10454-10459.

77. Pham M, Gross BA, Bendok BR, Awad IA, Batjer HH. Radiosurgery for angiographically occult vascular malformations. *Neurosurg Focus.* 2009;26(5):E16.

78. Gross BA, Batjer HH, Awad IA, Bendok BR. Brainstem cavernous malformations. *Neurosurgery.* 2009;64(5):E805-E818.

79. Yadla S, Jabbour PM, Shenkar R, Shi C, Campbell PG, Awad IA. Cerebral cavernous malformations as a disease of vascular permeability: from bench to bedside with caution. *Neurosurg Focus.* 2010;29(3):E4.

80. Krisht KM, Whitehead KJ, Niazi T, Couldwell WT. The pathogenetic features of cerebral cavernous malformations: a comprehensive review with therapeutic implications. *Neurosurg Focus.* 2010;29(3):E2.

81. Stockton RA, Shenkar R, Awad IA, Ginsberg MH. Cerebral cavernous malformations proteins inhibit Rho-kinase to stabilise vascular integrity. *J Exp Med.* 2010;207(4):881-896.

82. Fukuhara S, Sakurai A, Sano H, Yamagishi A, Somekawa S, Takakura N, Saito Y, Kangawa K, Mochizuki N. Cyclic AMP potentiates vascular endothelial cadherin-mediated cell-cell contact to enhance endothelial barrier function through an Epac-Rap1 signalling pathway. *Mol Cell Biol.* 2005;25(1):136-146.

83. Wilhelm S, Carter C, Lynch M, Lowinger T, Dumas J, Smith RA, Schwartz B, Simantov R, Kelley S. Discovery and development of sorafenib: a multikinase inhibitor for treating cancer. *Nat Rev Drug Discov.* 2006;5(10):835-844.

84. Wüstehube J, Bartol A, Liebler SS, Brütsch R, Zhu Y, Felbor U, Sure U, Augustin HG, Fischer A. Cerebral cavernous malformation protein CCM1 inhibits sprouting angiogenesis by activating DELTA-NOTCH signalling. *Proc Natl Acad Sci U S A.* 2010;107(28):12640-12645.

85. Moriarity JL, Wetzel M, Clatterbuck RE, Javedan S, Sheppard JM, Hoenig-Rigamonti K, Crone NE, Breiter SN, Lee RR, Rigamonti D. The natural history of cavernous malformations: a prospective study of 68 patients. *Neurosurgery.* 1999;44(6):1166-1171; discussion 1172-1173.

# Chapter 7

## Endothelial cell-specific Fgd5 involvement in vascular pruning defines neovessel fate in mice

C. Cheng, R.A. Haasdijk, D. Tempel, E.H.M. van de Kamp, R.L.J.M. Herpers
F.L. Bos, W.K. den Dekker, L.A.J. Blonden, R. de Jong, P.E. Bürgisser
I. Chrifi, E.A.L. Biessen, S. Dimmeler, S. Schulte-Merker, H.J. Duckers

## *Abstract*

**Objective** - New vessel formation contributes to organ development during embryogenesis and tissue repair in response to mechanical damage, inflammation, and ischemia in adult organisms. Early angiogenesis includes formation of an excessive primitive network that needs to be reorganised into a secondary vascular network with higher hierarchical structure. Vascular pruning - the removal of aberrant neovessels by apoptosis - is a vital step in this process. Although multiple molecular pathways for early angiogenesis have been identified, little is known about the genetic regulators of secondary network development.

**Methods and Results** - Using a transcriptomics approach, we identified a new endothelial specific gene named FYVE, RhoGEF, and PH domain-containing 5 (Fgd5) that plays a crucial role in vascular pruning. Gain- and loss-of-function studies demonstrate that Fgd5 inhibits neovascularisation, indicated by *in vitro* network-formation, aortic-ring, and coated-bead assays, and by *in vivo* coated-bead plug assays and studies in the murine retina model. Fgd5 promotes apoptosis-induced vaso-obliteration via induction of the Hey1-p53 pathway by direct binding and activation of Cdc42. Indeed, Fgd5 correlates with apoptosis in endothelial cells during vascular remodelling and was linked to rising $p21^{Cip1}$ levels in aging mice.

**Conclusion** - Here, we have identified Fgd5 as a new genetic regulator of vascular pruning by activation of endothelial cell-targeted apoptosis.

## *Introduction*

Vascularisation during development and regeneration plays a vital role in adult disease progression, including tumour growth and metastasis, arthritis, diabetic retinopathy, and cardiovascular disease. Vascular growth in both development and disease consists of a strictly orchestrated, multi-step process that requires integrated activation of several molecular pathways. During early vascular growth, a dense primary vascular network without functional arterial and venous distinction is formed in response to low-oxygen conditions. This primitive system, consisting of small capillaries, is relatively unstable, with tip and stalk cell vessel structures expanding and collapsing at a high rate. Transition of this primary network into a stable secondary vasculature with a defined arterial/venous hierarchy of larger vessels that branch into a restricted capillary field requires intensive vascular remodelling, a late angiogenic process that includes neovessel stabilisation and pruning of redundant vessel structures.[1,2]

The molecular regulation by angiogenic factors such as vascular endothelial growth factor (VEGF)-A and fibroblast growth factor (FGF) that promote growth of the primary vasculature has been studied extensively. In contrast, the key molecular pathways that regulate the reorganisation of this early network into the more mature secondary vascular structure are still largely undefined. For the process of vascular pruning, vaso-obliteration by apoptosis induced by hyperoxia has been described[3], but little is known about the molecular regulation of this important aspect in vascular remodelling that determines the fate of the neovasculature. Here, we define the function of an endothelial cell (EC) specific gene that plays a crucial role in apoptosis during vascular pruning.

Previously, we carried out a genome-wide expression profile analysis to identify potential trivial regulators in angiogenesis. A new gene named FYVE, RhoGEF, and PH domain-containing 5 (Fgd5) was discovered that showed specific expression in endothelial precursor cells in developing murine embryos and vasculature of zebrafish larvae and mature mice. The Fgd family members of Rho guanine-nucleotide exchange factors (GEF) include Fgd1 through Fgd6, as well as the Fgd1-related Cdc42-GEF[4-8], all sharing the Dbl homology, FYVE, and pleckstrin homology (PH) domains. Fgd1, Fgd4 and FRG have been shown to control Cdc42 activity via their Dbl homology domain by converting inactive GDP-bound Cdc42 into active GTP-bound Cdc42, resulting in altered capacities in actin cytoskeleton assembly, filopodia formation, and Jun N-terminal kinase pathway activation.[9-13] To date, the basic function of Fgd5 remains unknown.

Our studies, which incorporate gain- and loss-of-function of the Fgd5 gene, demonstrated *in vitro* and *in vivo* that Fgd5 induces vascular regression by pruning of redundant neovessels during neovascularisation. Fgd5 functions as a RhoGEF that binds and activates its direct target - Cdc42 - and therefore promotes Hey1-dependent p53-

mediated apoptosis in ECs. The Fgd5 mRNA level also correlates with rising p21$^{Cip1}$ levels in aging C57BL/6J wild-type mice, which coincides with a decline in CD31 expression. These findings identify Fgd5 as a new, critical regulator of neovasculature fate during late phase angiogenesis and demonstrate that Fgd5 may act as a defining factor for vascular regression in later adult life.

## *Methods*

A more detailed description of materials and methods is available in the Data Supplement (*online*). Summarised descriptions of the different techniques used in this study are supplied below.

This study was carried out in accordance with the Council of Europe Convention (ETS123)/Directive (86/609/EEC) for the protection of vertebrate animals used for experimental and other scientific purposes and with the approval of the National and Local Animal Care Committee.

**Isolation of Flk1-positive and Flk1-negative cells from mouse embryos**
First, 10.5 to 15.5 days post-fertilisation (dpf) FVB/N mouse embryos were harvested and digested to obtain single cell suspensions in 0.12% collagenase type I/phosphate-buffered saline (PBS) in 10% foetal calf serum (FCS) (Lonza, Breda, The Netherlands). Single cell suspensions were labelled with PE-conjugated anti-mouse Flk1 antibody 1:50 and Hoechst 1:100 (BD, Breda, The Netherlands), and sorted to > 90% purity for Flk1-positive/Hoechst-negative cells, using a BD FACSCanto$^{TM}$ cell-sorter (Breda, The Netherlands). Cells were dissolved in RLT-buffer and processed for qPCR analysis.

**qPCR and Western blot**
RNA was isolated using the RNeasy Mini Kit from Qiagen (Venlo, The Netherlands), checked for quality and quantity by capillary electrophoresis (Agilent 2100 Bioanalyser; Agilent Technologies, Amstelveen, The Netherlands), and reversed transcribed into cDNA. qPCR reactions were carried out by real-time fluorescence assessment of the SYBR$^{®}$ Green signal with the iCycler iQ$^{TM}$ Detection System (Bio-Rad, Veenendaal, The Netherlands). qPCR analysis was carried out for transcripts of mouse FRG, Fgd1 through Fgd6, eNOS, p21$^{Cip1}$ and CD31, as well as for human VEGFR-1 and 2, Notch 1 and 4, Dll4, jagged 1, ephrin B2 and B4, neuropilin 1 and 2, p53, and Hey1. Target mRNA expression levels are reported relative to the housekeeping genes - HPRT1 in murine samples and beta-actin in the human samples - as previously described (Supplemental table 1 and 2, *online*).[14]

For Western blot analysis, samples were lysed in NP40 Cell Lysis Buffer (Invitrogen, Bleiswijk, The Netherlands) and analysed on a 12.5% SDS-PAGE gel, followed by Western blotting using antibodies against p21[Cip1] and p53 1:1,000 (Abcam, Cambridge, UK), Rac1, RhoA and Cdc42 1:500 (Abcam, Cambridge, UK), and Fgd5 1:500 (BD, Breda, The Netherlands) for protein detection. Protein bands were visualised by the LI-COR Detection System (LI-COR Biotechnology, Cambridge, UK) as previously described.[15-17]

**Immunohistology of ventricle, aorta and carotid arteries**
Mouse ventricle, aorta and carotid arteries were embedded in OCT (Sakura Finetek, Hoge Rijndijk, The Netherlands) and snap-frozen in liquid nitrogen. Then, 5 μm cryosections were double-stained with Alexa Fluor®-conjugated isolectin GS-IB$_4$ 1:500 (Invitrogen, Bleiswijk, The Netherlands) and Fgd5 antibody 1:100 (BD, Breda, The Netherlands), followed by rhodamin-FITC-labelled anti-mouse IgG 1:500 (Invitrogen, Bleiswijk, The Netherlands) and goat FAB against mouse IgG (H+L) for blocking (Jackson ImmunoResearch Labs, West Grove, USA) as previously described.[18,19]

*In vivo* **coated-bead assay**
Mature SCID mice (age 10-15 weeks) were injected subcutaneously with 700 beads in 300 μl Matrigel (400 primary human umbilical vein endothelial cells (HUVEC) per bead; BD, Breda, The Netherlands) supplemented with 2.5 ng/ml rat fibrinogen and 20 ng/ml human FGF. For each animal, an adenovirus (pAd)-sham and pAd-Fgd5 expressing HUVEC-coated-bead plug was implanted in each flank. At day 8, solidified Matrigel plugs were retrieved, washed, fixed in 4% PFA/PBS, and imbedded in OCT (Sakura Finetek, Hoge Rijndijk, The Netherlands). For validation of transgene expression, qPCR analysis were carried out on isolated plugs obtained at different time points. Then, 5 μm cryosections were stained by haematoxylin and eosin staining, or using CD31 antibody 1:500 and rhodamin-labelled anti-rat IgG secondary antibody 1:500 (R&D systems, Abingdon, UK). For quantification of the percentage nuclei and percentage CD31-positive cells, data analysis was carried out using a commercial image analysis system (Clemex Technologies, Longueuil, Canada).

**Mouse model of retinal vascularisation**
Three-day old C57BL/6J pups were anesthetised by placement on ice. Then, 0.5 μl pAd-Fgd5 ($5 \times 10^7$ pfu) was injected into the left eye and 0.5 μl pAd-sham ($5 \times 10^7$ pfu) was injected into the right eye using a 33-Gauge needle (World Precision Instruments, Berlin, Germany). For Fgd5 silencing experiments, 100 nmol Accell Fgd5 targeting siRNA (si-Fgd5) was injected into the left eye and 100 nmol Accell scrambled non-targeting siRNA (si-sham) was injected into the right eye (Dharmacon, Etten-Leur, The Netherlands). For

rescue experiments with VEGFR-1, an active soluble form of VEGFR-1 was co-injected with 100 nmol Accell si-Fgd5. Depending on the assay, mice pups were killed at post-natal day 4, 6, 8, 11, 16 and 21, and retinas were stained with rhodamin-FITC-labelled isolectin GS-IB$_4$ or collagen IV antibody 1:200 (Millipore, Amsterdam, The Netherlands), followed by Alexa Fluor$^®$-conjugated anti-rabbit/mouse secondary antibodies 1:500 (Invitrogen, Bleiswijk, The Netherlands). Whole-mount retinas were visualised by confocal microscopy (LSM510-NLO/FCS; Carl Zeiss, Sliedrecht, The Netherlands) using a 10x lens to obtain high-resolution micrographs of the topical vascular layer. Post-processing was needed to reassembly the individual micrographs into an overview of the entire retina. Processed retina images were analysed using Angiosys Image Analysis Software 1.0 (TCS CellWorks, Buckingham, UK). At least 3 individual retinal flaps per mouse retina were assessed.

Adequate transgene expression and gene silencing were validated by qPCR analysis. For flow cytometric assessment of the retinal ECs, the retina was homogenised in 0.12% collagenase type I/PBS/10% FCS for 15 minutes, filtered through a 3 μm mesh (BD, Breda, The Netherlands), and stained with PE-conjugated anti-mouse Flk1 antibody 1:50, followed by Annexin V and propidium iodide (PI) staining (BD, Breda, The Netherlands). The percentage of apoptotic cells in the Flk1-positive population was quantified by flow cytometry on a BD FACSCanto$^{TM}$ (Breda, The Netherlands). For detection of cleaved caspase 3 and Fgd5, retinal cells were fixed and permeabilised using the Cytofix/Cytoperm System (BD, Breda, The Netherlands), followed by Fgd5 (Sigma-Aldrich, Zwijndrecht, The Netherlands) and secondary antibody staining with an allophycocyanin-labelled mouse anti-rabbit antibody, followed by FITC-labelled rabbit anti-cleaved caspase 3 and PE-labelled mouse anti-Flk1 antibody staining and subsequent quantification by flow cytometry on a BD FACSCanto$^{TM}$ (Breda, The Netherlands).

**Cell cultures**

HUVECs were cultured on gelatin-coated plates at 37°C in 5% $CO_2$ in EBM$^®$-2 medium supplemented with a commercial BulletKit, 10% FCS and 1% penicillin/streptomycin (Lonza, Breda, The Netherlands). Only cell cultures of passages three to six were used throughout the study.

For immunohistological staining, HUVECs were grown on cover slips and fixed in ice-cold acetone for 5 minutes, followed by permeabilisation in 0.1% Triton X/PBS, incubation with Fgd5 antibody 1:100 (BD, Breda, The Netherlands), and subsequent TSA-amplification of the signal (Roche, Woerden, The Netherlands). This was followed by incubation with Cdc42 or zyxin antibody 1:500 (Abcam, Cambridge, UK) and detection with 1:500 FITC-labelled anti-rabbit/rat IgG antibody (Invitrogen, Bleiswijk, The Netherlands). Cover slips were mounted with 4,6-diamidino-2-phenylindole (DAPI) in Vectashield$^®$ mounting medium (H-1200; Vector Laboratories, Burlingame, USA) and imaged by fluorescence microscopy (Carl Zeiss, Sliedrecht, The Netherlands).

**Cell proliferation, cell cycle and apoptosis assay**

Transfected HUVECs were synchronised in the G0/G1-phase by serum deprivation in EBM®-2 medium supplemented with a commercial BulletKit and 0.2% FCS for 12 hours. For cell growth assessment, cells were harvested and quantified using a haematocytometer (trypan blue negative) at different time points. We carried out 3-(4,5-dimethylthiazol-2-yl)-2,5-diphenyl tetrasodium bromide (MTT) uptake experiments for cell metabolism assessment according to the instruction manual (ATCC, Manassas, USA).

For cell cycle analysis, cells were harvested at 0, 4 and 12 hours after activation, fixed in 70% ethanol/PBS for 15 minutes on ice, stained with PI 1:300, and analysed by flow cytometry on a BD FACSCanto™ (Breda, The Netherlands).

For apoptosis analysis, cells were harvested at 0, 4 and 12 hours after activation, and stained for Annexin V and PI signals using an Annexin V Apoptosis Detection Kit (BD, Breda, The Netherlands), followed by analysis of the samples by flow cytometry on a BD FACSCanto™ (Breda, The Netherlands).

**Small G-protein activation assay and Fgd5 protein complex co-immunoprecipitation**

Rac1, RhoA and Cdc42 activation levels were measured using the G-LISA Detection System (Tebu-Bio, Heerhugowaard, The Netherlands).

For Fgd5 protein complex co-immunoprecipitation, magnetic beads (Dynabeads®; Invitrogen, Bleiswijk, The Netherlands) were coated and cross-linked with 2.5 μg Fgd5 antibody (BD, Breda, The Netherlands) before immunoprecipitation overnight at 4°C with protein cell lysates of transfected HUVECs (50 μg total protein in 100 μl incubation buffer supplied by the G-LISA Detection System). Beads were washed and protein samples were eluted with elution buffer (Invitrogen, Bleiswijk, The Netherlands) before analysis by Western blot on a 12.5% SDS-PAGE gel.

**Statistical analysis**

Data were reported as mean ± standard error of the mean (SEM). Statistical significance was evaluated by one-way ANOVA, as appropriate, followed by individual unpaired Student's *t*-test. In specific assays, repeated measurement analysis was applied. Significance was accepted at $P < 0.05$ (* $P < 0.05$, ** $P < 0.01$ in the figures).

## *Results*

### Fgd5 is specifically expressed in endothelial precursor cells during murine and zebrafish development and in fully differentiated endothelial cells

Fgd5 was specifically expressed in the Flk1-positive cell population during embryonic development in mice as shown by microarray and qPCR analysis. Fgd5 mRNA was predominantly expressed from 8.5 to 16.5 dpf Flk1-positive endothelial precursor cells, when the majority of the vascular structures were established (Figure 1A). Selection of endothelial precursor cells - based on the Flk1 cell surface marker - was further validated by microarray analysis, which showed a significant rise in the expression levels of well-known angiogenic genes such as angiopoietin 2, neuropilin 1 and 2, Tie1, Flt1, and Ets1 in the Flk1-positive compared with the Flk1-negative pool (data not shown).
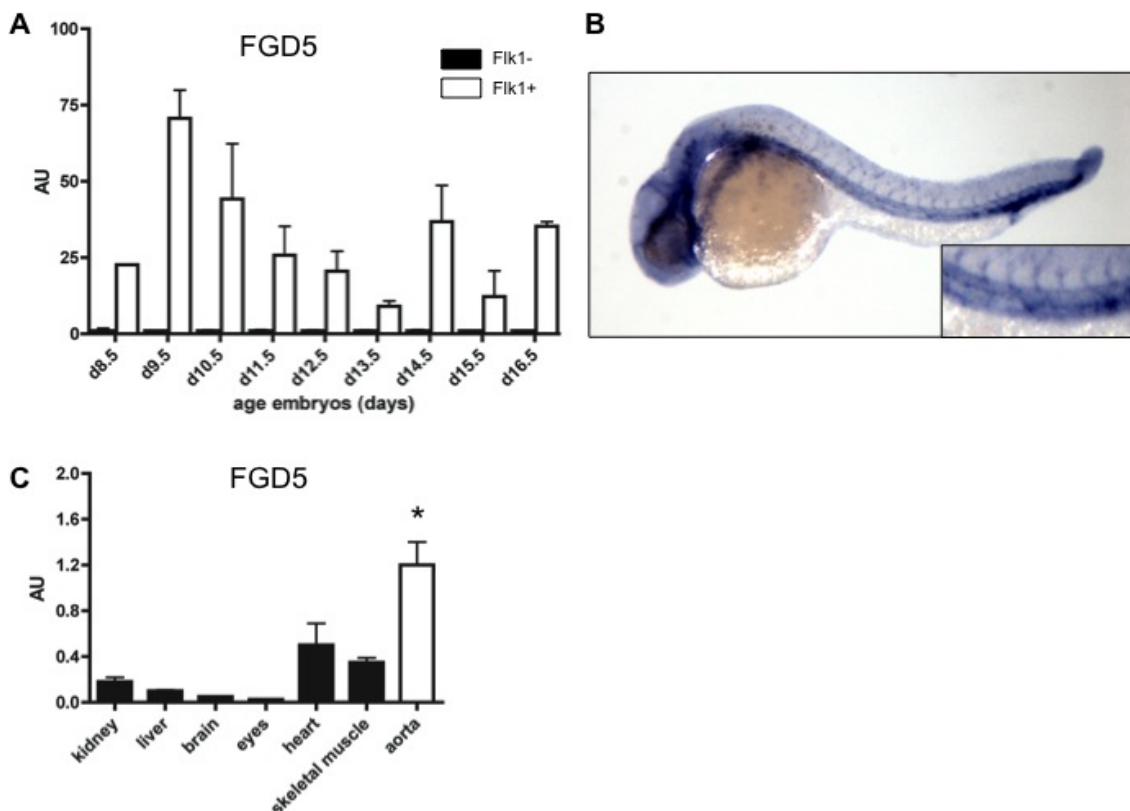


**Figure 1. Fgd5 is specifically expressed in endothelial cells.** (**A**) Endogenous expression level of Fgd5 in Flk1-positive angioblasts during murine embryonic development from 8.5 to 16.5 days post-fertilisation (dpf) compared with Flk1-negative cells as analysed by qPCR. The expression level of Fgd5 in Flk1-negative cells was arbitrarily set to one (n = 6; mean ± SEM). Fgd5 was upregulated at all time points. (**B**) Whole-mount *in situ* hybridisation of Fgd5 in zebrafish larvae at 26 hours post-fertilisation (hpf), lateral view, anterior is to the left. Fgd5 transcripts were localised in the developing vascular network, including main axial vessels - dorsal aorta and posterior cardinal vein - and intersegmental vessels (ISV). (**C**) qPCR analysis of Fgd5 expression in various tissues of mature C57BL/6J mice (n = 6; mean ± SEM).

Specific vascular expression of Fgd5 in the developing vascular tree was validated in zebrafish larvae by whole-mount *in situ* hybridisation (Figure 1B). Fgd5 mRNA in mature C57BL/6J mice was predominantly expressed in the aorta and carotid arteries compared with heart, skeletal muscle, kidney, liver, eye and brain tissue (Figure 1C), mimicking the expression profile of endothelial-specific markers including eNOS and CD31. The other Fgd family members showed a ubiquitous expression pattern (Figure 1D). *In vitro*, Fgd5 was specifically expressed in primary human arterial endothelial cells (HAEC) and HUVECs compared with non-relevant cells (HeLa and sarcoma cells) (Figure 1E), underlining endothelial-specific expression throughout different species and developmental stages.
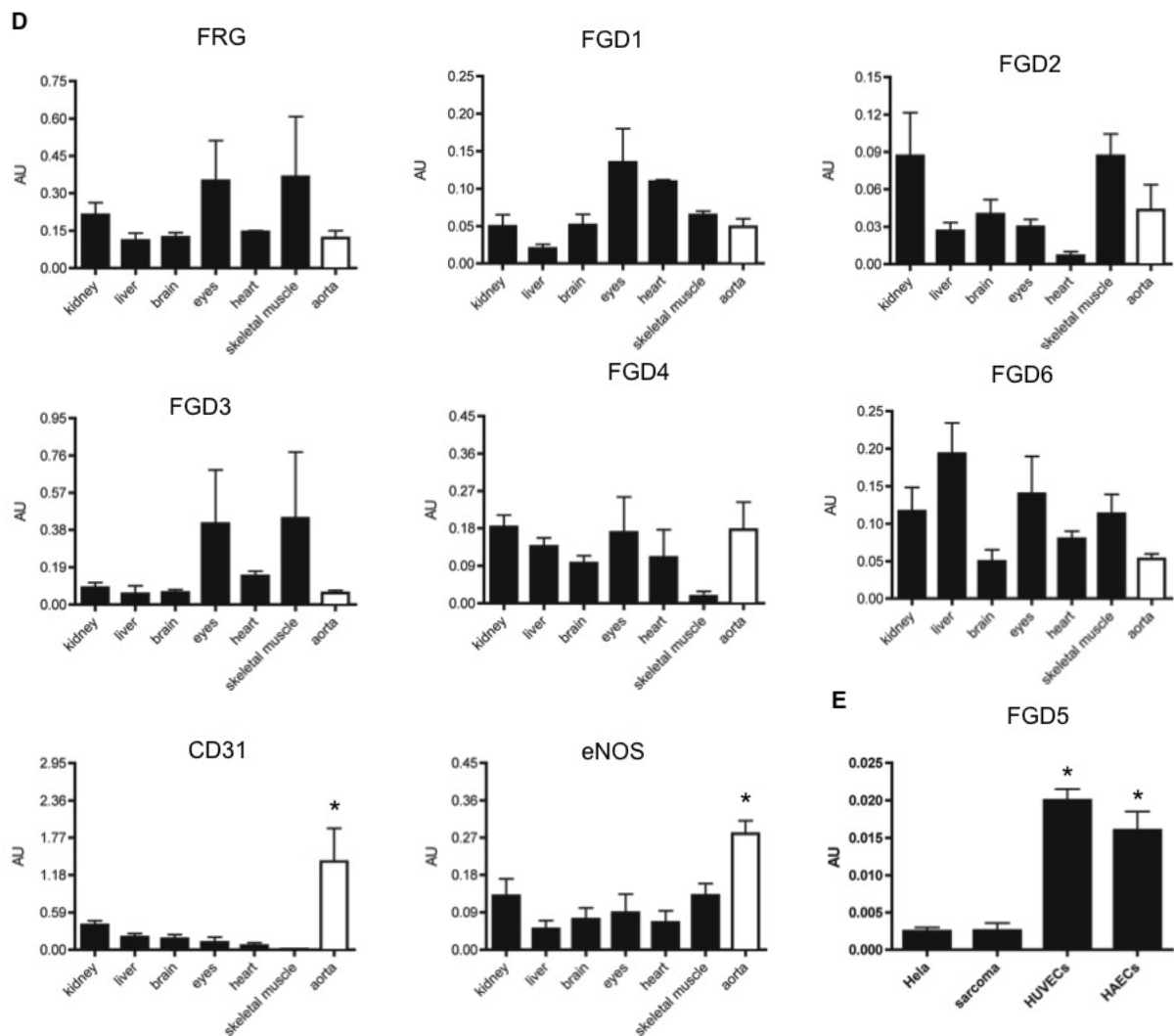


(**D**) qPCR analysis of the expression of the Fgd family members FRG, Fgd1, Fgd2, Fgd3, Fgd4 and Fgd6, and the expression pattern of vascular specific CD31 and eNOS (n = 4; mean ± SEM). (**E**) qPCR analysis of primary cell lines, including HUVECs and HAECs compared with non-relevant cell types - HeLa and sarcoma cells (n = 3; mean ± SEM).

Immunohistological analysis demonstrated selective Fgd5 expression in ECs in the microvasculature of the myocardium and in the endothelial lining of large blood vessels, including the aorta (Figure 1F, G). These findings were further confirmed by analysis of public gene expression databases (NCBI, Gene Expression Omnibus) (Supplemental figure 1, *online*). From these results, we conclude that Fgd5 is the predominant member of the Fgd family expressed in ECs during embryonic vascular development and in adult vasculature.
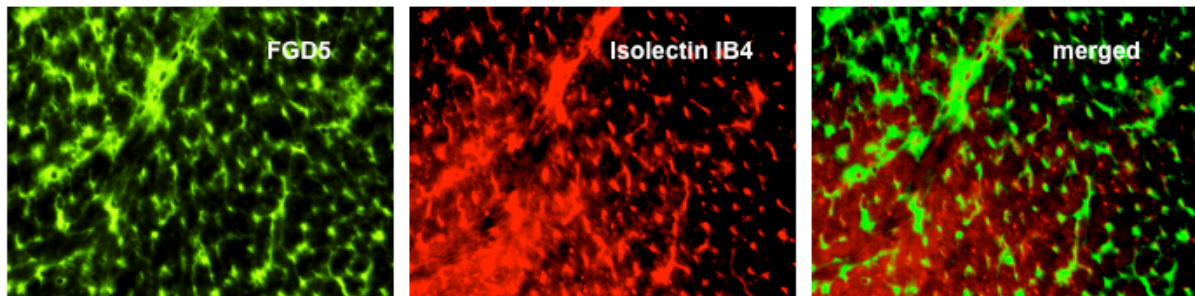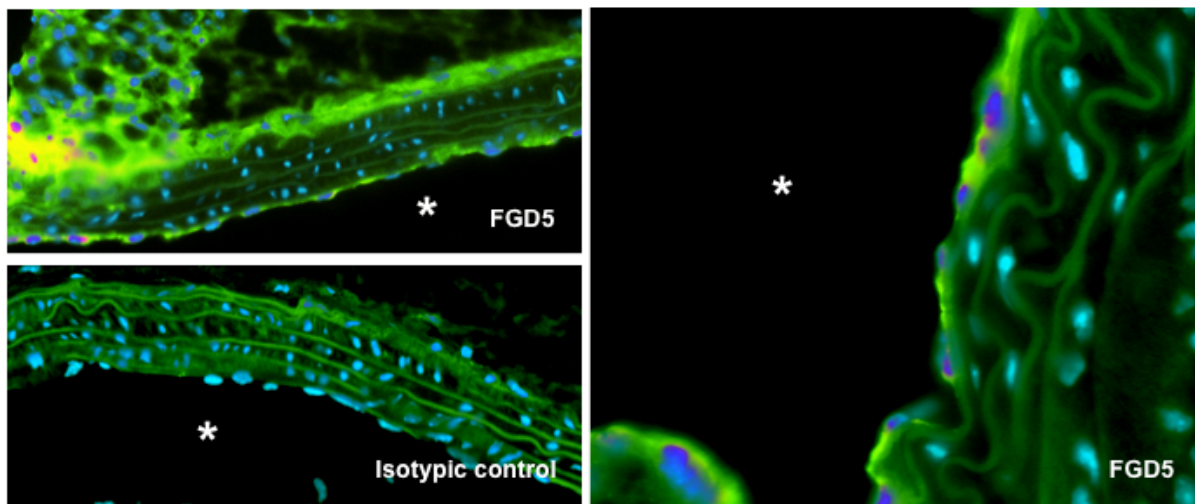


(**F**) Immunohistological staining of myocardium of mature C57BL/6J mice detected co-localisation of the Fgd5 protein (green) with the endothelial cell marker isolectin GS-IB$_4$ (red). (**G**) Immunohistological staining of aortas of mature C57BL/6J mice detected Fgd5 protein (green) in the endothelium and adventitia. Luminal area marked by an asterisk.

## Fgd5 diminishes angiogenesis *in vitro* and *in vivo*

Fgd5 function in HUVECs was assessed by gain- and loss-of-function studies by infection of adenovirus expressing murine or human Fgd5, or by transfection of Fgd5 targeting siRNA (Supplemental figure 2A-E, *online*). In a 2D matrigel network-formation assay, siRNA-mediated silencing of Fgd5 promoted network-formation (Supplemental figure 2F-I, *online*), whereas Fgd5 overexpression attenuated network-formation (Supplemental figure

2J-M, *online*). Similarly, in an *ex vivo* murine aortic-ring assay, adenovirus-mediated overexpression of murine Fgd5 significantly reduced vascular outgrowth (Supplemental figure 2N, O, *online*). In an established angiogenesis model using HUVECs-coated Cytodex® beads, Fgd5 overexpression also diminished capillary sprouting and lumen formation (Supplemental figure 2P-U, *online*). DAPI staining verified comparable numbers of cells attached to the beads at the initiation of the experiment (Supplemental figure 2V, *online*).

To assess the role of Fgd5 in angiogenesis *in vivo*, beads - coated with pAd-sham or pAd-Fgd5 infected HUVECs - were suspended in Matrigel and injected subcutaneously in immunodeficient SCID mice. Matrigel Fgd5 plugs harvested at day 8 after transplantation revealed reduced plug vascularisation, whereas the sham plugs showed an extensive neocapillary network (Figure 2A-D) and increased outgrowth of CD31-positive cells (Figure 2E, F). Human Fgd5 transgene expression in the plugs was validated at different time points by qPCR analysis and showed significantly higher levels of human Fgd5 mRNA in plugs with pAd-Fgd5 versus pAd-sham treated HUVECs (Figure 2G).
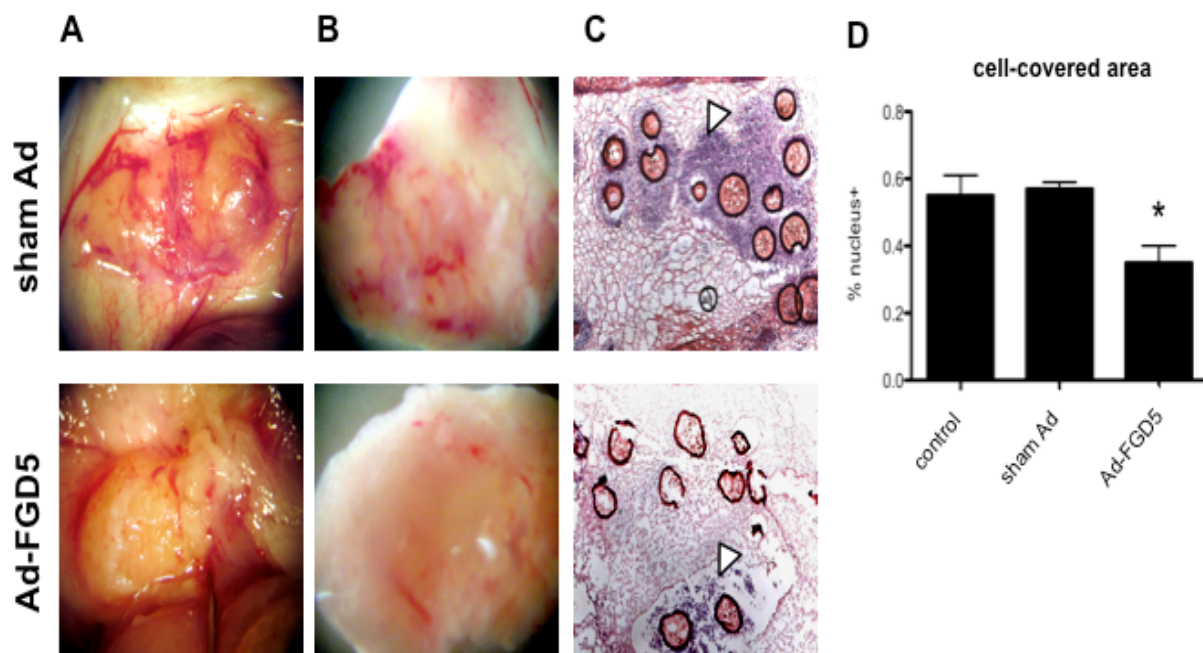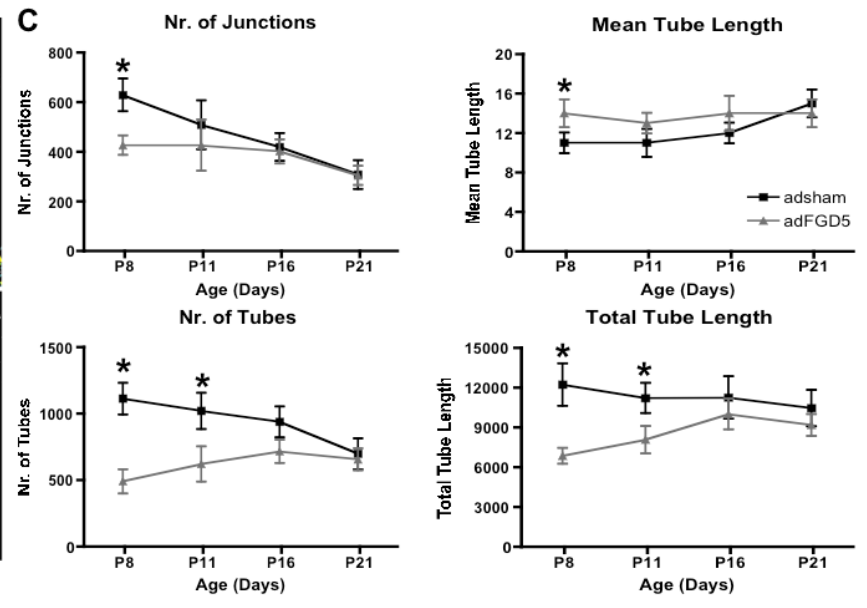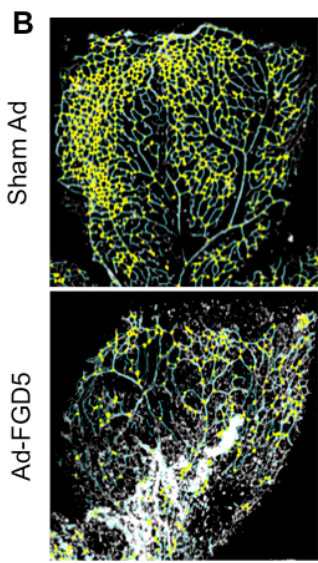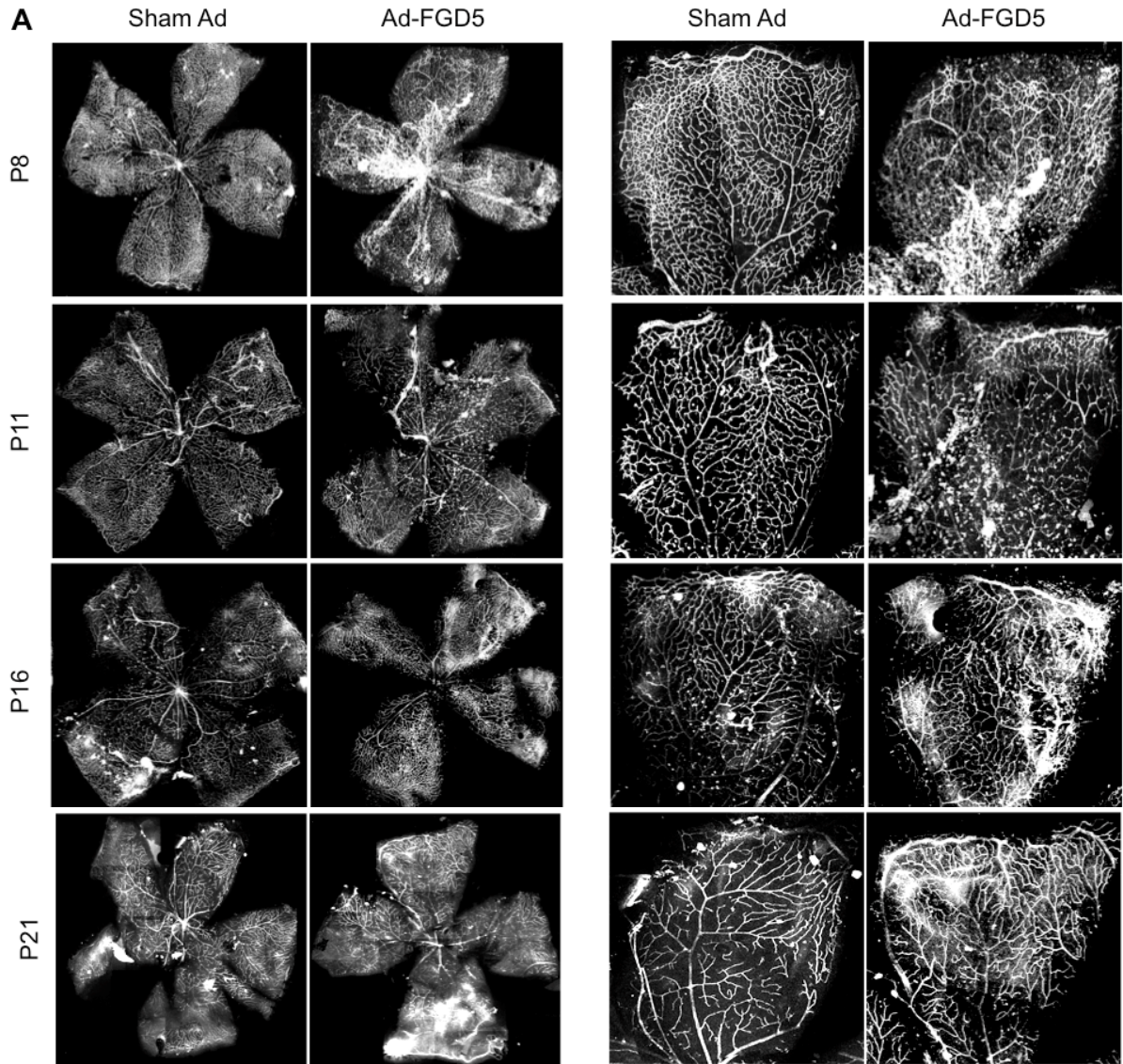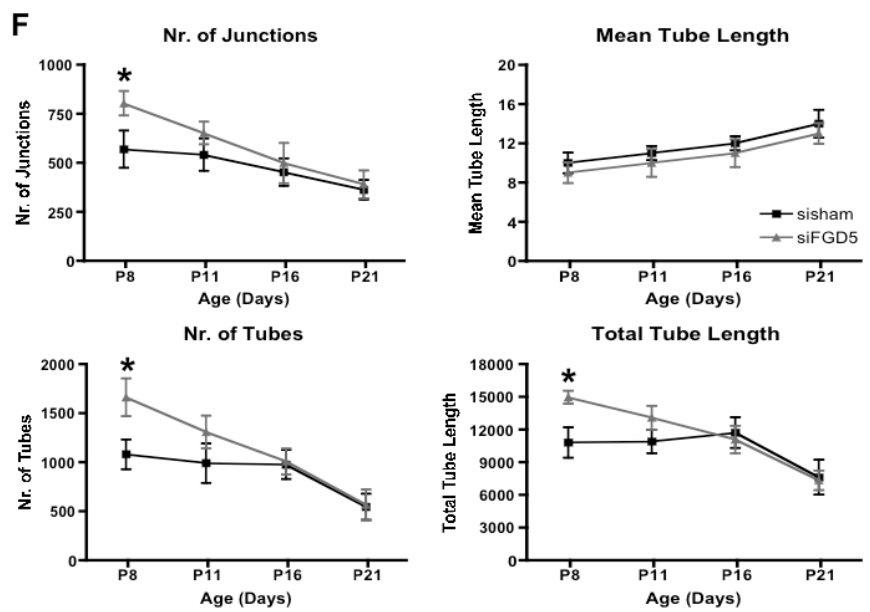


**Figure 2. Fgd5 inhibits angiogenesis in an *in vivo* coated-bead assay.** (**A**) Representative macroscopic pictures of subcutaneously injected matrigel plugs containing HUVEC-coated Cytodex® beads in SCID mice at day 8. HUVECs were infected with either pAd-Fgd5 or sham virus. (**B**) Representative macroscopic pictures of the matrigel plugs containing HUVEC-coated Cytodex® beads infected with pAd-Fgd5 or sham virus. Lack of vascularisation and accumulation of erythrocytes within the plugs is visible in the pAd-Fgd5 group compared with the sham virus infected control group. (**C**) Histological haematoxylin and eosin staining shows a decline in the accumulation of HUVECs on beads coated with pAd-Fgd5 infected HUVECs compared with the sham virus infected control group. White arrows point to perinuclear outgrowth. (**D**) Quantitative analysis of micrographs show the effect of Fgd5 on the percentage of cell covered plug area (mm$^2$ per bead) in the pAd-Fgd5 infected versus sham virus infected and non-infected controls (n = 8).
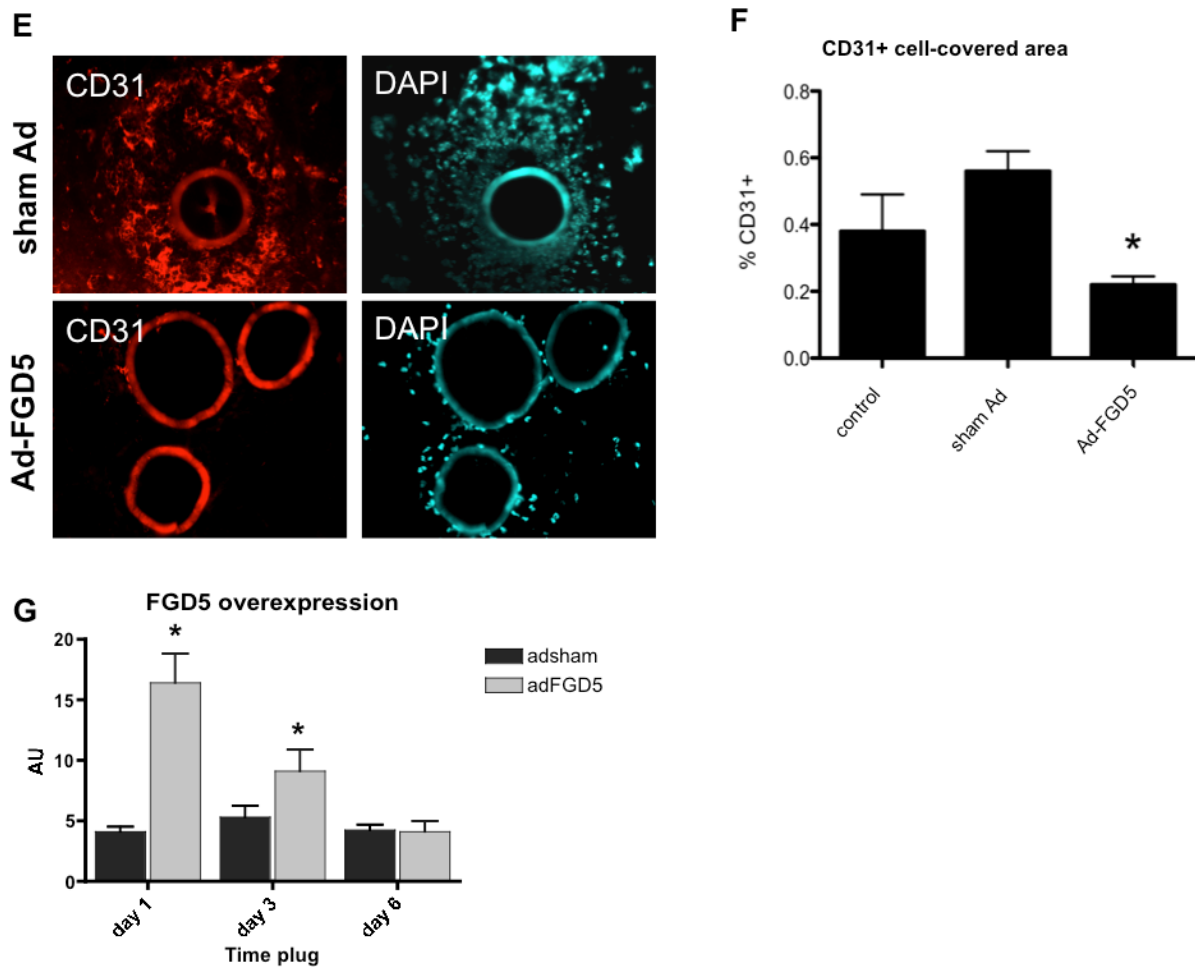
(**E**) Immunohistological staining reveals accumulation of CD31-positive endothelial cells (red) surrounding the Cytodex® beads (left hand panel), which co-localised with the DAPI-positive nuclei (blue) (right hand panel). The contours of the Cytodex® beads are visible by autofluorescence. (**F**) Quantitative analysis of the coated-bead assay show the effect of Fgd5 on the percentage CD31-positive surface area per bead ($mm^2$) in the pAd-Fgd5 group compared with the sham virus infected and non-infected control groups (n = 8; mean ± SEM). (**G**) Validation of human Fgd5 expression in the coated-beads as assessed by qPCR at different time points (n = 4; mean ± SEM).

Fgd5 function in angiogenesis was further assessed using an adenovirus expressing murine Fgd5 in murine postnatal vascular development (Figure 3A-C). Murine pAd-Fgd5 overexpression after intra-ocular injection at post-natal day 3 ($5x10^7$ pfu) reduced the vascular retinal network in the developing murine eye mainly at post-natal day 8 and 11 (Figure 3A) and is characterised by truncations in the superficial vasculature resulting in a decrease in total vascular tubule length, number of junctions and neocapillaries, whereas mean tubule length was increased at the earliest time point (Figure 3B, C).
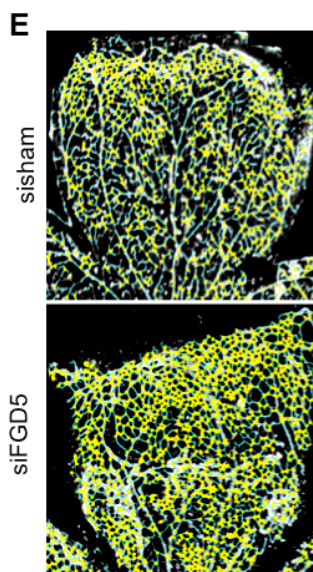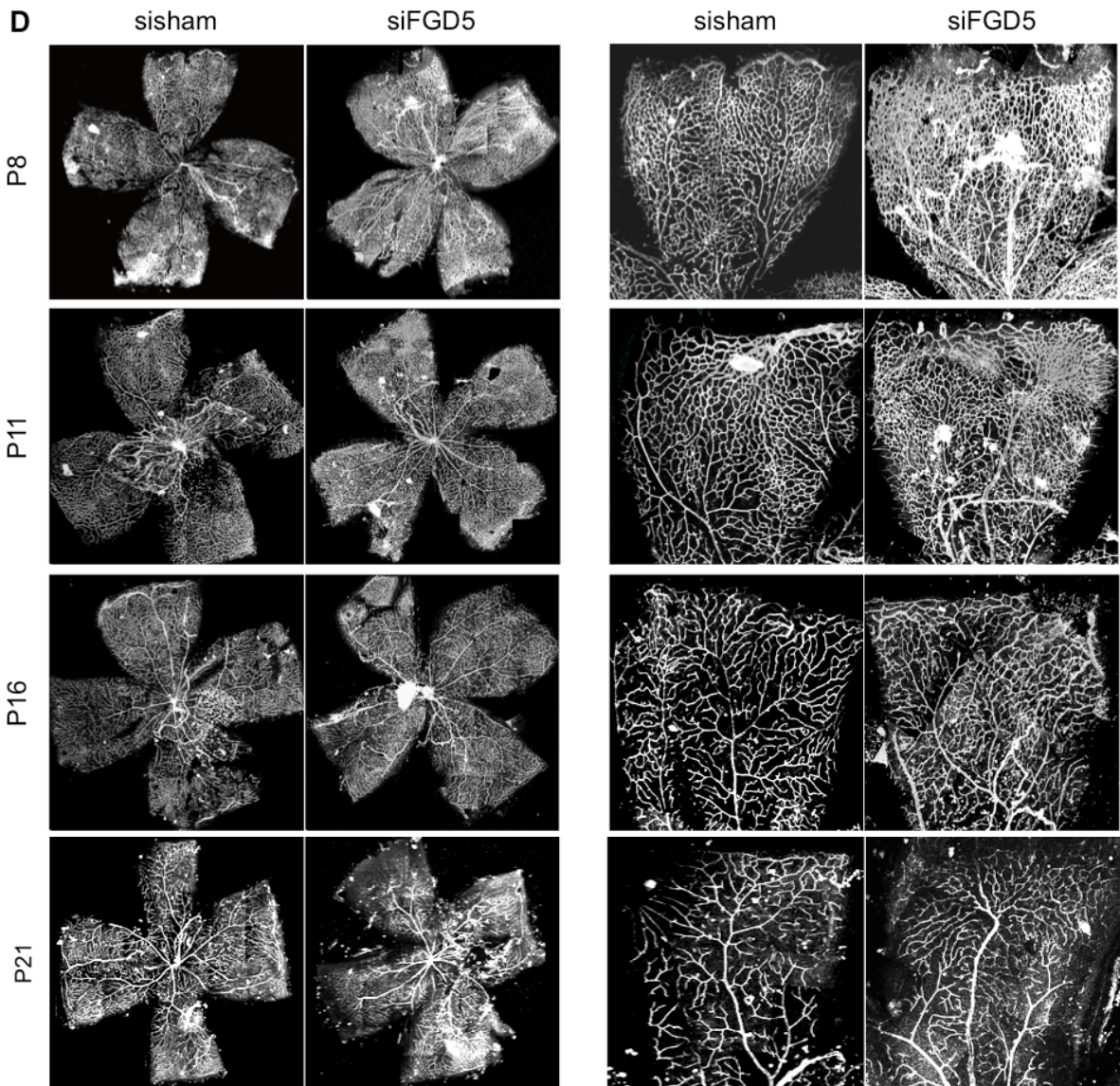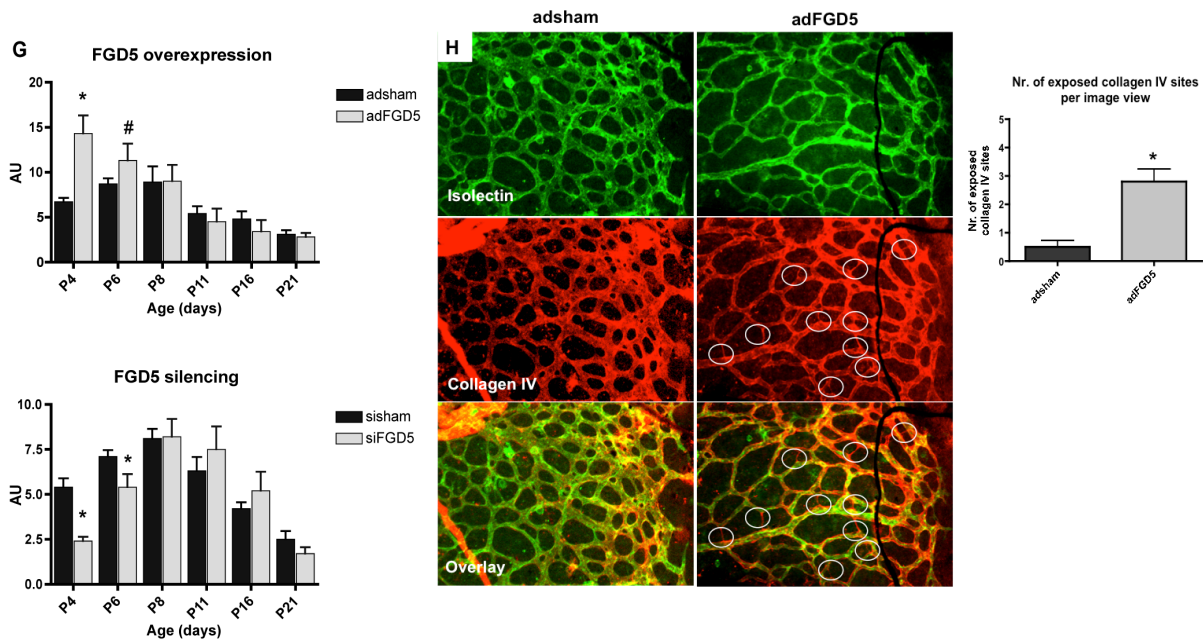
**Figure 3. Fgd5 inhibits angiogenesis the murine retina model.** (**A**) Effect of murine Fgd5 overexpression during retinal vascular development. Representative micrographs of the retinal vasculature visualised by whole-mount isolectin GS-IB$_4$ staining from 8 to 21days after birth. Whole-mount en-face staining of the retina (left hand panels) and high magnification examples of individual flaps (right hand panels) are shown. pAd-Fgd5 injection three days after birth severely impeded vascular development compared with sham virus controls. High magnification micrographs show disruption of vessels and shortened sprouts. (**B**) Representative examples of retinal flaps after processing by quantitative software (Angiosys Image Analysis Software 1.0): junctions (yellow dots) and vessels (blue lines) are shown. (**C**) Quantification of this experiment showed that Fgd5 overexpression induced a decrease in the number of junctions, number of tubules and total tubule length, whereas the mean tubule length was increased (n = 6; mean ± SEM). (**D**) Effect of murine siRNA-mediated silencing of endogenous Fgd5 during retinal vascular development. Representative micrographs of the retinal vasculature visualised by whole-mount isolectin GS-IB$_4$ staining from 8 to 21 days after birth. Whole-mount en-face staining of the retina (left hand panels) and high magnification examples of individual flaps (right hand panels) are shown. si-Fgd5 injection three days after birth supported a more excessive vascular network compared with scrambled non-targeting siRNA controls. High magnification micrographs show persistence of excessive sprouts and poor differentiation of veins and arteries by lack of pruning of the junctional vessels. (**E**) Representative examples of retinal flaps after processing by quantitative software (Angiosys Image Analysis Software 1.0): junctions (yellow dots) and vessels (blue lines) are shown. (**F**) Quantification of this experiment showed that Fgd5 silencing induced an increase in the number of junctions, number of tubules and total tubule length, whereas the mean tubule length was decreased (n = 5; mean ± SEM). (**G**) Validation of transfection efficiency by qPCR analysis: murine Fgd5 mRNA levels in the retina after infection with pAd-Fgd5 or sham virus (upper panel), and murine Fgd5 mRNA levels in the retina after treatment with siRNA targeting Fgd5 or scrambled non-targeting siRNA (lower panel) as assessed on different time points (n = 4; mean ± SEM). (**H**) Double-stained retinas 8 days after birth for isolectin GS-IB$_4$ (green, upper panel) and collagen IV (red, middle panel) shows exposed collagen IV basement membrane sheets due to vessel retraction in pAd-Fgd5 or sham virus treated retinas (indicated by white circles in the overlay, bottom panel). Quantification of exposed collagen IV sites shows that Fgd5 overexpression in the retina significantly increases neovessel retraction (n = 6; mean ± SEM).

siRNA-mediated Fgd5 knockdown substantiates these findings, because Fgd5 knockdown at post-natal day 3 resulted visa versa in an extended retinal vascular bed with persistence of excessive branches and tubule structures that failed to be removed during the vascular remodelling process (Figure 3D-F). qPCR analysis validated that murine Fgd5 mRNA expression in the pAd-Fgd5 treated retinas was significantly increased compared with treatment with pAd-sham up to post-natal day 6. Similarly, si-Fgd5 treated retinas showed a significant reduction in levels of endogenous Fgd5 at similar time points (post-natal day 4 and 6) compared with transfection with scrambled non-targeting siRNA treated retinas (Figure 3G). High-resolution representative retina examples of the Fgd5 gain- and loss-of-function are provided in the supplemental data (Supplemental figure 2W, *online*). Alteration in Fgd5 expression levels during retinal vascularisation did not affect the expansion rate of the vascular bed, as evidenced by the fact that the front of the network reached the border zone of the retina in all of the assessed conditions by post-natal day 8 (Figure 3A, D). This points toward a role in active pruning of pre-established neovessels rather than an inhibitory function in neovessel formation for Fgd5. To evaluate this further, pAd-Fgd5 treated retinas were assessed for neovessel retraction as visualised by whole-mount isolectin GS-IB$_4$/collagen IV staining. The number of exposed collagen IV basement membrane sheets at post-natal day 8 was significantly increased in Fgd5-overexpressed conditions compared with pAd-sham treated controls (Figure 3H). Further evidence was provided by FACS analysis, demonstrating that Fgd5 overexpression in the retinal bed decreased the percentage of Flk1-positive or CD31-positive (endothelial) cells (Figure 4A, B) at post-natal day 6 as a result of increased apoptosis, as revealed by Annexin V/PI analysis (Figure 4C, D). Combined, these data indicate that Fgd5 plays a significant role in the regression of the retinal vascular network.

**Fgd5 induces apoptosis in endothelial cells via a Hey1-p53 regulatory pathway**
The observed anti-angiogenic effects of Fgd5 may be attributed to changes in EC proliferation and survival. Fgd5 expressing HUVECs showed a reduced growth rate compared with pAd-sham infected controls (Supplemental figure 3A, B, *online*). In contrast, siRNA-mediated Fgd5 knockdown in HUVECs increased cell proliferation compared with si-sham controls (Supplemental figure 3C, *online*). Annexin V/PI FACS analysis demonstrated that Fgd5 overexpression promoted apoptosis, whereas siRNA-mediated Fgd5 silencing diminished apoptosis (Supplemental figure 3D, E, *online*). The increase in cell death coincided with rising p21$^{Cip1}$ and p53 protein levels (Supplemental figure 3F, G, *online*). These data imply that Fgd5 could be involved in p21$^{Cip1}$-associated cell cycle arrest and p53-dependent apoptosis, resulting in vascular regression. To elucidate the downstream signalling cascade involved in Fgd5-mediated vascular pruning, the gene expression for well-defined angiogenic modulators was determined by qPCR. Fgd5 knockdown inhibited VEGFR-1 and Flt1 mRNA expression, but promoted VEGFR-2, Kdr

and Flk1 mRNA expression, whereas Fgd5 overexpression decreased VEGFR-2 in favour of VEGFR-1 mRNA levels, thus promoting an anti-angiogenic state in the ECs (Supplemental figure 3H, *online*). In addition, Fgd5 knockdown was associated with the downregulation of Notch pathway genes, including Notch 1 and 4, and Dll4. Hey1, one of the key downstream transcriptional regulators of the Notch signalling pathway[20], was markedly downregulated by Fgd5 knockdown (Supplemental figure 3H, *online*). In contrast, Fgd5 overexpression induced reversed effects. Fgd5 knockdown or overexpression in HUVECs did not change mRNA expression of VEGF-A, jagged 1, ephrin B2 and B4, neuropilin 1 and 2 (Supplemental figure 3I, *online*). To investigate whether the process of Fgd5-mediated vascular pruning could be mediated by changes in the VEGFR-1:VEGFR-2 ratio, a soluble active form of VEGFR-1 was provided in si-Fgd5 treated retinas. Indeed, the restoration of VEGFR-1 bio-availability diminished the formation of excessive vascular structures that was associated with Fgd5 silencing (Supplemental figure 3J, *online*). Thus, Fgd5 could regulate the vascular pruning process by promoting VEGFR-1 versus VEGFR-2 bio-availability.
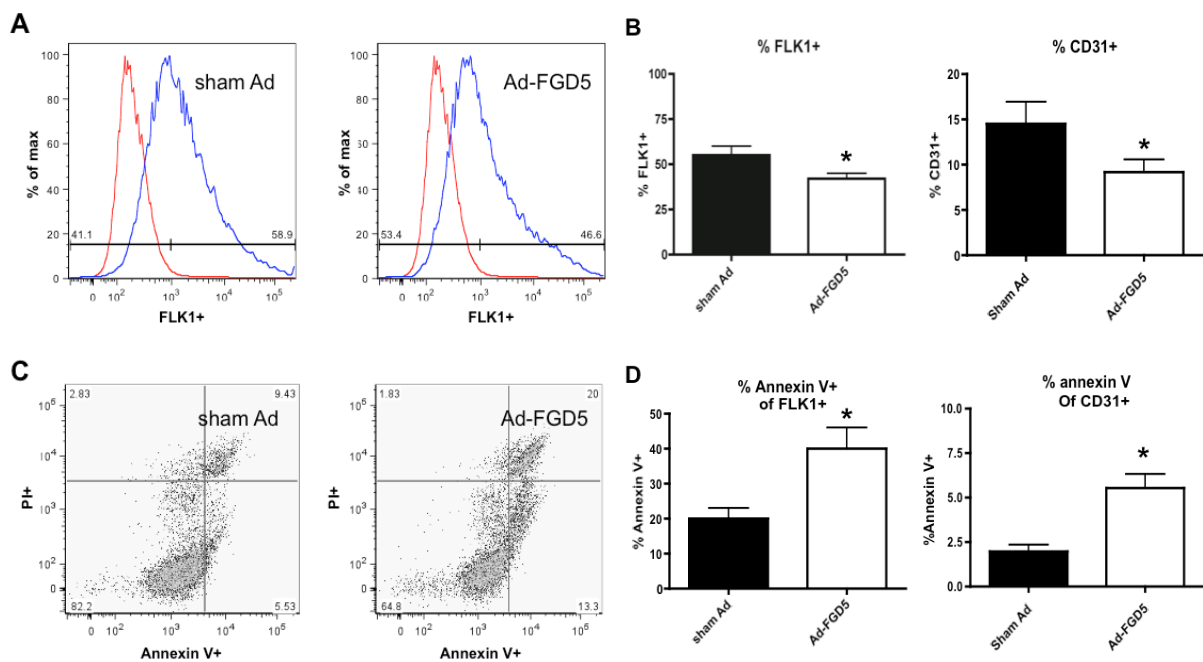


**Figure 4. Fgd5 expression affects retinal vascular development and correlates with apoptosis.** (**A**) Flow cytometric analysis of the percentage of Flk1-positive cells in the retina - infected with pAd-Fgd5 or sham virus - three days after injection. Red histograph represents the isotype control, blue histograph represents the Flk1-positive signal. (**B**) Bar graphs show the percentage of Flk1-positive cells and CD31-postive cells in the alive cell population. (**C**) Dot plot graphs of the percentage of dead cells, apoptotic cells and alive cells in the Flk1-positive population. (**D**) Quantification of the percentage of apoptotic cells in the Flk1-positive population (left graph) and the CD31-positive population (right graph) (Flk1 analysis: n = 6 and CD31 analysis: n = 4).

Hey1 was previously associated with p53-mediated apoptosis[21], suggesting that Hey1 could mediate Fgd5-induced apoptosis in ECs. Here, we assessed the function of Hey1 in Fgd5-mediated apoptosis. Hey1 knockdown in Fgd5 expressing HUVECs could rescue growth inhibition induced by Fgd5 (Figure 5A). It also diminished p21$^{Cip1}$ and p53 protein levels (Figure 5B, C) and reversed ECs from Fgd5-induced apoptosis (Figure 5D, E). PI-aided cell cycle analysis suggested that Fgd5 enhanced the sub-G1 apoptotic fraction, whereas the percentage of alive and proliferating cells decreased, i.e. decrease in G1 and S–G2 fraction in the pAd-Fgd5 group compared with the pAd-sham treated group (Figure 5F, G). This cytostatic effect was rescued by Hey1 knockdown in Fgd5 overexpressing ECs. Likewise, in an *in vitro* coated-bead assay, Fgd5-mediated inhibition of capillary outgrowth was reversed by concomitant Hey1 silencing (Figure 5H, I).
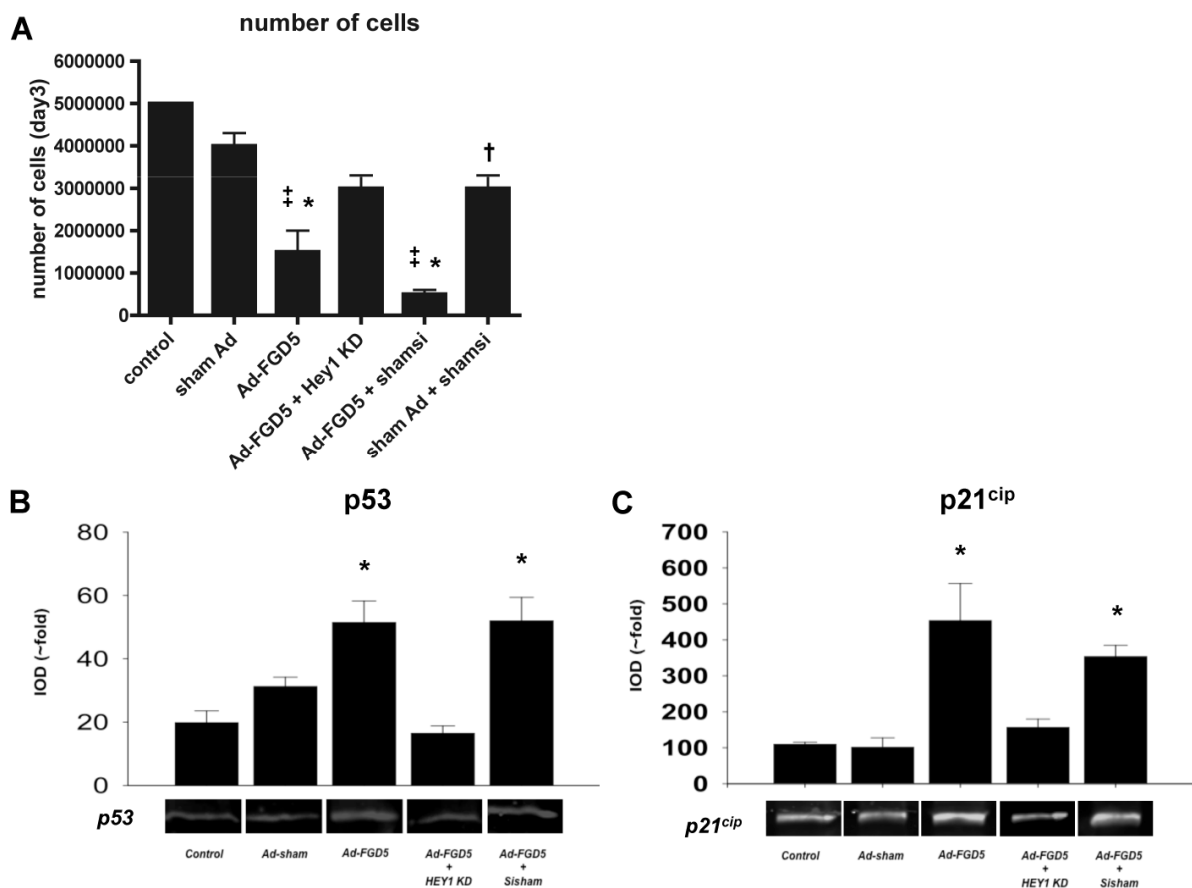


**Figure 5. Fgd5 induces apoptosis in endothelial cells via Hey1 activation.** (**A**) Number of HUVECs three days after infection with sham virus, pAd-Fgd5, pAd-Fgd5 with si-Hey1, pAd-Fgd5 with si-sham, or sham virus with si-sham. Representative immunoblots with corresponding graphs that show quantification of (**B**) p53 and (**C**) p21$^{Cip1}$ band densities in the examined groups (n = 4; mean ± SEM).

194
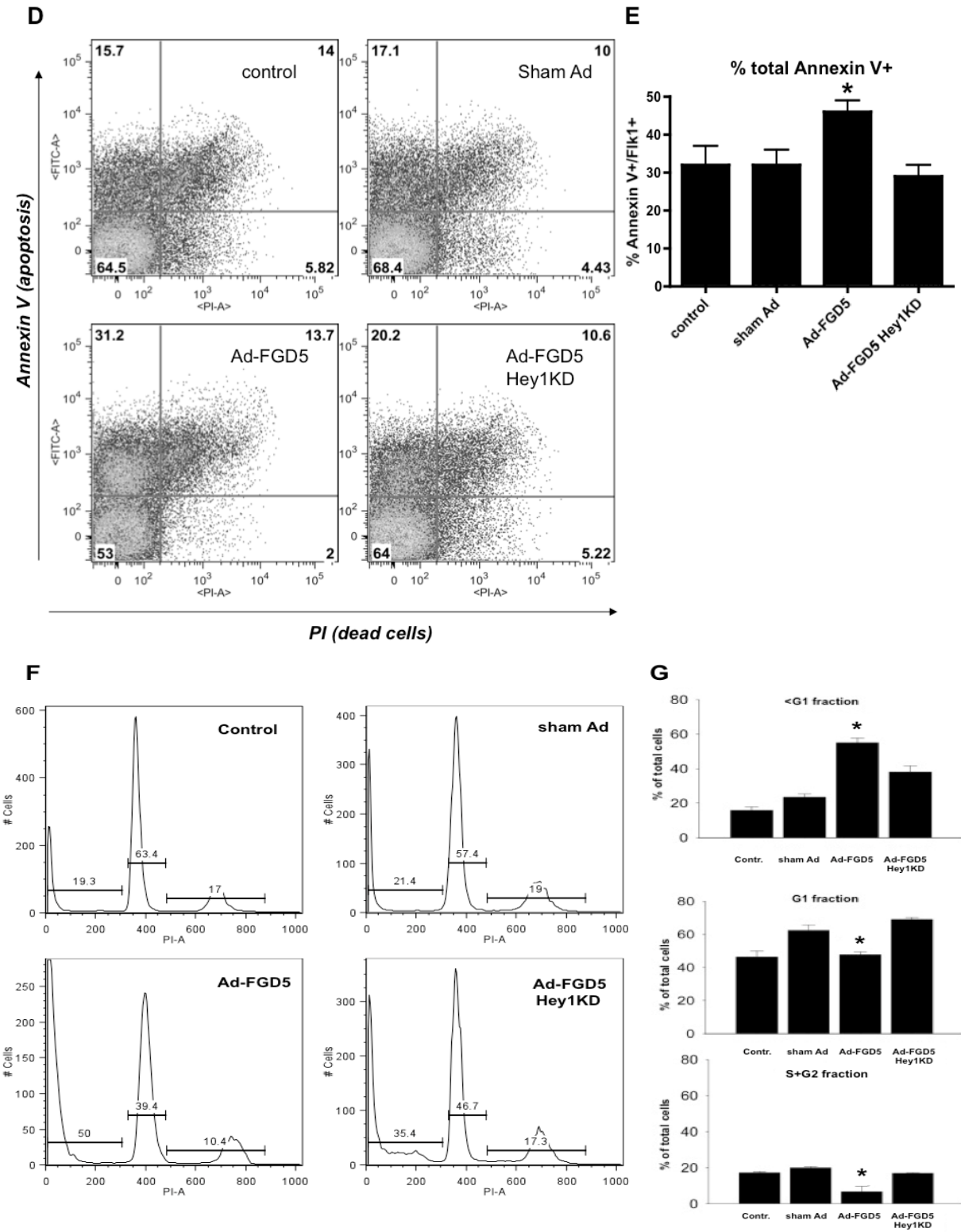
(**D**) Representative flow cytometric analysis of non-infected control HUVECs and HUVECs infected with sham virus, pAd-Fgd5 or pAd-Fgd5 with si-Hey1. (**E**) Quantification of the percentage of Annexin V-positive cells (n = 4; mean ± SEM). (**F**) Representative flow cytometric analysis of non-infected control HUVECs and HUVECs infected with sham virus, pAd-Fgd5 or pAd-Fgd5 with si-Hey1. (**G**) Quantification of the percentages of cells in the subG1, G1 and S–G2-fractions in the different experimental groups (n = 4; mean ± SEM).
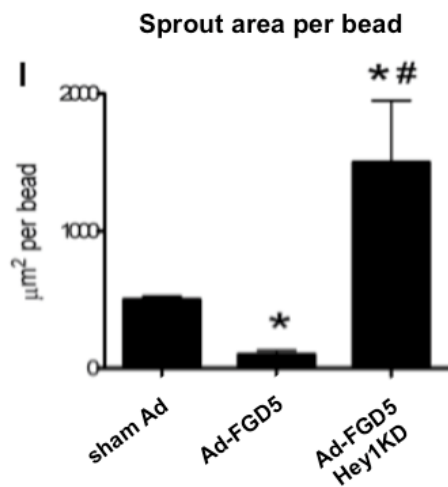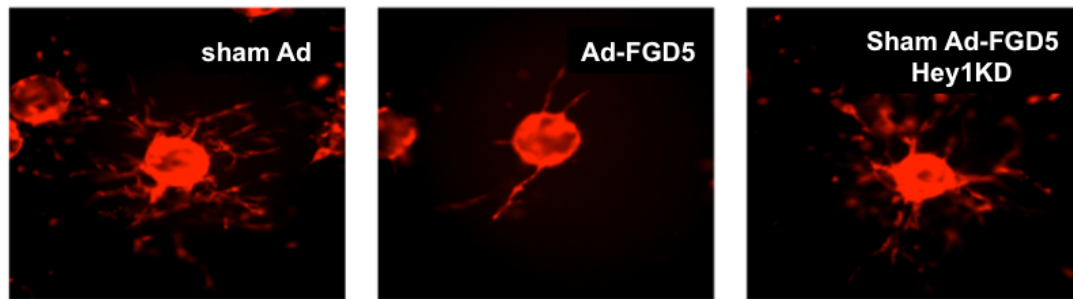
**(H)** Representative micrographs show phalloidin stained microvascular sprouting (red) of HUVECs coated on Cytodex® beads in matrigel. HUVECs were infected with sham virus, pAd-Fgd5 or pAd-Fgd5 with si-Hey1. **(I)** Quantitative analysis of the effect of Hey1 knockdown in Fgd5 overexpressing cells on the relative sprout area per bead (n = 3; mean ± SEM).

Further studies demonstrate that Fgd5-induced cell death was indeed mediated via p21$^{Cip1}$ and p53, because co-transfection of pAd-Fgd5 in HUVECs with p21$^{Cip1}$ or p53 targeting siRNA rescued these cells from apoptosis (Figure 6A, B) and reduced the sub-G1 apoptotic fraction while promoting the percentage of alive and proliferative cells as demonstrated by cell cycle analysis (Figure 6C, D). In addition, p53 silencing reversed the growth inhibitory effects of Fgd5 overexpression in the coated-bead assay (Figure 6E, F). These data support the pro-apoptotic function of Fgd5 in ECs during late neo-angiogenesis and demonstrate involvement of the Hey1-p21$^{Cip1}$-p53 signalling cascade in the induction of Fgd5-mediated apoptosis in ECs.
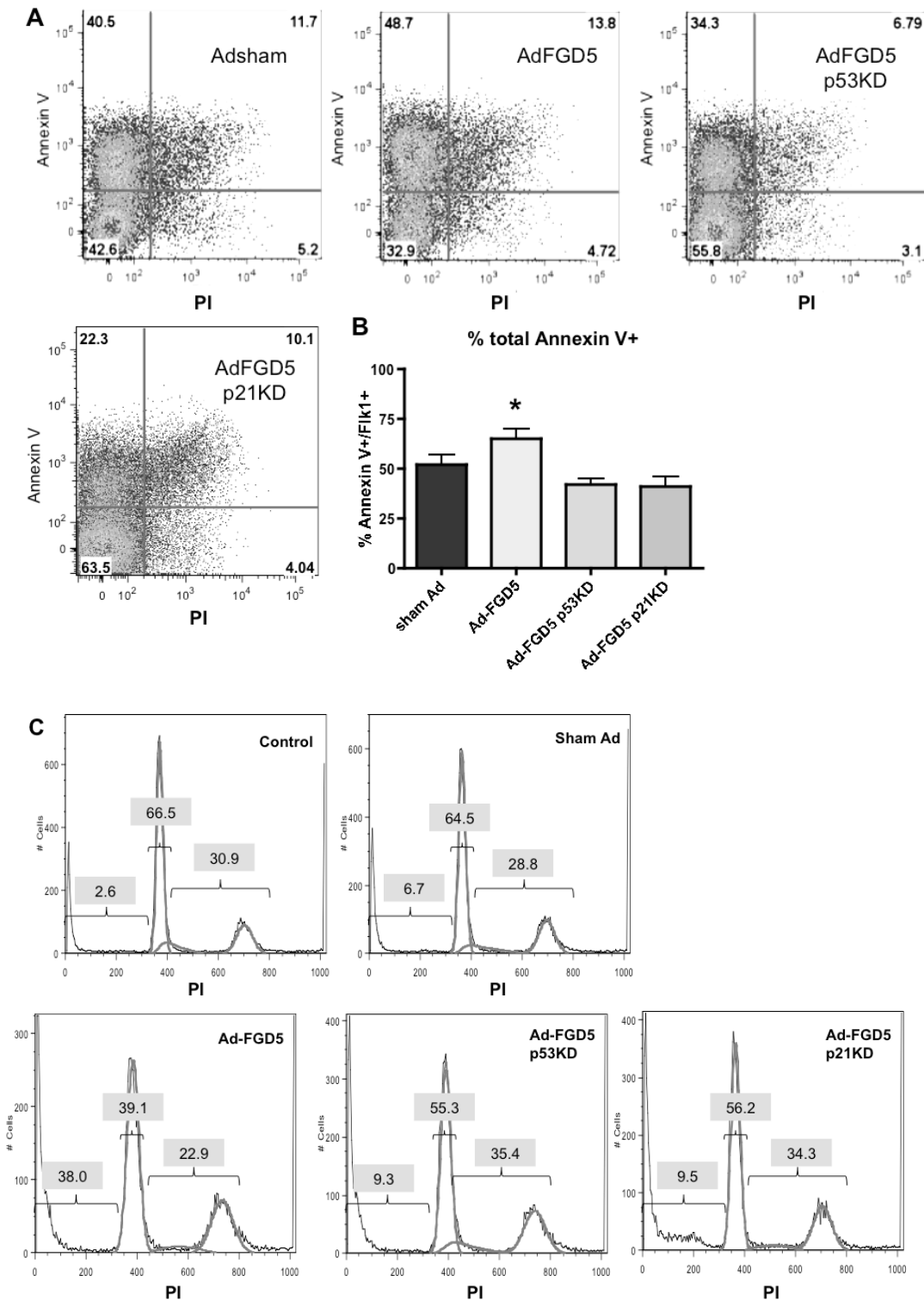
**Figure 6. Fgd5-mediated endothelial cell death depends on p21$^{Cip1}$ and p53 signalling.** (**A**) Representative flow cytometric analysis of HUVECs infected with sham virus, pAd-Fgd5, pAd-Fgd5 with si-p21$^{Cip1}$, or pAd-Fgd5 with si-p53. (**B**) Quantification of the percentage of Annexin V-positive cells (n = 4; mean ± SEM). (**C**) Representative flow cytometric analysis of non-infected control HUVECs and HUVECs infected with sham virus, pAd-Fgd5, pAd-Fgd5 with si-p21$^{Cip1}$, or pAd-Fgd5 with si-p53.

197
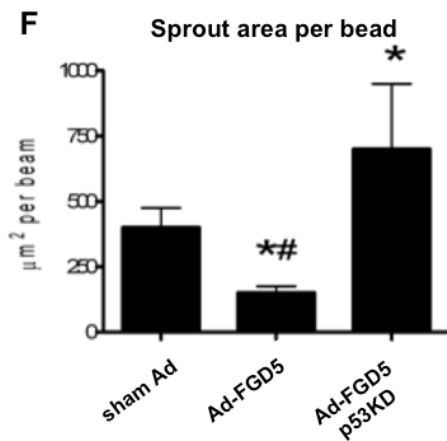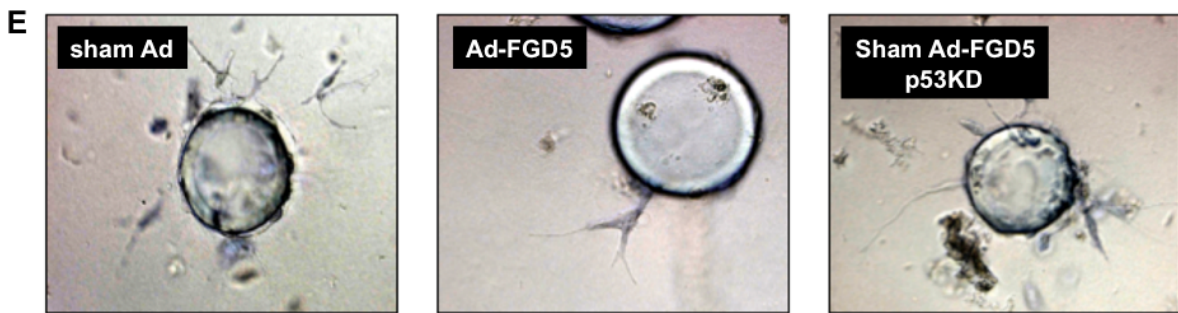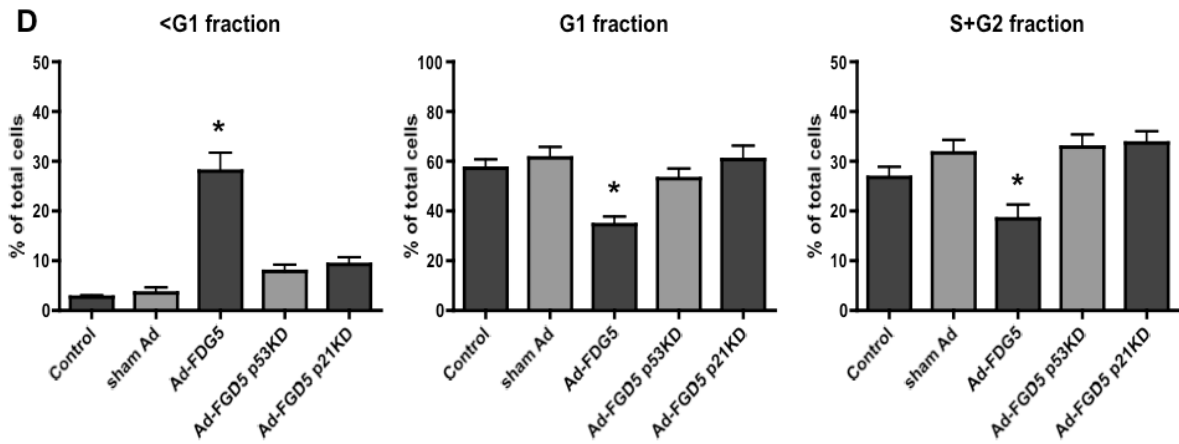
(**D**) Quantification of the percentages of cells in the subG1, G1 and S–G2-fractions in the different experimental groups (n = 4; mean ± SEM). (**E**) Representative micrographs show microvascular sprouting of HUVECs coated on Cytodex® beads in matrigel. HUVECs were infected with sham virus, pAd-Fgd5 or pAd-Fgd5 with si-p53. (**F**) Quantitative analysis of the effect of p53 knockdown in Fgd5 overexpressing cells on the relative sprout area per bead (n = 3; mean ± SEM).

**Fgd5 binds and activates Cdc42 small G-protein**

To determine the direct protein target of Fgd5, we assessed whether Fgd5 could bind and activate small G-proteins like its better-known family members. Fgd5 transgene expression in HUVECs did not alter total Cdc42, decreased Rac1 and increased RhoA protein levels (Figure 7A). However, co-immunoprecipitation using an antibody against Fgd5 identified Cdc42 as the selective binding partner of Fgd5 (Figure 7B), leading to specific activation of Cdc42 in a GEF-activity assay (Figure 7C-E). In addition, fluorescence microscopy showed co-localisation of endogenous Fgd5 with Cdc42 at the perinuclear site in the cytoplasm of ECs (Figure 7F, G). In contrast, Rac1 and RhoA activity was significantly reduced in response to Fgd5 overexpression. Because no direct binding of Fgd5 to Rac1 or RhoA was observed in the co-immunoprecipitation studies, these data suggest that the inhibition of Rac1 and RhoA activity is an indirect downstream effect of Fgd5.
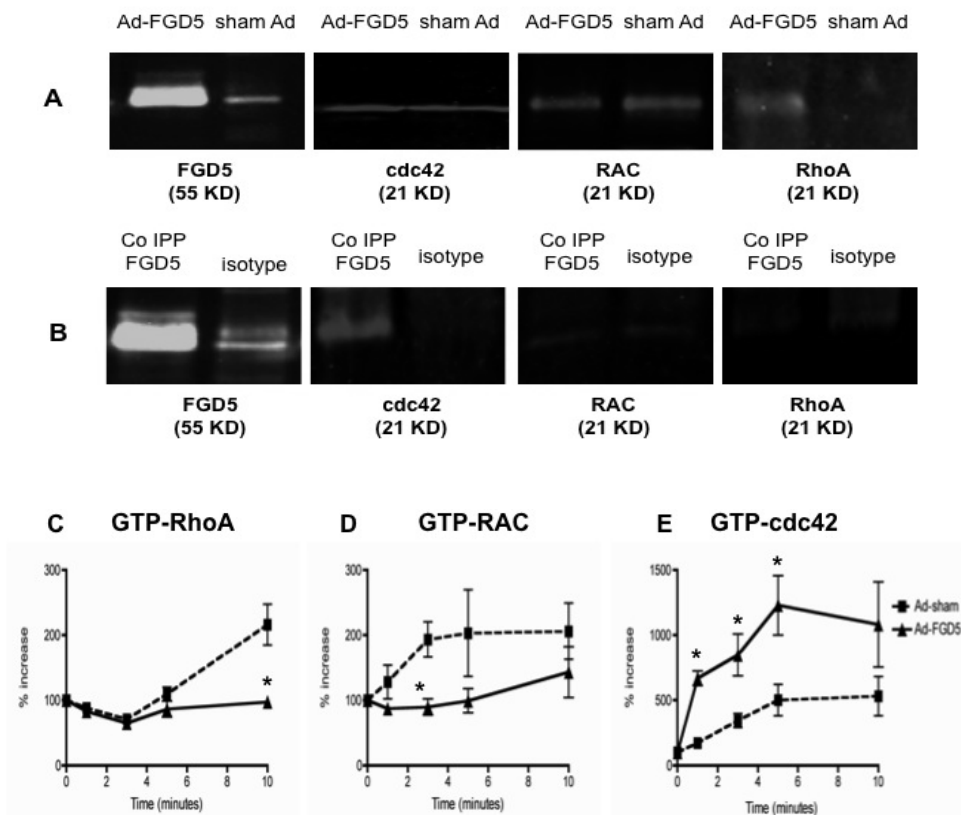


**Figure 7. Fgd5 binds and activates Cdc42 small G-protein.** (**A**) Western blot analysis of Rac1, RhoA and Cdc42 levels in HUVECs overexpressing Fgd5. (**B**) Immunoprecipitation of Fgd5 in HUVECs overexpressing Fgd5 showed co-immunoprecipitation of Cdc42, but not of Rac1 or RhoA. Immunoprecipitation using an IgG isotype control showed no effective pull down of Fgd5 or Cdc42 (shown are representative results of n = 3). Chemiluminescence measurement of the GTP-bound small G-proteins in HUVECs infected with sham virus or pAd-Fgd5, showing the levels of (**C**) RhoA-GTP, (**D**) Rac1-GTP and (**E**) Cdc42-GTP in response to serum activation (n = 4; mean ± SEM).
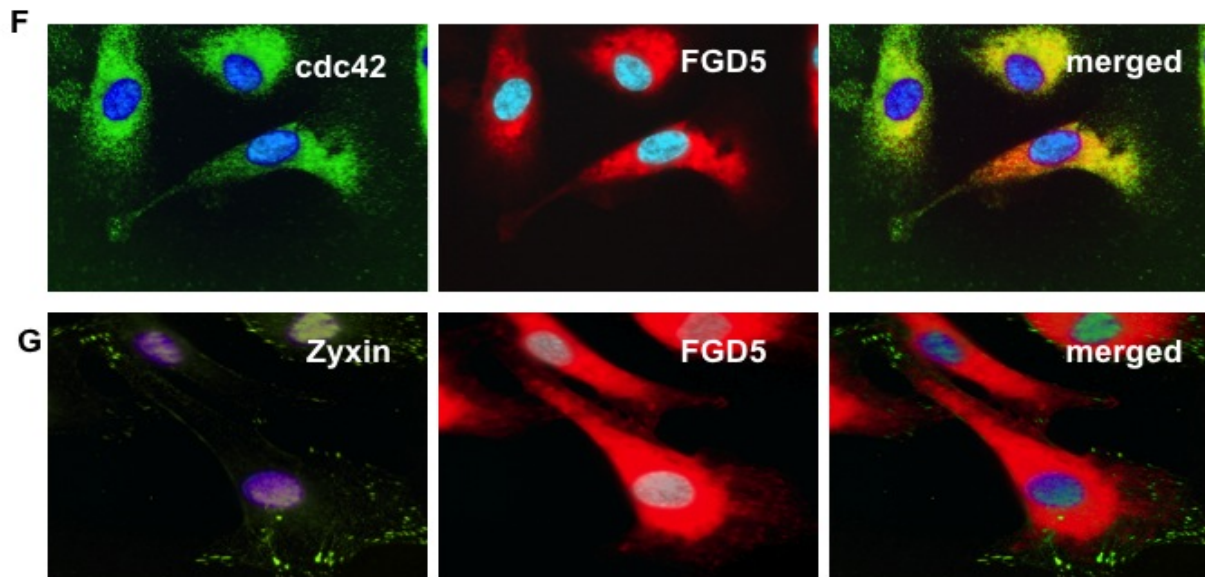
(**F**) Fgd5 was mainly located perinuclear in the cytoplasm and co-localises with Cdc42, as demonstrated by immunofluorescent staining. Fgd5 (red), Cdc42 (green), co-localised area (yellow) and nuclei (blue) (n = 3). (**G**) Fgd5 does not co-localise with zyxin - a focal adhesion marker - as demonstrated by immunofluorescent staining. Fgd5 (red), zyxin (green) and nuclei (blue) (n = 3).

**Fgd5 level correlates with vascular regression in aging**

Transgenic mice with constitutively activated Cdc42 show premature aging with failing DNA repair, accelerated cell senescence and increased p53-dependent apoptosis.[22] Similarly, Cdc42 activation in cell culture was previously associated with cell senescence[23] and apoptosis[24], whereas Cdc42 deletion in haematopoietic stem cells promoted proliferation by loss of p21$^{Cip1}$ regulation during cell cycle progression.[25] To assess the role of Fgd5 in aging-related vascular regression we carried out qPCR analysis of aging wild-type C57BL/6J mice ranging from early fully mature (37-41 weeks) to old (80-92 weeks) specimens. A significant increase in Fgd5 levels was observed in the oldest group of animals, which coincided with rising p21$^{Cip1}$ expression, whereas CD31 levels were diminished in the oldest group (Supplemental figure 4, *online*).

## *Discussion*

This study has several findings. First, Fgd5 is specifically expressed in both progenitor and mature ECs, in contrast to its family members FRG, Fgd1, Fgd2, Fgd3, Fgd4 and Fgd6, which show an ubiquitous expression in different cell types. In addition, this EC-specific expression is preserved throughout the evolution in different species. Second, Fgd5 inhibits

neovascularisation, as indicated by the results obtained *in vitro* from network-formation, aortic-ring and coated-bead assays. These findings were validated *in vivo* by results obtained from the coated-bead plug assay and the murine retina model. Third, Fgd5 binds and activates its direct downstream target - Cdc42. Fourth, Fgd5 inhibits neovascularisation by apoptosis-induced vaso-obliteration via induction of the Hey1-p53 pathway. Finally, Fgd5 indeed correlates with apoptotic marker expression in Flk1-positive ECs during vascular remodelling in the mouse retina, whereas high levels of Fgd5 expression were linked to rising p21$^{Cip1}$ mRNA levels in aging C57BL/6J wild-type mice.

Here, we define, for the first time to the best of our knowledge, the function of Fgd5 as an EC-specific GEF that plays a crucial role in apoptosis-induced vascular pruning during vascular remodelling.

Vascular growth and remodelling during development and disease are tightly regulated by stimulatory and inhibitory signals that determine the complexity of the vascular tree hierarchy. Here, we describe the inhibitory role of Fgd5 in vascular development, a member of the Fgd family of RhoGEF from which thus far no biological function was allocated. Fgd1 was the first Fgd member to be identified and mutations in the gene were proven to be responsible for Faciogenital Dysplasia or Aarskog-Scott syndrome.[8] Further studies indicated that Fgd1 functioned as a Cdc42-specific GEF, thereby activating Cdc42 signalling by exchanging bound GDP with GTP.[7] Fgd2, Fgd3, Fgd4 and FRG were identified by genetic searches as Fgd1 homologues[4-6], and were all subsequently associated with a specific role in Cdc42 activation with downstream effects on cell migration and morphology[9-13], whereas the function of Fgd5 and Fgd6 remained to be elucidated. Although the preserved Cdc42-GEF activity of the different Fgd members seemed to imply a redundancy in the protein family by overlapping function, the specific expression of Fgd5 in ECs points toward a unique role for this particular Fgd member in EC regulation. Similar to the other family members, Fgd5 comprises (in order) a Dbl homology adjacent to a PH domain, followed by a FYVE-finger domain and a second C-terminal PH domain. Although the Dbl homology domain is responsible for catalytic activity, the PH domain appears to be vital for localisation and full activation of this group of RhoGEFs.[6,12,13] Here, we show specific direct binding of Fgd5 to Cdc42 and demonstrate Fgd5-mediated activation of Cdc42. In addition, similar to recent findings that indicated co-localisation of Fgd1 with Cdc42 in the Golgi complex in HeLa cells[26], Fgd5 intracellular distribution in ECs was primarily co-localised with Cdc42 in the perinuclear region. Together, these data identify Cdc42 as the direct downstream target of Fgd5 and assign an EC-specific RhoGEF function to this gene.

Our data also demonstrated that the effect of Fgd5 could be attributed to p21$^{Cip1}$-mediated G1/S–G2 cell cycle arrest, followed by p53-mediated apoptosis. Transgenic overexpression of Fgd5 coincided with the upregulation of the Notch signalling pathway, including Notch 1 and 4, Dll4, and the downstream transcription factor Hey1. Genetic

regulation of these Notch genes could be induced after Fgd5-mediated Cdc42 activation via the p38-MAPK signalling pathway that regulates transcriptional activation.[27] More downstream of Cdc42 towards the process of apoptosis, recent studies have indicated that Hey1 triggered p53 activation through repression of HDMD2 transcription, indentifying a new direct link between Hey1 and p53.[21] Our experiments further showed that siRNA targeting of Hey1 in Fgd5 transgenic ECs inhibited Fgd5-induced G1/S–G2 cell cycle arrest and cell death by reverting protein levels of p21$^{Cip1}$ and p53 back to baseline. In addition, Hey1 knockdown of Fgd5 transgenic HUVECs restored the sprouting capacity of these cells in the *in vitro* coated-bead assay, whereas siRNA targeting of p21$^{Cip1}$ or p53 in Fgd5 transgenic ECs obtained similar effects on apoptosis and sprout-formation. Together, our data clearly indicate Fgd5-mediated cell death in ECs involves the Hey1-p21$^{Cip1}$-p53 pathway.

In our studies, we demonstrated that rising endogenous Fgd5 levels in the Flk1-positive ECs in the developing retinal vasculature were associated with the expression of the apoptosis marker cleaved caspase 3. Surprisingly, a large population of Flk1-postive/caspase 3-positive/Fgd5-negative cells was also observed next to the Flk1-positive/caspase 3-positive/Fgd5-positive subpopulation, which suggests that Fgd5-induced apoptosis is not the only regulatory mechanism of vascular pruning. Indeed, Ishida *et al*[3] have previously published that vascular regression in the murine retina was also regulated by infiltration of leukocytes. These cells induce apoptosis of the redundant vascular structure via a FasL-mediated process. In light of these findings, our data demonstrate that Fgd5 activation provides an additional mechanism that is partially responsible for the observed cell death of Flk1-positive ECs in the natural vascular pruning process.

Wang *et al*[22] demonstrated that during natural aging, Cdc42 activity in different organs was increased in wild-type mice. By targeting of Cdc42-GAP - which reverses Cdc42 from its active GTP-bound to its inactive GDP-bound state - they successfully created a murine strain with constitutively elevated Cdc42-GTP levels. These Cdc42-GAP-knockout animals had a prematurely aged phenotype with a failing DNA repair system and a considerably shortened average lifespan from 27 weeks to 12 months. In addition, increased apoptosis was observed in various cell types during organ development and aging, which was dependent on p21$^{Cip1}$ and p53 activation. Cdc42-GAP-null cells also showed early proliferative senescence compared with wild-type cells.[22] Cdc42 activation was previously associated with cell senescence[23] and apoptosis[24], whereas Cdc42 deletion in haematopoietic stem cells promoted cell proliferation by deregulating p21$^{Cip1}$ levels during cell cycle progression.[25] These studies suggested a direct link between Cdc42 activity and p53-mediated apoptosis, which was further affirmed in our findings in which GEF activity of Fgd5 elevated the level of Cdc42-GTP in ECs and coincided with Hey1-p53-induced cell death. Fgd5-induced apoptosis could be further confirmed *in vivo* because high endogenous levels of Fgd5 during retinal vascular development were linked to a rise in cleaved caspase

3 levels in ECs. More important, transgenic overexpression of Fgd5 in the developing murine retinal vasculature induced EC apoptosis and vascular regression, whereas Fgd5 silencing promoted survival of excessive vascular structures.

Thus far, we have established an important role for Fgd5 in vascular remodelling as an inducer of vascular pruning of redundant neovessels. In aging, an imbalance between Cdc42 deactivation and activation could result in elevated Cdc42 activity, which has severe effects on the proliferative and stress-responsive capacities of aging cells.[22] Thus, it would be interesting to study the level of Fgd5 expression not only in diseases with pronounced apoptosis-induced vascular regression, but also in the aging vasculature. In this study, we found a correlation between Fgd5 levels and increasing levels of p21$^{Cip1}$ expression in the highly vascularised hind limb tissue of aging wild-type mice, which coincided with a decline in CD31 EC marker expression. Currently, we are carried out further studies to elucidate the role of this EC-specific GEF in vascular regression in the natural aging process.

In conclusion, we have identified Fgd5 as a new genetic regulator of vascular pruning of redundant neovessels by activation of targeted apoptosis. In addition, Fgd5 function could prove to be a decisive factor in the survival and stability of aging vasculature.

## *References*

1. Benjamin LE, Hemo I, Keshet E. A plasticity window for blood vessel remodelling is defined by pericyte coverage of the preformed endothelial network and is regulated by PDGFβ and VEGF. *Development.* 1998;125(9):1591-1598.
2. Jain RK. Molecular regulation of vessel maturation. *Nat Med.* 2003;9(6):685-693.
3. Ishida S, Yamashiro K, Usui T, Kaji Y, Ogura Y, Hida T, Honda Y, Oguchi Y, Adamis AP. Leukocytes mediate retinal vascular remodelling during development and vaso-obliteration in disease. *Nat Med.* 2003;9(6):781-788.
4. Obaishi H, Nakanishi H, Mandai K, Satoh K, Satoh A, Takahashi K, Miyahara M, Nishioka H, Takaishi K, Takai Y. Fabrin, a novel Fgd1-related actin filament-binding protein capable of changing cell shape and activating c-Jun N-terminal kinase. *J Biol Chem.* 1998;273(30):18697-18700.
5. Pasteris NG, Nagata K, Hall A, Gorski JL. Isolation, characterisation and mapping of the mouse Fgd3 gene, a new Faciogenital Dysplasia (Fgd1; Aarskog syndrome) gene homologue. *Gene.* 2000;242(1-2):237-247.
6. Pasteris NG, Gorski JL. Isolation, characterisation and mapping of the mouse and human Fgd2 genes, Faciogenital Dysplasia (Fgd1; Aarskog syndrome) gene homologues. *Genomics.* 1999;60(1):57-66.

7. Zheng Y, Fischer DJ, Santos MF, Tigyi G, Pasteris NG, Gorski JL, Xu Y. The Faciogenital Dysplasia gene product Fgd1 functions as a Cdc42 Hs-specific guanine-nucleotide exchange factor. *J Biol Chem.* 1996;271(52):33169-33172.

8. Pasteris NG, Cadle A, Logie LJ, Porteous ME, Schwartz CE, Stevenson RE, Glover TW, Wilroy RS, Gorski JL. Isolation and characterisation of the Faciogenital Dysplasia (Aarskog-Scott syndrome) gene: a putative Rho/Rac guanine nucleotide exchange factor. *Cell.* 1994;79(4):669-678.

9. Miyamoto Y, Yamauchi J, Itoh H. Src kinase regulates the activation of a novel Fgd1-related Cdc42 guanine nucleotide exchange factor in the signalling pathway from the endothelin A receptor to JNK. *J Biol Chem.* 2003;278(32):29890-29900.

10. Hayakawa M, Matsushima M, Hagiwara H, Oshima T, Fujino T, Ando K, Kikugawa K, Tanaka H, Miyazawa K, Kitagawa M. Novel insights into Fgd3, a putative GEF for Cdc42, that undergoes SCF(FWD1/beta-TrCP)-mediated proteasomal degradation analogous to that of its homologue Fgd1 but regulates cell morphology and motility differently from Fgd1. *Genes Cells.* 2008;13(4):329-342.

11. Huber C, Mårtensson A, Bokoch GM, Nemazee D, Gavin AL. Fgd2, a Cdc42-specific exchange factor expressed by antigen-presenting cells, localises to early endosomes and active membrane ruffles. *J Biol Chem.* 2008;283(49):34002-34012.

12. Umikawa M, Obaishi H, Nakanishi H, Satoh-Horikawa K, Takahashi K, Hotta I, Matsuura Y, Takai Y. Association of frabin with the actin cytoskeleton is essential for microspike formation through activation of Cdc42 small G-protein. *J Biol Chem.* 1999;274(36):25197-25200.

13. Ono Y, Nakanishi H, Nishimura M, Kakizaki M, Takahashi K, Miyahara M, Satoh-Horikawa K, Mandai K, Takai Y. Two actions of frabin: direct activation of Cdc42 and indirect activation of Rac. *Oncogene.* 2000;19(27):3050-3058.

14. Cheng C, Tempel D, Oostlander A, Helderman F, Gijsen F, Wentzel J, van Haperen R, Haitsma DB, Serruys PW, van der Steen AF, de Crom R, Krams R. Rapamycin modulates the eNOS versus shear stress relationship. *Cardiovasc Res.* 2008;78(1):123-129.

15. Cheng C, Tempel D, den Dekker WK, Haasdijk RA, Chrifi I, Bos FL, Wagtmans K, van de Kamp EH, Blonden L, Biessen EA, Moll F, Pasterkamp G, Serruys PW, Schulte-Merker S, Duckers HJ. Ets2 determines the inflammatory state of endothelial cells in advanced atherosclerotic lesions. *Circ Res.* 2011;109(4):382-395.

16. Cheng C, Noordeloos AM, Jeney V, Soares MP, Moll F, Pasterkamp G, Serruys PW, Duckers HJ. Haem oxygenase-1 determines atherosclerotic lesion progression into a vulnerable plaque. *Circulation.* 2009:119(23):3017-3027.

17. Cheng C, Noordeloos AM, van Deel ED, Tempel D, den Dekker WK, Wagtmans K, Duncker DJ, Soares MP, Laman JD, Duckers HJ. Dendritic cell function in transplantation arteriosclerosis is regulated by haem oxygenase-1. *Circ Res.* 2010;106(10):1656-1666.

18. Cheng C, Tempel D, van Haperen R, van Damme LC, Algür M, Krams R, de Crom R. Activation of MMP8 and MMP13 by angiotensin II correlates to severe intra-plaque haemorrhages and collagen breakdown in atherosclerotic lesions with a vulnerable phenotype. *Atherosclerosis.* 2009;204(1):26-33.

19. Segers D, Helderman F, Cheng C, van Damme LC, Tempel D, Boersma E, Serruys PW, de Crom R, van der Steen AF, Holvoet P, Krams R. Gelatinolytic activity in atherosclerotic plaques is highly localised and is associated with both macrophages and smooth muscle cells *in vivo*. *Circulation.* 2007;115(5):609-616.

20. Fischer A, Schumacher N, Maier M, Sendtner M, Gessler M. The Notch target genes Hey1 and Hey2 are required for embryonic vascular development. *Genes Dev.* 2004;18(8):901-911.

21. Huang Q, Raya A, DeJesus P, Chao SH, Quon KC, Caldwell JS, Chanda SK, Izpisua-Belmonte JC, Schultz PG. Identification of p53 regulators by genome-wide functional analysis. *Proc Natl Acad Sci U S A.* 2004;101(10):3456-3461.

22. Wang L, Yang L, Debidda M, Witte D, Zheng Y. Cdc42 GTPase-activating protein deficiency promotes genomic instability and premature aging-like phenotypes. *Proc Natl Acad Sci U S A.* 2007;104(4):1248-1253.

23. Cho KA, Ryu SJ, Oh YS, Park JH, Lee JW, Kim HP, Kim KT, Jang IS, Park SC. Morphological adjustment of senescent cells by modulating caveolin-1 status. *J Biol Chem.* 2004;279(40):42270-42278.

24. Maillet M, Lynch JM, Sanna B, York AJ, Zheng Y, Molkentin JD. Cdc42 is an antihypertrophic molecular switch in the mouse heart. *J Clin Invest.* 2009;119(10):3079-3088.

25. Yang L, Wang L, Geiger H, Cancelas JA, Mo J, Zheng Y. Rho-GTPase Cdc42 coordinates haematopoietic stem cell quiescence and niche interaction in the bone marrow. *Proc Natl Acad Sci U S A.* 2007;104(12):5091-5096.

26. Egorov MV, Capestrano M, Vorontsova OA, Di Pentima A, Egorova AV, Mariggiò S, Ayala MI, Tetè S, Gorski JL, Luini A, Buccione R, Polishchuk RS. Faciogenital Dysplasia protein (Fgd1) regulates export of cargo proteins from the Golgi complex via Cdc42 activation. *Mol Biol Cell.* 2009;20(9):2413-2427.

27. Kang JS, Bae GU, Yi MJ, Yang YJ, Oh JE, Takaesu G, Zhou YT, Low BC, Krauss RS. A Cdo-Bnip-2-Cdc42 signalling pathway regulates p38alpha/beta-MAPK activity and myogenic differentiation. *J Cell Biol.* 2008;182(3):497-507.

# Chapter 8

## Tnfaip8l1 promotes angiogenesis by inhibition of endothelial cell apoptosis

D. Tempel, R.A. Haasdijk, F.L. Bos, D.M.A. Hermkens
P.E. Bürgisser, J.C. Sluimer, L. Bosman, E.A.L. Biessen
C. Cheng, S. Schulte-Merker, H.J. Duckers

## *Abstract*

**Objective** - During the initial phase of angiogenesis, proliferating endothelial cells (EC) are highly susceptible to apoptosis and need rescuing by biological anti-apoptotic cues to ensure neovasculature survival. Although the molecular mechanisms that govern the formation of a vascular network have been studied intensively, specific angiogenic factors that regulate EC apoptosis still need to be further identified.

**Methods and Results** - Using a transcriptomics approach to identify new regulators of angiogenesis, we identified Tumour necrosis factor alpha inducible protein like 1 (Tnfaip8l1), a gene of hitherto unknown function that was highly expressed in ECs. Vascular Tnfaip8l1 expression was predominantly restricted to angioblasts and adult ECs in mice and developing zebrafish. Gain- and loss-of-function assays *in vitro* and *in vivo* indicated that Tnfaip8l1 is involved in vascular development by inhibition of death effector domain-containing receptor-mediated apoptosis in ECs. Tnfaip8l1 proved to quench the activation of caspase 3 by inhibition of caspase 8 activity, leading to enhanced EC survival and vascular growth. EC and vasculature survival is crucial for safeguarding cardiac function after an ischemic insult. We demonstrate that the endothelial expression of Tnfaip8l1 was strongly increased after a myocardial infarction (MI), which suggests a role for Tnfaip8l1 in the neovascularisation response after MI.

**Conclusion** - Here, we present Tnfaip8l1 as a new regulator of EC survival during vascular growth-associated apoptosis and ischemic disease.

## Introduction

Survival of a newly formed or a fully established vascular network is highly dependent on external biological stimuli, which include secreted growth and chemotactic factors and the composition of microenvironment components that make up the supporting extracellular matrix. Cell apoptosis is commonly observed in fast expanding cell populations and during embryonic development. The dynamics of biological cues alternate from those that promote growth and expansion - such as VEGF-A and FGF - to those that promote vascular waning by active induction of apoptosis - such as FASL and TNFα.[1] A delicate balance between these pro-angiogenic and anti-angiogenic factors generally protects endothelial cells (EC) against apoptosis during vascular development, and ensures survival of selective neovessels for further maturation into a functional vascular network.[2] In addition, increasing evidence suggests that EC apoptosis may actively counteract neovascular growth.[3,4] In vascular-related pathology, EC apoptosis often contributes to disease progression. For example, in atherosclerosis, loss of the endothelium in the cap region of atherosclerotic lesions triggers atherothrombosis[5], while in early myocardial infarction (MI) response, active protection of ECs against apoptosis is crucial for fast recovery of the myocardium.[6,7] In contrast, disease progression in cancer may be held back by an effective decline in blood flow due to EC apoptosis and subsequent vascular degradation. Although the importance of EC apoptosis is clearly demonstrated by earlier reports, the molecular regulators that orchestrate EC and thus vascular network survival remain to be determined. Here, we describe the function of a new gene with specific endothelial expression and potent anti-apoptotic activity.

Previously, we studied the expression profile of Flk1-positive angioblasts in embryos during different days of murine embryonic development.[8] We found that Tumour necrosis factor alpha inducible protein like 1 (Tnfaip8l1) is one of the ~2,000 genes that were > 1.90 fold upregulated in Flk1-positive angioblasts compared with Flk1-negative cells. Tnfaip8l1 is a member of the Tnfaip8 subfamily, which includes Tnfaip8l1, Tnfaip8l2, Tnfaip8l3 and Tnfaip8.[9] All family members contain a death effector domain (DED)-like domain homologous to DED II of Fas-associated death domain-like interleukin-1b-converting enzyme (FLICE/caspase 8)-inhibitory proteins (FLIP). DEDs are commonly found in proteins that regulate or mediate the process of apoptosis.[10] FLIPs block death domain-containing receptor-DEDs, thereby interfering with the activation of caspase 8.[11,12] Unlike FLIPs, Tnfaip8 inhibits apoptosis by inhibiting caspase 8 activity and caspase 3 activation in cells *in vitro*.[13,14] Tnfaip8l2 has been shown to bind to caspase 8 and influence its activity in immune cells.[15] However, the function of Tnfaip8l1, and more specifically its role in ECs, is currently unknown. Given the specific expression of Tnfaip8l1 in Flk1-positive angioblasts during vascular development, we sought to define the potential role of Tnfaip8l1 within the process of vascularisation.

Here, we demonstrate that Tnfaip8l1 is specifically expressed in the zebrafish and mouse vasculature during embryonic development, but also in adult ECs. Tnfaip8l1 overexpression reduced endothelial apoptosis and promoted vascular network formation *in vitro* and *in vivo*. Vice Versa, knockdown of Tnfaip8l1 by short hairpin RNA (shRNA) lentivirus infection resulted in enhanced endothelial apoptosis and diminished network formation *in vitro* and *in vivo*. Further studies *in vitro* showed that Tnfaip8l1 inhibited TNFα and FasL-induced endothelial apoptosis, by inhibiting the activation of caspase 3 by reducing the activity of cleaved caspase 8 *in vitro*. Furthermore, after a MI - a condition in which EC survival and high levels of TNFα play a crucial role in cardiac protection - the endothelial expression of Tnfaip8l1 strongly increased, suggesting a role for Tnfaip8l1 in the repair mechanism after MI.

Taken together, these data indicate that Tnfaip8l1 functions as a pro-angiogenic factor by enhancing EC survival during vascular development and after an ischemic event. Considering its potent anti-apoptotic nature, Tnfaip8l1 might be an interesting target for the development of therapeutic agents for the protection of the degradation sensitive (neo)vasculature in vascular disease or during the treatment of cancer.


## *Methods*

A more detailed description of materials and methods is available in the Data Supplement (*online*). Summarised descriptions of the different techniques used in this study are supplied below.


**Animals**

All experiments were carried out in accordance with the Council of Europe Convention (ETS123)/Directive (86/609/EEC) for the protection of vertebrate animals used for experimental and other scientific purposes and with the approval of the National and Local Animal Care Committee. C57BL/6J mice were obtained from The Jackson Laboratory (Bar Harbor, USA), and maintained and bred under standard laboratory conditions. Wild-type zebrafish and the transgenic zebrafish line Tg(Fli1:eGFP)[y1] were kept and bred under standard laboratory conditions.


**Isolation of Flk1-positive angioblasts from murine embryos**

Developing mouse embryos were collected at different days during development. After proteolytic dissociation of the embryos, the single cell suspensions were incubated with PE-conjugated anti-mouse Flk1 antibody 1:50 (555308; BD, Breda, The Netherlands) and Hoechst (Sigma-Aldrich, Zwijndrecht, The Netherlands). Cell suspensions were sorted for

> 90% purity for Flk1-positive/Hoechst-negative cells using a BD FACSCanto[TM] cell-sorter (Breda, The Netherlands). Flk1-negative/Hoechst-negative cells served as a control.

## Zebrafish whole-mount *in situ* hybridisation and morpholino injection

Template DNA for *in situ* probe generation was obtained by direct amplification of target genes from genomic DNA. Primers for probe generation were designed to span exons of at least 250 base pairs in size to ensure probe specificity. Reverse primers were tagged with a T3 RNA polymerase promotor tail to allow direct *in vitro* transcription and generation of antisense probes after PCR purification. Primer sequences used were: 5'-CTC TAG TTT GGA GGG CAA TAG-3' (forward) and 5'-AAT AAG GCA CGA GAT CTT CC-3' (reverse) (Biolegio, Nijmegen, The Netherlands). Antisense RNA probes were labelled with a digoxigenin RNA Labeling Mix from Roche (Woerden, The Netherlands). Whole-mount *in situ* hybridisation was carried out as previously described.[16] Coarse *in situ* transcript detection was automated using the Intavis AG *in situ* robot followed by manual *in situ* transcript detection to increase the signal to noise ratio.

Morpholinos (MO) (Gene Tools, Philomath, USA) were diluted in Milli-Q water containing 0.2% phenol red. One cell stage embryos were injected with different dosages of MO as described previously.[17] MO sequences used were: 5'-TGG TGC TGA ACG AGT CCA TGA TGG TC-3' for the MO Tnfaip8l1-ATG, 5'-CTT GTA TCC GGT TCA AAT GGG G-3' for the MO Tnfaip8l1-UTR and 5'-CTC TTA CCT CAG TTA CAA TTT ATA-3' for the MO control.

Zebrafish embryos were mounted in 1% low melting point agarose in a culture dish with a cover slip replacing the bottom. Imaging was carried out with a Leica Microsystems SP5 confocal microscope using a 10x, 20x or 40x objective with digital zoom. Angiography was carried out as previously described.[18]

## Mouse model of retina vascularisation

Two-day old C57BL/6J mice pups were anesthetised by placement on ice. Either 1 µl of adenovirus expressing murine Tnfaip8l1 ($5x10^7$ pfu) or 1 µl Tnfaip8l1 targeting siRNA (1.33 µg/µl) (Thermo Fisher Scientific, Breda, The Netherlands) was injected into the left eye using a 33-Gauge needle (World Precision Instruments, Berlin, Germany). As a control either 1 µl of sham virus ($5x10^7$ pfu) or 1 µl scrambled non-targeting siRNA (1.33 µg/µl) (Thermo Fisher Scientific, Breda, The Netherlands) was injected into the right eye. Mice pups were killed five days after intra-ocular injection and eyes were enucleated. Retinas were stained with Alexa Fluor® 488-conjugated isolectin GS-IB$_4$ 1:200 (I21411; Invitrogen, Bleiswijk, The Netherlands) before microscopic assessment. Four different regions per retina were used to analyse the newly formed vasculature. Adequate transgene-expression was validated by qPCR analysis.

For the TUNEL assay, retinas were briefly fixed in 4% PFA, embedded in paraffin and cut longitudinally into 5 μm sections. Sections were dehydrated and labelled using a TUNEL staining kit (CardioTACS *In Situ* Apoptosis Detection Kit, R&D systems, Abingdon, UK) according to the instruction manual, followed by counterstaining with nuclear fast red. TUNEL positive cells were quantified using a commercial image analysis system (Clemex Technologies, Longueuil, Canada).

### *In vitro* analysis of Tnfaip8l1 in HUVEC

Primary cultures of human umbilical vein endothelial cells (HUVEC) were cultured in EBM®-2 medium supplemented with a commercial BulletKit (Lonza, Breda, The Netherlands) under normoxic conditions (21% $O_2$). Passages three and five were used throughout the study. HUVECs were infected using either a lentivirus encoding shRNA targeting human Tnfaip8l1, a lentivirus expressing human Tnfaip8l1 or a sham lentivirus in culture medium supplemented with 10 μg/ml diethylaminoethyl (DEAE)-dextran at $37^{o}C$. After 72 hours gene and protein expressions were verified by qPCR and Western blot analysis as described below. To induce apoptosis HUVECs were stimulated with TNFα (10 ng/ml) (BD, Breda, The Netherlands) or FasL (1 ng/ml) (Sigma-Aldrich, Zwijndrecht, The Netherlands) for 8 hours.

### 2D matrigel network-formation assay

*In vitro* network-formation was studied on BioCoat Matrigel tissue culture plates (BD, Breda, The Netherlands). 72 hours after lentiviral infection, HUVECs were plated at 30,000 cells/well in 96-well plates pre-coated with a solution of Matrigel basement membrane matrix. After 18 hours of incubation at 37°C, cells were visualised by Calcein-AM uptake (BD, Breda, The Netherlands). Network-formation was examined using an inverted fluorescence microscope and the photographs were subsequently analysed using Angiosys Image Analysis Software 1.0 (TCS CellWorks, Buckingham, UK). 4,6-diamidino-2-phenylindole (DAPI) in Vectashield® mounting medium (H-1200; Vector Laboratories, Burlingame, USA) was added to assess the cell number after 18 hours.

### Apoptosis and cell cycle assay

For the apoptosis analysis, cells were harvested 72 hours after infection, stained for Annexin V and propidium iodide (PI) signals using an Annexin V Apoptosis Detection Kit (BD, Breda, The Netherlands), followed by analysis of the samples by flow cytometry on a BD FACSCanto™ (Breda, The Netherlands).

For the cell cycle analysis, HUVECs were harvested and fixed in 70% ethanol/phosphate-buffered saline (PBS) for 24 hours at $4^{o}C$, stained with PI and analysed by flow cytometry on a BD FACSCanto™ (Breda, The Netherlands).

**Caspase 8 activity assay**

Caspase 8 activity in infected HUVECs was assessed with a commercial Caspase 8 (Colorimetric) Assay Kit (Abcam, Cambridge, UK), according to the instruction manual.

Briefly, HUVECs were harvested and lysed with the supplied lysis buffer. Protein concentration was determined by a colorimetric protein assay, followed by optical spectroscopy (Bio-Rad, Veenendaal, The Netherlands). After addition of DTT and IETD-$p$NA substrate, 200 µg of protein was incubated at $37^{o}$C for 2 hours. Samples were spectrophotometrically read at 405 nm.

**Immunohistology of embryos and heart samples**

Murine embryos at embryonic day (E)12.5 and murine heart samples - with or without MI - were embedded in paraffin and cut longitudinally into 5 µm sections. The sections were rehydrated and incubated with FITC-conjugated lectin GS (Sigma-Aldrich, Zwijndrecht, The Netherlands) and Tnfaip8l1 (Santa Cruz Biotechnology, Heidelberg, Germany) in 5% bovine serum albumin (BSA)/PBS for 90 minutes at room temperature. Sections were washed in PBS and incubated for 30 minutes with an Alexa Fluor$^{®}$ 546-conjugated donkey anti-goat IgG (Invitrogen, Bleiswijk, The Netherlands). After washing, sections were cover slipped with DAPI in Vectashield$^{®}$ mounting medium (H-1200; Vector Laboratories, Burlingame, USA). Data analysis was carried out using a commercial image analysis system (Clemex Technologies, Longueuil, Canada).

Human heart samples - with or without MI - were collected and processed by the Experimental Vascular Pathology group (Maastricht UMC+, The Netherlands). The paraffin sections were rehydrated and incubated with goat anti-human Tnfaip8l1 (Santa Cruz Biotechnology, Heidelberg, Germany) in 5% BSA/PBS o/n at $4^{o}$C. Sections were washed in PBS and incubated for 90 minutes with Alexa Fluor$^{®}$ 546 donkey anti-goat IgG (Invitrogen, Bleiswijk, The Netherlands). After washing, sections were mounted with Vectashield$^{®}$ hard-set mounting media (Vector Laboratories, Burlingame, USA).

**Statistical analysis**

Data were analysed by one-way ANOVA, as appropriate, followed by individual unpaired Student's *t*-test. Significance was accepted at $P < 0.05$ (* $P < 0.05$, ** $P < 0.01$ in the figures). All data are presented as mean ± standard error of the mean (SEM), unless otherwise stated.

# *Results*

**Tnfaip8l1 expression during development in mice and zebrafish and in the adult murine vasculature**

To evaluate the expression of Tnfaip8l1, we compared Flk1-positive angioblasts to the Flk1-negative background during embryonic murine development by qPCR analysis. Tnfaip8l1 was higher expressed in Flk1-positive angioblasts compared with the Flk1-negative background from 8 to 16 days post-fertilisation (dpf) (Figure 1A). Vascular expression of Tnfaip8l1 was also validated in developing zebrafish larvae by whole-mount *in situ* hybridisation. Tnfaip8l1 was detected in the dorsal aorta, intersegmental vessels (ISV) and the pro-nephric duct (Figure 1B).
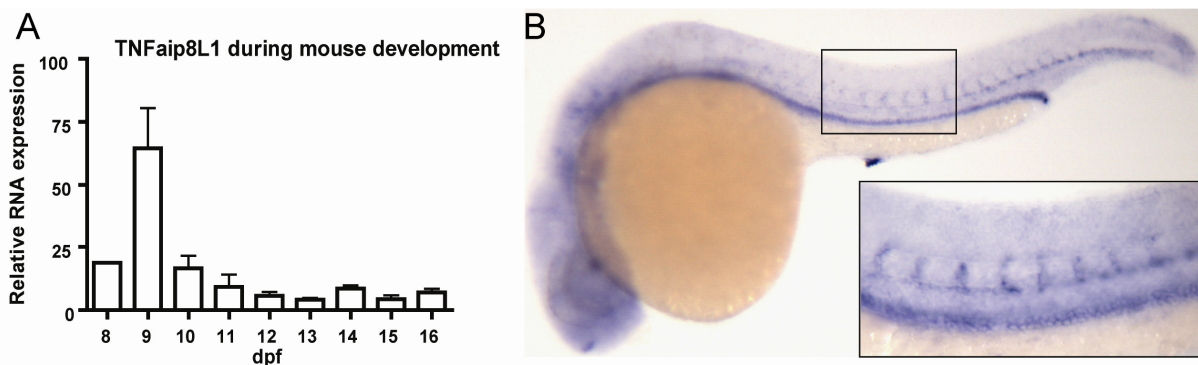


**Figure 1. Tnfaip8l1 expression during development in mice and zebrafish and in the adult murine vasculature.** (**A**) Tnfaip8l1 mRNA expression in Flk1-positive cells during mouse development. (**B**) Global whole-mount *in situ* expression profiles for Tnfaip8l1 shows apparent vascular expression patterns at 24-28 hours post-fertilisation.

The endothelial expression was further confirmed by immunohistological analysis of a 12.5 dpf murine embryo. Tnfaip8l1 protein expression was identified in the vasculature of a developing embryo (Figure 1C). Tnfaip8l1 protein expression was also observed in the blood vessels in the heart of a adult mouse (Figure 1D). This finding was further supported by different primary cells isolated by laser dissection from adult murine hearts. Tnfaip8l1 expression in ECs was at least 1.75 higher compared with other vascular cell types, including smooth muscle cells (SMC), cardiomyocytes and fibroblasts (Supplemental figure 1A, *online*). Strikingly, RNA analysis of other Tnfaip8 family members - Tnfaip8 and Tnfaip8l2 - did not show a similar endothelial expression pattern as observed for Tnfaip8l1 (Supplemental figure 1B, C, *online*). These data demonstrate that Tnfaip8l1 is predominantly expressed in vascular ECs in zebrafish and mice.
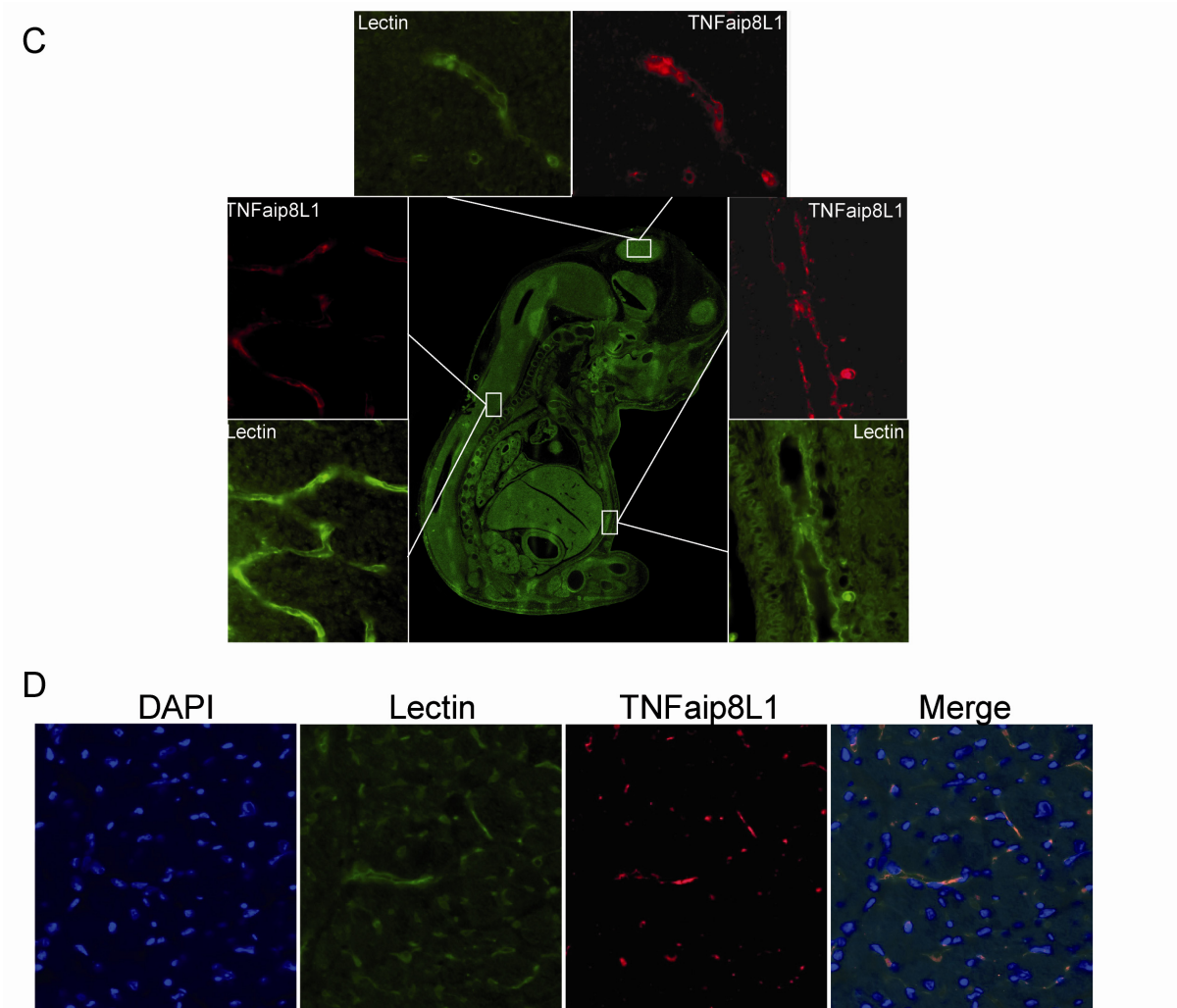
(**C**) Immunohistological example of a 12.5 dpf mouse embryo, showing co-localisation between lectin (green) and Tnfaip8l1 (red). (**D**) Immunohistological example of an adult mouse heart, showing endothelial specific expression of Tnfaip8l1 by a double staining of lectin and Tnfaip8l1.

## Tnfaip8l1 enhances network-formation *in vitro*

The angiogenic effect of Tnfaip8l1 was assessed *in vitro*, using the well established network-formation assay in Matrigel. Using a lentivirus - encoding a shRNA targeting human Tnfaip8l1 - we were able to inhibit gene and protein expression in HUVECs by 48% and 61%, respectively, compared with a sham lentivirus (Figure 2A-C). Overexpression of Tnfaip8l1 was studied by infection with a lentivirus - containing the full-length cDNA of human Tnfaip8l1. Lentiviral infection of the Tnfaip8l1 cDNA construct increased the gene and protein expression of Tnfaip8l1 by 121% and 68%, respectively, compared with a sham lentivirus (Figure 2A-C). In contrast, neither knockdown, nor overexpression of Tnfaip8l1 in HUVECs affected the gene expression of its family members - Tnfaip8 and Tnfaip8l2 (Figure 2D, E). Interestingly, also neither knockdown, nor overexpression of Tnfaip8l1 in

HUVECs affected the expression of VEGFR-2, which was previously reported for its family member Tnfaip8 (Figure 2F).
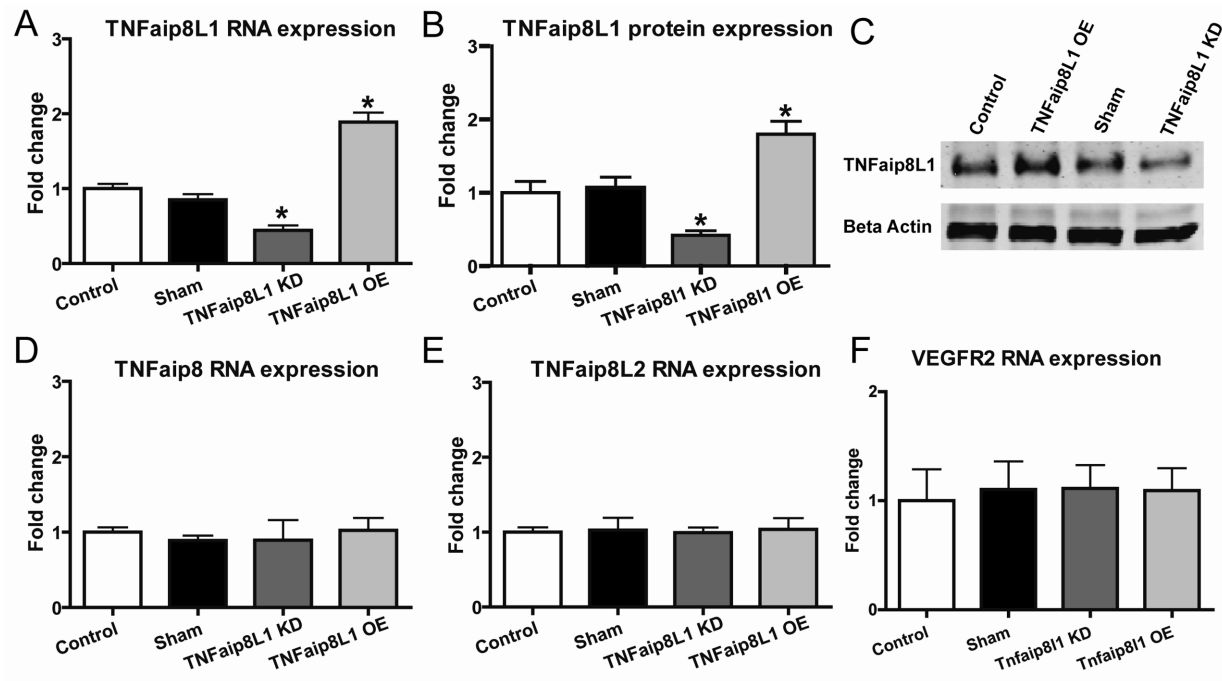


**Figure 2. Tnfaip8l1 enhances network-formation *in vitro*.** Tnfaip8l1 (**A**) mRNA and (**B, C**) protein expression in HUVECs was reduced after infection with a lentivirus encoding a Tnfaip8l1 targeting shRNA construct, without affecting the mRNA expression of its genetic family members: (**D**) Tnfaip8, (**E**) Tnfaip8l2 and (**F**) VEGFR-2. Tnfaip8l1 overexpression in HUVECs with a lentivirus containing the full-length cDNA of human Tnfaip8l1 resulted in an increase of Tnfaip8l1 (**A**) mRNA and (**B, C**) protein, without changes in mRNA expression levels of its direct family members: (**D**) Tnfaip8, (**E**) Tnfaip8l2, and (**F**) VEGFR-2.

In the 2D matrigel network-formation assay, knockdown of Tnfaip8l1 diminished the number of tubules and junctions of sprouting cells by 43% and 41%, respectively, compared with sham transfected HUVECs (Figure 2G-I). In addition, overexpression of Tnfaip8l1 enhanced the number of tubules and junctions by 1.46 and 1.41 fold, respectively, compared with sham infected HUVECs (Figure 2G-I). Nuclear staining with DAPI observed a difference in cell number after 18 hours of network-formation (Supplemental figure 2, *online*). Network-formations with Tnfaip8l1 knockdown showed a reduction in the number of cells, as seen by the reduction of nuclei. In contrast, overexpression of Tnfaip8l1 showed a higher number of cells compared with control and sham conditions. These findings provide evidence for a pro-angiogenic function of Tnfaip8l1.
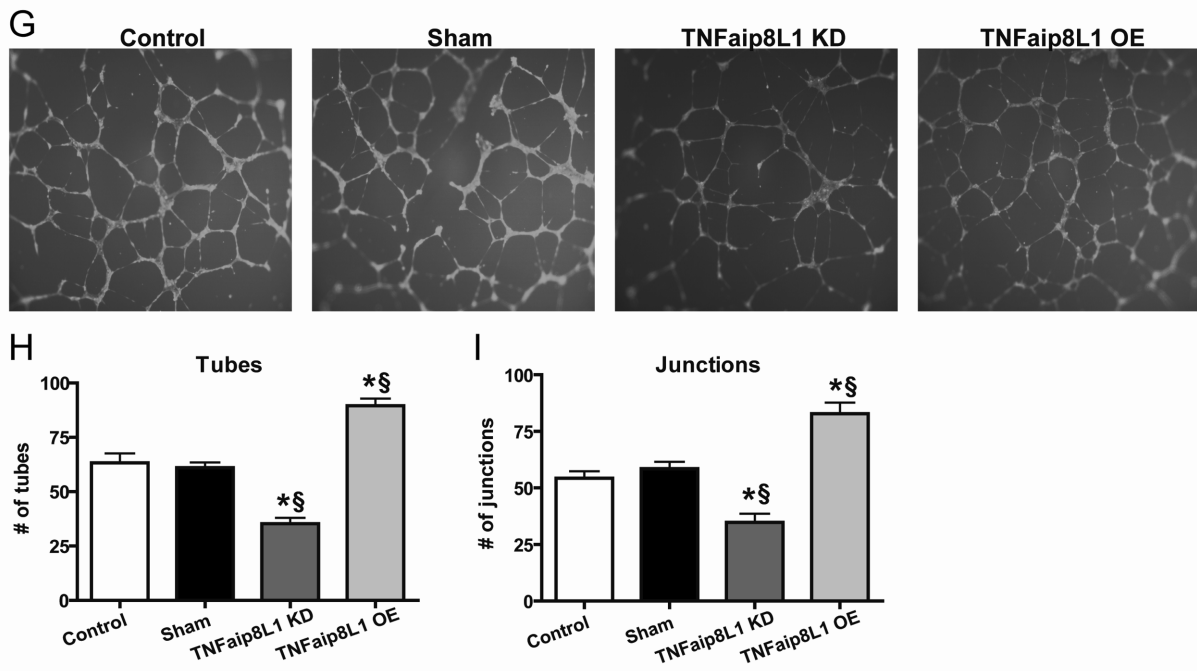
(**G**) Lentiviral infected HUVECs were cultured in a 2D matrigel to induce network-formation. Tubules were visualised by Calcein-AM dye fluorescence and were subsequently assessed by fluorescence microscopy. Knockdown of Tnfaip8l1 showed a decrease in angiogenic capacity of HUVECs as indicated by a decrease in (**H**) number of tubules and (**I**) number of junctions. (**H, I**) In contrast, Tnfaip8l1 overexpression increased the angiogenic capacity of HUVECs (n = 4 for each group; * $P < 0.05$ versus control, § $P < 0.05$ versus sham).

## Tnfaip8l1 enhances *in vivo* endothelial sprouting in zebrafish larvae and the murine retina

Next, we addressed the *in vivo* function of Tnfaip8l1 in the developing vasculature of zebrafish larvae. We used an ATG and UTR MO that silenced the zebrafish orthologue of Tnfaip8l1. Tg(Fli1:eGFP)[y1] zebrafish larvae were injected with either the ATG or UTR MO. Both Tnfaip8l1 targeting MOs diminished the formation of ISVs (Figure 3A, C). Angiographies at 2.5 dpf in Tnfaip8l1-silenced zebrafish larvae confirmed the absence of functional ISVs, indicated by the lack of luminal flow (Figure 3B).

Furthermore, the effect of Tnfaip8l1 was also assessed during postnatal angiogenesis in the murine retina model. Tnfaip8l1 knockdown in retinas from mice pups - using targeting siRNA - reduced Tnfaip8l1 mRNA expression levels by 68% compared with scrambled non-targeting siRNA transfected controls (Figure 3D). Overexpression *in vivo* was assessed using adenovirus - containing the full-length cDNA of murine Tnfaip8l1. Tnfaip8l1 expression was increased 1.8 fold after adenoviral injections compared with sham adenoviral injections (Figure 3D). Neither knockdown, nor overexpression of Tnfaip8l1 affected the mRNA expression of Tnfaip8 and Tnfaip8l2 in murine retinas as verified by qPCR analysis (Figure 3E, F). Evaluation of the retina vasculature by whole-mount

isolectin GS-IB$_4$ staining showed a reduction of the vascular network upon Tnfaip8l1 silencing compared with scrambled non-targeting siRNA (Figure 3G). In contrast, overexpression of Tnfaip8l1 in the retina resulted in increased vascular network-formation compared with sham adenoviral infection (Figure 3G). Combined, these *in vivo* data clearly demonstrate that Tnfaip8l1 plays a vital role in angiogenesis.
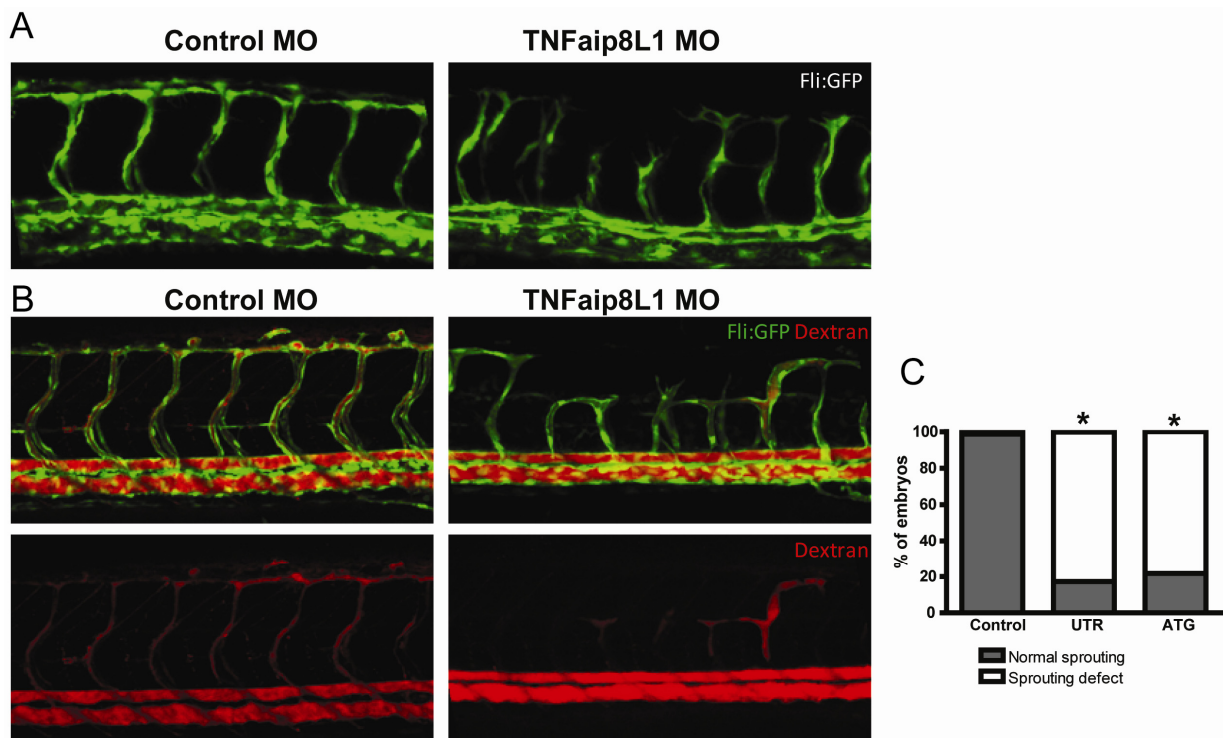


**Figure 3. Tnfaip8l1 enhances *in vivo* endothelial sprouting in zebrafish larvae and the murine retina.** (**A**) Confocal analysis of Tg(Fli1:eGFP)^s843 zebrafish larvae at 1 dpf showed normal development of the vasculature in uninjected larvae. Tnfaip8l1 larvae displayed normal development of the major blood vessels, but had abnormally formed ISVs. (**B**) Angiographies at 2.5 dpf in Tnfaip8l1-silenced zebrafish larvae demonstrated normal flow in the vasculature with the exception of the lacking ISVs. Abnormally formed ISVs still showed some perfusion. (**C**) Quantification of zebrafish larvae with normal or abnormal vasculature after morpholino silencing (n = 150 per group; * *P* < 0.05 versus control).
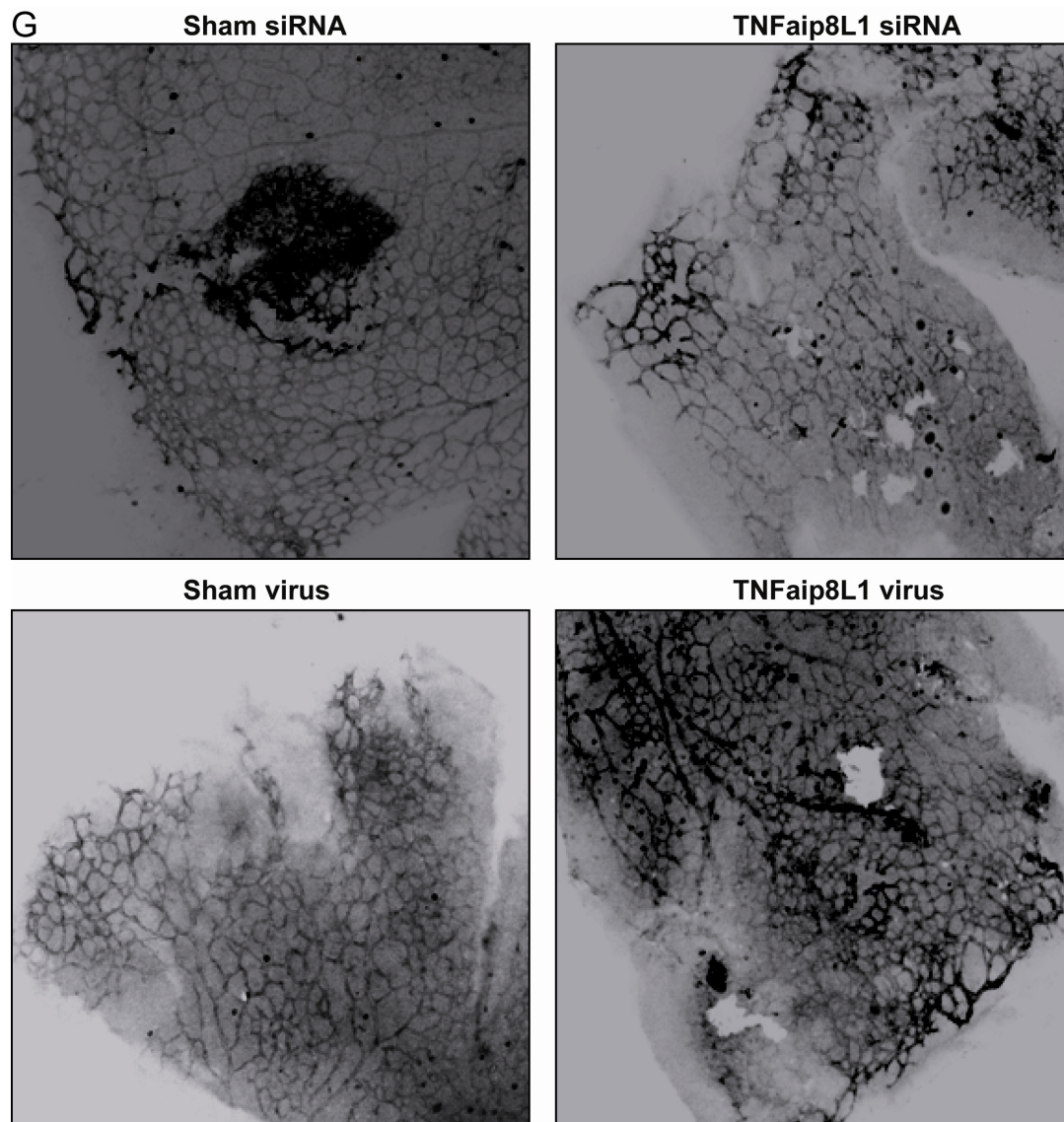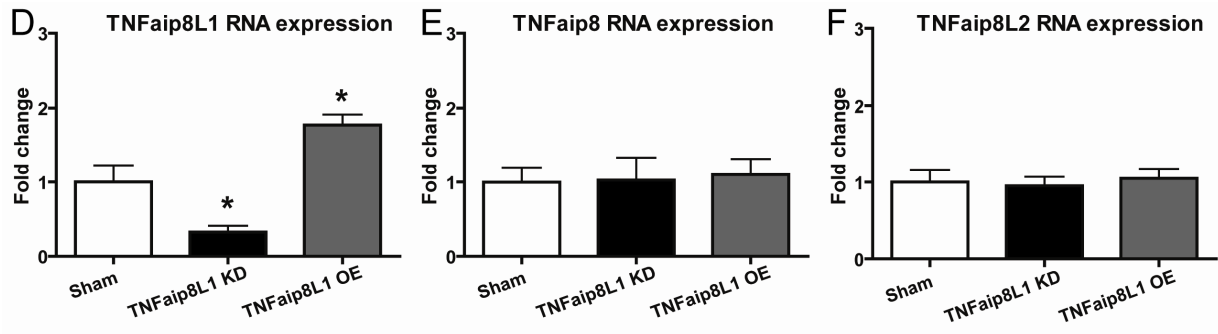
(**D**) Tnfaip8l1 mRNA expression during postnatal retinal vascular development in mice was reduced after transfection with Tnfaip8l1 targeting siRNA, whereas the expression of (**E**) Tnfaip8 and (**F**) Tnfaip8l2 remained unchanged. Adenoviral overexpression of (**D**) Tnfaip8l1 did not affect the expression of (**E**) Tnfaip8 and (**F**) Tnfaip8l2 (n = 5 per group; * $P < 0.05$ versus sham). (**G**) Knockdown of Tnfaip8l1 in the murine retina from day 2 after birth greatly diminished the vascular network at day 7 compared with sham treated retinas. Overexpression of Tnfaip8l1 in these retinas enhanced the complexity of the vascular network.

**Tnfaip8l1 inhibits endothelial cell apoptosis without affecting the cell cycle**

Since Tnfaip8l1 is implicated in angiogenesis, we studied the effects of Tnfaip8l1 on EC specific apoptosis and cell cycle progression. Flow cytometric analysis of apoptosis by Annexin V/PI staining revealed that Tnfaip8l1 knockdown promoted apoptosis in HUVECs under normal growth conditions, resulting in approximately a 2 fold increase of both early and late apoptotic cells in subconfluent cell cultures compared with sham transfected HUVECs (Figure 4A-D). In confluent cell cultures the apoptotic effect of Tnfaip8l1 knockdown was not observed (data not shown). In addition, overexpression of Tnfaip8l1 in subconfluent HUVEC cultures diminished both early and late apoptosis under normal growth conditions compared with sham transfected HUVECs (Figure 4A-D). The different effect on apoptosis found between confluent and subconfluent HUVECs suggested a difference in expression. Using qPCR analysis this idea was confirmed, subconfluent HUVECs showed a higher mRNA expression of Tnfaip8l1 compared with confluent HUVECs (Supplemental figure 3A, *online*). Cell cycle progression of HUVECs was assessed by PI flow cytometric analysis. Neither knockdown, nor overexpression affected cell cycle progression in cultured HUVECs (Figure 4E-G).
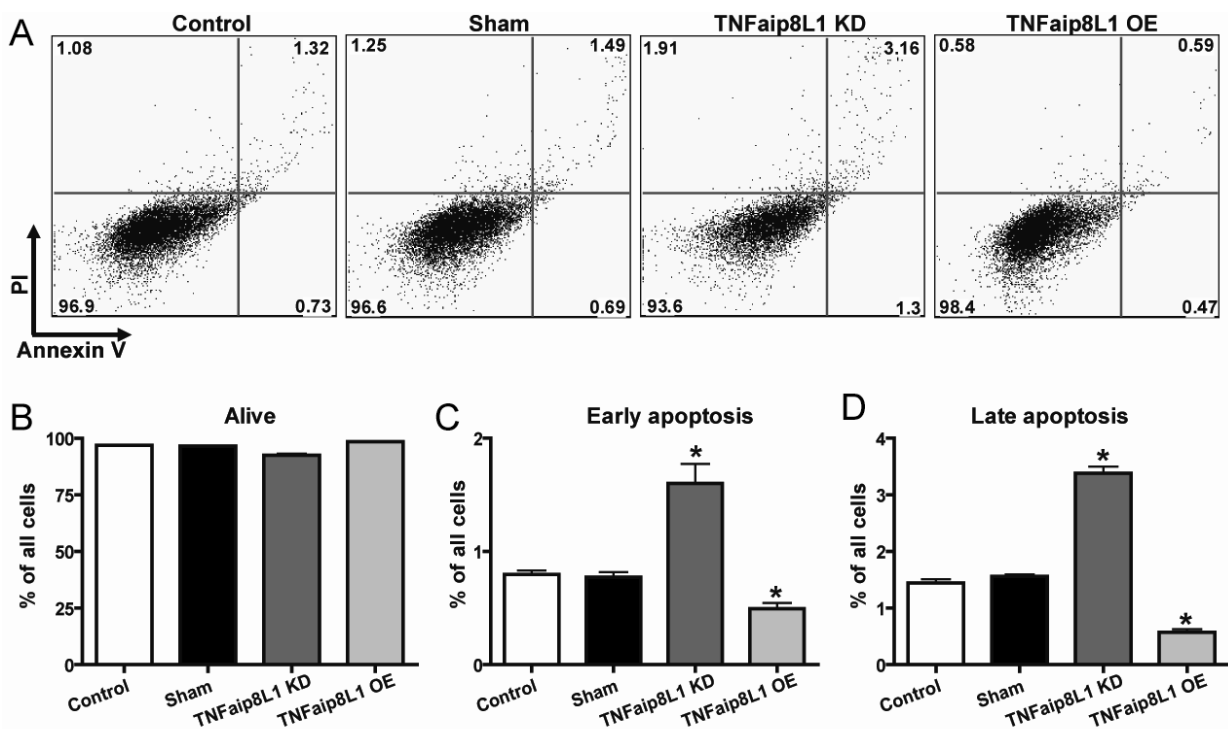


**Figure 4. Tnfaip8l1 inhibits endothelial cell apoptosis without affecting the cell cycle.** (**A**) Representative flow cytometric analysis of apoptosis in HUVECs 5 days after lentiviral infection. Knockdown of Tnfaip8l1 enhanced apoptosis of HUVECs under normal culture conditions. Apoptosis of HUVECs was diminished by overexpression of Tnfaip8l1. (**B-D**) Quantification of (**B**) living, (**C**) early apoptotic and (**D**) late apoptotic HUVECs (n = 8 per group; * $P < 0.05$ versus naïve).
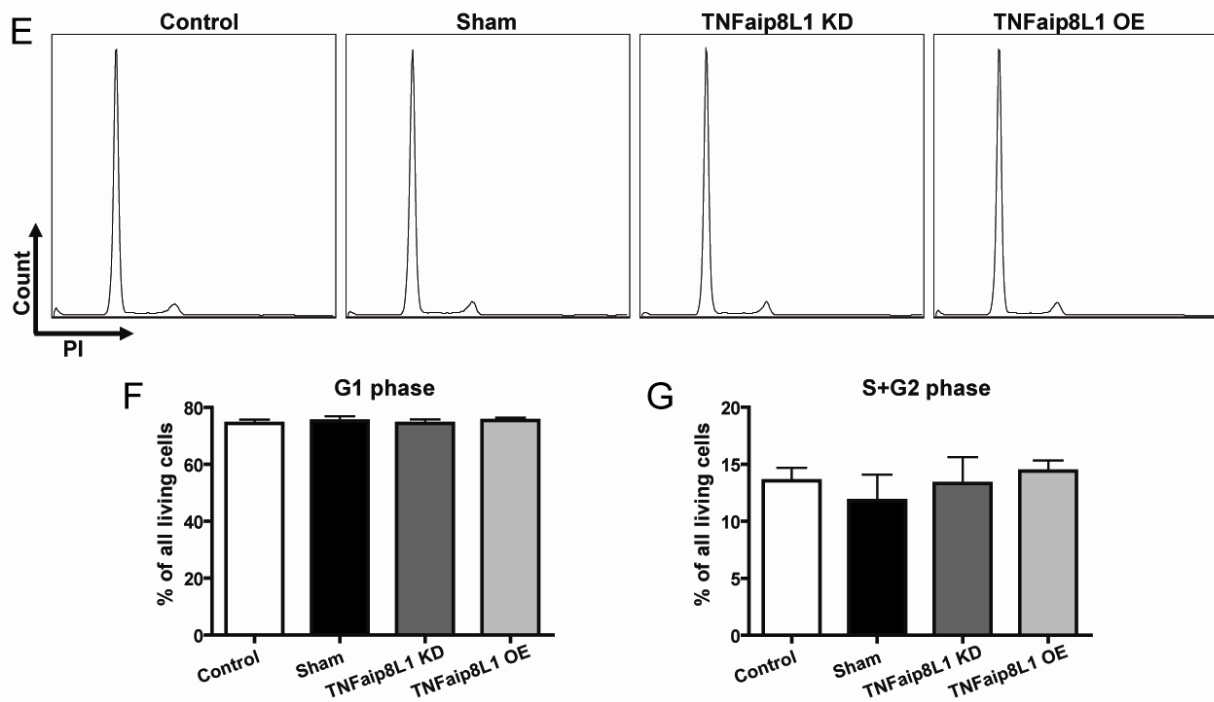
(**E**) Representative flow cytometric analysis of the cell cycle in HUVECs 5 days after lentiviral infection. Knockdown or overexpression of Tnfaip8l1 did not affect the cell cycle in HUVEC. Quantification of the (**F**) G1 and (**G**) combined S–G2-phase after cell cycle analysis in HUVECs (n = 8 per group; * $P < 0.05$ versus naïve).

To evaluate if Tnfaip8l1 is involved in regulating apoptosis during vascular development, we assessed apoptosis in murine retinas using a TUNEL staining. Tnfaip8l1 silencing revealed an increase in the number of TUNEL-positive nuclei compared with scrambled non-targeting siRNA (Figure 5A, B). Vice versa, overexpression of Tnfaip8l1 in the retina resulted in a reduction in apoptotic nuclei compared with sham adenoviral infection (Figure 5A, B). These data suggest that Tnfaip8l1 may aid new vascular growth by providing protection to ECs from apoptosis.
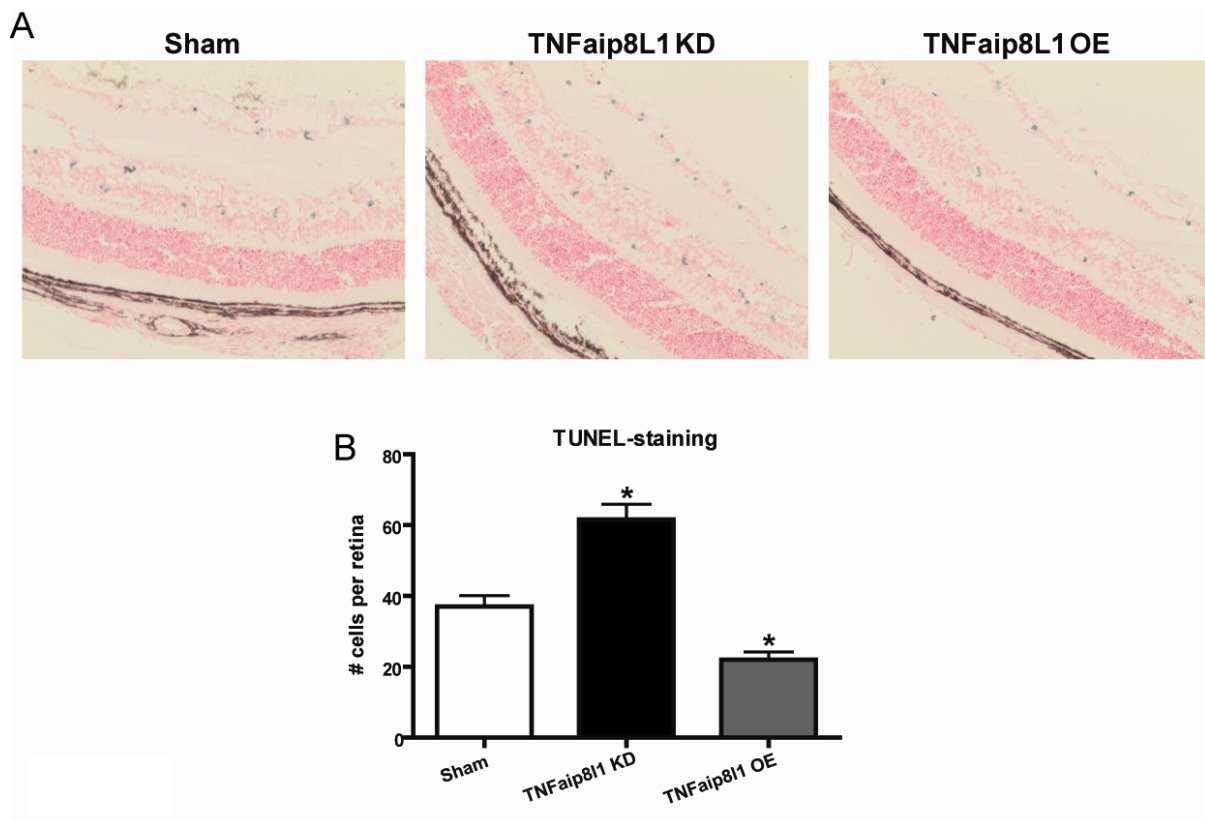
**Figure 5. Tnfaip8l1 inhibits *in vivo* apoptosis in the murine retina.** (**A**) Representative TUNEL staining of retina sections depicting apoptotic cells. Knockdown of Tnfaip8l1 in the murine retina model enhanced the number of apoptotic cells compared with sham treated retinas at day 3 post-injection. Overexpression of Tnfaip8l1 in these retinas reduced the number of TUNEL-positive cells. (**B**) Quantification of TUNEL-positive cells in the retina (n = 5 per group; * $P < 0.05$ versus sham).

## Tnfaip8l1 diminishes TNFα and FasL-induced endothelial apoptosis

Since DED-containing proteins - like the Tnfaip8 family - reduce DED-containing receptor-mediated apoptosis - including TNFα and FasL-mediated apoptosis - we proceeded with an in-depth analysis of Tnfaip8l1 to establish its role in these types of apoptotic signalling. Flow cytometric analysis of apoptosis in subconfluent HUVECs revealed that transgenic expression of Tnfaip8l1 inhibited apoptosis, as shown by a decrease in both early and late apoptotic cells compared with sham transfected HUVECs in response to TNFα (Figure 6A-D) or FasL stimulation (Figure 6E-G). Knockdown of Tnfaip8l1 in combination with TNFα or FasL stimulation further enhanced EC apoptosis, but provided unquantifiable results due to the minimal amount of cells detected. In confluent HUVEC cultures, similar effects were observed after TNFα stimulation, but in a lesser degree than seen in subconfluent HUVECs (Supplemental figure 3B-D, *online*). Combined, these data validate that Tnfaip8l1 plays a crucial role in TNFα and FasL-triggered apoptosis, especially in proliferating ECs.
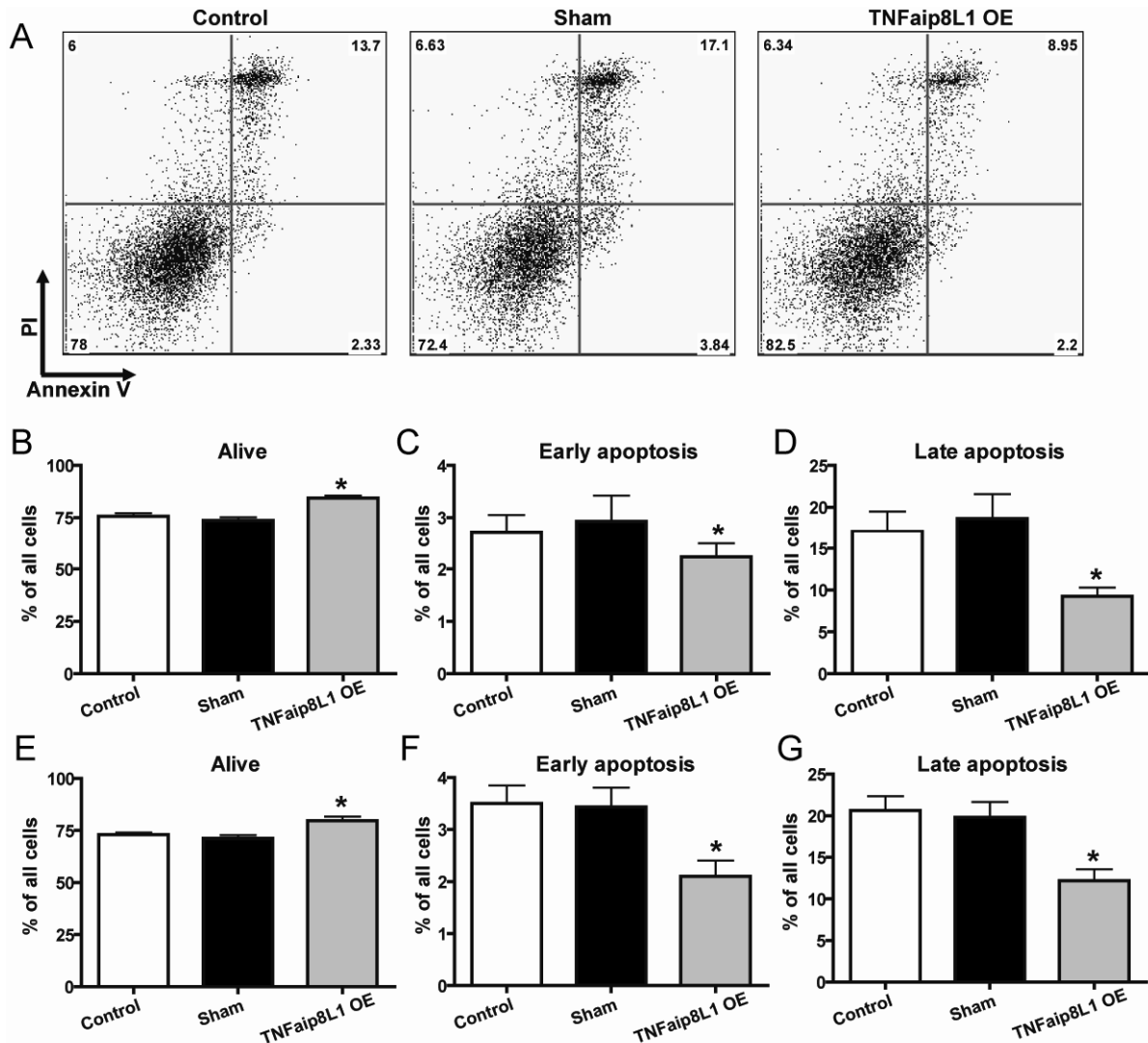
**Figure 6. Tnfaip8l1 diminishes TNFα and FasL-induced endothelial apoptosis.** (**A**) Representative flow cytometric analysis of apoptosis in lentiviral infected HUVECs 8 hours after TNFα stimulation. TNFα-induced apoptosis was reduced in HUVECs with Tnfaip8l1 overexpression. (**B-D**) Quantification of (**B**) living, (**C**) early apoptotic and (**D**) late apoptotic HUVECs after TNFα stimulation of subconfluent cultures (n = 5 per group; * $P <$ 0.05 versus naïve). (**E-G**) Quantification of (**E**) living, (**F**) early apoptotic and (**G**) late apoptotic HUVECs after FasL stimulation of subconfluent cultures (n = 5 per group; * $P <$ 0.05 versus naïve).

## Tnfaip8l1 reduces caspase 8 activity and activated caspase 3 levels

Since a family member of Tnfaip8l1 diminishes DED-containing receptor-mediated apoptosis by inhibiting caspase 8 activity, which subsequently reduces activated caspase 3 levels, we also investigated whether Tnfaip8l1 inhibits caspase 8 activity, influence the amount of caspase 8 and the downstream activated caspase 3. Therefore, we carried out protein expression analysis on TNFα-stimulated HUVEC cultures. Tnfaip8l1 overexpression (as validated by Figure 7A, D) did not affect the level of activated cleaved

caspase 8 (Figure 7B, D). In contrast, cleaved caspase 3 levels were significantly reduced by 59% compared with sham lentivirus treated HUVECs (Figure 7C, D). Next, we measured caspase 8 enzyme activity using an IETD-*p*NA cleavage assay. Transgenic Tnfaip8l1 expression inhibited caspase 8 enzyme activity by 54% compared with sham lentivirus treated HUVECs (Figure 7E). Taken together, these observations clearly indicate that Tnfaip8l1 protects ECs from TNFα-induced apoptosis by directly intervening in the caspase 8 - caspase 3 activation pathway.
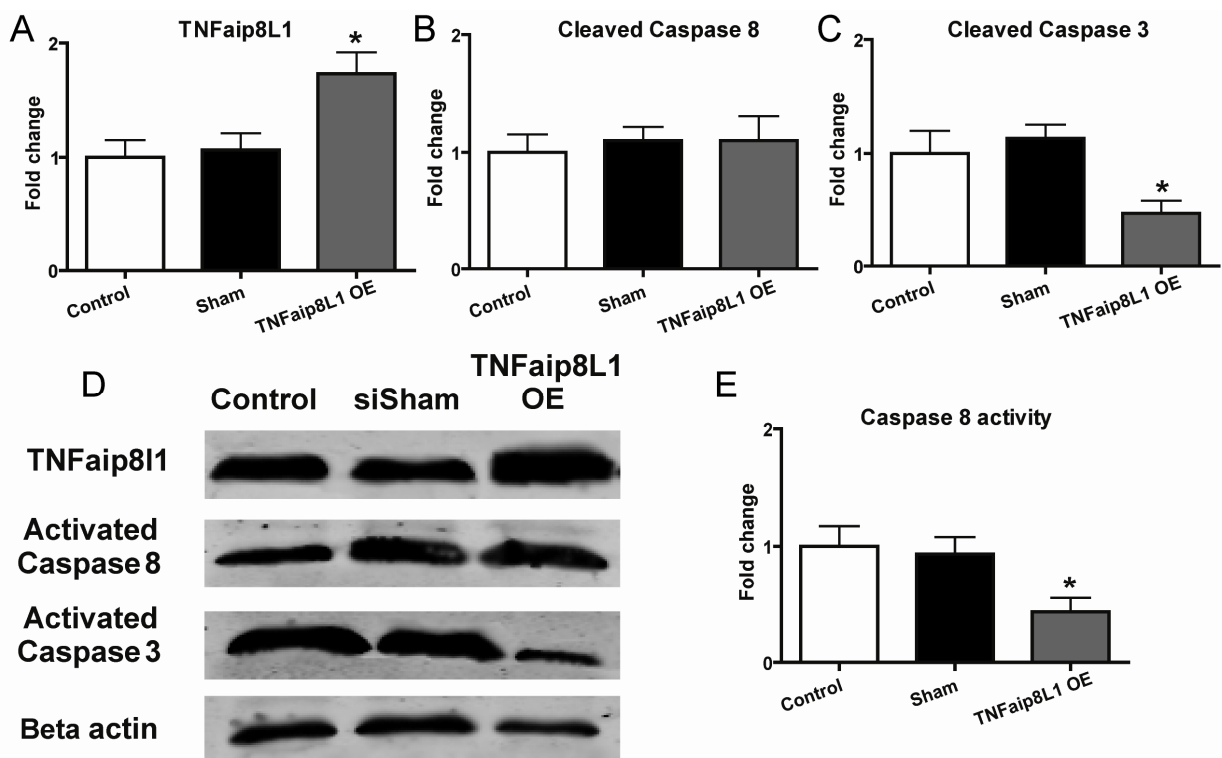


**Figure 7. Tnfaip8l1 reduces caspase 8 activity and activated caspase 3 levels.** (**A**) Protein expression of Tnfaip8l1 is increased after lentiviral overexpression in HUVECs. (**B**) Protein expression of activated caspase 8 is not affected by Tnfaip8l1 overexpression. (**C**) Protein expression of activated caspase 3 is decreased by Tnfaip8l1 overexpression. (**D**) Representative immunoblots of Tnfaip8l1, activated caspase 8 and activated caspase 3 in lentiviral infected HUVECs 8 hours after TNFα stimulation. (**E**) Tnfaip8l1 overexpression diminished caspase 8 activity in lentiviral infected HUVECs 8 hours after TNFα stimulation (n = 5 per group; * $P < 0.05$ versus sham).

**Tnfaip8l1 is upregulated in cardiac endothelial cells after myocardial infarction**

Apoptosis of vascular cells during an ischemic cardiac event plays an important role in the recovery of heart function. Previous studies reported a local rise in TNFα[19] and an increase in cleaved caspase 3 levels[20] after MI, suggesting that regulation by the Tnfaip8 subfamily may be involved. To investigate if Tnfaip8l1 is indeed involved in the initial phase after an MI, we carried out immunohistological analysis of murine cardiac tissue, 2 days after the

induction of an MI. Tnfaip8l1 protein expression was clearly enhanced in the capillaries after an MI compared with sham operated animals (Figure 8A, B). This was further supported by laser capture of the ECs from these hearts, followed by qPCR analysis. Tnfaip8l1 mRNA expression in murine ECs was significantly upregulated 2 days after induction of MI compared with sham operated animals (Supplemental figure 4, *online*), providing an indication that high Tnfaip8l1 levels might be important in this disease.
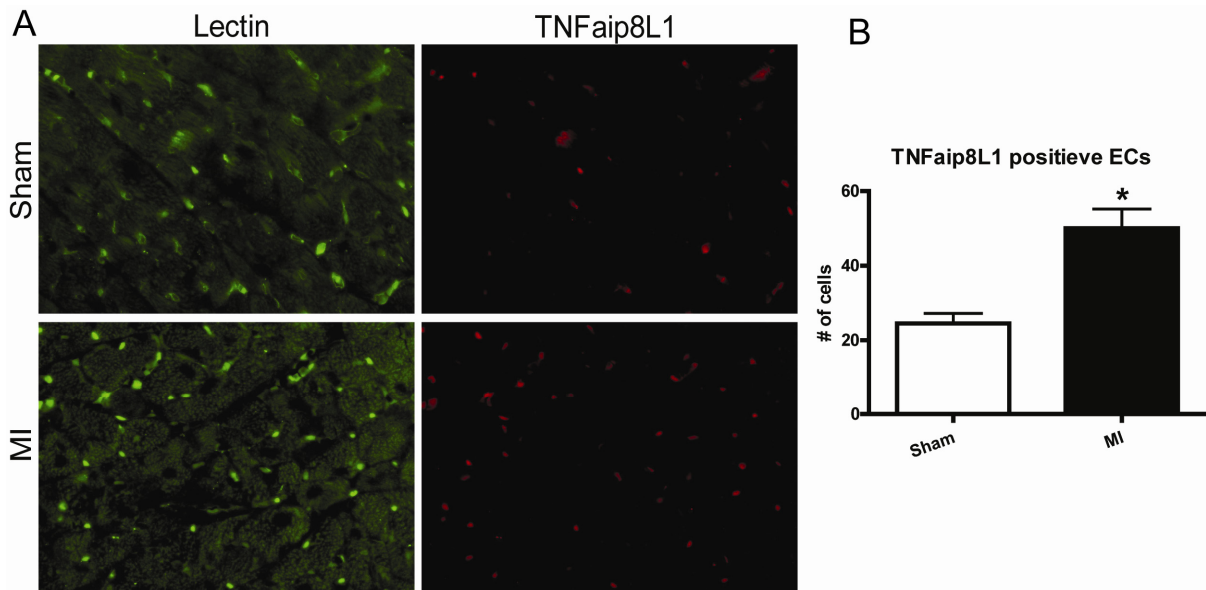


**Figure 8. Tnfaip8l1 is upregulated in cardiac endothelial cells after myocardial infarction.** (**A**) Protein expression of Tnfaip8l1 in murine hearts after MI induction. Endothelial Tnfaip8l1 expression (red) is increased after MI as seen by co-localisation with lectin (green). (**B**) Quantification of Tnfaip8l1 expressing endothelial cells after an MI in murine hearts (n = 5 per group; * $P < 0.05$ versus sham operated animals).

Next, we evaluated if the mouse data would reflect the human condition. We therefore carried out immunohistological evaluation of Tnfaip8l1 expression in human MI samples and revealed that Tnfaip8l1 protein expression was increased after an MI (Figure 8C). Further *in vitro* analysis showed that the endothelial expression of Tnfaip8l1 is not enhanced by hypoxia, but rather by increasing levels of TNFα (Supplemental figure 5A, B, *online*). These data suggest that Tnfaip8l1 is involved in an inflammatory reaction after an human ischemic event and would be a potential target for development of therapeutics.
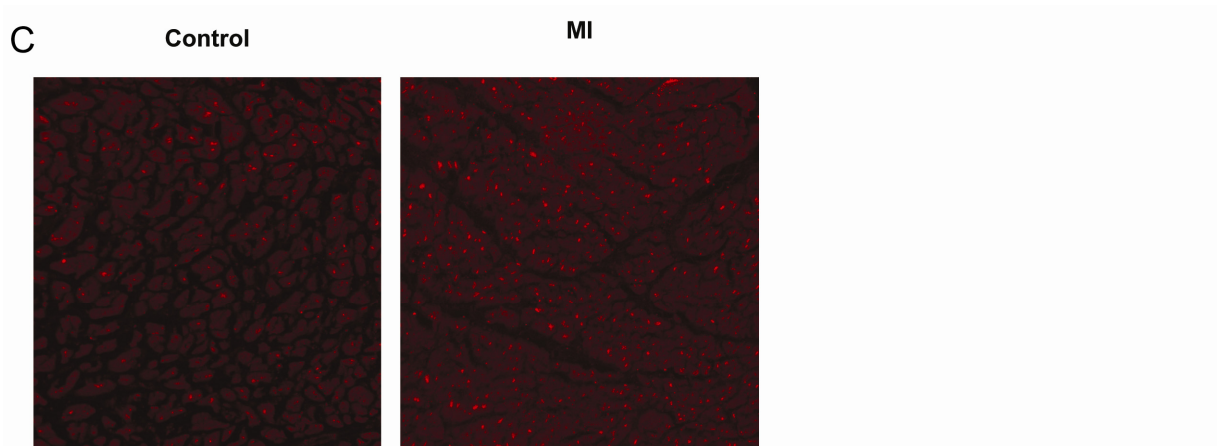
(**C**) Representative cross sections of normal human heart tissue or heart tissue that has suffered an MI. Tnfaip8l1 protein expression is increased after MI in human cardiac tissue (red fluorescence).

## *Discussion*

In the current study, we demonstrate that Tnfaip8l1 stimulates vascularisation by promoting EC survival by inhibition of DED-containing receptor-mediated apoptosis. Our data showed that Tnfaip8l1 is specifically expressed in both embryonic and adult vasculature. Tnfaip8l1 is predominantly expressed in ECs, in contrast to its family members Tnfaip8 and Tnfaip8l2 that show preferential expression in other vascular cell types. Moreover, the vascular expression is preserved in different species. Loss of Tnfaip8l1 inhibited angiogenesis, as indicated by the *in vitro* data obtained from 2D matrigel network-formation assays and the *in vivo* data from the murine retina model and zebrafish larvae development. In contrast, overexpression of Tnfaip8l1 resulted in enhanced angiogenesis in *in vitro* Matrigel cultures and *in vivo* models. The observed effects of Tnfaip8l1 on angiogenesis could be attributed to inhibition of DED-containing receptor-mediated EC apoptosis by inhibition of caspase 8 enzyme activity, resulting in reduced levels of cleaved caspase 3.

We identified Tnfaip8l1 in a screen for new molecular regulators of vascularisation during murine development by gene expression profiling. Although functions of its family members Tnfaip8 and Tnfaip8l2 have been described[13-15], thus far no biological function has yet been attributed to Tnfaip8l1. Our data showed that Tnfaip8l1 is highly expressed in angioblasts and ECs, and is preserved between species, suggesting functional importance in ECs, especially during blood vessel development. This was confirmed by further gain- and loss-of-function studies both *in vitro* and *in vivo* in human ECs, zebrafish larvae and newborn mice pups, demonstrating that the function of Tnfaip8l1 was evolutionary and

functionally preserved. *In vitro* experiments also demonstrated that gain- and loss-of-function of Tnfaip8l1 did not alter the level of its family members Tnfaip8 and Tnfaip8l2, and thus is not compensated by its family members in ECs, excluding possible redundancy. This was further supported by data obtained from studies *in vivo* in which neither knockdown, nor overexpression of Tnfaip8l1 in murine retinas affected the gene expression of family members Tnfaip8 and Tnfaip8l2.

Angiogenesis is dependent on the dynamic balance between pro-angiogenic and anti-angiogenic factors. One essential issue during angiogenesis is EC survival. Actually, many of the known pro-angiogenic and anti-angiogenic factors function at least partly by regulating EC survival and apoptosis.[1,2] Pro-angiogenic growth factors - including VEGF, Ang1 and FGF - are well known for their effect on EC proliferation. However, they also stimulate the expression of anti-apoptotic proteins like survivin, thus inhibiting EC apoptosis.[21-23] Inhibition of VEGF signalling results in enhanced EC apoptosis and reduced angiogenesis.[24] In contrast, anti-angiogenic factor Thrombospondin 1 (TSP1) functions by binding to CD36, activating downstream caspase 3 and enhancing EC apoptosis. Interestingly, the anti-apoptotic effect of TSP1 is restricted to proliferating ECs and was not observed in quiescent ECs, suggesting that proliferating ECs are more sensitive to apoptosis.[25]

In line with these findings, we observed that in non-confluent EC cultures, Tnfaip8l1 knockdown resulted in an increase of apoptotic cells, whereas overexpression of Tnfaip8l1 reduced the apoptosis in HUVECs, suggesting that Tnfaip8l1 has an anti-apoptotic effect in proliferating ECs. Similar to TSP1, we found that Tnfaip8l1 had no effect on apoptosis in confluent cell cultures. This suggests that the anti-apoptotic effect of Tnfaip8l1 may only apply to proliferating ECs. This was further supported by the higher expression of Tnfaip8l1 in proliferating ECs compared with quiescent ECs.

In addition, we found that cell cycle of HUVECs was not altered by Tnfaip8l1 expression, implying that the observed effects were only caused by EC apoptosis and not partially by influencing proliferation. Other investigators have previously reported that knockdown of Tnfaip8 also reduced viability of microvascular ECs, but did not mention if this was in dividing or confluent cells.[26]

The effect on apoptosis by Tnfaip8l1 *in vitro* was further supported by the data obtained *in vivo* from mice retinas. Knockdown of Tnfaip8l1 enhanced the number of apoptotic cells in the treated retina, as visualised by TUNEL staining. In comparison, overexpression of Tnfaip8l1 in the eye reduced the number of TUNEL-positive nuclei.

The family member Tnfaip8 was previously implicated to inhibit DED-containing receptor-mediated apoptosis in cancer cells.[13,14] Two well-known mechanisms of apoptosis are potentially involved in this process: the FasL pathway and the TNF-mediated pathway.[27] During pathological angiogenesis, peak levels of these pro-apoptotic ligands accumulate and provide the perfect microenvironment for the Tnfaip8l1 activity, but also

during physiological angiogenesis there is evidence for a possible involvement of the Tnfaip8 subfamily. Several *in vivo* studies in mice with a deficiency in the TNFα or FasL signalling have shown that loss of these signalling cascades reduces EC apoptosis and enhanced physiological angiogenesis in murine retinas.[28-30] We also observed enhanced EC apoptosis in our *in vitro* cultures in response to TNFα and FasL stimulation. *In vivo*, TNFα and FasL secretion tend to be facilitated by non-ECs. *In vitro*, the cultured ECs can become a source of these apoptotic ligands in response to stress, as indicated by our findings, and thus contributing to their own cell death.

Our *in vitro* data in which we demonstrate that transgenic expression of Tnfaip8l1 could diminish ECs from TNFα and FasL-induced apoptosis, point towards a crucial role in ensuring survival of especially dividing ECs in response to stimulation by these pro-apoptotic ligands.

In the early stages of DED-containing receptor-mediated apoptosis, the death-inducing signalling complex (DISC) is formed, which consists of the multimerised death receptors, Fas-associated death domain (FADD) and caspase 8.[31,32] This complex cleaves and activates caspase 8, which in its turn activates caspase 3 by cleavage, ultimately resulting in the execution of apoptosis.[33] In our study, we could not observe an effect of Tnfaip8l1 on the processing of caspase 8, as shown by Western blot, suggesting that Tnfaip8l1 works downstream of DISC formation. Indeed, we observed that Tnfaip8l1 reduced caspase 8 activity. We found that in addition to the reduced caspase 8 activity, the amount of activated caspase 3 was reduced as well, suggesting that Tnfaip8l1 functions as inhibitor of activated caspase 8. In line with our data, other investigators have shown that family member Tnfaip8 also reduced apoptosis in cancer cells by inhibition of caspase 8 activity and thus subsequently reduce caspase 3 activation.[14] The other family member Tnfaip8l2 has also previously been linked to caspase 8 activity in the immune homeostasis[15], again underlining the role of this family in the regulation of caspase 8. As mentioned before, family member Tnfaip8 function was previously described in microvascular ECs: knockdown of Tnfaip8 was reported to reduce the expression of VEGFR-2[26], a well known regulator in EC survival and mitogenesis.[34] In light of our findings, these reports suggest that Tnfaip8l1 and Tnfaip8 both are capable to promote EC survival through two distinct processes.

EC survival and proliferation are crucial in repairing and maintaining the myocardium after an infarction.[6,7] Early after MI the cardiac tissue produces high levels of TNFα[18], possibly creating a hostile environment for the proliferating ECs, making them more sensitive for apoptosis. In our murine MI model, we observed a strong upregulation of Tnfaip8l1 in cardiac ECs. Evaluation of human heart tissues showed similar results. Tnfaip8l1 protein expression increased in human cardiac tissue after an infarction. *In vitro*, we observed that this endothelial specific increase is a result of enhanced TNFα expression and not by the ischemia itself. These findings suggest a role for Tnfaip8l1 during the

neovascularisation response following an MI, making it a potential target for new therapeutic approaches to stimulate or protect the vasculature after an ischemic insult. Currently, we are generating a mouse line with inducible EC specific knockdown of Tnfaip8l1 to study its role in MI.

Similarly to ischemia, tumours are known to produces high levels of TNFα.[35] Angiogenesis is a key feature of a growing tumour[36], giving rise to the thought that Tnfaip8l1 may play a role in EC survival during tumour angiogenesis. Further studies in Tnfaip8l1 will elucidate the function of this endothelial prevalent anti-apoptotic protein in disease onset and progression.

In summary, the current study allocates for the first time the biological function of Tnfaip8l1 and demonstrates that Tnfaip8l1 acts as a potent inhibitor of DED-containing receptor-mediated apoptosis in ECs. Tnfaip8l1 inhibits the activation of caspase 3 by reducing caspase 8 activity, leading to enhanced EC survival and vascular growth, both in developmental vascular network-formation, as well as in neovascularisation after an adult ischemic event.

## *References*

1. Pandya NM, Dhalla NS, Santani DD. Angiogenesis - a new target for future therapy. *Vascul Pharmacol.* 2006;44(5):265-274.
2. Tang DG, Conti CJ. Endothelial cell development, vasculogenesis, angiogenesis and tumour neovascularisation: an update. *Semin Thromb Hemost.* 2004;30(1):109-117.
3. Belloni D, Verschini L, Foglieni C, Dell'Antonio G, Caligaris-Cappio F, Ferrarini M, Ferrero E. Bortezomib induces autophagic death in proliferating human endothelial cells. *Exp Cell Res.* 2010;316(6):1010-1018.
4. Merchan JR, Kovács K, Railsback JW, Kurtoglu M, Jing Y, Piña Y, Gao N, Murray TG, Lehrman MA, Lampidis TJ. Anti-angiogenic activity of 2-deoxy-D-glucose. *PLoS One.* 2010;5(10):e13699.
5. Napoli C. Oxidation of LDL, atherogenesis and apoptosis. *Ann N Y Acad Sci.* 2003;1010:698-709.
6. Maulik N. Angiogenic signal during cardiac repair. *Mol Cell Biochem.* 2004;264(1-2):13-23.
7. Prech M, Grajek S, Marszalek A, Lesiak M, Jemielity M, Araszkiewicz A, Mularek-Kubzdela T, Cieslinski A. Chronic infarct-related artery occlusion is associated with a reduction in capillary density. Effects on infarct healing. *Eur J Heart Fail.* 2006;8(4):373-380.

8.  Cheng C, Haasdijk RA, Tempel D, van de Kamp EH, Herpers R, Bos F, den Dekker WK, Blonden LA, de Jong R, Bürgisser PE, Chrifi I, Biessen EA, Dimmeler S, Schulte-Merker S, Duckers HJ. Endothelial cell-specific Fgd5 involvement in vascular pruning defines neovessel fate in mice. *Circulation.* 2012;125(25):3142-3158.

9.  Zhang S, Zhang Y, Wei X, Zhen J, Wang Z, Li M, Miao W, Ding H, Du P, Zhang W, He M, Yi F. Expression and regulation of a novel identified Tnfaip8 family is associated with diabetic nephropathy. *Biochim Biophys Acta.* 2010;1802(11):1078-1086.

10. Park HH, Lo YC, Lin SC, Wang L, Yang JK, Wu H. The death domain superfamily in intracellular signalling of apoptosis and inflammation. *Annu Rev Immunol.* 2007;25:561-586.

11. Eberstadt M, Huang B, Chen Z, Meadows RP, Ng SC, Zheng L, Lenardo MJ, Fesik SW. NMR structure and mutagenesis of the FADD (Mort1) death-effector domain. *Nature.* 1998;392(6679):941-945.

12. Xiao CW, Yan X, Li Y, Reddy SA, Tsang BK. Resistance of human ovarian cancer cells to tumour necrosis factor alpha is a consequence of nuclear factor kappaB-mediated induction of Fas-associated death domain-like interleukin-1beta-converting enzyme-like inhibitory protein. *Endocrinology.* 2003;144(2):623-630.

13. Kumar D, Whiteside TL, Kasid U. Identification of a novel tumour necrosis factor-alpha-inducible gene, SCC-S2, containing the consensus sequence of a death effector domain of Fas-associated death domain-like interleukin-1beta-converting enzyme-inhibitory protein. *J Biol Chem.* 2000;275(4):2973-2978.

14. You Z, Ouyang H, Lopatin D, Polver PJ, Wang CY. Nuclear factor-kappaB-inducible death effector domain-containing protein suppresses tumour necrosis factor-mediated apoptosis by inhibiting caspase 8 activity. *J Biol Chem.* 2001;276(28):26398-26404.

15. Sun H, Gong S, Carmody RJ, Hilliard A, Li L, Sun J, Kong L, Xu L, Hilliard B, Hu S, Shen H, Yang X, Chen YH. TIPE2, a negative regulator of innate and adaptive immunity that maintains immune homeostasis. *Cell.* 2008;133(3):415-426.

16. Thisse C, Thisse B. High-resolution *in situ* hybridisation to whole-mount zebrafish embryos. *Nat Protoc.* 2008;3(1):59-69.

17. Nasevicius A, Ekker SC. Effective targeted gene 'knockdown' in zebrafish. *Nat Genet.* 2000;26(2):216-220.

18. Weinstein BM, Stemple DL, Driever W, Fishman MC. Gridlock, a localised heritable vascular patterning defect in the zebrafish. *Nat Med.* 1995;1(11):1143-1147.

19. Nian M, Lee P, Khaper N, Liu P. Inflammatory cytokines and postmyocardial infarction remodelling. *Circ Res.* 2004;94(12):1543-1553.

20. Zidar N, Dolenc-Strazar Z, Jeruc J, Stajer D. Immunohistochemical expression of activated caspase 3 in human myocardial infarction. *Virchows Arch.* 2006;448(1):75-79.

21. Hayes AJ, Huang WQ, Mallah J, Yang D, Lippman ME, Li LY. Angiopoietin 1 and its receptor Tie2 participate in the regulation of capillary-like tubule formation and survival of endothelial cells. *Microvasc Res.* 1999;58(3):224-237.

22. Mesri M, Morales-Ruiz M, Ackermann EJ, Bennett CF, Pober JS, Sessa WC, Altieri DC. Suppression of vascular endothelial growth factor-mediated endothelial cell protection by survivin targeting. *Am J Pathol.* 2001;158(5):1757-1765.

23. Papapetropoulos A, Fulton D, Mahboubi K, Kalb RG, O'Connor DS, Li F, Altieri DC, Sessa WC. Angiopoietin 1 inhibits endothelial cell apoptosis via the Akt/survivin pathway. *J Biol Chem.* 2000;275(13):9102-9105.

24. Alon T, Hemo I, Itin A, Pe'er J, Stone J, Keshet E. Vascular endothelial growth factor acts as a survival factor for newly formed retinal vessels and has implications for retinopathy of prematurity. *Nat Med.* 1995;1(10):1024-1028.

25. Jiménez B, Volpert OV, Crawford SE, Febbraio M, Silverstein RL, Bouck N. Signals leading to apoptosis-dependent inhibition of neovascularisation by Thrombospondin 1. *Nat Med.* 2000;6(1):41-48.

26. Zhang C, Chakravarty D, Sakabe I, Mewani RR, Boudreau HE, Kumar D, Ahmad I, Kasid UN. Role of SCC-S2 in experimental metastasis and modulation of VEGFR-2, MMP1 and MMP9 expression. *Mol Ther.* 2006;13(5):947-955.

27. Lavrik I, Golks A, Krammer PH. Death receptor signalling. *J Cell Sci.* 2005;118(Pt 2):265-267.

28. Davies MH, Eubanks JP, Powers MR. Increased retinal neovascularisation in Fas ligand-deficient mice. *Invest Ophthalmol Vis Sci.* 2003;44(7):3202-3210.

29. Gardiner TA, Gibson DS, de Gooyer TE, de la Cruz VF, McDonald DM, Stitt AW. Inhibition of tumour necrosis factor-alpha improves physiological angiogenesis and reduces pathological neovascularisation in ischemic retinopathy. *Am J Pathol.* 2005;166(2):637-644.

30. Kaplan HJ, Leibole MA, Tezel T, Ferguson TA. Fas ligand (CD95 ligand) controls angiogenesis beneath the retina. *Nat Med.* 1999;5(3):292-297.

31. Varfolomeev EE, Schuchmann M, Luria V, Chiannilkulchai N, Beckmann JS, Mett IL, Rebrikov D, Brodianski VM, Kemper OC, Kollet O, Lapidot T, Soffer D, Sobe T, Avraham KB, Goncharov T, Holtmann H, Lonai P, Wallach D. Targeted disruption of the mouse Caspase 8 gene ablates cell death induction by the TNF receptors, Fas/Apo1 and DR3, and is lethal prenatally. *Immunity.* 1998;9(2):267-276.

32. Juo P, Kuo CJ, Yuan J, Blenis J. Essential requirement for caspase 8/FLICE in the initiation of the Fas-induced apoptotic cascade. *Curr Biol.* 1998;8(18):1001-1008.

33. Scaffidi C, Fulda S, Srinivasan A, Friesen C, Li F, Tomaselli KJ, Debatin KM, Krammer PH, Peter ME. Two CD95 (Apo1/Fas) signalling pathways. *EMBO J.* 1998;17(6):1675-1687.

34. Ferrara N, Gerber HP, LeCouter J. The biology of VEGF and its receptors. *Nat Med.* 2003;9(6):669-676.

35. Wang X, Lin Y. Tumour necrosis factor and cancer, buddies or foes? *Acta Pharmacol Sin.* 2008;29(11):1275-1288.

36. Folkman J. Role of angiogenesis in tumour growth and metastasis. *Semin Oncol.* 2002;29(Suppl 16):15-18.

# Chapter 9

Discussion and conclusion

Development of the vascular network consist of the differentiation of angioblasts into endothelial cells (EC) and the assembly into primitive vascular tubules, followed by the formation of new capillaries by sprouting from pre-existing small blood vessels. In addition to normal embryonic development of the vascular network, vessel formation contributes also to the pathogenesis of diseases like atherosclerosis, myocardial infarction and cancer. Identifying the molecular players in the regulation of angiogenesis provides further insight in the progress of many diseases and aids the development of novel therapies.

## *Gene expression analysis*

To identify new molecular players involved in angiogenesis, we carried out a genome-wide microarray screen for genes specifically expressed in Flk1-positive angioblasts at embryonic day (E)10.5 and 11.5 of vascular development during mouse embryogenesis. Upregulated genes were further verified in zebrafish by whole-mount *in situ* hybridisation and subsequent morpholino (MO)-knockdown technology to assess its biological function, which was validated in a murine retina model. In depth analysis of the molecular mechanism took place by *in vitro* assays, while the functional implications of the gene was eventually elucidated in knockout mice.

Gene expression analysis resulted in a list of candidate genes involved in the regulation of angiogenesis, including 9430020K01Rik (KIAA1462), Klf7, Tagln2, Thsd1, CCM1-3, Tnfaip8l1 and Fgd5. In this thesis, we describe in more detail the biological function of these genes in vessel formation.

### 9430020K01Rik and Klf7 are required for endothelial cell proliferation

The study described in chapter 2 focuses on the essential role of 9430020K01Rik in EC proliferation during vascular development. In spite of missing an one-to-one orthologue to zebrafish to verify the biological function of 9430020K01Rik, the gene was very interesting because of its association with coronary artery disease (CAD), which has been found previously.[1] Knockdown of 9430020K01Rik in the murine retina model suppressed blood vessel formation in the retina. Similar results were found in 9430020K01Rik-knockout mice, in which vascular density was also diminished in cardiac tissue. This phenotype was validated by *in vitro* 2D matrigel experiments. Further characterisation of the role of 9430020K01Rik in cultured ECs revealed that cell proliferation was decreased, due to a blockade in G1–S-phase transition after 9430020K01Rik knockdown. Based on liquid chromatography-mass spectrometry (LC-MS), we identified catenin (cadherin-associated protein), delta 1 (CTNND1) as a binding partner of 9430020K01Rik. Both proteins were co-localised at the cell membrane. It has been shown that free CTNND1 in the cytoplasm

forms a complex with RhoA-GDP, which results in the inhibition of GDP dissociation.[2] We hypothesised that complex formation of 9430020K01Rik with CTNND1 lowers the affinity of CTNND1 for RhoA-GDP and allows activation of RhoA-GDP by local guanine nucleotide exchange factors (GEF). Loss of 9430020K01Rik will result in less RhoA activation and downstream signalling, which is indeed reflected by our studies in cultured ECs. RhoA signalling regulates cell cycle progression or EC proliferation through G1–S-phase transition by two distinct pathways: via (i) Rho-associated coiled-coil containing protein kinase (ROCK) or (ii) the mammalian homolog of Drosophila diaphanous (mDia). Mainly changes in ROCK activity were associated with an increased risk of CAD by causing endothelial dysfunction and subsequent damage of the intimal layer. Loss of 9430020K01Rik could result in less EC turnover to repair endothelial damage, accelerating the progress of atherosclerosis. The activity of ROCK is inhibited by cytoplasmic p21$^{Cip1/Waf1}$, a member of the Cip/Kip family of cyclin-dependent kinase (CDK) inhibitors.[3-5] The expression of p21$^{Cip1/Waf1}$ is regulated by Krüppel-like factor 7 (Klf7), suggesting a potential role of Klf7 in EC proliferation. In our research, described in chapter 3, EC proliferation was indeed inhibited by Klf7 due to a blockade in G1–S-phase transition. However, this time the phenotype was effected by overexpression of the target gene, indicating an opposite effect of 9430020K01Rik and Klf7 on the RhoA-ROCK pathway (Figure 1). In spite of this, both genes were upregulated around 8 to 9 days post-fertilisation (dpf) of murine embryonic development: at 8 dpf 9430020K01Rik was highest upregulated compared with Klf7, whereas at 9 dpf it was the other way around. Taken together, a peak of Klf7 expression next to an increase in 9430020K01Rik expression may indicate a negative feedback loop or fine tuning mechanism of cell cycle progression by Klf7. In addition, Klf7 has been identified recently as one of the core regulators of several pathways associated with the onset or progression of CAD.[6] For this reason Klf7 and 9430020K01Rik can be both of great interest for the development of novel therapies against CAD.

**The role of Tagln2 during endothelial cell migration**
One of the next steps after ROCK or mDia activation in RhoA-regulated EC proliferation are changes in cell shape and cellular contractility, both generated by actin cytoskeleton dynamics.[3] Modulation of the actin cytoskeleton is important during different phases of the cell cycle, including cytokinesis - physical separation of daughter cells at the end of mitotic cell division (M-phase).[7] In non-dividing cells there is a significant role for actin cytoskeleton flexibility in many different processes, like EC migration and vascular integrity. In chapter 4 we describe the role of Transgelin 2 (Tagln2) in EC migration. Knockdown of Tagln2 in zebrafish resulted in ectopic sprouting of intersegmental vessels (ISV) at a later stage of development. Also in a murine retina model and *in vitro* migration assays we observed an increase in cell migratory properties after downregulation of Tagln2.

Similar results of enhanced cell motility has been found in hepatocellular carcinoma cells (HCC), where inactivation of Tagln2 led to less actin depolymerisation.[8] For that reason Tagln2 is also known as a tumour suppressor gene. Cancer cell spreading as well as tumour vascularisation are decisive factors in disease progression. Because of the late moment of ectopic sprouting of ISVs during zebrafish development, we hypothesised that migratory deficiencies were the result of a prolonged angiogenic behaviour of ECs within the ISVs. Normally, angiogenic behaviour is induced by VEGFR-2 signalling to make cells more sensitive for directional clues in their environment and is downregulated after tip cell fusion of two newly formed vessel branches. Prolonged VEGFR-2 signalling - reflected by increased VEGFR-2 synthesis - results in enhanced cell motility.[9-12] In our study, VEGFR-2 synthesis in cultured ECs was indeed increased after Tagln2 silencing. This would suggest that Tagln2 not only suppress cell motility through actin-binding and depolymerisation, but also by a negative feedback loop on VEGFR-2 signalling in migratory cells.

The actin-binding affinity of Tagln2 is regulated via PFTK1-dependent phosphorylation. PFTK1 - also known as CDK14 - is mainly active during the G2–M-phase of the cell cycle and forms a complex with cyclin Y. The activity of a broad spectrum of cyclin-CDK complexes is inhibited by Cip/Kip family members, including p27$^{Kip1}$, which is a downstream effector of the earlier mentioned RhoA signalling pathway. During cytokinesis at the end of the M-phase, RhoA signalling stimulates actin filament formation.[5,7,8,13] Taking these observations in consideration, RhoA-mDia may activate the ubiquitin ligase SKP2 and subsequent p27$^{Kip1}$ degradation, releasing the inhibition on cyclin-CDK complexes, allowing CDK14 to lower the actin-binding affinity of Tagln2 followed by actin depolymerisation in dividing cells (Figure 1).

**Vessel stabilisation and the role of Thsd1 and CCM proteins**
In the second part of this thesis, the research focuses more on vascular integrity and vessel stabilisation. Actin cytoskeleton flexibility and its regulation play an important role in this process. In chapter 5 we explain the role of Thrombospondin type I domain 1 (Thsd1) as regulator of endothelial barrier function during angiogenesis. Knockdown of Thsd1 in zebrafish and in the developing retinal vasculature of neonatal mice resulted in vascular haemorrhages. In a cultured monolayer of Thsd1-silenced ECs we showed that cell-cell barrier function was diminished in a transwell permeability assay. The endothelial barrier function is determined by cell morphology and junctional strength. Exposing the molecular mechanism we demonstrated that Thsd1 mediates Rac1 activation via CRT-LRP1 complex binding and downstream signalling via the FAK-PI3K cascade. Next to RhoA, Rac1 is also one of the small GTPases of the Rho family, which regulates the assembly of the actin cytoskeleton and related cell morphology. Rac1 activity plays a crucial role in the process of cell spreading by lamellipodia formation, while it suppress RhoA-induced stress fibre formation.[14,15] Analysis of the actin cytoskeleton during cell adhesion of Thsd1-silenced

ECs showed a clear delay in actin cytoskeleton spreading as compared with non-targeting siRNA transfected and untransfected controls. In addition, activation of Rac1 preserves cell-cell junction formation and thereby endothelial barrier function.[16,17] Based on immuno-histochemistry we indeed observed a reduced co-localisation of VE-cadherin with the actin cytoskeleton at the junctional sites, which suggests a weakening of the cell-cell junctions. Actin cytoskeleton reorganisation and strengthening of the cell-cell junctions due to Thsd1 expression may not only increase endothelial barrier function, but can also indicate the entrance of a quiescent EC phenotype. The last is also characterised by a reduction in VEGFR-2 signalling.[18] In chapter 4 we showed that VEGFR-2 signalling was negatively regulated by Tagln2. Taken together, it should be interesting to analyse Tagln2 activity at 9 dpf of murine embryonic development, because of the high expression level of Thsd1 at this day. As shown in Figure 1, Thsd1 will not only activate Rac1 signalling, but also diminish the RhoA pathway, which may eventually lead to an increase in Tagln2 activity and subsequent downregulation of VEGFR-2 signalling.

In addition of Thsd1, other proteins are involved in the regulation of the endothelial barrier function, including cerebral cavernous malformation (CCM) proteins 1-3. Mutations in these genes lead to the development of abnormal vascular structures particularly in the brain, also known as capillary-venous malformations. An overview from molecular pathogenesis to genetic counselling and clinical management is described in chapter 6. We noticed that CCM1-3 all have an essential role in the regulation of the Rho-GTPases, arranging cell polarity and adhesion to the extracellular matrix (ECM) and neighbouring cells. Especially RhoA is inhibited by CCM1-3 (Figure 1), suggesting less stress fibre formation and an increase in cell spreading, which results in enhanced endothelial barrier function.[19,20] CCM proteins are also involved in focal adhesion assembly, vessel maturation and vessel quiescence, as shown by the inhibitory effect of CCM1 on ICAP1α binding affinity to integrin, preventing blockage of integrin signalling, and the modulating effect of CCM2 on the actin cytoskeleton flexibility. In summary, CCM1-3 as well as Thsd1 play essential roles in vessel stabilisation.

**The role of Fgd5 and Tnfaip8l1 in endothelial cell apoptosis and vessel regression**
After vessel stabilisation aberrant vessels will regress by apoptosis - also known as vascular pruning - which is studied in the last part of this thesis. The study described in chapter 7 focuses on the role of FYVE, RhoGEF, and PH domain-containing 5 (Fgd5) in EC apoptosis. Fgd5 is a member of the FGD family of GEFs which regulates Cdc42 activity.[21,22] Based on co-immunoprecipitation and Cdc42 GEF-activity assays, we observed that Fgd5 also binds and activates Cdc42. From previous studies it is known that Cdc42 can induce apoptosis via phosphorylation of p21-activated serine/threonine kinase (PAK), while a more recent study has demonstrated that PAK blocks apoptosis via inhibition of caspase 8 signalling and degradation of the Bcl2 family proteins.[23-25] Given

these contradictory results, we hypothesised that Fgd5 may induce apoptosis via an alternative pathway. qPCR analysis determined that knockdown of Fgd5 was associated with downregulation of the Notch pathway genes, which leads to diminished transcription of Hey1 and p21$^{Cip1/Waf1}$. Hey1 is associated with p53-mediated apoptosis, while p21$^{Cip1/Waf1}$ blocks cell cycle progression.[26-28] Indeed, we observed that overexpression of Fgd5 resulted in p21$^{Cip1/Waf1}$-mediated cell cycle arrest and subsequent cell death induced by the Hey1-p53 pathway, which could be rescued by Hey1 knockdown (Figure 1). In addition, overexpression of Fgd5 resulted in a shift of the VEGFR-1 versus VEGFR-2 expression ratio, which leads to a more quiescent phenotype of ECs. The effect of Fgd5 on EC proliferation, apoptosis and VEGFR-2 signalling supports a regulatory role of Fgd5 in vascular pruning.

In chapter 8 we described the role of Tumour necrosis factor alpha inducible protein 8 like 1 (Tnfaip8l1) in apoptosis which is opposite in comparison with Fgd5. During vascular development, EC survival is important to prevent to early regression of newly formed blood vessels. Mainly proliferating ECs are more sensitive to apoptosis.[29] Knockdown of Tnfaip8l1 inhibited angiogenesis *in vitro* as well as *in vivo*, while overexpression of Tnfaip8l1 enhanced vascular development. Unravelling the molecular mechanism showed that Tnfaip8l1 mediates a reduction of caspase 8 activity, which results in reduced levels of cleaved caspase 3 (Figure 1). Caspase 3 normally activates ROCK1, which finally results in membrane blebbing, one of the first events in the execution phase of apoptosis.[30,31] The observed anti-apoptotic effect of Tnfaip8l1 was only found in proliferating cells. In addition, Tnfaip8l1 had no effect on the cell cycle itself. Just like Fgd5, expression of Tnfaip8l1 during murine development is highest around 9 dpf. However, Fgd5 is mostly active in the aberrant vessels, while Tnfaip8l1 is more active in proliferating ECs and sprouting vessels. Further, it is important to realise that the same period of embryonic development in human compared with mice is relatively fourteen-times longer. To gain more insight into the exact moment of co-expression of different genes during murine development, we have to fine tune at E9, because all genes described in this thesis, except Tagln2, were highly upregulated then.
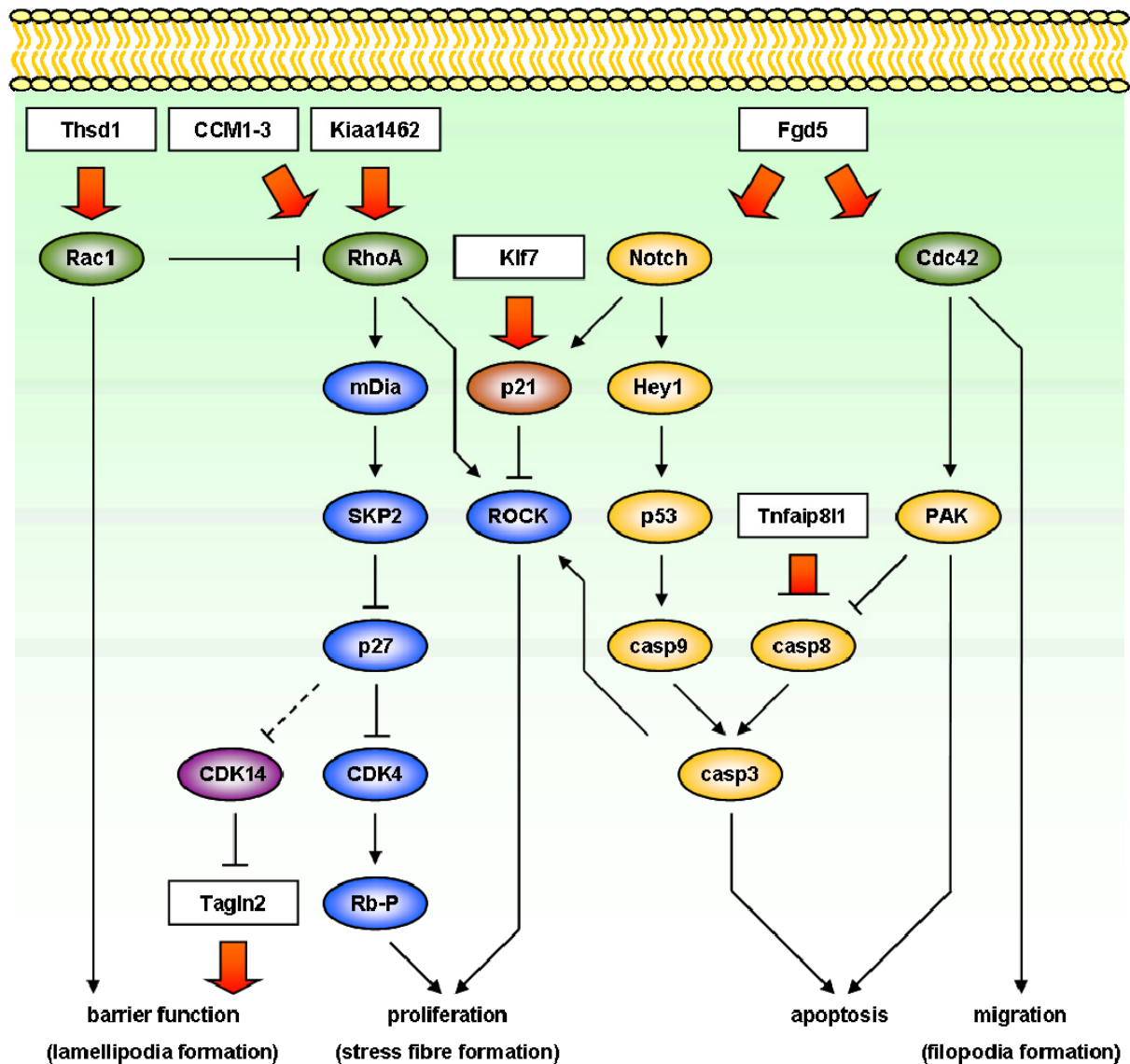
**Figure 1. Overview of the biological function of genes involved in angiogenesis.** Simplified reproduction of the molecular pathways that link up the genes involved in the regulation of angiogenesis described in this thesis. The pathways shown are based on studies in cultured ECs. Signalling from p27 to CDK14 is uncertain and remains to be elucidated. Red/orange arrows indicate the level at which these pathways are regulated in a positive or negative way by the examined genes (see text for more details).

## *Therapeutic implementation*

The leading cause of death in the world are cardiovascular diseases. Hypertension, smoking, dyslipidemia and diabetes mellitus are important risk factors for (ischemic) CAD and stroke.[32] Scientific progression made it increasingly clear that genetic aberrations also play an important role in the aetiology of vascular pathologies. For that reason, insight in the genetic regulation of cardiovascular development can provide clues to develop novel or additional therapies. Some of the genes identified in our microarray screen are already associated with cardiovascular diseases, such as 9430020K01Rik and Klf7 which were recently identified with several pathways associated with the onset or progression of CAD.[1,6] Both genes are involved in the regulation of ROCK activity (Figure 1). Clinical studies has demonstrated a correlation between elevated ROCK activity and impaired endothelial function in CAD patients.[33,34] Thus, inhibition of ROCK might be an attractive therapeutic target. Animal studies with the ROCK inhibitor Y-27632 showed indeed limited atherosclerotic plaque formation, whereas treatment with fasudil in patients with CAD showed a reduction of the overactivity of ROCK.[35-38] Interestingly, the 'pleiotropic' effects of statins - one of the main pharmacological options in the treatment of atherosclerosis - are also due to inhibited ROCK activity via indirect inhibition of the small GTPases of the Rho family.[39] In addition to the overactivity of ROCK, neovascular integrity further determines the progression and destabilisation of atherosclerotic lesions, since extravasation of erythrocytes from newly formed vessels leads to an increase in inflammatory response, expansion of the necrotic core and intraplaque haemorrhaging. Inward vessel growth sprouted from the vasa vasorum is driven by intraplaque hypoxia and subsequent VEGF secretion, another important therapeutic target.[40,41] VEGF blockage using monoclonal anti-VEGF antibodies is mainly studied in tumour angiogenesis. These blockers inhibit vascular branching and induces vessel destruction, which leads to tumour starvation. However, aggravation of hypoxia may also promote tumour invasiveness. Paradoxically, vessel normalisation and stabilisation of the vessel wall must prevent this.[42,43] Here, Thsd1 may have a beneficial role. After that, Thsd1 may also diminish the progression of atherosclerotic plaque vulnerability. Delivery of Thsd1 in mice already showed a lower percentage of intraplaque erythrocytes and a decrease in intraplaque Dextran-FITC leakage (chapter 5). In addition, new techniques have been developed to deliver angiogenic factors via cell beads containing genetically modified mesenchymal stem cells. Animal studies already showed a potential therapeutic benefit of this new approach after infusion in acute myocardial infarction.[44] In future cell bead studies that incorporate EC protective genes, Tnfaip8l1 may also be a potential candidate for overexpression, since it is upregulated during the neovascularisation response following myocardial infarction. Finally, it is

important to realise that the outcome of molecular interference in the signal transduction pathways depends on many different factors, including:

- the level at which these pathways are interrupted: blockage of a receptor may influence a wide range of different pathways, while further downstream the effect is more directed
- the intracellular location of the target protein: for example, in the nucleus p21$^{\text{Cip1/Waf1}}$ inhibits cyclin-CDK complexes, whereas located in the cytoplasm p21$^{\text{Cip1/Waf1}}$ will inhibit ROCK activity[5]
- the phase of the cell cycle in which a cell will be: for example, proliferating cells are more sensitive for Tnfaip8l1 than quiescent cells
- the availability of alternative pathways: blockage of a specific pathway may be rescued by an alternative one
- interaction between different cell types: in this thesis the research was focused on ECs only, but blood vessels are build up of distinct cell types. For example, in vessel stabilisation not only an increase in stabilisation of cell-cell junctions between ECs is important, but also the attraction of pericytes

Therefore, it's very precise to recover an imbalance of pro-angiogenic and anti-angiogenic factors. Genes described in this thesis may not only be a therapeutic target, but can also be used in personalised medicine to provide a genetic profile of hereditary risk factors in the development of cardiovascular diseases. Based on these information, preventive interventions can be considered.


## *Conclusion*

This thesis describes the biological function of genes involved in the regulation of angiogenesis. Gain- and loss of function studies have been carried out in ECs for each gene separately. However, the regulation of vascular development is a balance of pro-angiogenic and anti-angiogenic factors, which linked up accurately in different cell types. Therefore, multifactorial analyses in ECs and subsequent the vasculature as a whole will be the next step.

# *References*

1.  Erdmann J, Willenborg C, Nahrstaedt J, Preuss M, König IR, Baumert J, Linsel-Nitschke P, Gieger C, Tennstedt S, Belcredi P, Aherrahrou Z, Klopp N, Loley C, Stark K, Hengstenberg C, Bruse P, Freyer J, Wagner AK, Medack A, Lieb W, Grosshennig A, Sager HB, Reinhardt A, Schäfer A, Schreiber S, El Mokhtari NE, Raaz-Schrauder D, Illig T, Garlichs CD, Ekici AB, Reis A, Schrezenmeir J, Rubin D, Ziegler A, Wichmann HE, Doering A, Meisinger C, Meitinger T, Peters A, Schunkert H. Genome-wide association study identifies a new locus for coronary artery disease on chromosome 10p11.23. *Eur Heart J.* 2011;32(2):158-168.
2.  Anastasiadis PZ, Moon SY, Thoreson MA, Mariner DJ, Crawford HC, Zheng Y, Reynolds AB. Inhibition of RhoA by p120 catenin. *Nat Cell Biol.* 2000;2(9):637-644.
3.  Wozniak MA, Chen CS. Mechanotransduction in development: a growing role for contractility. *Nat Rev Mol Cell Biol.* 2009;10(1):34-43.
4.  Nunes KP, Rigsby CS, Webb RC. RhoA/Rho-kinase and vascular diseases: what is the link? *Cell Mol Life Sci.* 2010;67(22):3823-3836.
5.  Denicourt C, Dowdy SF. Cip/Kip proteins: more than just CDKs inhibitors. *Genes Dev.* 2004;18(8):851-855.
6.  Vangala RK, Ravindran V, Ghatge M, Shanker J, Arvind P, Bindu H, Shekar M, Rao VS. Integrative bioinformatics analysis of genomic and proteomic approaches to understand the transcriptional regulatory program in coronary artery disease pathways. *PLoS One.* 2013;8(2):e57193.
7.  Schiel JA, Childs C, Prekeris R. Endocytic transport and cytokinesis: from regulation of the cytoskeleton to midbody inheritance. *Trends Cell Biol.* 2013;23(7):319-327.
8.  Leung WK, Ching AK, Chan AW, Poon TC, Mian H, Wong AS, To KF, Wong N. A novel interplay between oncogenic PFTK1 protein kinase and tumour suppressor Tagln2 in the control of liver cancer cell motility. *Oncogene.* 2011;30(44):4464-4475.
9.  Nakayama M, Nakayama A, van Lessen M, Yamamoto H, Hoffmann S, Drexler HC, Itoh N, Hirose T, Breier G, Vestweber D, Cooper JA, Ohno S, Kaibuchi K, Adams RH. Spatial regulation of VEGF receptor endocytosis in angiogenesis. *Nat Cell Biol.* 2013;15(3):249-260.
10. Gaengel K, Niaudet C, Hagikura K, Laviña B, Muhl L, Hofmann JJ, Ebarasi L, Nyström S, Rymo S, Chen LL, Pang MF, Jin Y, Raschperger E, Roswall P, Schulte D, Benedito R, Larsson J, Hellström M, Fuxe J, Uhlén P, Adams R, Jakobsson L, Majumdar A, Vestweber D, Uv A, Betsholtz C. The sphingosine-1-phosphate receptor S1PR1 restricts sprouting angiogenesis by regulating the interplay between VE-cadherin and VEGFR-2. *Dev Cell.* 2012;23(3):587-599.

11. Galan Moya EM, Le Guelte A, Gavard J. PAKing up to the endothelium. *Cell Signal.* 2009;21(12):1727-1737.

12. Abraham S, Yeo M, Montero-Balaguer M, Paterson H, Dejana E, Marshall CJ, Mavria G. VE-cadherin-mediated cell-cell interaction suppresses sprouting via signalling to MLC2 phosphorylation. *Curr Biol.* 2009;19(8):668-674.

13. Niehrs C, Acebron SP. Mitotic and mitogenic Wnt signalling. *EMBO J.* 2012;31(12):2705-2713.

14. Dickson BJ. Rho-GTPases in growth cone guidance. *Curr Opin Neurobiol.* 2001;11(1):103-110.

15. Huveneers S, Danen EH. Adhesion signalling - crosstalk between integrins, Src and Rho. *J Cell Sci.* 2009;122(Pt 8):1059-1069.

16. Waschke J, Burger S, Curry FR, Drenckhahn D, Adamson RH. Activation of Rac1 and Cdc42 stabilises the microvascular endothelial barrier. *Histochem Cell Biol.* 2006;125(4):397-406.

17. Wójciak-Stothard B, Potempa S, Eichholtz T, Ridley AJ. Rho and Rac but not Cdc42 regulate endothelial cell permeability. *J Cell Sci.* 2001;114(Pt 7):1343-1355.

18. Potente M, Gerhardt H, Carmeliet P. Basic and therapeutic aspects of angiogenesis. *Cell.* 2011;146(6):873-887.

19. Borikova AL, Dibble CF, Sciaky N, Welch CM, Abell AN, Bencharit S, Johnson GL. Rho-kinase inhibition rescues the endothelial cell cerebral cavernous malformation phenotype. *J Biol Chem.* 2010;285(16):11760-11764.

20. Crose LE, Hilder TL, Sciaky N, Johnson GL. Cerebral cavernous malformation 2 protein promotes smad ubiquitin regulatory factor 1-mediated RhoA degradation in endothelial cells. *J Biol Chem.* 2009;284(20):13301-13305.

21. Huber C, Mårtensson A, Bokoch GM, Nemazee D, Gavin AL. Fgd2, a Cdc42-specific exchange factor expressed by antigen-presenting cells, localises to early endosomes and active membrane ruffles. *J Biol Chem.* 2008;283(49):34002-34012.

22. Hayakawa M, Matsushima M, Hagiwara H, Oshima T, Fujino T, Ando K, Kikugawa K, Tanaka H, Miyazawa K, Kitagawa M. Novel insights into Fgd3, a putative GEF for Cdc42, that undergoes SCF(FWD1/beta-TrCP)-mediated proteasomal degradation analogous to that of its homologue Fgd1 but regulates cell morphology and motility differently from Fgd1. *Genes Cells.* 2008;13(4):329-342.

23. Molli PR, Li DQ, Murray BW, Rayala SK, Kumar R. PAK signalling in oncogenesis. *Oncogene.* 2009;28(28):2545-2555.

24. Gnesutta N, Minden A. Death receptor-induced activation of initiator caspase 8 is antagonised serine/threonine kinase PAK4. *Mol Cell Biol.* 2003;23(21):7838-7848.

25. Yoshii S, Tanaka M, Otsuki Y, Fujiyama T, Kataoka H, Arai H, Hanai H, Sugimura H. Involvement of alpha-PAK-interacting exchange factor in the PAK1-c-Jun NH(2)-terminal kinase 1 activation and apoptosis induced by benzo[a]pyrene. *Mol Cell Biol.* 2001;21(20):6796-6807.

26. de la Pompa JL, Epstein JA. Coordinating tissue interactions: Notch signalling in cardiac development and disease. *Dev Cell.* 2012;22(2):244-254.

27. Huang Q, Raya A, DeJesus P, Chao SH, Quon KC, Caldwell JS, Chanda SK, Izpisua-Belmonte JC, Schultz PG. Identification of p53 regulators by genome-wide functional analysis. *Proc Natl Acad Sci U S A.* 2004;101(10):3456-3461.

28. Fischer A, Schumacher N, Maier M, Sendtner M, Gessler M. The Notch target genes Hey1 and Hey2 are required for embryonic vascular development. *Genes Dev.* 2004;18(8):901-911.

29. Jiménez B, Volpert OV, Crawford SE, Febbraio M, Silverstein RL, Bouck N. Signals leading to apoptosis-dependent inhibition of neovascularisation by thrombospondin-1. *Nat Med.* 2000;6(1):41-48.

30. Sebbagh M, Renvoizé C, Hamelin J, Riché N, Bertoglio J, Bréard J. Caspase 3-mediated cleavage of ROCK1 induces MLC phosphorylation and apoptotic membrane blebbing. *Nat Cell Biol.* 2001;3(4):346-352.

31. Coleman ML, Sahai EA, Yeo M, Bosch M, Dewar A, Olson MF. Membrane blebbing during apoptosis results from caspase-mediated activation of ROCK1. *Nat Cell Biol.* 2001;3(4):339-345.

32. Ohira T, Iso H. Cardiovascular disease epidemiology in Asia: an overview. *Circ J.* 2013;77(7):1646-1652.

33. Nohria A, Grunert ME, Rikitake Y, Noma K, Prsic A, Ganz P, Liao JK, Creager MA. Rho-kinase inhibition improves endothelial function in human subjects with coronary artery disease. *Circ Res.* 2006;99(12):1426-1432.

34. Shimokawa H, Takeshita A. Rho-kinase is an important therapeutic target in cardiovascular medicine. *Arterioscler Thromb Vasc Biol.* 2005;25(9):1767-1775.

35. Surma M, Wei L, Shi J. Rho-kinase as a therapeutic target in cardiovascular disease. *Future Cardiol.* 2011;7(5):657-671.

36. Zhou Q, Gensch C, Liao JK. Rho-associated coiled-coil-forming kinases (ROCKs): potential targets for the treatment of atherosclerosis and vascular disease. *Trends Pharmacol Sci.* 2011;32(3):167-173.

37. Mallat Z, Gojova A, Sauzeau V, Brun V, Silvestre JS, Esposito B, Merval R, Groux H, Loirand G, Tedgui A. Rho-associated protein kinase contributes to early atherosclerotic lesion formation in mice. *Circ Res.* 2003;93(9):884-888.

38. Shimokawa H, Morishige K, Miyata K, Kandabashi T, Eto Y, Ikegaki I, Asano T, Kaibuchi K, Takeshita A. Long-term inhibition of Rho-kinase induces a regression of arteriosclerotic coronary lesions in a porcine model *in vivo*. *Cardiovasc Res.* 2001;51(1):169-177.

39. Zhou Q, Liao JK. Pleiotropic effects of statins - basic research and clinical perspectives. *Circ J.* 2010;74(5):818-826.

40. Michel JB, Virmani R, Arbustini E, Pasterkamp G. Intraplaque haemorrhages as the trigger of plaque vulnerability. *Eur Heart J.* 2011;32(16):1977-1985, 1985a, 1985b, 1985c.

41. Moreno PR, Purushothaman KR, Sirol M, Levy AP, Fuster V. Neovascularisation in human atherosclerosis. *Circulation.* 2006;113(18):2245-2252.

42. Goel S, Duda DG, Xu L, Munn LL, Boucher Y, Fukumura D, Jain RK. Normalisation of the vasculature for treatment of cancer and other diseases. *Physiol Rev.* 2011;91(3):1071-1121.

43. Crawford Y, Ferrara N. VEGF inhibition: insights from preclinical and clinical studies. *Cell Tissue Res.* 2009;335(1):261-269.

44. Houtgraaf JH, de Jong R, Monkhorst K, Tempel D, van de Kamp E, den Dekker WK, Kazemi K, Hoefer I, Pasterkamp G, Lewis AL, Stratford PW, Wallrapp C, Zijlstra F, Duckers HJ. Feasibility of intracoronary GLP-1 eluting CellBead[TM] infusion in acute myocardial infarction. *Cell Transplant.* 2013;22(3):535-543.

# Chapter 10

**Summary**

**Samenvatting**

# *Summary*

Cardiovascular diseases are a major cause of death in the Western world. To gain more insight into the origin of these diseases, first of all it is important to understand normal development and functioning of the cardiovascular system in more detail. During embryonic development, the vascular network is formed by the assembly of tubular structures out of single cells (vasculogenesis) from which new vessel branches will develop (angiogenesis). These processes are regulated by proteins which building plan is encoded by our genetic material. Such part of genetic material - coding a specific protein - is also known as a gene. Changes (mutations) of a gene may result in the formation of a non-functioning protein and subsequent disturbances in blood vessel development. This thesis describes the search for genes involved in blood vessel development and their role within this process.

The identification of genes involved in blood vessel formation started with the isolation of cells from the vessel wall of mouse embryos at the embryonic stage of blood vessel development. Gene expression profiles of these isolated cells were determined. To validate gene expression in the developing vascular network, the expression of the zebrafish orthologues were examined. When positive, the genes were silenced one-by-one. Once a disturbance in blood vessel development occurred, the findings in the zebrafish were further validated in the developing retinal vasculature of neonatal mice and in primary cultures of human umbilical vein endothelial cells (HUVEC). In total, seven genes were studied in more detail in this thesis.

Chapter 2 describes the function of 9430020K01Rik (KIAA1462). Previous research has shown a link between mutations in this gene and the development of cardiovascular diseases. Silencing of 9430020K01Rik in the developing retinal vasculature of neonatal mice resulted in suppressed blood vessel formation. Supplementary research in HUVEC showed a disturbance in the regulation of cell proliferation. Many different proteins are involved in this process. These proteins can bind to each other and subsequently influence their activity. A series of proteins that stimulate or inhibit each other's activity, is also known as a signalling cascade. By using molecular techniques, it has been determined that 9430020K01Rik binds CTNND1 in order to influence the RhoA signalling cascade, which finally regulates cell proliferation. Knockdown of 9430020K01Rik in HUVEC resulted in a decrease of ROCK activity - an important protein in the RhoA signalling cascade. From literature it is known that disturbances of ROCK activity could be linked to the onset of cardiovascular diseases.

Chapter 3 describes the function of Klf7. Overexpression of Klf7 in HUVEC resulted in an increased activity of $p21^{Cip1/Waf1}$. It is known that $p21^{Cip1/Waf1}$ has an inhibitory effect on ROCK activity and in that way blocks cell proliferation. Supplementary research showed indeed a decrease of cell proliferation in HUVEC overexpressing Klf7.

Chapter 4 describes the function of Tagln2. Silencing of Tagln2 in zebrafish showed an apparently normal development of the vasculature. During a later stage of embryonic development excessive sprouting of intersegmental vessels occurred. Tagln2 depletion in the murine retinal vascular development model resulted in increased migration of the vascular plexus toward the retinal border. Since these effects occurred at a later stage of embryonic development, we hypothesised that the process of vessel development continuous as a result of remained sensitivity of vascular cells to growth promoting factors in the environment. From literature it is known that these remained sensitivity is caused by overexpression of specific receptors (VEGFR-2) at the cell surface. Indeed, Tagln2-silenced HUVEC showed an overexpression of VEGFR-2. Based on these findings, we conclude that Tagln2 plays an important role in preventing excessive sprouting of new blood vessels.

Chapter 5 describes the function of Thsd1. In zebrafish as well as in the murine retinal vascular development model, Thsd1 depletion resulted in vascular haemorrhaging, possibly by a loss of vascular integrity. The barrier function of the vessel wall is determined by cell shape and binding strength between two cells. Silencing of Thsd1 in HUVEC resulted in impaired actin cytoskeleton organisation and a weakening of cell-cell junctions. The actin cytoskeleton eventually determine cell shape. Molecular research showed an interaction of Thsd1 with the CRT-LRP1 complex and downstream Rac1 signalling. It is known that Rac1 signalling regulates actin cytoskeleton organisation and the binding strength between two cells. Beside the strong effects of Thsd1 knockdown on vascular integrity under normal conditions, massive bleeding were also found in atherosclerosis after silencing of Thsd1, which may result in an increase of disease progression. In mice, we have shown that overexpression of Thsd1 resulted in less haemorrhages of atherosclerotic plaques. This provides opportunities for the development of new therapies.

Chapter 6 provides an overview of the aetiology of vascular malformations in the brain caused by mutations in the three CCM genes (CCM1-3). These genes regulates different signalling cascades which finally determine cellular binding strength between two different cells or between the cell and its surrounding structures. Disturbances in binding strength could result in blood vessel dilatation and subsequently haemorrhaging.

Chapter 7 describes the function of Fgd5. Overexpression of Fgd5 in HUVEC resulted in an increase of programmed cell death, also known as apoptosis. It is known that Fgd5 belongs to a protein family which regulates the Cdc42 signalling cascade. An important protein in this signalling cascade is PAK. In literature a discussion is going on about the stimulating or inhibiting effect of PAK on apoptosis. Based on the contradictory findings,

we suspect that Fgd5 regulates an alternative signalling cascade to stimulate apoptosis. Research has shown that this is the p53 signalling cascade. After that, Fgd5 also impaired cell proliferation and stimulate cell quiescence, due to a proportionately decrease of the amount of VEGFR-2 at the cell surface and a subsequent impaired sensitivity to growth promoting factors in the environment. Based on these findings, we conclude that Fgd5 stimulates vascular pruning.

Chapter 8 describes the function of Tnfaip8l1. In zebrafish as well as in the murine retinal vascular development model, Tnfaip8l1 depletion resulted in impaired vessel formation. Supplementary research in HUVEC showed an increase of apoptosis, while on the other hand overexpression of Tnfaip8l1 in HUVEC resulted in a decrease of apoptosis. These effects were only found in dividing cells. It is known that dividing cells are more sensitive to apoptosis. Molecular research showed that Tnfaip8l1 inhibited caspase 8 activity. Caspase 8 normally induce the apoptotic signalling cascade. Based on these findings, we conclude that Tnfaip8l1 has a protective role against apoptosis in developing and newly formed blood vessels.

Taken together, this thesis showed the function of seven genes involved in the development of new blood vessels. The current findings may form a foundation for future medical developments. One of the possibilities is the improvement or development of new therapies to promote vessel growth after cardiac ischemia, or inhibition of vascular development on the other hand to impair tumour growth. Another possibility is genetic screening in patients and their families. Based on genetic testing, it is also possible to determine whether someone has a genetic predisposition for the development of cardiovascular diseases. However, there is still a long way to go…

## *Samenvatting*

Hart- en vaatziekten vormen een belangrijke doodsoorzaak in de westerse wereld. Om meer inzicht te krijgen in het ontstaan van deze ziekten, is het van belang om allereerst de normale ontwikkeling en het functioneren van het hart- en vaatstelsel beter te begrijpen. Tijdens de embryonale ontwikkeling ontstaat een netwerk van bloedvaten door het samenkomen van losse cellen die een buisvormige structuur vormen (vasculogenese) van waaruit zich nieuwe bloedvaten vertakken (angiogenese). De aansturing van deze processen geschiedt door eiwitten waarvan het bouwplan vastligt in het erfelijk materiaal. Zo'n stukje erfelijk materiaal dat codeert voor een specifiek eiwit, wordt ook wel gen genoemd. Veranderingen (mutaties) in een gen kunnen zorgen voor een niet goed functionerend eiwit, waardoor een verstoring kan optreden in de vorming van nieuwe bloedvaten. Dit proefschrift beschrijft de zoektocht naar genen betrokken bij de aanleg van nieuwe bloedvaten en hun functie binnen dit proces.

De zoektocht naar genen betrokken bij vaatvorming begon met het isoleren van cellen uit de bloedvatwand van muizenembryo's in de periode waarin het netwerk van bloedvaten wordt gevormd. In deze cellen is gekeken welke genen op dat moment actief waren. Vervolgens is onderzocht of deze genen eveneens actief waren in het vaatstelsel van de zebravis. Indien dit het geval was, werden deze genen stuk voor stuk uitgeschakeld. Zodra er hierdoor een verstoring optrad in de vorming van nieuwe bloedvaten, werden deze genen verder bestudeerd in het oog van de muis en in menselijke donorcellen afkomstig uit de bloedvatwand van een navelstreng (HUVEC). In totaal worden er in dit proefschrift zeven genen nader bestudeerd.

In hoofdstuk 2 wordt de functie van 9430020K01Rik (KIAA1462) beschreven. Eerder onderzoek heeft al een verband aangetoond tussen mutaties in dit gen en het ontstaan van hart- en vaatziekten. Uitschakeling van 9430020K01Rik in het oog van de muis zorgde voor minder bloedvaten in het netvlies. Aanvullend onderzoek in HUVEC liet zien dat er een verstoring was opgetreden in de aansturing van celdeling. Bij het delen van een cel zijn vele verschillende eiwitten betrokken. Deze eiwitten kunnen aan elkaar binden en zo elkaars activiteit beïnvloeden. Een aaneenschakeling van eiwitten die elkaars activiteit stimuleren of remmen, wordt ook wel signaalroute genoemd. Middels moleculaire technieken is vastgesteld dat 9430020K01Rik bindt aan het eiwit CTNND1 en op deze wijze de RhoA signaalroute aanstuurt, waardoor uiteindelijk celdeling kan plaatsvinden. Uitschakeling van 9430020K01Rik in HUVEC deed de activiteit van ROCK, een belangrijk eiwit in de RhoA signaalroute, afnemen. Vanuit de literatuur is bekend dat afwijkingen in de activiteit van het eiwit ROCK, het ontstaan van hart- en vaatziekten tot gevolg kan hebben.

In hoofdstuk 3 wordt de functie van Klf7 beschreven. Een verhoogde hoeveelheid Klf7 in HUVEC zorgde voor een toegenomen activiteit van het eiwit p21$^{Cip1/Waf1}$. Bekend is dat p21$^{Cip1/Waf1}$ een remmend effect heeft op de activiteit van het eiwit ROCK en op deze wijze celdeling kan blokkeren. Vervolgonderzoek toonde inderdaad een blokkade van de celdeling aan van HUVEC met een verhoogde hoeveelheid Klf7.

In hoofdstuk 4 wordt de functie van Tagln2 beschreven. Uitschakeling van Tagln2 in de zebravis liet aanvankelijk een normale aanleg van het vaatstelsel zien. Pas in een later ontwikkelingsstadium trad er een wildgroei van bloedvaten rondom de wervelkolom op. In het oog van de muis zorgde uitschakeling van Tagln2 ervoor dat het netwerk van bloedvaten zich veel sneller verplaatste richting het uiteinde van het netvlies. Aangezien deze effecten pas optreden in een later ontwikkelingsstadium, veronderstelden wij dat het proces van vaatgroei mogelijk door bleef gaan doordat de bloedvaten gevoelig bleven voor groei stimulerende factoren in de omgeving. Vanuit de literatuur is bekend dat een verlengde waarneming van deze factoren wordt veroorzaakt door een verhoogde productie van specifieke antennes (VEGFR-2), gepositioneerd aan de buitenkant van de cel. HUVEC waarin Tagln2 was uitgeschakeld liet inderdaad een verhoogde productie zien van VEGFR-2. Op basis van deze bevindingen concluderen wij dat Tagln2 een belangrijke rol speelt bij het voorkomen van een overmatige groei van nieuwe bloedvaten.

In hoofdstuk 5 wordt de functie van Thsd1 beschreven. Zowel in de zebravis als in het oog van de muis had uitschakeling van Thsd1 het optreden van bloedingen tot gevolg, mogelijk door een verstoring van de barrièrefunctie van de bloedvatwand. Deze barrièrefunctie wordt bepaald door de vorm van de cel en de bindingssterkte tussen twee cellen. Uitschakeling van Thsd1 in HUVEC resulteerde in een vertraagde opbouw van het celskelet en een verzwakking van de cel-cel verbindingen. Het celskelet bepaald de uiteindelijke vorm van de cel. Moleculair onderzoek toonde aan dat Thsd1 bindt aan het CRT-LRP1 eiwitcomplex en op deze wijze de Rac1 signaalroute aanstuurt. Bekend is dat deze signaalroute de opbouw van het celskelet en de bindingssterkte tussen twee cellen reguleert. Niet alleen onder normale omstandigheden liet de uitschakeling van Thsd1 een duidelijk effect zien op de vaatstabilisatie, maar ook gedurende aderverkalking zorgde een verminderde productie van Thsd1 voor bloedingen. Dergelijke bloedingen bij aderverkalking kunnen het verloop van de ziekte doen versnellen. In muizen hebben we kunnen aantonen dat een verhoogde hoeveelheid Thsd1 het aantal bloedingen bij aderverkalking kan laten doen afnemen. Dit biedt mogelijkheden voor de ontwikkeling van nieuwe therapieën.

In hoofdstuk 6 wordt een overzicht gegeven van het ontstaan van vaatafwijkingen in de hersenen, veroorzaakt door mutaties in de drie CCM genen (CCM1-3). Deze genen sturen meerdere signaalroutes aan die de bindingssterkte tussen twee cellen en tussen de cel en zijn omgeving bepaald. Een verstoring in deze bindingssterkte kan zorgen voor verwijding van het bloedvat met mogelijk bloedingen tot gevolg.

In hoofdstuk 7 wordt de functie van Fgd5 beschreven. Een verhoogde hoeveelheid Fgd5 in HUVEC zorgde voor een toename van geprogrammeerde celdood, ook wel apoptose genoemd. Bekend is dat Fgd5 onderdeel uitmaakt van een eiwitfamilie die de Cdc42 signaalroute aanstuurt. Een belangrijk eiwit in deze signaalroute is PAK. Er bestaat in de literatuur discussie of dit eiwit apoptose nu stimuleert, dan wel remt. Gezien deze tegenstrijdige bevindingen, verwachtten wij dat Fgd5 mogelijk een alternatieve signaalroute aanstuurt om zo apoptose te bevorderen. Onderzoek heeft aangetoond dat het hier gaat om de p53 signaalroute. Verder zorgt Fgd5 via deze signaalroute ervoor dat cellen minder delen en juist meer tot rust komen. Dit wordt mede bereikt doordat verhoudingsgewijs de hoeveelheid VEGFR-2 aan de buitenkant van de cel afneemt, waardoor de cellen minder gevoelig worden voor groei stimulerende factoren in de omgeving. Alle bevindingen in ogenschouw nemende, concluderen wij dat Fgd5 zorgt voor het verwijderen van het teveel aan nieuw ontstane bloedvaten.

In hoofdstuk 8 wordt de functie van Tnfaip8l1 beschreven. Zowel in de zebravis als in het oog van de muis had uitschakeling van Tnfaip8l1 een vermindering van het aantal bloedvaten tot gevolg. Aanvullend onderzoek in HUVEC liet een toename van apoptose zien. Daarentegen zorgde een verhoogde hoeveelheid Tnfaip8l1 in HUVEC voor een afname van apoptose. Deze effecten werden alleen waargenomen in delende cellen. Bekend is dat delende cellen gevoeliger zijn voor apoptose. Moleculair onderzoek toonde aan dat Tnfaip8l1 de activiteit van het eiwit caspase 8 remt. Dit eiwit induceert normaal gesproken de signaalroute die apoptose bevorderd. Op basis van deze gegevens concluderen wij dat Tnfaip8l1 een beschermende rol heeft tegen apoptose van nog ontwikkelende of net nieuw gevormde bloedvaten.

Samengevat laat dit proefschrift de functie zien van een zevental genen bij de aanleg van nieuwe bloedvaten. De huidige bevindingen kunnen de basis vormen voor medisch vervolgonderzoek. Zo valt te denken aan het ontwikkelen van nieuwe of verbeteren van reeds bestaande therapieën ter bevordering van de vaatgroei na een hartinfarct, of juist de remming van vaatgroei bij de bestrijding van tumoren. Ook in het erfelijkheidsonderzoek bij patiënten kunnen deze bevindingen een grote rol spelen. Middels genetisch onderzoek naar mutaties in deze genen kan mogelijk in de toekomst nog nauwkeuriger bepaald worden of iemand een erfelijke aanleg heeft voor het ontstaan van hart- en vaatziekten. Vooralsnog ligt er echter nog een lange weg voor ons open…

# Appendix

Curriculum Vitae

PhD portfolio

List of publications

Dankwoord

## *Curriculum Vitae*

Remco Haasdijk (1978) studeerde biologie aan de Rijksuniversiteit Groningen en de Radboud Universiteit Nijmegen, waar hij *cum laude* afstudeerde. Ook behaalde hij aan deze universiteit zijn artsexamen. Hij werkte als arts-assistent op de afdeling kindergeneeskunde en klinische genetica. In 2008 startte hij met zijn promotieonderzoek in het laboratorium voor Experimentele Cardiologie van het Erasmus MC te Rotterdam onder leiding van dr. H.J. Duckers. Zijn vrije tijd verdeelt hij over zijn grote passies wandelen en het bezoeken van balletvoorstellingen.

## *PhD portfolio*

**Erasmus MC**
University Medical Center Rotterdam

**Summary of PhD training and teaching**

| | |
|---|---|
| Name PhD student | Remco Haasdijk |
| Erasmus MC Department | Experimental Cardiology |
| Research School | COEUR |
| PhD period | May 2008 - April 2014 |
| Promotor | Prof.dr. D.J.G.M. Duncker |
| Supervisors | Dr. H.J. Duckers |
| | Dr. C. Cheng |

**PhD training**

| | Year | Workload (ECTS) |
|---|---|---|
| **General academic skills** | | |
| • Course in Animal Experimentation | 2001 | 3.0 |
| • GCP training | 2010 | 0.3 |
| • 'Basiscursus regelgeving en organisatie voor klinisch onderzoekers' (BROK) | 2010 | 0.5 |
| • English Biomedical Writing and Communication | 2011 | 4.0 |
| **Research skills** | | |
| • Practical introduction to laser scanning microscopy (OIC) | 2008 | 0.6 |
| **In-depth courses** | | |
| • 'Grasduinen in Genome Browsers' (MolMed) | 2007 | 0.6 |
| • Vascular Biology (Netherlands Heart Foundation) | 2008 | 2.0 |
| • Molecular Biology in Cardiovascular Research (COEUR) | 2009 | 1.5 |
| • Intensive Care Research (COEUR) | 2009 | 1.5 |
| • Pathophysiology of Ischemic Heart Disease (COEUR) | 2009 | 1.5 |
| • Cardiac Function and Adaptation (Netherlands Heart Foundation) | 2009 | 2.0 |
| • Cardiovascular Medicine (COEUR) | 2009 | 1.5 |

| | Year | Workload (ECTS) |
|---|---|---|
| **Presentations** | | |
| • Symposium Dutch Atherosclerosis Society, Ede, The Netherlands (poster) | 2009 | 0.3 |
| • COEUR PhD course (oral) | 2009 | 1.5 |
| • Dutch-German Joint Meeting, Rotterdam, The Netherlands (poster) | 2010 | 0.9 |
| • COEUR PhD day (poster) | 2010 | 0.8 |
| • COEUR PhD course (oral) | 2011 | 1.5 |
| • American Heart Association, Orlando (Florida), USA (poster) | 2011 | 0.3 |
| • Keystone Symposium, Snowbird (Utah), USA (poster) | 2012 | 0.3 |
| **National and international conferences** | | |
| • National | | |
|   - Symposium Dutch Atherosclerosis Society, Ede, The Netherlands | 2009 | |
|   - Cardio Vascular Conference, Noordwijkerhout, The Netherlands | 2011 | 0.3 |
| • International | | |
|   - Dutch-German Joint Meeting, Rotterdam, The Netherlands | 2010 | |
|   - American Heart Association, Orlando (Florida), USA | 2011 | 1.2 |
|   - Keystone Symposium, Snowbird (Utah), USA | 2012 | 1.5 |
| **Seminars and lectures** | | |
| • COEUR research seminars | | |
|   - Gene and cell based therapies of CV disease | 2008 | 0.4 |
|   - Imaging of carotid bifurcation atherosclerosis | 2008 | 0.4 |
|   - Surgical and percutaneous aortic valve implantation: indications, techniques and follow-up | 2009 | 0.4 |
|   - Hypertension | 2009 | 0.4 |
|   - New developments in percutaneous revascularisation | 2009 | 0.4 |
|   - Novel aspects of intensive care research | 2009 | 0.4 |
|   - Left ventricular hypertrophy and genetics | 2009 | 0.4 |
|   - Identification of novel genetic regulators of vessel formation | 2011 | 0.4 |

**Teaching activities**

| | Year | Workload (ECTS) |
|---|---|---|
| Supervising Bachelor/Master theses<br>• Student of LILLE 1 University - Science and Technology, Lille, France (F. Moreaux)<br>• Student of Avans Hogeschool, Breda, The Netherlands (J. Vermeer)<br>• Student of Avans Hogeschool, Breda, The Netherlands (E. van Reenen) | 2009<br><br>2011<br><br>2012 | 1.4<br><br>1.4<br><br>1.4 |
| | Total | 35.0 |

## List of publications

Tempel D, de Boer GMJ, van Deel ED, **Haasdijk RA**, Duncker DJGM, Cheng C, Schulte-Merker S, Duckers HJ. Apelin enhances cardiac neovascularisation after myocardial infarction by recruiting aplnr+ circulating cells. *Circulation Research* 2012; 111 (5): 585-598.

Cheng C, **Haasdijk RA**, Tempel D, van de Kamp EHM, Herpers RLJM, Bos FL, den Dekker WK, Blonden LAJ, de Jong R, Bürgisser PE, Chrifi I, Biessen EAL, Dimmeler S, Schulte-Merker S, Duckers HJ. Endothelial cell-specific Fgd5 involvement in vascular pruning defines neovessel fate in mice. *Circulation* 2012; 125 (25): 3142-3158.

Sluiter I, van Heijst AFJ, **Haasdijk RA**, Kempen MB, Boerema-de Munck A, Reiss I, Tibboel D, Rottier RJ. Reversal of pulmonary vascular remodelling in pulmonary hypertensive rats. *Experimental and Molecular Pathology* 2012; 93 (1): 66-73.

Cheng C, **Haasdijk RA**, Tempel D, den Dekker WK, Chrifi I, Blonden LAJ, van de Kamp EHM, de Boer GMJ, Bürgisser PE, Noordeloos AM, Rens JAP, ten Hagen TLM, Duckers HJ. PDGF-induced migration of vascular smooth muscle cells is inhibited by haem oxygenase-1 via VEGFR-2 upregulation and subsequent assembly of inactive VEGFR-2/PDGFR-β heterodimers. *Arteriosclerosis, Thrombosis and Vascular Biology* 2012; 32 (5): 1289-1298.

**Haasdijk RA**, Cheng C, Maat-Kievit AJ, Duckers HJ. Cerebral cavernous malformations: from molecular pathogenesis to genetic counselling and clinical management. *European Journal of Human Genetics* 2012; 20 (2): 134-140.

Cheng C, Tempel D, den Dekker WK, **Haasdijk RA**, Chrifi I, Bos FL, Wagtmans K, van de Kamp EHM, Blonden LAJ, Biessen EAL, Moll F, Pasterkamp G, Serruys PWS, Schulte-Merker S, Duckers HJ. Ets2 determines the inflammatory state of endothelial cells in advanced atherosclerotic lesions. *Circulation Research* 2011; 109 (4): 382-395.

Klaren PHM, **Haasdijk R**, Metz JR, Nitsch LMC, Darras VM, van der Geyten S, Flik G. Characterisation of an iodothyronine 5'-deiodinase in gilthead seabream (*Sparus auratus*) that is inhibited by dithiothreitol. *Endocrinology* 2005; 146 (12): 5621-5630.

van Heijst AFJ, **Haasdijk R**, Groenman FA, van der Staak FHJM, Hulsbergen-van de Kaa CA, de Krijger RR, Tibboel D. Morphometric analysis of the lung vasculature after Extra Corporeal Membrane Oxygenation treatment for pulmonary hypertension in newborns. *Virchows Archiv* 2004; 445 (1): 36-44.

**Haasdijk RA**, den Dekker WK, Tempel D, Szulcek R, Bos FL, Hermkens DMA, Chrifi I, Brandt MM, van de Kamp EHM, Blonden LAJ, van Bezu J, Sluimer JC, Biessen EAL, van Nieuw Amerongen GP, Schulte-Merker S, Cheng C, Duckers HJ. Thsd1: a new regulator of endothelial barrier function in vascular development and advanced atherosclerosis. *Submitted*

**Haasdijk RA**, Hermkens DMA, Tempel D, Demmers JAA, van de Kamp EHM, Blonden LAJ, Schulte-Merker S, Cheng C, Duckers HJ. 9430020K01Rik (KIAA1462): a new regulator of endothelial cell proliferation in angiogenesis. *Submitted*

**Haasdijk RA**, Cheng C, Tempel D, Herpers RLJM, Bürgisser PE, van de Kamp EHM, Blonden LAJ, Schulte-Merker S, Duckers HJ. Tagln2 is essential for endothelial cell migration in angiogenesis. *Submitted*

**Haasdijk RA**, Tempel D, Bürgisser PE, van de Kamp EHM, Blonden LAJ, Cheng C, Duckers HJ. Klf7 regulates endothelial cell proliferation and differentiation in angiogenesis. *Submitted*

Tempel D, **Haasdijk RA**, Bos FL, Hermkens DMA, Bürgisser PE, Sluimer JC, Bosman L, Biessen EAL, Cheng C, Schulte-Merker S, Duckers HJ. Tnfaip8l1 promotes angiogenesis by inhibition of endothelial cell apoptosis. *Submitted*

Tempel D, den Dekker WK, Yu ML, **Haasdijk RA**, Bürgisser PE, Serruys PWS, Schulte-Merker S, Cheng C, Duckers HJ. Apelin enhances atherosclerotic lesion size and vulnerability by increasing endothelial activation. *Submitted*

Tempel D, Bürgisser PE, Bos FL, **Haasdijk RA**, Cheng C, Schulte-Merker S, Duckers HJ. Grrp1 affects the organisation of the microtubule cytoskeleton in endothelial cells. *Submitted*

Tempel D, van Dessel L, Bos FL, Bürgisser PE, **Haasdijk RA**, Cheng C, Schulte-Merker S, Duckers HJ. Plvap is crucial during angiogenesis through stabilisation of caveolae. *Submitted*

Cheng C, Hermkens DMA, Chrifi I, Tempel D, **Haasdijk RA**, Brandt MM, van Dijk CGM, Bürgisser PE, van de Kamp EHM, Haitsma DB, Zhu C, Mustafa DAM, Blonden LAJ, Kros JM, Schulte-Merker S, Duckers HJ. Cgnl1 controls endothelial function and tubule assembly during vascular growth of human and murine endothelial cells. *Submitted*

## *Dankwoord*

'*Alvorens de Universiteit van Rotterdam te verlaten en als geneeskundige/bioloog het maatschappelijk leven in te treden rust op mij de plicht, een voor mij hoogst aangename plicht, een woord van hulde en dank te richten tot de Hoogleeraren van de natuur- en wiskundige en van de geneeskundige faculteiten, aan wie ik mijne opleiding te Rotterdam, Utrecht, Amsterdam, Nijmegen, Leuven en Groningen heb te danken. Gretig vat ik de heden mij geschonken gelegenheid aan, U allen, Hooggeleerde Heeren! openlijk mijn' hartelijken dank te zeggen èn voor de bijzondere welwillendheid, waarmede Gij mij van den aanvang tot het einde van mijn studietijd zijt te gemoet gekomen, èn voor het onderwijs dat ik van U heb mogen genieten. Zonder die welwillendheid zou het mij niet mogelijk zijn geweest den stap te doen, noch minder dien te volbrengen, waartoe ik den moed gevoelde te besluiten!*'

Bovenstaande tekst is gebaseerd op de uiting van dank door mevrouw Dr. Aletta H. Jacobs (1854-1929) op 8 maart 1879 in haar academisch proefschrift - Over localisatie van physiologische en pathologische verschijnselen in de groote hersenen (Stads- en Handels-Stoomdrukkerij van L. Oppenheim, Groningen) - ter verkrijging van den graad van Doctor in de geneeskunde aan de Rijksuniversiteit te Groningen. Zij vormt voor mij een groot voorbeeld.

Geheel in deze traditie zou ik daarom dank willen brengen aan een ieder die mij heeft gevormd gedurende mijn academische loopbaan.

**Erasmus MC Rotterdam**
Prof.dr. Duncker, beste Dirk-Jan, fijn dat je als promotor wilde optreden. Je scherpe blik was een waar genoegen!

Dr. Duckers, beste Eric, het was een bijzondere ervaring om onder jouw leiding werkzaam te mogen zijn geweest! De congresbezoeken in Amerika en de afdelingsborrels bij jou thuis heb ik zeer gewaardeerd.

Mevr. Dr. Cheng, beste Caroline, dank voor al de steun die je mij hebt gegeven zodat dit proefschrift tot een goed einde mocht komen!

**Hubrecht Instituut Utrecht**
Prof.dr. Schulte-Merker, dear Stefan, thank you for the pleasant cooperation. The zebrafish work that takes place within your research group, forms an important foundation for this thesis. I would also like to thank you for being a member of the supervisory committee.

**Vrije Universiteit Amsterdam**

Dr. Van Nieuw Amerongen, beste Geerten, dank dat ik gebruik mocht maken van de ECIS faciliteiten bij je op het lab. Ook Jan van Bezu en Robert Szulcek wil ik bedanken voor hun ondersteuning bij de experimenten. Met veel plezier heb ik mijn werkzaamheden bij jullie mogen uitvoeren! Zonder het VU-busje naast de telefoon bij mijn beide grootouders en zo vele anderen zou dit niet mogelijk zijn geweest.

**Radboudumc Nijmegen**

Prof.dr. Kollée, onder uw leiding kon ik op de afdeling kindergeneeskunde mijn klinische, alsmede mijn onderzoeksvaardigheden tot ontplooiing brengen.

Dr. Van Heijst, beste Arno, dank voor je enthousiaste begeleiding. Je toonde altijd een grote betrokkenheid bij het wetenschappelijk onderzoek! Door jouw vertrouwen in mij, kon ik mij vormen tot een klinisch onderzoeker. Tijdens de periode van het onderzoeksproject bij jou op de afdeling neonatologie bood je me altijd de krenten in de pap aan, waaronder een symposiumbezoek in Aachen, het houden van een mondelinge voordracht op het NVK-congres te Veldhoven en de vele werkbesprekingen met professor Tibboel in het Sophia Kinderziekenhuis te Rotterdam, maar ook het neonataal transport per ambulance vanuit Oss vond ik een geweldige ervaring. Je stelregel: '*maak het jezelf niet te moeilijk*' heb ik helaas pas veel te laat ter harte genomen, maar al doende leert men. Dank voor alles!

Mevr. Van Wolferen, beste Corrie, jij mag in deze rij zeker niet ontbreken. Dank voor je ondersteuning en bemoediging als het wel eens tegenzat. Je attendeerde me altijd weer op de lichtpuntjes als ik ze soms even niet meer zag. Met een groot genoegen kijk ik terug op de NVK-congressen welke ik samen met jou mocht bezoeken. Je hebt me hier leren 'shoppen' bij de industrie, waarvan ik nog vele malen plezier heb gehad bij andere wetenschappelijke bijeenkomsten. Ook stelde je me in de gelegenheid om te netwerken tijdens het informele deel van het congres. Niet alleen tijdens het werk bood je de nodige ondersteuning, maar ook bij het lopen van de Nijmeegse vierdaagse. Ik keek altijd uit naar je sms'jes. Zonder dit zou ik de 'Via Gladiola' nooit hebben gehaald. In één woord geweldig!

**Radboud Universiteit Nijmegen**

Prof.dr. Flik, beste Gert, vaak denk ik nog terug aan de woorden die je hebt gesproken tijdens de uitreiking van het doctoraal diploma Biologie. Deze hebben een diepe indruk op mij achtergelaten. Je bent iemand die de waarde van mensen inziet! Iedereen bij jou op de afdeling organismale dierfysiologie is van even groot belang, ongeacht rang of stand. Met zeer veel plezier heb ik me dan ook gestort op de stage die ik bij je mocht lopen. Ook aan de uitreiking van de L.M. van Nieuwenhovenprijs koester ik warme herinneringen. Veel, veel dank!

274

Dr. Klaren, beste Peter, werkoverleg met jou was altijd heel gezellig. Je bood de ruimte om met eigen ideeën te komen en stuurde bij waar nodig. De deur van je kamer stond altijd open en ik kon dan ook met al m'n vragen bij je terecht. Dank voor alle sprankelende momenten!

**Katholieke Universiteit Leuven (België)**

Mevr. Prof.dr. Darras, dank voor de geboden gastvrijheid bij u op het Laboratorium voor Vergelijkende Endocrinologie. Het was mij een waar genoegen de Vlaamse normen en waarden te mogen ervaren. Ik heb mij dan ook erg thuis gevoeld bij u op het labo!

Dr. Van der Geyten, beste Serge, vele goede gesprekken hebben wij mogen voeren op een van de gezellige terrasjes in Leuven. Op het labo heerste ook altijd een goede sfeer. Met veel humor kon je dingen uitleggen. Het mooiste was toch wel dat we voor het scannen van de gelelectroforese in witte jas buitenom naar de buren moesten. Ook van de labuitjes naar de Belgische Ardennen heb ik erg genoten, waarvoor mijn dank!

**Rijksuniversiteit Groningen**

Prof.dr. Luiten, onder uw toezicht is in de eerste twee jaar van de studie Biologie de basis gelegd waarop mijn verdere academische loopbaan rust.

Susan en Carien, dank dat jullie mijn paranimfen wilden zijn.

Al deze mensen hebben mij in academisch maar ook in persoonlijk opzicht gevormd tot wie ik nu ben. De grootste les die ik van hen allen heb mogen leren, is dat elke ontmoeting - hoe lang of hoe kort deze ook is - van waarde is en je doet laten veranderen. Carl Gustav Jung (1875-1961) verwoorde dit als volgt: '*De ontmoeting tussen twee persoonlijkheden is als het contact tussen twee chemische stoffen. Indien er een reactie optreedt, zullen beiden veranderen.*'

Verder dank aan al diegenen die ik hier niet met naam en toenaam heb genoemd, maar zonder wie dit proefschrift nooit tot stand zou zijn gekomen.

Tot slot wil ik nog in het bijzonder mijn ouders bedanken voor alle ruimte die zij mij geven om mijn dromen te verwezenlijken, maar bovenal dank aan de Ene die nooit loslaat het werk waaraan zijn hand eenmaal begonnen is…

*Remco*